OIL-IN-WATER NANOEMULSIONS AS MUCOSAL VACCINE ADJUVANTS: CHARACTERIZATION, MECHANISM, FORMULATION, AND DEVELOPMENT OF A NANOEMULSION-BASED *BURKHOLDERIA CENOCEPACIA* VACCINE

by

Paul Edward Makidon

A dissertation submitted in partial fulfillment
of the requirements for the degree of
Doctor of Philosophy
(Biomedical Engineering)
in The University of Michigan
2009

Doctoral Committee:

Professor James R. Baker Jr., Chair

Professor Victor J. DiRita

Professor John J. LiPuma

Associate Professor Joseph L. Bull

Dedication

To the loving memory of my Grandparents Jack and LaVern McJilton…

Ring the bells
that still can ring…
Forget your perfect offering
There is a crack…
A crack in everything…
That's how the light gets in.
--Leonard Cohen

To my wife Jennifer, son Gavin, and child on the way…

Love itself holds no boundaries.

And to my mother Pamela….

You are my compass, my anchor, and my guide.

Acknowledgements

Committee: James R. Baker, Jr., Victor J. DiRita, John J. LiPuma, and Joseph L. Bull

I am greatly honored and humbled to have had the pleasure of **Dr. James R. Baker Jr.**'s mentorship**.** He is a true pioneer in science. His constant vigilance, encouragement, and support have helped to guide me through this seemingly endless process. In those rare moments when all else seemed lost, Dr. Baker, without hesitation, would have a suggestion that in retrospect was beyond insightful. I will always be amazed by his abilities. As with all great scientists, his work load is immense and his days are long. I hope that some day in the not too distant future, he will take a *real* vacation.

It was a great pleasure to have an opportunity to work with **Dr. LiPuma**, **Dr. Bull**, and **Dr. DiRita.** Your knowledge and insight have been invaluable to my progress. I am especially thankful to Dr. LiPuma for his support and encouragement on the *Burkholderia* studies. Your lessons also went beyond scientific detail and I feel that I have better scientific insight because of time spent with you. Dr. Bull was particularly helpful in the physical analysis of the nanoemulsion. I will look forward to his continued guidance and colleagueship. Dr. Dirita's suggestions for improvements on separating the outer membrane protein proved critical for the progress of the development of the *Burkholderia* vaccine. I am also looking forward to his continued guidance as my career progresses.

I am particularly indebted to the scientists and managers at the Michigan Nanotechnology Institute for Medicine and Biological Sciences (**MNIMBs**). One

could not ask for a more supportive and knowledgeable group of people. Without them, my progression would have been stifled.

Dr. Ania Bielinska has been a real source of strength for me (sometimes emotional, sometimes scientific). We are true comrades in the art of venting! Her support and guidance are well appreciated. I am a better scientist and perhaps a better person having known her. Someday, we will write that truly eloquent paper. Dr. Bielinska was the co-author of the manuscript that Chapter 2 of this dissertation was based off of.

Dr. Luz Blanco (Lupi) has been a constant source of support and mentorship for me. Together, we tackled the ominous task of determining the mechanism of adjuvant activity. I will look forward to more of those tennis games with her. Dr. Blanco was the co-author of the yet to be published manuscript that Chapter 3 of this thesis was based off of.

Dr. Shradda Nigavekar was like a lighthouse in a vast see of fog for me. Her calming presence and clarity of thought will not be forgotten. It is because of her, that I have a finer appreciation for the art of patience.

Jessica Knowlton is probably one of the most capable scientists I know. What is truly amazing, she is also one of the best people I know. Without her efforts, my project would still be in the dark ages. She mentioned to me once that she just truly wants to make the world a better place. I think that it is safe to say that she is well on her way to success in this regard.

As a graduate student, **Jeffry Groom, II** is a rising star. His work was instrumental in the development of the *Burkholderia cenocepacia* vaccine. I expect great things to come for Jeffrey.

I was once told that I am the only graduate student in history to have a support staff. I have to agree. I would like to acknowledge important contributions of **Kasia Janczak**, **Nick Mank**, **Allison Scott**, **Mike Beer**, **Whitney Hovan, Claire Vereij, Gloria Lippens, Donna Gauss, Dr. Peter Cao**, **Dr. Siva Rathinavelu**, **Dr. Jola Kukowska**, **Dr. Andrjez Myc**, **Dr. Michele Gerber, and Dr. Erby Wilkinson** to this work. Of special note, I also need to thank **Dr. Pascale Leroueil** for her suggestion to hit “ALT F9”. She will know what I mean!

I am grateful to the faculty and staff at the Unit for Laboratory Animal Medicine **(ULAM)** at the University of Michigan for support throughout my residency in Comparative Medicine and my graduate studies. I am especially grateful to my ULAM mentors **Dr. Howard Rush** and **Dr. Jean Nemzek**.

I would finally like to thank **my family**. I owe them a debt for your support and love that I can never repay (though I may die trying). Without their love, completing this task would have been impossible and meaningless.

I have been financially supported by a T32 RR07008 from the Natl Ctr Research Resources of NIH. This research has been a Funded by Bill & Melinda Gates Foundation through Grand Challenges in Global Health Initiative 37868 and by a grant from the Haas Foundation for Cystic Fibrosis.

Table of Contents

Dedication ii
Acknowledgements iii
List of Figures ix
List of Tables xix
List of Abbreviations xx

CHAPTER 1 INTRODUCTION 1
1.1 BACKGROUND 1
1.2 CURRENT AND HISTORICAL APPROACHES TO VACCINE ADJUVANTS 2
1.3 MUCOSAL VACCINATION 3
1.4 NANOMEULSIONS 6
1.5 NANOEMULION AS A MUCOSAL VACCINE ADJUVANT 7
1.6 NANOEMULISON-BASED THERMAL STABLE, AND NEEDLE-FREE VACCINES FOR DEVELOPING POPULATIONS 7
1.7 CURRENT INSIGHTS INTO THE MECHANISM OF NE ADJUVANT 8
1.8 EFFECTS OF FORMULATION OF NE-BASED VACCINES ON THERMAL STABILITY AND DELIVERY THROUGH NASAL SPRAYER DEVICES 9
1.9 DEVELOPMENT OF A NE-BASED *BURKHOLDERIA CENOCEPACIA* VACCINE 10
1.10 OUTLINE AND THESIS ORGANIZATION 11
1.11 REFERENCES 13

CHAPTER 2 PRE-CLINICAL EVALUATION OF A NOVEL NANOEMULSION-BASED HEPATITIS B MUCOSAL VACCINE 19
2.1 BACKGROUND 19

2.2 EXPERIMENTAL METHODS 21
2.3 RESULTS 31
2.4 DISCUSSION 38
2.5 CONCLUSIONS AND SUMMARY 42
2.6 TABLES 43
2.7 FIGURES 45
2.8 REFERENCES 54

CHAPTER 3 NANOEMULSION NASAL MUCOSAL ADJUVANT MECHANISM OF ACTION: INDUCTION OF ANTIGEN SAMPLING AND ROLE OF IL6 61
3.1 BACKGROUND 61
3.2 EXPERIMENTAL METHODS 62
3.3 RESULTS 69
3.4 DISCUSSION 75
3.5 CONCLUSSIONS AND SUMMARY 78
3.6 FIGURES 79
3.6 FIGURES 79
3.7 REFERENCES 90

CHAPTER 4 FORMULATION AND DEVELOPMENT OF NANOEMULSION-BASED VACCINES AND DELIVERY THROUGH NASAL SPRAYER DELIVERY SYSTEMS 94
4.1 BACKGROUND 94
4.2 EXPERIMENTAL METHODS 96
4.3 RESULTS 107
4.4 DISCUSSION 110
4.5 CONCLUSIONS AND SUMMARY 114
4.6 FIGURES 115
4.7 TABLES 124
4.8 REFERENCES 126

CHAPTER 5 NASAL IMMUNIZATION WITH A NANOEMULSION-BASED BURKHOLDERIA CENOCEPACIA OUTER MEMBRANE PROTEIN VACCINE PROTECTS AGAINST EXPERIMENTAL LUNG INFECTIONS IN MICE 130
5.1 BACKGROUND 130
5.2 EXPERIMENTAL METHODS 131
5.3 RESULTS 139
5.4 DISCUSSION 145
5.5 CONCLUSIONS AND SUMMARY 149
5.6 FIGURES 150
5.7 TABLES 158
5.8 REFERENCES 160

CHAPTER 6 CONCLUSIONS AND OUTLOOK 164

List of Figures

Figure 1.1	**Artist rendition of the microbiocidal activity of nanoemulsion.**	**12**
Figure 1.2	**Cartoon showing the comparison of the emulsion to a micelle**	**12**
Figure 2.1	**Stability of HBsAg. A) Silver stained SDS-PAGE: Analysis of freshly prepared vs. 72 hour incubated HBs antigen mixed with 20% NE. Conditions of the incubation are specified above the gel. HBsAg monomer and dimer are indicated with arrows at 24 kDa and 48 kDa bands. B) Western blot: The protein configuration is identical to as described for SDS-PAGE. HBsAg is detected using a polyclonal anti-HBsAg antibody for all incubation conditions.**	**45**
Figure 2.2	**HBsAg interaction with NE droplets. Zeta potential: A) The zeta potential was measured for HBsAg (2.5 mg/ml), 20% NE and mixture of HBsAg with NE (HBsAg-NE) in water and PBS. Surface charge is reported in mV units. Particle sizing: Size distribution was measured using a laser diffraction particle-sizer. Analysis of HBsAg alone B), NE alone C), and NE with 10 mg/ml of HBsAg D). Data was processed and analyzed using Fraunhofer optical modeling and number weighted averaging (number %). Single population intensity peaks indicate monodisperse populations of HBsAg (28 nm), NE (349 nm), and HBsAg-NE (335 nm). E) Calorimetric titration of HBsAg with NE: 25 injections of 1% NE (10 µl/injection) were introduced into a sample cell containing HBsAg (600 µg/ml in PBS) at 30°C. The upper panel shows differences between the sample and reference cell containing PBS. The lower panel shows enthalpy per injection of NE injected versus injection number. An exothermic reaction was measured following the addition of nanoemulsion to an antigen solution. Addition of nanoemulsion to the antigen solution became less energetic as the total concentration of nanoemulsion increased, suggesting that the antigen was being depleted. ΔCp was calculated to be -1.44 [77].**	**46**

Figure 2.3 **Development of IgG response in serum. Effect of NE adjuvant: Mice were immunized intranasally with HBsAg-NE consisting of 20 µg of HBsAg mixed with 0% to 40% concentrations of NE A). Significant statistical difference with *p-value* <0.05 was observed between all HBsAg-NE formulations and HBsAg-PBS vaccine. Antigen dose escalation: Mice were immunized intranasally with 1 µg to 40 µg HBsAg mixed with 20% NE B). A significant statistical difference with *p value* < 0.05 was observed between all 5 µg to 40 µg HBsAg-NE formulations and 1 µg HBsAg-NE vaccine. Serum anti-HBsAg IgG antibody concentrations are presented as mean of endpoint titers in individual sera ±SEM. * indicates a statistical difference (*p-value* <0.05) in the anti-HBsAg IgG titers. Arrows indicate vaccine administration.** **47**

Figure 2.4 **Comparison of mucosal NE-based with conventional aluminum-based injectible HBsAg vaccine. Time course of antibody response: Mice were immunized with 20 mg HBsAg. Antigen was mixed with 20% NE for intranasal administration (HBsAg-NE), or adsorbed on aluminum hydroxide (HBsAg-Alu) for intramuscular injections A). Serum anti-HBsAg IgG antibody concentrations are presented as mean of endpoint titers in individual sera ± SEM. * indicates a statistical difference (*p-value* <0.05) in the anti-HBsAg IgG titers. Arrows indicate vaccine administration. Avidity of anti-HBsAg IgG: Analysis of sera from mice immunized i.n. with HBsAg-NE and with i.m. injections of HBsAg-Alu vaccines B). Avidity indexes (AI) were assessed using 1.5 M NaSCN as a discriminating salt concentration. Each circle represents individual AI and lines indicate mean AI value for each group obtained in two independent assays. Serum anti-HBsAg IgG subclass: Anti-HBsAg IgG subclass pattern in mice immunized nasally with HBsAg-NE and injected i.m. with HBsAg-Alu vaccine C). Analysis of sera collected at 22 weeks after initial immunization. The results are presented as ratio of the specific subclass IgG to the overall IgG titer. * indicates statistical difference (*p-value* <0.05) between NE-based and alum-based immunizations.** **48**

Figure 2.5 **Characterization of immune response mucosal and cellular responses to HBsAg-NE. Mucosal antibody measurements were performed in BAL fluids obtained 23 weeks after i.n immunization with HBsAg-NE vaccines. IgA detection: The anti-HBsAg IgA detection was performed with 1:2 dilutions of BAL A). Results are presented as mean values of OD at 405 nm ±SEM. IgG detection: The anti-HBsAg IgG antibody concentrations are presented as end point titers B). Antigen-specific cytokine expression. Pattern of Th1 (IFN-γ and TNF-α) and Th2 (IL4, IL5 and IL10) cytokine expression in vitro in splenocytes from mice intranasally immunized with HBsAg-NE C). Splenocytes were obtained at 23 weeks after initial immunization from mice with HBsAg-20% NE. Results are presented as fold increase of the cytokine production over levels detected in non-stimulated splenocyte cultures.** **49**

Figure 2.6 **Immunogenicity in rats and guinea pigs. Rats and guinea pigs were immunized intranasally with either 5 µg or 20 µg HBsAg mixed with 20% NE. Serum anti-HBsAg IgG antibody concentrations are presented as mean of endpoint titers in individual sera ± SEM. Data represents anti-HBsAg end titers measured 3 weeks after a single dose (1 dose) vaccination and after two vaccinations (2 doses) measured at 7 weeks.** **50**

Figure 2.7 **In vitro analyses of HBsAg-NE stability. The comparison of HBsAg-NE stored at test temperature conditions to freshly prepared formulation using SDS-PAGE followed by silver staining (S) or Western immunoblotting (W) is shown. Lanes are labeled according to sample storage conditions as follows- 1: fresh, 2: 4°C, 3: 25°C and 4: 40°C. Samples were stored for A) 6 weeks, B) 3 months, C) 6 months or D) 1 year (52 weeks) at the three test temperatures. Each lane contains 0.5 µg of antigen. Arrow indicates the HBsAg major band. E) Particle size comparison of NE alone to freshly mixed HBsAg-NE and formulation stored up to a year. Mean diameter of particles is shown in microns ± SD.** **51**

Figure 2.8 **In vivo analyses of HBsAg-NE stability. HBsAg specific antibody responses to freshly prepared HBsAg-NE or HBsAg-NE stored under real-time (4°C), accelerated (25°C) and stressed (40°C) temperature conditions are depicted. CD-1 mice were vaccinated with either freshly prepared or stored HBsAg-NE and boosted at 6 weeks. Serum anti-HBsAg IgG antibody concentrations are presented as a mean of endpoint titers in individual sera ± SD. Comparison of serum IgG elicited by freshly prepared HBsAg-NE to formulation stored for A) 6 weeks, B) 3 months, C) 6 months or D) 1 year at indicated temperatures. * indicates a statistical difference (*p- value*<0.05) in the anti-HBsAg IgG titers between freshly mixed and stored formulation. Arrows indicate vaccine administration.** **52**

Figure 2.9 **Histopathological analysis of nasal tissue exposed to NE adjuvant or HBsAg-NE. Mice: CD-1 mice were vaccinated with HBsAg-NE and primed at 2 weeks. A–B) Photomicrographs of H&E stained nasal epithelium collected from mice 14 days following the boost vaccination. Only normal tissue architecture was recorded which indicates a lack of (sub) chronic cytotoxicity or inflammation. C) Nasal epithelium collected 24 hours following boost vaccination with HBsAg-NE scored as a +1 grade change according to methodology as described is shown as an example of architectural change. The arrow indicates a single microscopic focus of accumulation of mucoid material and debris in the nasal passages. However, no evidence of epithelial necrosis or inflammatory infiltration of the nasal epithelium is detected. D) Nasal epithelium collected 24 hours following boost vaccination with HBsAg-NE scored as a +2 grade. The arrow indicates a single microscopic focus of accumulation of mucoid material and debris in the nasal passages in the absence of inflammatory changes. Architectural change demonstrated in C and D are considered incidental and can be observed in non-vaccinated mice. Rats and guinea pigs: Nasal epithelium was collected 14 days following final boost vaccination from rats E–F) and guinea pigs G–H) treated a total of 3 doses of HBsAg-NE administered 14** **53**

days apart. Normal tissue architecture is observed suggesting lack of toxicity or inflammation. Dogs: Nasal biopsies were collected 24 hours following the final dose in dogs treated with a total of three doses of NE adjuvant. NE was delivered using a Pfeiffer multidose wide angle sprayer pump in 200 µl/dose I) or 400 µl/dose J). No evidence of inflammation or cytotoxicity was detected.

Figure 3.1 *In vitro* NE adjuvant induces antigen internalization into murine dendritic-like cells and enhances lipid staining of Jaws II dendritic-like cells. By fluorescent microscopy, internalization of OVA-Alexa 488 (green fluorescence) into Jaws II dendritic-like cells was demonstrated in A through C, the nuclei is stained blue with DAPI. The A image shows the cells treated with the cell culture media; B shows cells treated with just fluorescent OVA-Alexa 488 10ug/ml; and C shows the cells after 2 h exposed to fluorescent OVA-Alexa 488 10 ug/ml plus 0.001% NE. Using FACs internalization of OVA-Alexa 647 into bone marrow dendritic-like cells was measured in D through F. Bone-marrow derived DC treated with cells culture media in D, just OVA-Alexa 647 in E and OVA-Alexa 647 plus NE 0.01% in F. In G and H are shown images of Nile red staining of Jaws II dendritic-like cells pretreated with NE in G or pretreated with just PBS in H. 79

Figure 3.2 Histopathological analysis of nasal tissue sections. Shown are photomicrographs of hematoxylin-eosin staining of coronal tissue sections of paraffin embedded heads using an Olympus BX 51 microscope. First row A to C shows control mouse nasally inoculated with PBS alone (A using 4x objective; B using 20x objective; and C using a 40x objective). The second row D to F are pictures from a mouse treated with 20% NE alone (D using 4x objective; E using 20x objective; and F using a 40x objective). And in the last row G to I a set of potomicrographs of the mouse nasally vaccinated with 20% NE plus 10 µg of HBsAg (G using 4x objective; H using 20x objective; and I using a 40x objective). 80

Figure 3.3 *In vivo* NE promotes broad sampling activity by nasal epithelial cells. Shown here are the analyses of Z scanning of murine nasal epithelium after 30 m nasal vaccination with QDOTs (red) using laser confocal microscopy: galleries in A, C, and E and the respective 3D reconstruction views in B, D, and F (see supplemental material with the respective 3D animations) using the Imaris software. Figures A and B show the nasal epithelium of a mouse immunized with QDOTs plus PBS; C and D show the nasal epithelium of a mouse vaccinated with QDOTs plus 20% NE; E and F show the nasal epithelium from a mouse immunized with QDOTs and CTB. Just before euthanasia 2 µl of the UE-1-FITC (green) lectin were added to the nares to label the surface of the M cells, and the samples of nasal tissues were mounted with ProLong containing DAPI (blue nuclei). 81

Figure 3.4 ***In vivo*** **NE promotes nasal epithelial cells' sampling activity without disruption of the epithelial barrier. Images of the TEM analysis of murine nasal epithelium 24 h after nasal inoculation are shown from A through F. Shown in A through E is the nasal epithelium of a mouse treated with 20% NE adjuvant; the vesicle-like material was measured (average diameter is 0.479 microns). D and E show the nasal epithelium of a mouse nasally inoculated with QDOTs plus NE adjuvant; in the D overview (magnification 7,900 x) the white square shows the area amplified in the E view at up to 130,000 x magnification. In E the vesicle-like structure containing clumps of QDOTs, the diameter measured 0.455 microns on average and the QDOT-like material spread in the cytoplasm measured on average 0.005 microns. In Figure F shows a picture of the nasal epithelium of a control animal without treatment.** **82**

Figure 3.5 ***In vivo*** **effect of NE adjuvant in E-GFP trafficking towards lymphoid tissues. Mice were nasally inoculated either with E-GFP in PBS (A, B, and C) or with E-GFP with 20% NE (D, E and F). After 24 h, cryo-sections of tissues were prepared and analyzed using an inverted fluorescent microscope (magnification 40 x). Showing in A and D: the nasal epithelium; in B and E: the submandibular lymphoid nodules; and in C and F: the thymus. G and F show the profile of fluorescence through the red line is shown for tissue sections of olfactory bulb obtained after 24 h of nasal vaccination. The tissue sections were stained with anti E-GFP antibody in G or without the primary antibody in H from a mouse nasally vaccinated with 20% NE plus E-GFP.** **83**

Figure 3.6 ***In vivo*** **NE adjuvant promotes co-localization of E-GFP with DC. After 24 h of nasal inoculation, frozen sections of the tissues were prepared. In A through D, frozen tissue sections were stained with anti-DEC205 antibody (red: PE conjugated) and, in E through H, with anti-CD11c (red: PE conjugated) and were analyzed by laser confocal microscopy profiles. Profiles measure the fluorescence intensity through a red line in each image. ProLong (molecular Probes) containing DAPI was used to prepare the samples for microscopy analysis and to stain the nuclei blue. Profiles A, E, C, and G were obtained from mice immunized with NE plus E-GFP and profiles B, F, D, and H are from mice immunized with just E-GFP. Profiles A and B show the nasal epithelium; C, D, E and F are profiles from the thymus; and G and H profiles show spleen sections.** **84**

Figure 3.7 ***In vivo*** **effect of the NE adjuvant in the dissemination of quantum dots after nasal vaccination of mice. Groups of 4 mice were nasally inoculated with QDOTs plus 20% NE, column a; QDOTs in PBS, column b; QDOTs plus 20% NE plus GM1 (0.35 mM), column c; and 20% NE only, column d. Then through time and up to 8 days the whole mouse fluorescence was measured in the IVIS Imaging System 200 Spectrum series bioluminometer from Xenogen at the Center for Molecular Imaging, University of Michigan. The fifth mouse in each group to the right is a naïve mouse. One mouse died in the group treated with the NE from a nasopharyngeal obstruction.** **85**

Figure 3.8 **Effect of NE adjuvant in cytokines and neutrophils infiltration into the nasal lumenal cavity and identification of IL6 producing cells. After nasal inoculation, the cytokine profile was determined in nasal-bronchoalveolar lavage after 24 hours A) by Luminex assay. After 24 h the cellular content of the lavage were pelleted (cytospin) and microscopically analyzed for the presence and number of neutrophils after Giemsa staining B). Shown are the averages ± SEM of 5 different focal views for each group, *: *p-value* <0.01 by student's t-test analyses. Nasal epithelium was harvested from mice 24 hours after treatment with rPA-NE C) or rPA alone D). The tissues were probed with wheat germ agglutinin (WGA) lectin [green] and anti-Il6 antibodies [red].** **86**

Figure 3.9 **Antigen specific antibodies produced in the IL6 deficient mice. Shown are the rPA specific antibodies induced after 14 weeks of vaccine (prime at 0 week and boost at 4 weeks) in the IL6 deficient (IL6 -/-) and the wild type C57BL/6 (WT) mice. It is shown in A the serum end titers reach for IgG and in B the sIgA from bronchoalveolar lavage, respectively. All the animals were immunized by the nasal route except those vaccinated with Alum plus rPA (intramuscular injection). *p<0.05 and **p<0.01 as determined by Mann Whitney analysis in A, and student's t- test in B, respectively.** **87**

Figure 3.10 **Anti-PA IgG subclass analysis in IL6-/- mutant and WT mice. Immunization with rPA-NE produced over 10 fold prevalence of IgG1 over IgG2b subclass IgG in IL6-/- mice, and balanced pattern of IgG1 and IgG2b in WT mice. Low titers of IgG2a subclass were detected in both strains of mice. * indicate significant IgG2b titer difference between IL6-/- and WT mice (*p-value* <0.05).** **88**

Figure 3.11 **Gene expression patterns changes following i.n. treatment with either NE or NEP407 A) Hierarchal clustering of over 1400 gene transcripts up-regulating with NE or NEP407 treatment for 6 or 24 hours and B) Clustering of a group of 38 genes regulating inflammatory expression patterns. Statistical analysis of gene expression was performed using Bioconductor analysis and the DAVID acquisition program. Gene transcription was considered changed when detected as ≥ 2 fold difference as compared to non-treated controls. Red = up-regulation and green = down regulation, yellow = not changed.** **89**

Figure 4.1 **Evaluation of the effects of diluent on OVA-NE thermostability- Particle size characterization of NE OVA-NE. Particle size was not significantly different (*p-value* < 0.05) for either OVA-NE with 150 mMol PBS or 0.9% NaCl at any time during the study.** **115**

Figure 4.2 **Physico-chemical Evaluation of the effects of diluent on OVA-NE The comparison of OVA-NE stored at room temperature conditions to freshly prepared formulation using SDS-PAGE followed by silver staining or Western immunoblotting is shown. Lanes are labeled according to sample storage conditions as follows- Lane 1: MW standard, lane 2: OVA (non-incubated), lanes 3-4: fresh prepared versus stored OVA-NE with 0.9% NaCl, lanes 5-6: fresh prepared versus stored OVA-NE with 150 mMol PBS. Samples were stored for A) 6 weeks, B) 6 months (0.9% NaCl** **116**

mixtures) and 8 months (PBS mixtures), or C) 8 months (0.9% NaCl mixtures) and 10 months (PBS mixtures). Each lane contains 0.5 µg of antigen.

Figure 4.3 *In vivo* potency evaluation of the effects of diluent on OVA-NE. OVA specific antibody responses to freshly prepared OVA-NE or OVA-NE stored at room temperature (25°C) conditions are depicted. CD-1 mice were vaccinated with either freshly prepared or stored OVA-NE and boosted at 6 weeks. Control mice were not vaccinated. Serum anti-OVA IgG antibody concentrations measured at 6 weeks following boost vaccination are presented as a mean of endpoint titers in individual sera ± SD. Comparison of serum IgG elicited by freshly prepared OVA-NE to formulation stored for 8 months (OVA-NE with 150 mMol PBS) or 10 months (OVA-NE with 0.9% NaCl). No statistical differences (*p-value* <0.05) between freshly mixed and stored formulation IgG titers were observed. 117

Figure 4.4 Effects of dispensing OVA-NE through commercially available nasal sprayers on NE stability. A) Particle size characterization of NE and B) OVA-NE. Note that particle size did not change after dispensing NE or OVA-NE through either the BD Accuspray or Pfeiffer sprayer systems. 118

Figure 4.5 Physico-chemical evaluation of the effects of spraying OVA-NE through the Pfeiffer SAP-62602 or the BD Accuspray. A) The comparison of OVA-NE mixtures dispensed through either the BD Accuspray (left panel) or Pfeiffer sprayers (right panel) to freshly prepared (non-dispensed) formulations using SDS-PAGE followed by silver staining is shown. Lanes are labeled according to sample storage conditions as follows—Lane 1: MW standard, lanes 2-5: pre-dispensed OVA-NE (NE concentrations are listed above the respective lanes), lanes 6-9: post-dispensed OVA-NE, lane 10: OVA (non-dispensed). Each lane contains 0.5 mg of antigen. B) Comparison of AlkP enzymatic activity AlkP-OVA in pre-dispensed mixtures versus samples dispensed through the BD Accuspray and Pfeiffer sprayers. Activity in post-dispensed samples was not significantly different (*p-value* < 0.05) in comparison to pre-dispensed mixtures for either sprayer system. 119

Figure 4.6 Evaluation of the effects of spraying OVA-NE through the Pfeiffer SAP-62602 or the BD Accuspray on *in vivo potency.* Antibody responses to OVA-NE actuated through either the BD Accuspray or Pfeiffer sprayer systems compared to non-sprayed mixtures are depicted. Mice were vaccinated with 20% NE + 20 µg OVA A) or 20% NE + 5 µg OVA B) and boosted at 6 weeks. Serum anti-OVA IgG antibody concentrations measured at 0, 4 and 8 weeks following prime vaccination are presented as a mean of endpoint titers in individual sera ± SD. No statistical difference (*p-value* <0.05) between sprayed and non-sprayed IgG titers was observed for either sprayer system. 120

Figure 4.7 Evaluation of consistency in dispensed NE volume using commercially available nasal sprayer systems. A) Spectrophotometric analysis and B) spray weight characterization of the volume of NE dispensed in a single spray 121

using either the BD Accuspray or Pfeiffer sprayer systems. Variation in spray volume is presented as a mean of optical density or spray weight ± SD. The difference in measured optical density and spray weight between the Pfeiffer and BD sprayers is explained by the inherent dead space within the BD sprayer nozzle and does not reflect a difference in the ability to deliver NE.

Figure 4.8 Rheological evaluation and surface tension characterization of NE and HbsAg-NE. A) Shear viscosity of solutions of NE at various concentrations and HBsAg-NE are depicted. Rheological measurements were performed using an AR-G2 (TA Instruments, Newcastle, DE) control stress rheometer by linearly increasing the shear stress from 10^{-1} (s^{-1}) to 10^{3} (s^{-1}). B) A hysteresis curve was generated by gradually increasing the shear rate from 10^{-1} (s^{-1}) to 10^{2} (s^{-1}) where shear rate remained constant at 10^{2} (s^{-1}) for 30 minutes. The shear rate was then gradually returned to the starting point under the same conditions. Viscosity (η) is reported in Pa-s units. C) Changes in surface tension at varying NE concentrations calculated using capillary rise tensiometry. Note that as the concentration of NE from 2.5 to 20% (and therefore surfactant concentration) increases, a statistically significant (*p*-value < 0.5) decrease in surface tension was observed. However, no significant change in surface tension was observed in the HBsAg-NE and 40% NE mixtures as compared to the 2.5% NE. 122

Figure 4.9 Plume Geometry and Spray-pattern characteristics for nasal sprayer systems. Influence in pump design on the emission of HBsAg-NE. Plume geometry is represented for A) Pfeiffer and C) BD Accuspray devices. Spray pattern is visualized at a distance of 3-cm from the pump orifice for B) Pfeiffer and D) BD Accuspray units. 123

Figure 5.1 OMP Analysis A) The 4-12% SDS-PAGE was loaded on a volumetrically normalized basis to track the progression of the protein from its most crude form to its cleanest form. In lane A, protein from the supernatant produced after the 6000xG centrifugation was loaded. An equal volume of the supernatant from the 100,000xG centrifugation was loaded into lane B. Lane C was loaded with the Crude OMP (the re-suspended pellet fraction of the 100,000xG spin). Lanes D-J were loaded with the endotoxin-depleted OMP fractions (the successive flow-through portions of the endotoxin column). Lanes K-N were loaded with the endotoxin column retentant fractions (the successive fluid regenerated from the column after the addition of sodium deoxycholate). B) Western blot probed with serum from mice immunized with the endotoxin-depleted OMP prep at 1:1000 in 5% Milk/PBST and secondarily probed with an AP-conjugated anti-mouse antibody. C) Western blot probed with serum from mice immunized with the OMP in PBS prep at 1:1000 in 5% Milk/PBST and secondarily probed with an AP-conjugated anti-mouse antibody. D) Agarose gel electrophoresis of the OMP preparation. Lane 1 is loaded with a DNA ladder. Lane 2 is loaded with the cell lysate (WCL) before separation by high speed centrifugation, Lane 3 is loaded with the resulting supernatant following the 150

100,000xG spin (lane B in the Silver and western blot above), Lane 4 is loaded with the crude OMP preparation (lane C in the Silver and western blot above), and lane 5 is loaded with the endotoxin (ET) depleted OMP fraction (lane E in the Silver and western blot above).

Figure 5.2 Humoral immune response to *B. cenocepacia* OMP-NE. IgG response in serum post-immunization with the OMP preparation with or without nanoemulsion. Response was measured via ELISA using plates coated with the OMP preparation. Significant statistical difference with *p value* <0.05 were observed for the 6 and 9 week (2 and 5 weeks following boost) samples between nanoemulsion-adjuvanted OMP formulations and OMP-PBS formulations for either concentration. Serum anti-OMP IgG antibody concentrations are presented as mean of endpoint titers in individual sera ±SEM. * indicates a statistical difference (*p-value* <0.05) in the anti-OMP IgG titers. 151

Figure 5.3 Mucosal and splenic cytokine response analysis of *B. cenocepacia* OMP-NE. A) Mucosal response to the OMP vaccination with or without nanoemulsion. IgA and IgG measured in BAL solution via ELISA using plates coated with the OMP preparation. The OD levels were normalized to total protein content within the samples. B) Cytokine profiling of splenocytes of mice immunized with 5 µg OMP + 20% NE. Cytokines were measured in media taken from splenocytes activated with endotoxin-depleted OMP preparation. 1.5ug OMP prep was used to activate $4x10^4$ splenocytes in RPMI medium. Media was removed from the splenocytes on day 3 post-activation and analyzed using the Mouse Cytokine/Chemokine Kit from Linco. Data is represented as fold change in vaccinated mice vs. naïve mice. 152

Figure 5.4 IgG Subtype Analysis. Serum from naïve mice and mice immunized with 5 µg OMP +/- 20% NE was analyzed for antibody subtype distribution. The results are presented as ratio of the specific subclass IgG to the overall IgG titer. * indicates statistical difference (*p-value* <0.05) between IgG2b and IgG1 subtypes. 153

.

Figure 5.5 Evaluation of the immunogenic effects of LPS and of the 17 KDa OmpA. A) In order to determine the antigen specificity of the response to the OMP preparation-based vaccine, 96 well plates were coated with either crude OMP preparation, endotoxin-depleted OMP preparation, or LPS for standard ELISA serum IgG analysis using serum from mice vaccinated with 15 µg OMP-20% NE. Results are presented as mean values of OD at 405 nm ±SEM. The levels of responses were compared to LPS only. B) Silver-stained SDS gel and western blots of the crude OMP preparation (lane 2), the enzymatically digested crude OMP preparation (lane 3), the endotoxin-depleted OMP preparation (lane 4), and the enzymatically digested endotoxin-depleted OMP preparation (lane 5). A protein ladder was loaded into lane 1. Western blots were probed with serum from either OMP in PBS or OMP-NE immunized mice as indicated. 154

Figure 5.6 **Serum Neutralization Assay. A) Serum diluted 1:5 from immunized or naïve mice was mixed in equal volumes with *B. cenocepacia* (10^7 CFU) and broth and incubated 48 hours at 37°C. Following incubation, the solution was plated out on BCSA plates and incubated for 72 hours at 37°C for colony enumeration. The percent reduction in CFU was plotted against samples with naïve serum. A statistical difference (*p-value* <0.05) in neutralizing activity was observed between serum from mice immunized with OMP-NE and serum from mice immunized with OMP in PBS formulations. B) Cross neutralizing activity of the antibodies produced from mice vaccinated mice, serum from mice immunized with 15 µg OMP + 20% NE was diluted 1:3 and mixed with equal volumes of *B. multivorans* (10^7 CFU) and broth and incubated 48 hours at 37°C. As above, the solution was plated out on BCSA plates and incubated for 72 hours at 37°C for colony enumeration following incubation. The percent reduction in CFU was plotted against samples with naïve serum. A statistical difference (*p-value* <0.05) in neutralizing activity was observed between serum from mice immunized with OMP-NE and serum from naïve mice.** **155**

Figure 5.7 **Pulmonary and splenic colonization assay. A) and B) Vaccinated or naïve mice (n=5/group) were placed under general anesthesia and were challenged with $5X10^7$ *B. cenocepacia* in PBS. The mice were euthanized at 6 days post-challenge. Lungs and spleens were homogenized under sterile conditions in PBS and the homogenate was diluted. The dilution samples were plated to BCSA plates and incubated 72 hours at 37°C prior to CFU enumeration.** **156**

Figure 5.8 **Morbidity monitoring. A) Change in body weight and B) change in subcutaneous temperature in CD-1 mice following pulmonary challenge with $5x10^7$ *B. cenocepacia* organisms. * indicates a statistic difference in subcutaneous temperature of vaccinated versus non-vaccinated mice (*p-value* < 0.05).** **157**

List of Tables

Table 2.1	**Consistency of nanoemulsion particle size.**	**43**
Table 2.2	**Pre-clinical toxicology evaluation.**	**44**
Table 4.1	**Droplet size analysis of dispensing HBsAg-NE through commercial BD Accuspray or Pfeiffer sprayer systems. Each data column represents the average ± SD of six actuations. %CV is the coefficient of variance.**	**124**
Table 4.2	**Spray pattern and plume geometry characterization of dispensing HBsAG-NE through commercial BD Accuspray or Pfeiffer sprayer systems. Each data column represents the average ±SD of six actuations. %CV is the coefficient of variance.**	**125**
Table 5.1	**Sequence alignment of OmpA-like domains. The sequence underlined was obtained from the analysis of the high immune reactive protein in the outer membrane preparation of *B. cenocepacia*. Shown are the sequence alignments resulting from the BLAST analysis. The eleven residues in red are strictly conserved among all the Omp-A family members characterized as described by Grisot and Buchanan (2004).**	**158**
Table 5.2	**Total leukocyte and polymorphonuclear leukocyte serum enumeration following challenge. Vaccinated or naïve mice (n=5/group) were placed under general anesthesia and were trans-tracheally challenged with $5X10^7$ *B. cenocepacia* in PBS. The mice were euthanized at 4 or 6 days post-challenge and blood from a cardiac puncture was collected in tubes with EDTA. The blood was analyzed for total and mononuclear lymphocytes using the HEMAVETH 950 analyzer. * indicates statistical difference (*p value* <0.05) between immunized and non-immunized animals.**	**159**

List of Abbreviations

Alexa	Alexafluor dye
APCs	Professional antigen presenting cells
BAL	Bronchioalveolar lavage
BSA	Bovine serum albumin
Bcc	*Burkholderia cepacia* complex
CMI	Cell mediated immunity
CFU	Colony forming unit
CF	Cystic Fibrosis
CNS	Central nervous system
CTB	Cholera toxin subunit B
CTL	Cytotoxic T lymphocyte
DC	Dendritic cell
E-GFP	Enhaced green fluorescent protein
FACS	Fluorescence-activated cell sorting
FDA	Food and Drug Administration
GRAS	Generally recognized as safe
HBsAg	Hepatitis B surface antigen
ISCOMSs	Immune stimulating complexes
LD90	Lethal dose to 90% of recipients

MNIMBs	Michigan Nanotechnology Institute for Medicine and Biological Science
NE	Nanoemulsion
NaCl	Sodium chloride
NALT	Nasal associated lymphoid tissue
NF-κB	Nuclear Factor Kappa Beta
NLR	Nod-like receptor
OMP	Outer membrane protein
OVA	Ovalbumin
PBS	Phosphate buffered saline
rPA	Recombinent protective antigen from *Bacillus anthracis*
Th1	T helper cell type 1 response
Th2	T helper cell type 2 response
TLR	Toll-like receptor
VLP	Virus-like particles
WHO	World Health Organization

CHAPTER 1
INTRODUCTION

1.1 BACKGROUND

The historical approach to vaccine development seems paradoxical, given that the majority of effort has been directed toward producing vaccines that drive systemic and not mucosal responses yet the vast majority of infections occur at the enteric, respiratory, and reproductive mucosal surfaces [1-4]. Despite this irony, traditional vaccines are arguably some of the most significant public health achievements of the 20th century and have been credited with saving more lives and preventing more illnesses than any medical treatment [5]. However, vaccine-preventable diseases continue to cause significant morbidity and mortality, especially in developing countries [6]. There is currently a great interest in developing a new generation of mucosal vaccines but progress has been hampered by a lack of safe and effective adjuvants [4]. Nanoemulsions (NEs), originally developed as microbiocidal materials by the Michigan Nanotechnology Institute for Medicine and Biological Sciences (MNIMBs), were unexpectedly discovered to stimulate both mucosal and systemic immunity. This serendipitous finding has led to research into the optimization of NEs as mucosal vaccine adjuvants. It is from this perspective that this thesis is organized to address the characterization and mechanism of NE-associated immune induction, formulation optimization, their deliverability, and the development of NE-based vaccines.

1.2 CURRENT AND HISTORICAL APPROACHES TO VACCINE ADJUVANTS

Adjuvants are immunological agents that are added with antigens in vaccine preparations to induce co-stimulatory activity and enhance immune responses to the antigen [7]. Modern adjuvants were first identified in the 1920s, when it was empirically discovered that microbial components were highly co-stimulatory. Since this time, more than 100 adjuvant preparations have been described and formulated using chemicals, oils and lipids, mammalian proteins, plant material, and microbial components [8-10]. The exact mechanism of adjuvant action for most of these agents is complex and often multi-factorial and has remained obscure. However, the general immunological mechanistic effects required for the adjuvant effect include 1) increasing the biological or immunological half-life of vaccine antigens by providing a "depot" effect to prolong the persistence of the antigen through prevention of proteolytic destruction; 2) improving antigen delivery and presentation through innate and dendritic cell activation via receptor-mediated endocytosis or pinocytosis; and 3) inducing the production of immunomodulatory cytokines [10-14]. Each of these activities appears to be important in the induction of the type of immunity that is effective in protection against a pathogen.

Several classes of modern vaccine adjuvants have been tested in humans and animals and include mineral salts (e.g., aluminum- and calcium-based), surface active microparticles (e.g., non-ionic block polymer surfactants), bacterial products (e.g., monophosphoryl lipid A), cytokines (e.g., IL12), polyanions (e.g., dextran), carriers (e.g, tetanus toxoid), living vectors (e.g., canarypox virus), and vehicles (e.g., liposomes), among others. Out of all of these, the only adjuvants approved in the United States and elsewhere for human use are aluminum salts, virosomes, and MF59 emulsions [15]. Unfortunately, these compounds have failed to significantly enhance many subunit vaccine antigens in people, or to stimulate cytotoxic T-cell responses. [10, 12]. This failure has, in part, inspired the search for a new generation of vaccine adjuvants.

Most traditional adjuvants, which have been referred to as “the immunologist's dirty little secret” [16], are inadequate to meet the needs of a new generation of vaccines. To begin, the majority of approved and experimental adjuvants are, in reality, broadly pro-inflammatory compounds. While inflammation is useful in augmenting T helper cell type 2 (Th2) humoral immune responses to antigens and toxins, this approach has significant limitations and safety considerations [17]. Aluminum and potassium salts, which are pro-inflammatory adjuvants, have been shown to be poorly capable of stimulating an effective cytotoxic lymphocyte (CTL) and cell-mediated (CMI) immunity critical for inactivation of intracellular pathogens, viruses, parasites, or mycobacteria [18, 19]. What is more, surface active particulate adjuvants such as liposomes, immune stimulating complexes (ISCOMs), emulsions, and microparticles, have been demonstrated to stimulate both humoral and CMI immunity, but they often require the addition of pro-inflammatory immunostimulants and have considerable stability issues [20, 21]. Most importantly, safety considerations have greatly limited the ability of many experimental adjutants from being tested in people [22]. This suggests the need for an entirely new approach to the development of novel vaccine adjuvants.

1.3 MUCOSAL VACCINATION

The ideal vaccine could be delivered at a single site providing both humoral and cell-mediated protection, not only at the location of administration, but also throughout the body [23]. The mucosal route of vaccination has been explored because of the potential to affect this type of ideal response. This route of vaccination is attractive and offers several advantages over the traditional parenteral means. To begin with, infectious agents transmitted through mucosal surfaces may be better prevented through mucosal immunity primarily by secreted immunoglobulins (IgA and IgG) which both inhibit the initial stages of disease (e.g. colonization) and block its development and generalization of the infection [23]. A classic example of this is the inhibition of *Vibrio cholerae* colonization due to mucosal antibodies directed against the bacteria itself and the

toxin it produces (cholera toxin) [24, 25]. Secondly, a mucosal response appears to be non-compartmentalized, and a vaccine placed on one mucosal surface, such as the upper respiratory tract, can yield protective mucosal immunity on other mucosal surfaces, such as the vagina [26]. This suggests that mucosal vaccines can be directed towards an accessible mucosal site, such as the nasal cavity, and still yield protective activation of effector B and T cells—CTLs and natural killer (NK) cells—and production of secretory IgA and IgG directed against gut or genital urinary infectious agents [23]. Importantly, mucosal vaccines are typically easy to administer and often do not require needle delivery by highly trained medical workers, thereby improving compliance, potentially reducing the cost, and enhancing the safety of vaccination. This is particularly important in developing countries where single-use needles are not always utilized because of financial limitations. Finally, mucosal vaccines may provide longer-lasting immunity to pathogens, such as was observed with the oral vs. the injectable polio vaccine [27].

Despite these advantages, very few mucosal vaccines have been approved in the United States or elsewhere. This handful of licensed vaccines includes those developed to prevent polio, *Salmonella typhi*, *V. cholerae*, rotavirus, and influenza [25, 28-30]. The lack of progress in new mucosal vaccines has been due, in part, to the lag in knowledge of our understanding of mucosal immunity and the complexity of characterizing and quantifying a mucosal immune response compared to the much less complicated task of measuring a humoral response elicited by parenteral vaccines [23]. In Chapters 2-5, with special emphasis on Chapter 3 of this thesis, we discuss novel and innovative ways in which a mucosal response was evaluated.

Recent advances in the science of vaccinology have created an array of promising mucosal vaccines that can be delivered to the respiratory, gastrointestinal, and genitourinary tracts using intranasal, oral, and vaginal routes [31]. Unfortunately, there are a number of technical limitations associated with

these mucosal vaccines. The first is that many of them involve live organisms. These vaccines require special handling or freezing of the material until use. This creates logistical problems, even in the industrialized world, where one of the major limitations to the use of FluMist® vaccine for influenza was the need to keep this material frozen until use. Also, the use of live pathogens in the current population can be risky given the increased number of people who are affected with immunosuppressive conditions. Equally important is the lack of understanding in the specific mechanisms mucosal adjuvant activity. Many immunologists believe that mucosal vaccines work by loading antigen into dendritic cells or the "M" cells on the surface of the mucosa. However, the methods to target these cells are still in the experimental phase. Regardless, most current mucosal adjuvants stimulate inflammation through some type of toxin or a microbiologic component that binds to Toll-like receptors (TLR) [32].

The list of experimental mucosal adjuvants is expanding and includes cholera toxin, *Pseudomonas* or *E. coli* enterotoxins, lipopolysaccharide, muramyl dipeptide, CpG oligonucleotides, copolymers of lactic acid and glycolic acids, proteosomes, cochleates, and virus-like particles (VLP), among others [33-39]. These compounds activate dendritic cells and produce inflammatory cytokines that augment the immune response and overcome natural tolerance. Also, Proteosome™ adjuvant formulations that use outer membrane proteins of *Neisseria meningitidis* to produce non-specific inflammation can induce serum IgG, mucosal IgA, and protection against an influenza challenge [40]. Most of these toxins result in a robust, cellular or Th1 type of response; however, despite the efficacy of many prototype mucosal vaccines, there are concerns about safety that may limit their use. For example, an inactivated influenza nasal vaccine formulated with an enterotoxin has been associated with the development of autoimmunity and Bells Palsy and had to be withdrawn from use [41]. Cholera toxin has even been found in the central nervous system (CNS) after nasal immunization, making it unlikely to be approved in a vaccine for humans [42]. Hypersensitivity reactions to bacterial antigens may be a limiting

factor in the use of these types of vaccines. As a result, it is unclear that mucosal vaccines based on these inflammatory toxins will ever be approved for use in general populations. Recent studies have shown that inclusion of cytokines in mucosal vaccines, particularly IL12, can enhance immune responses [43]. However, the tolerability of cytokine adjuvants in people remains to be seen. Thus, effective mucosal vaccines depend on the development of safe and effective adjuvants.

1.4 NANOMEULSIONS

Nanoemulsions (NEs) were developed as a microbiocidal substance at the University of Michigan and licensed to NanoBio Corp. (Ann Arbor, MI) in 2000. They are novel oil-in-water nanoscale (<400 nm) emulsion formulations that contain low concentrations of surfactants such as N cetyl pyridinium chloride (CPC), co-surfactants such as Tween 80, ethanol, water, and ultra-purified soybean oil (64%). These components are listed by the FDA as food additives that are generally recognized as safe (GRAS). NEs are manufactured by mixing the water-immiscible lipid phase into an aqueous phase through high stress mechanical extrusion. This process yields a monodisperse population of lipid droplets ranging in diameter from 200 to 400 nm. NEs are remarkably stable and maintain integrity for at least 12 months, even under accelerated stability conditions [44, 45].

The mechanism of microbiocidal activity has been reported to be related to the fusion of the nanoemulsion surfactant with the cell wall or viral envelope, causing disruption and death of the organism (Figure 1.1) [45, 46]. The emulsion droplets are therefore small enough to act as micelles in disrupting bacterial cell walls (Figure 1.2). NEs have demonstrated microbiocidal activity against enveloped viruses, bacteria, fungi, and spores [44-48].

The structure of the NE appears to play a vital role in its function [49-51], allowing application to mucosal, skin and gastrointestinal surfaces at

therapeutically useful concentrations without irritation or disruption of tissue. NEs easily penetrate intact epidermis and dermis and are not inflammatory to the tissue [52]. In general, NEs have exceptional safety profiles and are non-toxic and well tolerated when applied to mucosal tissue in numerous animal models [53].

1.5 NANOEMULION AS A MUCOSAL VACCINE ADJUVANT

Most fortuitously, the discovery that the NE may have mucosal adjuvant activity was made while the microbiocidal activity of the material was being studied. This finding occurred during studies designed to demonstrate that placing the NE into the nasal cavity of mice could protect them from a subsequent respiratory challenge with an LD90 of influenza virus. The mice were successfully protected from the challenge even two hours after the material was placed into the nares. Interestingly, these same mice were protected from influenza pneumonitis when challenged again three weeks later, even without reapplication of the nanoemulsion. Moreover, they were shown to have high titers of anti-influenza antibodies. Subsequent studies documented that placing NE-killed influenza virus in the sinus with the NE produced strong protective immunity [54, 55]. Most recently, our group has documented the efficacy of NE mixed with live influenza virus or with β-propiolactone-inactivated Wisconsin influenza virus [54, 55], recombinant anthrax PA [56], vaccinia virus [57], recombinant HIV gp 120 [58], and recombinant hepatitis B surface antigen [52]. These findings in conjunction with the safety profile support the further development of the NE as a nasopharyngeal adjuvant for humans.

1.6 NANOEMULISON-BASED THERMAL STABLE, AND NEEDLE-FREE VACCINES FOR DEVELOPING POPULATIONS

The World Health Organization (WHO) estimates that as many as 2.4 million children die every year from vaccine-preventable diseases despite the availability of effective vaccines [59]. Most of these deaths occur in developing populations where a disparity in vaccination rates results from the need for costly sterile

needles, the requirements for cold-chain vaccine handling, political strife, weak health service delivery systems, underfunding, and poor management [60]. This astounding rate of mortality constitutes a global health emergency and suggests that a new approach to a vaccination strategy in developing populations is urgently needed. Thankfully, there has recently been increasing awareness and interest in addressing this disparity in the public and private sectors. Recognizing the NE's potential to overcome some of the logistical obstacles to mass-vaccination of undeveloped populations, the Bill and Melinda Gates Foundation through their Grand Challenges in Global Health initiative charged the Michigan Nanotechnology Institute for Medicine and Biological Sciences (MNIMBs) in 2005 with developing a heat-stable and needle-free vaccine for prevention of hepatitis B. Chapter 2 presents the pre-clinical evaluation of the NE-based recombinant hepatitis B vaccine (HBsAg-NE) developed as a result of this challenge. We report that needle-free nasal immunization with HBsAg-NE could be a safe and effective hepatitis B vaccine or could provide an alternative booster administration for the parenteral hepatitis B vaccines. We found that the vaccine induces a Th1-associated cellular immunity and may also provide therapeutic benefit to patients with chronic hepatitis B infection who lack the cellular immune responses to adequately control viral replication. The long-term stability of this vaccine formulation at elevated temperatures suggests a direct advantage in the field, since potential excursions from cold-chain maintenance could be tolerated without a loss in therapeutic efficacy.

1.7 CURRENT INSIGHTS INTO THE MECHANISM OF NE ADJUVANT

We have demonstrated that the NE is capable of robust adjuvant activity with a number of antigen systems [52, 55, 61-63]. The mechanism of immune induction associated with the NE adjuvant, however, has yet to be defined. In preliminary *in vivo* studies, we have been unable to detect a substantial inflammatory response induced by the NE in histological analysis of different tissues [53] . We have previously described a Th1 polarized response in mice following intranasal immunization with NE-based vaccines [52, 61, 62]. Chapter 3 examines the

apparently unique adjuvant mechanism associated with the NE on a gross physiological, cellular, and molecular level. In this chapter, we report that the NE adjuvant enhances antigen internalization in the nasal epithelium and induces DC trafficking towards lymphoid tissues without inducing inflammation or massive cellular infiltration. We hypothesize that nasally administered NE adjuvant mimics microbial strategies to invade eukaryotic cells and promote antigen presentation phenomena by innate immune cells, which ultimately leads to a specific immune response. We also discuss the involvement of IL6 cytokine in the signaling pathway.

1.8 EFFECTS OF FORMULATION OF NE-BASED VACCINES ON THERMAL STABILITY AND DELIVERY THROUGH NASAL SPRAYER DEVICES

The ultimate utility of NE-based vaccines will not only depend on their immunogenicity but also on the ability of the NE to stabilize antigen and to be delivered needle-free efficiently. Chapter 4 addresses the effects of the diluent on thermal stability and potency. This chapter also evaluates the suitability of using commercially available nasal sprayer devices for dispensing NE-based vaccines. In this chapter, we report the stability and potency of PBS-diluted antigen-NE mixtures for up to 8 months when stored at room temperature and of NaCl-diluted mixtures for up to 6 months. Further, we demonstrate that the NE-based vaccines are not physically or chemically altered and retain their potency following actuation through two commercially available nasal sprayer devices. Parameters affecting nasal deposition were evaluated, including volume consistency, viscosity, surface tension, droplet size distribution, spray pattern, and plume geometry. Based on this work, we report that the NE-based vaccines are expected to be efficiently deposited in inductive tissues mainly in the anterior region of the human sinus and therefore do not require specially engineered delivery devices.

1.9 DEVELOPMENT OF A NE-BASED *BURKHOLDERIA CENOCEPACIA* VACCINE

Our group has formerly demonstrated successful experimental NE-based vaccines using whole viral and recombinant antigens. In Chapters 2 and 3, we have reasonably defined the profile of NE-associated immunity and described the overall mechanism of immune induction. With this knowledge, we were interested in evaluating the potential to develop a NE-based vaccine using a pathogen derived category of antigen. In Chapter 5, we examine the development of a *Burkholderia cenocepacia* outer membrane protein (OMP)-based NE vaccine. *B. cenocepacia* is one of at least 17 bacterial strains comprising the *Burkholderia cepacia* complex (Bcc) and is a leading cause of death in cystic fibrosis (CF) patients. Bcc organisms are opportunistic bacteria associated with incessant infection and progressive lung disease that culminates in pulmonary failure and death for CF patients [64]. Most Bcc species form biofilm and are highly resistant to antibiotics, and therefore therapeutic intervention aimed at clearing the infection is often unsuccessful [65]. At present there is no available vaccine or effective treatment for this disease. A successful mucosal vaccine may offer a critical life-line to CF patients. Chapter 5 discusses the development of a NE-based *B. cenocepacia* OMP (OMP-NE) experimental vaccine. In this chapter, we report robust mucosal and systemic immune responses after vaccination with OMP-NE. Using a mouse model of chronic pulmonary infection, we observed enhanced clearance of *B. cenocepacia* from the lungs of vaccinated animals, which correlated with the production of serum antibody capable of neutralizing *B. cenocepacia*. Mice vaccinated with OMP-NE showed fewer signs of systemic illness and became less septic following experimental infection with *B. cenocepacia*. Additionally, we demonstrated that administration of a *B. cenocepacia* OMP vaccine resulted in the production of cross-neutralizing antibodies capable of inactivating *B. multivorans.* Our results indicate that the NE can effectively adjuvant OMP for intranasal immunization and mucosal immunity to *B. cenocepacia* elicited by intranasal vaccination with OMPs, and the NE (OMP-NE) could prevent the early steps of colonization and infection with *Bcc organisms.*

1.10 OUTLINE AND THESIS ORGANIZATION

This thesis examines the potential for a nanoemulsion to serve as a nasopharyngeal adjuvant. Chapter 2 addresses the pre-clinical evaluation of a novel nanoemulsion-based hepatitis B mucosal vaccine in regard to the physico-chemical characterization of the vaccine and to the characterization of immunity, thermostabilty, and safety in multiple animal models. Chapter 3 focuses on the mechanism of the NE-adjuvant action, the induction of antigen sampling, and the evaluation of the role of IL6 in the adjuvant activity. Chapter 4 discusses formulation development of NE-based vaccines and their delivery through nasal sprayer delivery systems. Chapter 5 demonstrates the development of a NE-based *Burkholderia cenocepacia* vaccine. Chapter 6 serves as a summary of this thesis and provides direction for relevant future studies.

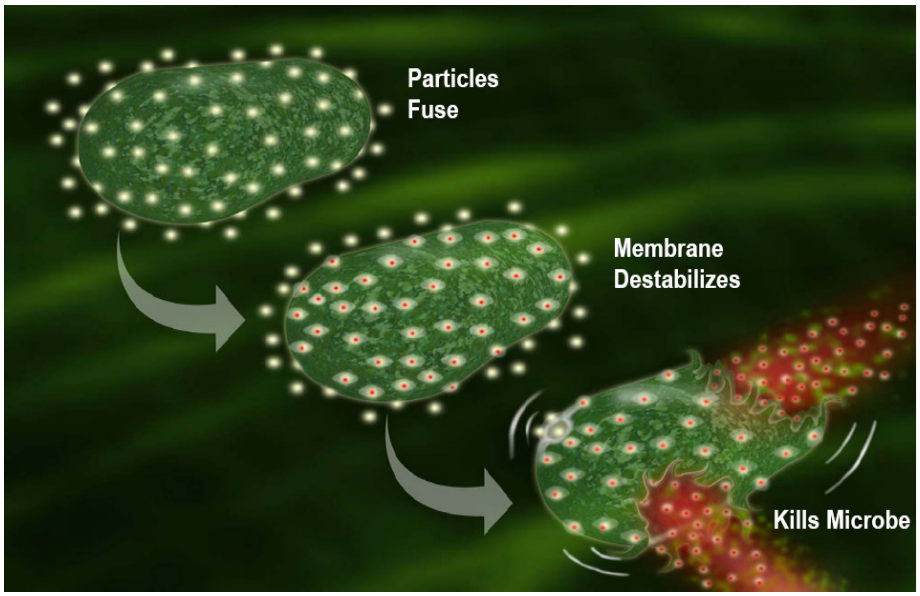

Figure 1.1. Artist rendition of the microbiocidal activity of nanoemulsion.

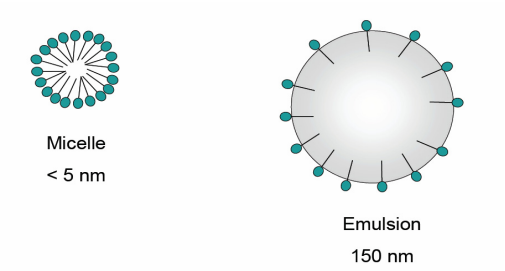

Figure 1.2. Cartoon showing the comparison of the emulsion to a micelle

1.11 REFERENCES

1. Medina, E. and C.A. Guzman, *Modulation of immune responses following antigen administration by mucosal route.* FEMS Immunol Med Microbiol., 2000. 27(4): p. 305-311.

2. Ogra, P.L., Mucosal Immunoprophylaxis, in Mucosal Vaccines, H. Kiyono, P.L. Ogra, and J.R. McGhee, Editors. 1196, Academic Press: San Diego, CA. p. 5-7.

3. Boyaka, P.N., et al., *Mucosal vaccines: an overview.*, in Mucosal Immunology, a.J.B. J. Mestecky, and M. E. Lamm, and L. Mayer, and J. R. McGhee, and W. Strober, Editor. 2005, Elsevier/Academic Press: Amsterdam. p. 855-873.

4. Holmgren, J. and C. Czerkinsky, *Mucosal immunity and vaccines. .* Nat. Med. , 2005. 11: p. S45-S53.

5. FDA, *Statement by William Egan PH.D. acting office director, Office of Vaccine Research and Review, Center for Biologics Evaluation and Review, Committee on Government Reform, U.S. House of Representatives*, U.F.a.D. Adminstration, Editor. 2000, US Food and Drug Adminstration: Washington, D. C.

6. Heininger, U., *The success of immunization-shovelling its own grave? .* Vaccine, 2004. 22(15-16): p. 2071-2072.

7. Janeway, C.A.J., et al., *Innate Immunity*, in *Immunobiology the immune system in health and disease* C.A.J. Janeway, et al., Editors. 2005, Taylor & Francis/Garland Science: New York. p. 54.

8. Hunter, R.L., *Overview of vaccine adjuvants: present and future.* Vaccine, 2002. 20(Suppl 3): p. S7-S12.

9. Vogel, F.R. and M.F. Powell, *A compendium of vaccine adjuvants and excipients.* Pharm Biotechnol, 1995. 6: p. 141-228.

10. Edelman, R., *The development and use of vaccine adjuvants.* Mol Biotechnol., 2002. 21(2): p. 129-148.

11. Davies, G., *Vaccine adjuvant formulation: a relatively neglected field that is crucial to vaccine success.* Expert Reviews of Vaccines, 2008. 7(3): p. 287-291.

12. Cox, J.C. and A.R. Coulter, *Adjuvants--a classification and review of their modes of action.* Vaccine, 1997. 15(3): p. 248-56.

13. Stills, H.F., Jr., *Adjuvants and antibody production: dispelling the myths associated with Freund's complete and other adjuvants.* Ilar Journal, 2005. 46(3): p. 280-93.

14. Lanzavecchia, A., *Receptor-mediated antigen uptake and its effect on antigen presentation to class II-restricted T lymphocytes.* Annu Rev Immunol, 1990. 8: p. 773-93.

15. Valiante, N.M., D.T. O'Hagan, and J.B. Ulmer, *Innate immunity and biodefence vaccines.* Cellular Microbiology, 2003. 5(11): p. 755-760.

16. Morley, S.C. and P.M. Allen, *Taking a Toll Road to Better Vaccines.* Immunity, 2008. 28(5): p. 602-604.

17. Allison, A.C., *Squalene and squalane emulsions as adjuvants.* Methods (Duluth), 1999. 19(1): p. 87-93.

18. Gupta, R.K., et al., *Vaccine Design: The Subunit and Vaccine Approach*, ed. M.F. Powell and M.J. Newman. 1995, New York: Plenum. 229-248.

19. Wijburg, O.L., et al., *The role of macrophages in the induction and regulation of immunity elicited by exogenous antigens.* Eur J Immunol, 1998. 28(2): p. 479-87.

20. Vajdy, M., et al., *Mucosal adjuvants and delivery systems for protein-, DNA- and RNA-based vaccines.* Immunology & Cell Biology, 2004. 82(6): p. 617-27.

21. Martinon, F., et al., *Induction of virus-specific cytotoxic T lymphocytes in vivo by liposome-entrapped mRNA.* European Journal of Immunology, 1993. 23(7): p. 1719-22.

22. Podda, A. and D.G. Giuseppe, *MF59 Adjuvant Emulsion*, in *New Generation Vaccines*, M.M. Levine, et al., Editors. 2004, Informa Health Care: New York.

23. Neutra, M.R. and P.A. Kozlowski, *Mucosal vaccines: the promise and the challenge.* Nature Reviews Immunology, 2006. 6: p. 148-158.

24. Blanco, L.P. and V.J. DiRita, *Antibodies enhance interaction of Vibrio cholera with intestinal M-like cells.* Infect Immun, 2006. 74(12): p. 6957-6964.

25. Levine, M.M., *Immunization against bacterial diseases of the intestine.* J. Pediatr. Gastroenterol. Nutr. , 2000. 31: p. 336-355.

26. Kozlowski, P.A., et al., *Comparison of the oral, rectal, and vaginal immunization routes for induction of antibodies in rectal and genital tract secretions of women.* Infect Immun, 1997. 65: p. 1387-1394

27. Salk, D., A.L. van Wezel, and J. Salk, *Induction of long-term immunity to paralytic poliomyelitis by use of non-infectious vaccine.* Lancet, 1984. **8**(2): p. 1317-1321.

28. Modlin, J.F., *Poliomyelitis in the United States: the final chapter?* JAMA 2004. 292: p. 1749-1751.

29. Kapikian, A.Z., et al., *Efficacy of a quadrivalent rhesus rotavirus-based human rotavirus vaccine aimed at preventing severe rotavirus diarrhea in infants and young children.* J. Infect. Dis. , 1996. 174: p. S65-S72.

30. Belshe, R.B., et al., *The efficacy of live attenuated, cold-adapted, trivalent, intranasal influenza virus vaccine in children.* N. Engl. J. Med., 1998. 338: p. 1405-1412.

31. Levine, M.M. and G. Dougan, *Optimism over vaccines administered via mucosal surfaces. .* Lancet, 1998. 351(9113): p. 1375-1376.

32. Ebensen, T., et al., *The Bacterial Second Messenger cdiGMP Exhibits Promising Activity as a Mucosal Adjuvant.* Clin Vaccine Immunol., 2007. 14(8): p. 952-958.

33. Lowell, G.H., *Proteosomes for Improved Nasal, Oral, or Injectable Vaccines*, in *New Generation Vaccines*, M.M. Levine, et al., Editors. 1997, Marcel Dekker: New York. p. 193-206.

34. Tacket, C.O., et al., *Enteral immunization and challenge of volunteers given enterotoxigenic E. coli CFA/II encapsulated in biodegradable microspheres.* Vaccine, 1994. 12(14): p. 1270-1274.

35. Lambert, J.S., et al., *A Phase I safety and immunogenicity trial of UBI(R) microparticulate monovalent HIV-1 MN oral peptide immunogen with parenteral boost in HIV- 1 seronegative human ubjects. .* Vaccine, 2001. 19: p. 23-24.

36. Fries, L.F., et al., *Safety and Immunogenicity of a Proteosome-Shigella flexneri 2a Lipopolysaccharide Vaccine Administered Intranasally to Healthy Adults. .* Infect Immun, 2001. 69(7): p. 4545-4553.

37. Chaicumpa, W., et al., *Immunogenicity of liposome-associated and refined antigen oral cholera vaccines in Thai volunteers. .* Vaccine 1998. 16(7): p. 678-684.

38. Moldoveanu, Z., et al., *CpG DNA, a novel immune enhancer for systemic and mucosal immunization with influenza virus.* Vaccine, 1998. 16(11-12): p. 1216-1224.

39. Gould-Fogerite, S., et al., *Lipid matrix-based subunit vaccines: a structure-function approach to oral and parenteral immunization.* AIDS Res. Hum. Retroviruses, 1994. 10(Suppl 2): p. S99-103:S99-103.

40. Palante, M., et al., *Nasal immunization with subunit proteosome influenza vaccines induces serum HAI.* Vaccine, 2002. 20(1-2): p. 218-225.

41. Mutsch, M., et al., *Use of the inactivated intranasal influenza vaccine and the risk of Bell's palsy in Switzerland. .* N Engl J Med 2004. 350: p. 896-903.

42. Armstrong, M.E., et al., *Proinflammatory responses in the murine brain after intranasal delivery of Cholera toxin : Implications for the use of ab toxins as adjuvants in intranasal vaccines.* The Journal of infectious diseases, 2005. 192(9): p. 1628-1633.

43. Rao, J.B., et al., *IL-12 Is an Effective Adjuvant to Recombinant Vaccinia Virus-Based Tumor Vaccines.* J. Immunol., 2004. 24(6): p. 1581-1588.

44. Baker Jr., J.R., et al., *Method for inactivating bacteria including bacterial spores*, U.S Patent # 6, 832, Editor. 2000.

45. Hamouda, T., et al., *A novel surfactant nanoemulsion with a unique non-irritant topical antimicrobial activity against bacteria, enveloped viruses and fungi.* Microbiological Research, 2000. 156(1): p. 1-7.

46. Hamouda, T., et al., *A novel surfactant nanoemulsion with a unique non-irritant topical antimicrobial activity against bacteria, enveloped viruses and fungi.* Microbiol Res, 2001. 156(1): p. 1-7.

47. Hamouda, T. and J.R. Baker, *Antimicrobial mechanism of action of surfactant lipid preparations in enteric Gram-negative bacilli.* Journal of Applied Microbiology, 2000. 89(3): p. 397-403.

48. Myc, A., et al., *The fungicidal activity of novel nanoemulsion (X8W60PC) against clinically important yeast and filamentous fungi.* Mycopathologia, 2002. 155(4): p. 195-201.

49. Florence, A.T., *Nonionic surfactant vesicles: Preparation and characterization.* . Liposome Technology, ed. G. Gregoriadis. 1993: CRC Press, Boca Raton, Florida.

50. Gregoriadis, G. and A.T. Florence, *Liposomes in drug delivery. Clinical, diagnostic and ophthalmic potential.* Drugs, 1993. 45(1): p. 15-28.

51. Wasan, K.M. and G. Lopez-Berestein, *The past, present, and future uses of liposomes in treating infectious diseases.* Immunopharmacol Immunotoxicol, 1995. 17(1): p. 1-15.

52. Makidon, P.E., Bielinska, A. U., Nigavekar, S. S., Janczak, K. W., Knowlton, J., Scott, A. J., Mank, N., Cao, Z., Rathinavelu, S., Beer, M. R., Wilkinson, E., Blanco, L. P., Landers, J. J., Baker, J. R., Jr., *Pre-Clinical Evaluation of a Novel Nanoemulsion-Based Hepatitis B Mucosal Vaccine.* PLoS ONE, 2008. 3(8): p. 1-15.

53. Makidon, P.E., et al., *Pre-Clinical Evaluation of a Novel Nanoemulsion-Based Hepatitis B Mucosal Vaccine.* PLoS ONE, 2008. 3(8): p. e2954.

54. Hamouda, T., et al. *A Novel Nanoemulsion Adjuvant Enhancing The Immune Response from Intranasal Influenza Vaccine in Mice* in *National Foundation for Infectious Disease, the Eleventh Annual Conference on Vaccine Research*. 2008. Baltimore, MD.

55. Myc, A., et al., *Development of immune response that protects mice from viral pneumonitis after a single intranasal immunization with influenza A virus and nanoemulsion.* Vaccine, 2003. 21(25-26): p. 3801-14.

56. Bielinska, A.U., et al., *Mucosal immunization with a novel nanoemulsion-based recombinant anthrax protective antigen vaccine protects against Bacillus anthracis spore challenge.* Infect Immun, 2007. 75(8): p. 4020-9.

57. Bielinska, A.U., et al., *A novel, killed-virus nasal vaccinia vaccine.* Clinical and Vaccine Immunology, 2008. 15(2): p. 348-358.

58. Bielinska, A.U., et al., *Nasal immunization with a recombinant HIV gp120 and nanoemulsion adjuvant produces Th1 polarized responses and neutralizing antibodies to primary HIV-1 isolates.* AIDS Research and Human Retroviruses, 2008. 24(2): p. 271-281.

59. WHO, *Word Health Statistics 2008*, in *Inequiteis in Health Care and Health Outcome*. 2008, World Health Organization: Geneva. p. 36-46.

60. Miller, M.A. and J.T. Sentz, *Disease and Mortality in Sub-Saharan Africa*, in *Disease and Mortality in Sub-Saharan Africa*, D.T. Jamison , et al.,

Editors. 2006, The Internation Bank for Reconstruction and Development/The World Bank: Washington, D. C.

61. Bielinska, A.U., et al., *Nasal immunization with a recombinant HIV gp120 and nanoemulsion adjuvant produces TH1 polarizatied responses and neutralizing antibodies to primary HIV-1 isolates.* AIDS Research and Human Retroviruses, 2007. 24: p. 271-281.

62. Bielinska, A.U., et al., *Mucosal Immunization with a Novel Nanoemulsion-Based Recombinant Anthrax Protective Antigen Vaccine Protects against Bacillus anthracis Spore Challenge.* Infect Immun, 2007. 75: p. 4020-4029.

63. Bielinska, A.U., et al., *A novel killed-virus nasal vaccinia virus vaccine.* Clinical and Vaccine Immunology, 2008. 15: p. 348-358.

64. LiPuma, J.J., *Update on Burkholderia cepacia complex.* Current Opinion in Pulmonary Medicine, 2005. 11: p. 528-533.

65. LiPuma, J.J., et al., *In vitro activity of a novel nanoemulsion against Burkholderia and other multi-drug resistant cystic fibrosis-associated bacterial species.* Antimicrob Agents Chemother. , 2008. Epub ahead of print.

CHAPTER 2
PRE-CLINICAL EVALUATION OF A NOVEL NANOEMULSION-BASED HEPATITIS B MUCOSAL VACCINE

2.1 BACKGROUND

Infection with hepatitis B virus (HBV) remains an important global health concern, despite the availability of multiple prophylactic vaccines. The World Health Organization (WHO) estimates that more than 2 billion persons have been infected with the virus. The current prophylactic vaccines require a regimen of three intramuscular (i.m.) injections, have a 10%-15% non-responders rate, and are ineffective for limiting HBV replication in chronic carriers [1-3]. Large scale vaccination programs are also limited in developing populations due to compliance issues secondary to the three dose vaccination schedule, the requirement for cold storage and the availability of sterile needles [4, 5]. This has limited the use of hepatitis B vaccine in these populations and is partly responsible for 8%-10% of the population in areas of Africa, Asia and South America being chronically infected with HBV [6]. Chronic HBV infection increases the risk of developing liver cirrhosis, hepatocellular carcinoma and other associated complications leading to increased mortality [7]. This suggests the need for a new strategy on hepatitis B vaccination for the developing world.

Hepatitis B surface antigen (HBsAg) is a major structural protein of HBV and is a protective immunogen in experimental animals and in humans [8-10]. The hepatitis B surface (HBs) proteins are synthesized as large (L), medium (M) and small (S) envelope sub-units, which self assemble into virus-like lipid-anchored particles (about 22 nm in size) [11, 12]. The majority of commercially available recombinant HBsAg vaccines (including Recombivax HB; Merck, and Engerix-B; GSK) consist of yeast derived HBs-S antigen particles adsorbed to an

aluminum salt (alum) adjuvant [1,13]. While alum is generally well tolerated and is considered safe, some adverse effects have been reported [14,15]. Further, alum has been shown to elicit predominantly a Th2 polarization of immune response, which is associated with cellular immunity that is ineffective at producing CD8 responses to virally infected cells [16]. Since cellular immunity is essential for an efficient response against some infections and elimination of some viral pathogens [17], it would be desirable to develop anti-viral vaccine(s) capable of inducing cell-mediated immunity, in addition to a robust and durable antibody response [17, 18]. Currently available hepatitis B vaccines have comparable thermo-stability profiles requiring unbroken cold chain storage (between 2°C and 8°C) in order to retain potency [19, 20]. The higher costs associated with guaranteed cold chain, from point of manufacture to point of use, also contribute to the inaccessibility of these vaccines. Thus, an efficacious vaccine requiring fewer injections and a less stringent cold storage requirement would directly benefit underserved populations.

Mucosal immunization is an attractive alternative to parenteral vaccines because it can produce both systemic and mucosal immunity and avoids the need for sterile needles [21, 22]. However, development of mucosal vaccines remains limited by lack of effective mucosal adjuvants [23, 24]. Studies have evaluated several potential mucosal adjuvants for hepatitis B vaccines including recombinant cholera toxin (CT) [25], lipid microparticles [26], CpG oligonucleotides [27, 28], cationic particles [29], PLG microspheres [30] or hepatitis B core antigen (HBcAg) [31-33]. CT has been limited from use in humans due to its potential to cause CNS inflammation. Unfortunately, a CpG-adjuvanted injectable hepatitis B vaccine was recently placed on clinical hold due to inflammatory issues in a patient, further calling into question the safety of pro-inflammatory adjuvants. No other adjuvant, with the exception of HBcAg, has even been tested in clinical trials [34-36]. This underlines the need for new nontoxic mucosal adjuvants.

This study evaluates the formulation, immunogenicity, thermal stability and pre-clinical safety of a novel mucosal, needle-free hepatitis B vaccine. These vaccine formulations are composed of recombinant HBsAg using nanoemulsions (NEs) (NanoBio Corporation, Ann Arbor, MI) as mucosal adjuvants. NEs are nanoscale (<400 nm) emulsions formulated with surfactants, distilled water, refined soybean oil and ethanol as a solvent. Initially developed as broad-spectrum antimicrobial agents [37, 38, 39], NEs proved effective as mucosal adjuvants for a range of antigens from whole influenza and vaccinia viruses to recombinant anthrax protective antigen and HIV gp120 [40-43]. In animals, these experimental NE-based vaccines do not produce local inflammation as is observed with alum-based vaccines [15]. However, these formulations are effective in inducing Th1 biased immune response and cellular immunity [41], and remain stable for at least three years at 25°C (Hamouda T., NanoBio, personal communication). These inherent advantages of NE provided a rationale for evaluating it as a mucosal adjuvant in a candidate nasal vaccine for prevention of hepatitis B infection.

2.2 EXPERIMENTAL METHODS

Adjuvant and antigen

Nanoemulsion (NE, W_{80}5EC formulation) was supplied by NanoBio Corporation, Ann Arbor, MI. Nanoemulsion was manufactured by emulsification of cetyl pyridinium chloride (CPC, 1%), Tween 80 (5%) and ethanol (8%) in water with soybean oil (64%) using a high speed emulsifier, with resultant mean droplet size of less than 400 nm in diameter. W_{80}5EC is formulated with surfactants and food substances that are 'Generally Recognized as Safe' (GRAS) by the FDA, and can be economically manufactured under Good Manufacturing Practices (GMP). The nanoemulsion is stable for at least 3 years at 25°C. Recombinant HBs antigen *adw* serotype used for immunizations (HBsAg) was supplied by Human Biologicals Institute (Indian Immunologics, Ltd., Hyderabad, India). The

antigen protein was purified from Pichia pastoris transfected with plasmid pPIC3K using standard methods according to Indian Immunologicals SOP and GMP procedures. HBsAg was dissolved in PBS (pH 7.03) and endotoxin level was determined to be <7.5 EU/20 µg of protein; below international standard of ≤30 EU/20 µg of protein.

General reagents

Phosphate buffered saline (1x PBS and 10x PBS, pH 7.4) was purchased from Cellgro (Mediatech, Inc). Deionized water was prepared using a Milli-Q® Ultrapure Water Purification system (Millipore, Billerica, MA). The bovine serum albumin (BSA) was purchased from Sigma. Alkaline phosphatase (AP) conjugated rabbit anti-mouse IgG (H&L), IgG1, IgG2a, IgG2b, IgG3, IgA (α chain specific), goat anti-rat IgG (H&L), and goat anti-guinea pig IgG (H&L) secondary antibodies were purchased from Rockland Immunochemicals, Inc.

Particle sizing studies

HBsAg-NE formulations were prepared by vigorously mixing concentrated NE with HBsAg and PBS. Mixtures contained a final concentration of 0.5 mg/ml or 2.5 mg/ml of antigen mixed in 1%, 20%, or 40% (v/v) NE concentrations and normalized to 1x PBS. The lipid-phase NE droplets were sized by quasi-elastic light scattering using an LS230 instrument (Beckmann-Coulter, Fullerton, CA) following manufacturer's protocols. In brief, between 10 µl and 30 µl of NE-antigen mixtures were diluted into a flow chamber containing 1 L of deionized water. Particle size distributions were calculated using number weighting, and statistics were generated from the average of three 60 second measurement cycles. Sample concentration was optimized based on PIDS obscuration, and PIDS data was included in the instrument's Fraunhofer model calculation.

HBsAg analysis

The integrity of HBsAg protein was analyzed using sodium dodecylsulphate-polyacrylamide gel electrophoresis (SDS-PAGE) and Western blotting techniques. HBsAg was mixed in 20% NE at 0.5 mg/ml and 2.5 mg/ml concentrations. Aliquots of each of the HBsAg-NE mixtures were incubated at 4°C, 25°C and 40°C for up to 72 hrs. For PAGE analysis, the HBsAg samples were resuspended in 1% SDS, reduced with β-mercaptoethanol (BME, 2.5%) and boiled for 15 minutes. The electrophoresis was performed in duplicates using 0.5ug HBsAg, 4–12% Bis-Tris PAGE gels (Invitrogen), and MES SDS Running Buffer. One gel of each duplicate was stained using the SilverQuest Silver Staining Kit (Invitrogen). For Western blots, gels were transferred onto Immobilon-P PVDF membrane (Millipore) in NuPAGE transfer buffer according to Invitrogen's protocol. The membranes were blocked for 1 hr in 5% Milk/PBST and were probed with a polyclonal goat anti-HBsAg (Abcam). Alkaline phosphatase-(AP) conjugated anti-goat (Sigma) secondary antibodies were used with 1-Step NBT/BCIP AP substrate (Pierce) for protein detection.

Zeta potential measurement

Zeta potential measurements were obtained using a NICOMP™ 380ZLS (PSS.NICOMP, Santa Barbara, CA). Samples containing 20% NE mixed with 2.5 mg/ml HBsAg were prepared by vigorously mixing concentrated NE and HBsAg. Test mixtures were diluted in either PBS or de-ionized water. Zeta potential was measured in 200 x diluted samples at 25°C.

Isothermal titration calorimetry

The interaction of the amphiphilic HBsAg with the lipid phase of NE was studied using an isothermal titration microcalorimeter (VP-ITC MicroCalorimeter, Microcal™). HBsAg solutions in PBS aliquots were prepared from concentrated stock and introduced into the calorimetric reaction and reference vessels (1.3 ml). Chambers were then gently agitated until temperature equilibrium with the

surroundings was reached. Concentrated NE (50% wt) was diluted in PBS to 1% (v/v). After the sample vessel had reached the equilibrium conditions, the NE solution was added in discrete injections using a syringe, into the calorimetric reaction vessel under continuous stirring (either 30°C or 40°C). The experimentally observed change of energy corresponding to a given injection of NE was measured and plotted using software (Origin 7SR4 v. 7, Origin Lab Corp., Northhampton, MA). The change in heat capacity of binding (ΔCp) was calculated using the following equation: $\Delta Cp = (\Delta H^{\circ}_{T2} - \Delta H^{\circ}_{T1})/T2-T1$ where ΔH is calculated enthalpy and T is vessel temperature [71].

Preparation of HBsAg-NE vaccine

HBsAg-NE formulations were prepared 30 to 60 minutes prior to immunization by vigorously mixing HBsAg protein solution with concentrated NE using PBS as diluent. For intranasal immunizations HBsAg-NE doses ranged from 1 μg to 40 μg HBsAg mixed with 5% to 40% NE. For intramuscular immunizations with the HBsAg/aluminum hydroxide vaccine (HBsAg-Alu), antigen was adsorped onto 0.5 mg/ml aluminium hydroxide (Sigma) following the adsorption procedure described in [72] to obtain formulation similar to that of Engerix® (GlaxoSmithKline).

Animals

Pathogen-free, outbred CD-1 mice (females 6–8 weeks old), inbred BALB/c mice (females 6–8 weeks old), and Hartley guinea pigs (females 10–11 weeks old) were purchased from Charles River Laboratories. Pathogen free Sprague Dawley rats (females 7–8 weeks old) and specific pathogen free (SPF) purpose-bred American standard beagles (females, 6 month old) were obtained from Harlan and Covance, respectively. Animals used in these studies were housed in SPF conditions with food and water available ad libitum in accordance to the standards of the American Association for Accreditation of Laboratory Animal Care. Mice were housed with 5 to a cage. Rats and guinea pigs were

housed 3 to a cage. Dogs were housed in floor pens with soft bedding and in a rotating group setting. Daily exercise was provided as enrichment. All procedures performed on animals within this study were conducted in accordance with and by approval of the University of Michigan University Committee on Use and Care of Animals (UCUCA).

Immunization procedures

CD-1 mice (n=5 per group for immunogenicity studies, n=10 per group for stability studies) were vaccinated with two administrations of HBsAg-NE vaccine six weeks apart. Both intranasal (i.n.) and intramuscular (i.m.) immunizations were performed in mice anaesthetized with isoflurane using IMPAC$^{6®}$ anesthesia delivery system. For i.n. administration, animals were held in a supine position and 8 µl (4 µl/nare) of HBsAg-NE vaccine was administered slowly to the nares using a micropipette tip. For i.m. immunization, the 50 µl of HBsAg-Alu vaccine was injected into apaxial muscle. Rats, and guinea pigs (n=5 per group) were also manually restrained in a supine position and 100 µl (50 µl/nare) of HBsAg-NE vaccine was administered slowly to the nares using a micropipette tip.

Blood, bronchioalveolar lavage, and splenocyte collection

Blood samples were obtained from the saphenous vein in mice, rats, and guinea pigs and from the superficial cephalic vein in dogs at various time points during the course of the experiments. The terminal murine sample was obtained by cardiac puncture post-euthanasia. Serum was separated from whole blood by centrifugation at 1500 x g for 5 minutes after allowing coagulation for 30 to 60 minutes at room temperature. Serum samples were stored at -20°C until analyzed.

Bronchioalveolar lavage (BAL) fluid was obtained from mice euthanized by an overdose of isoflurane. A 22 gauge catheter (Angiocath, B-D) attached to a

syringe was inserted into the distal trachea. The lungs were infused twice with 0.5 ml of PBS containing 10 μM DTT and 0.5 mg/ml aprotinin and approximately 1 ml of aspirate was recovered. BAL samples were stored at -20°C until analyzed.

At the time of euthanasia, spleens were harvested from mice and mechanically disrupted to obtain single-cell splenocyte suspension in PBS, which was used for in vitro determination of cytokine response. Red blood cells were removed by lysis with ACK buffer (150 mM NH_4Cl, 10 mM $KHCO_3$, 0.1 mM Na_2EDTA), and the remaining cells were washed twice in PBS. For the cytokine expression assays, splenocytes were resuspended in RPMI 1640 medium supplemented with 2% FBS, 200 nM L-glutamine, and penicillin/streptomycin (100 U/ml and 100 μg/ml).

Determination of IgG and IgA antibodies in serum and BAL fluid

Mouse, rat, and guinea pig anti-HBsAg specific IgG and mouse anti-HBsAg specific IgA levels were determined by ELISA. Microtiter plates (NUNC) were coated with 5 μg/ml (100 μl) of HBsAg in a coating buffer (50 mM sodium carbonate, 50 mM sodium bicarbonate, pH 9.6) and incubated overnight at 4°C. The protein solution was removed and plates were incubated with blocking buffer (PBS with 1% dry milk) for 30 minutes at 37°C. After the blocking solution was aspirated, the plates were used immediately or stored sealed at 4°C until needed. For antibody detection, serum and BAL samples were serially diluted in 0.1% BSA in PBS. The 100 μl/well aliquots were incubated in HBsAg coated plates for 1 hour at 37uC. Plates were washed three times with PBS containing 0.05% Tween 20, followed by 1 hour incubation with either species specific anti-IgG or IgA alkaline phosphatase (AP)-conjugated antibodies, then washed three times and incubated with AP substrate Sigma FastTM (Sigma). The colorimetric reaction was stopped with 1 N NaOH according to the manufacturer's protocol, and optical density (OD) measured using a Spectra Max 340 ELISA reader

(Molecular Devices, Sunnyvale, CA) at 405 nm and the reference wavelength of 690 nm. The antibody concentrations are presented as endpoint titers defined as the reciprocal of the highest serum dilution producing an OD above cutoff value. The cutoff value is determined as OD of the corresponding dilution of control sera+2 (standard deviations) and plate background [73,74]. Normalization of IgG was performed at UMHHC diagnostic laboratory using an ADVIA Centaur anti-HBsAg assay.

Determination of IgG avidity

The avidity index (AI) was determined by ELISA using mouse serum as described by Vermont et al. [75] with minor modifications. Sodium thiocyanate (NaSCN) was used for dissociation of low avidity antibody-antigen binding. Optimal assay conditions for determination of AI were established in an ELISA assay using 0 M to 3 M range of NaSCN concentrations. We have identified that incubation with 1.5 M NaSCN solution resulted in reduction of antibody binding that was discriminating between serum samples. In each assay, serial dilutions of immune serum were incubated with HBsAg as described above for standard ELISA. To differentiate antibody binding, the wells were incubated with either PBS or with 1.5 M NaSCN at room temperature for 15 minutes. Subsequently wells were washed three times and incubated with anti-mouse IgG AP-conjugate as described above. The AI was calculated as percentage of antibody titer which remained bound to antigen after incubation with NaSCN in comparison to the standard ELISA protocol.

Luminex analysis of cytokine expression

Freshly isolated mouse murine splenocytes were seeded at $4x10^6$ cells/ml (RPMI 1640, 2% FBS) and incubated with HBsAg (5 μg/ml) or control PHA-P mitogen (2 μg/ml) for 72 hours. Serum and cell culture supernatants were harvested and analyzed for the presence of cytokines. These assays were

performed using Luminex® Multiplex21 multi-analyte profiling beads (Luminex Corporation, Austin, TX), according to the manufacturer's instructions.

Analyses of thermostability of HBsAg-NE

For vaccine thermostability studies, the formulation was made by vigorously mixing HBsAg and NE to achieve a dose of 2.5 mg/ml recombinant protein in 20% NE and a final buffered solution of 1x PBS. The vaccine was then aliquoted into sterile glass vials with Teflon-coated caps (Wheaton) and stored at either 4±-2°C, 25±2°C or 40±2°C. Temperatures were monitored for the period of the study by Lufft OPUS10 thermographs (PalmerWahl). At time points of 6 weeks, 12 weeks (3 months), 24 weeks (6 months) and 52 weeks (1 year), an aliquot was withdrawn and used for in vitro as well as in vivo analyses. For in vitro analyses 0.5 mg of antigen contained in vaccine product was electrophoresed per lane and detected by silver staining and Western blotting (as described above); NE particle size was also determined (as described above). In vivo immunogenicity studies were done by intranasal vaccinations (primed at 0 and boosted at 6 weeks) of about 8 week old female CD-1 mice (n =10 per group) and testing serum IgG titers at 2, 3, 5, 8, 10 and 12 weeks as described above.

Comprehensive toxicity assessments

Acute and (sub) chronic toxicity responses to either NE or HBsAg-NE were assessed in mice, rats, guinea pigs, and dogs. We have evaluated numerous species in order to minimize the effects of animal model biasing. The end points of the study were histopathological evaluation of exposed tissues and of highly perfused organs. Metabolic changes were also measured using serum biochemical profile analysis.

The clinical status of each animal including the nasal cavity, body weight, body temperature, and food consumption was assessed throughout the study.

Mice were non-surgically implanted with programmable temperature transponders (IPTT-3000, Bio Medic Data Systems, Inc.) for non-invasive subcutaneous temperature measurement with a handheld portable scanner (DAS-6002, Bio Medic Data Systems, Inc.). Euthanasia by isoflurane asphyxiation was performed in mice whereas rats and guinea pigs were euthanized by barbiturate overdose. A complete necropsy, which included the gross pathological examination of the external surface of the body, all orifices, and the cranial thoracic and abdominal cavities and their contents, was performed on all rodent species at the time of death. Vaccine exposed tissues and highly perfused organs including the sinus cavity, lungs, esophagus, trachea, brain, heart, liver, kidneys, spleen, stomach, intestines, pancreas, and adrenals were collected and immediately fixed in 10% buffered formalin (Fisher Scientific).

In order to assess safety and tolerability of the adjuvant, NE was delivered to dogs using a wide angle nasal sprayer pump (Pfeiffer 62602, 415 screw enclosure). The containers used were Saint Gobain Desqueres 5-mL U-SaveTM Type 1 amber glass bottles with a 415 neck finish. The dose volume for the sprayer pump was 130 µl. Dogs received either 260 µl (130 µl/nare) or 520 µl (260 µl/nare) administered every 14 days for a total of 3 doses as outlined in Table 2. Rostral nasal sinus punch biopsy samples were collected 24 hours following the final treatment. For the biopsy procedure, dogs were anesthetized with ketamine/diazepam/butorphanol (10 mg/kg, 0.5 mg/kg, 3 mg/kg) and maintained on 2.5% isoflurane after endotracheal intubation. The anterior sinus cavity and external nares were sterilely prepared. A sterile dermal punch biopsy instrument (Miltex, 4 mm) was introduced approximately 1.5 cm into ventral portion of the anterior sinus cavity. Hemostasis was achieved using 4-0 PDS suture material. Tissues obtained for biopsy were immediately fixed in 10% buffered formalin (Fisher Scientific). Butorphanol (3 mg/kg) administration was continued every 8 hours for three days following the biopsy procedure for analgesic management.

Histopathological analysis

Harvested tissues were fixed in 10% formalin solution for at least 24 hours. Sinus tissues including bone were decalcified for 48 hours using Cal-EXTM II (Fisher Scientific) prior to trimming and embedding in paraffin. For mice, rats, and guinea pigs, four standard cross sections of the nasal passages including the brain were taken [76]. Tissue blocks were processed in xylene and paraffin embedded for multi-sections and slide preparation. Routine hematoxylin and eosin (H&E) staining of each slide was carried out and blindly examined by a veterinary pathologist. Histopathological lesions were scored on a histological grading scale ranging from 0 to 10 based on severity and distribution. The histopathology of the nasal cavity was scored using very strict criteria. Any finding other than pristine was given a positive score. A single small focus of accumulation of amorphous material and/or the presence of any cell damage no matter how slight was scored as +1 (Figure 2.9C). More than one focus of accumulation of material and/or cell damage was scored as +2 (Figure 2.9D). More than 3 foci of accumulation of material and/or cell damage or multiple locally extensive areas of pathology were scored as +3. The lesions graded as +4 to +6 were associated with increasing severity and more extensive distribution of lesions including the presence of lesions in more than one section. These lesions could be associated with morbidity. The +7 and above had increasing degrees of inflammation. Mortality would be given a score of +10.

Hematological and serum biochemical profile analysis

Whole blood samples were collected from rats and guinea pigs 2 weeks following the final vaccine dose. Dogs were phlebotomized every 14 days and at the study termination at day 43. A portion of the blood was placed in VacutainerTM tubes containing EDTA (BD) and a portion was placed in serum separator VacutainerTM tubes (BD). Anti-coagulated blood was processed to determine hematological parameters (lymphoyctes, monocytes, eosinophils, basophils, red blood cells, hemoglobin, hematocrit, mean corpuscular hemoglobin, mean corpuscular volume, mean corpuscular hemoglobin

concentration, and platelets) in a HEMAVETH 950 hematology analyzer (Drew Scientific, Inc., Oxford, CT) in accordance to manufacturer's recommendation. Hematological data was compared to species laboratory reference values as established by the Animal Diagnostic Laboratory at the University of Michigan. Serum samples were analyzed using a VetTest Chemistry AnalyzerH (Idexx, Westbrook, Maine). A complete chemistry panel including albumin, alkaline phosphatase, alanine aminotransferase, amylase, aspartate aminotransferase, total calcium, total cholesterol, creatinine, glucose, phosphorous, total bilirubin, total protein, blood urea nitrogen, sodium, potassium, chloride, globulin, and creatine kinase was performed. Biochemical data was compared to species laboratory reference values as established by the Animal Diagnostic Laboratory at the University of Michigan.

Statistical Analysis

Results are expressed as mean ± standard error of the mean (SEM) or ± standard deviation (SD). Statistical significance was determined by ANOVA (analysis of variance) using the Student t and Fisher exact tests or a Bonferroni's Multiple comparison analysis. The analyses were done with 95% confidence limits and two-tailed tests. A *p-value* < 0.05 was considered to be statistically significant.

2.3 RESULTS

Characterization of vaccine formulation

The candidate hepatitis B vaccine was formulated from two components; recombinant HBsAg and NE (HBsAg-NE). The formulation was characterized by evaluating the stability of its components, as well as the physical interaction of the antigen with NE.

To characterize NE stability, emulsion droplet size was analyzed in a broad range of concentrations (1% to 40%) both alone and mixed with either low (0.5 mg/ml) or high (2.5 mg/ml) concentrations of HBsAg. The effect of temperature on the mixing of antigen and NE of was evaluated by incubating each of the formulations at either 4°C, 25°C, or 40°C for 72 hours. The lipid droplet size was stable and uniform in both concentrations of antigen (the average size for all conditions calculated as 349±17 nm), and droplet size of the mixture was not altered by either temperature or NE concentration (Table 2.1).

HBsAg integrity in the emulsion was evaluated using SDS-PAGE and Western blot (Figures 2.1A and 2.1B). NE also did not interfere with the electrophoresis or immunoblotting procedures. After treatment with SDS, HBsAg protein migrated as a band that corresponded to HBsAg monomer (Mw≈24 kDa) with a minor fraction at twice this molecular weight representing dimer, and this pattern was not altered by prior mixing in NE. In addition, antigenic recognition was retained in HBsAg mixed in NE as identified in Western Blots using a polyclonal goat antiserum raised to native HBsAg (Figure 2.1B). No degradation products of HBsAg were detected in either analysis and no significant aggregation appeared to occur during mixing or incubation with NE.

The surface charge of the vaccine formulation was determined by measuring the zeta potential and was compared to NE and HBsAg solutions with deionized water and PBS buffer used as diluents. In either diluent, HBsAg had negative zeta potential as has been previously reported in literature (Figure 2.2A) [44]. In contrast, there was a decrease in the positive zeta potential of the NE after mixing with the HBsAg. This suggests an electrostatic association between the negatively charged HBsAg particles and cationic CPC-containing emulsion [45]. The drop in charge of the emulsion was more pronounced when the HBsAg/NE formulation was made with deionized water as compared to buffers such as PBS (Figure 2.2A).

The interaction of HBsAg with NE was further examined using laser diffraction particle sizing and isothermal titration calorimetry (ITC). Two independent and differently sized peaks for NE and HBsAg were observed before mixing, however after formulation only a single peak was detected with a dynamic diameter of ≈300 nm (Figures 2.2B, 2.2C, and 2.2D and Figure 2.1). The absence of two separate peaks again indicated an association between the lipid phase and HBsAg protein, and suggested that no significant fraction of the antigen remained independent from the lipid in the aqueous phase of NE. Thermodynamic analysis of the interaction between the HBsAg and the NE using ITC showed a spontaneous exothermic reaction with a calculated change in heat capacity of binding (ΔCp) of -1.44 indicating an energetically favorable interaction (Figure 2.2E).

Optimization the immunogenicity of the nasal HBsAg-NE vaccine

Immunogenicity of the HBsAg-NE vaccine formulation was optimized by conducting in vivo adjuvant and antigen dose escalation studies. To optimize the NE concentration for the vaccine, CD-1 mice were intranasally (i.n.) immunized with 20 μg of HBsAg mixed with a range of NE concentrations from 5% to 40% using antigen in PBS as a control. After a single immunization with 20 μg of HBsAg in either 10%, 20% or 40% NE, similar end-point serum anti-HBsAg IgG titers averaging over 10^4 were achieved (Figure 2.3A). In contrast, significantly lower serum titers ($<10^2$) were generated after immunization with 5% NE and low, inconsistent antibody responses were detected in mice nasally vaccinated with HBsAg in PBS (Figure 2.3A). Booster immunization at six weeks caused the serum anti-HBsAg IgG titers to increase over 10 fold in all groups except in the animal immunized with HBsAg in PBS where no effect was observed. The highest anti-HBsAg antibody endpoint titers, exceeded 10^6 at 6 to 8 weeks after boost, were achieved when the animals were vaccinated with either 20% or 40% NE. The HBsAg-NE vaccine also produced persistent antibody responses with serum anti-HBsAg IgG titers of 10^4–10^5 at 6 months after initial vaccination

regardless of the concentration of NE used for vaccination. Thus, the lowest optimal NE concentration was determined to be 20%.

To optimize the antigen concentration in the NE vaccine, mice were i.n. immunized with 1 µg, 5 µg 20 mg and 40 µg of HBsAg mixed with 20% NE (Figure 2.3B). After a single vaccination anti-IgG HBsAg antibody responses showed a dose dependent relationship with highest titers in the 20 µg HBsAg-NE group and significantly weaker antibody responses in mice vaccinated with 1 µg of HBsAg. After a second immunization at six weeks, the anti-HBsAg IgG titers increased approximately 10 fold exceeding 10^4, except in animals immunized with 1 µg HBsAg in NE. Intranasal immunizations with equivalent amounts of HBsAg mixed in PBS again produced only sporadic and weak antibody responses with titers less than 10^2 (data not shown). This indicated that 20 µg of HBsAg appeared in the optimal antigen dose.

Immunogenicity of HBsAg-NE immunization

The humoral and cell-mediated immune responses to the optimized HBsAg-NE vaccine were characterized in vivo in mice. Intranasal vaccination with either 20 µg HBsAg-20% NE or i.m. injection of 20 µg HBsAg-Alu resulted in comparable, high levels of anti-HBsAg serum IgG antibodies reaching 10^5 to 10^6 titers within 8 weeks after primary vaccination (Figure 2.4A). HBsAg-Alu induced a slightly more rapid response, producing higher IgG titers than HBsAg-NE at 2 weeks after primary vaccination (*p-value* <0.05), but this difference disappeared after a single booster immunization. Both HBsAg-NE and HBsAg-Alu vaccines produced equivalent, durable immune responses with serum anti-HBsAg IgG end point titers of 10^4 to 10^5 being maintained up to 6 months after vaccination. Nasal vaccination with HBsAg-NE elicited serum titers in mice that when normalized with standardized human anti-HBsAg serum indicated an antibody index ≥1000 IU/ml (data not shown). This index is compatible with protective immunity in humans.

Analysis of serum IgG anti-HBsAg avidity at 23 weeks indicated significantly higher antibody avidity in HBsAg-NE immunized animals as compared to IgG from HBsAg-Alu vaccinated mice (*p-value* =0.034) (Figure 2.4B). While the overall titers were equivalent, analysis of serum IgG subclass indicated that i.n. HBsAg-NE vaccination produced anti-HBsAg IgG with a prevalence of IgG2b (and IgG2a) over IgG1 subclass antibodies, while consistent with previous reports [46, 47] the HBsAg-Alu vaccine produced mainly IgG1 subclass antibodies (Figure 4C). This suggests a Th1 response to the NE-based vaccine vs. the traditional Th2 response associated with alum. Immunization with HBsAg-NE composed of *adw* serotype surface antigen also produced cross-reacting IgG antibodies against the heterologous *ayw* serotype (data not shown).

Mucosal immune responses were characterized in bronchioalveolar lavage (BAL) fluid of immunized animals. HBsAg specific IgA and IgG antibodies were detected in BAL samples obtained at the conclusion of the study (23 weeks after initial immunization) from mice immunized intranasally with HBsAg-NE (Figure 2.5A and B, respectively). These animals also had detectable serum levels of IgA anti-HBsAg (data not shown). No anti-HBsAg antibodies were detected in BALs or serum in mice immunized with antigen administered in PBS or in intramuscularly immunized mice despite high serum titers.

HBsAg specific cellular responses were characterized in splenocytes of immunized outbred CD-1 mice obtained at 18 weeks after last immunization. The cells were stimulated with HBsAg and then evaluated for specific cytokine production (Figure 2.5C). The cytokine expression pattern included high production of the Th1-type cytokines IFN-γ and TNF-α (ranging from 5 to 40 fold) and lower increases (≤ 2 fold) in the expression of Th2-type cytokines IL-4, IL-5 and IL-10. This pattern of expression suggested a Th1 bias of cell-mediated response.

The serum IgG response elicited by HBsAg-NE vaccine was also studied in two alternative rodent species to ensure that the immunization effect was not species specific. Rats and guinea pigs were immunized with 5 μg and 20 μg doses of HBsAg mixed with 20% NE (Figure 2.6). After a single vaccination, animals showed a dose dependent response with the highest IgG antibody titers in the 20 mg HBsAg-NE group. After a second administration at five weeks, the anti-HBsAg IgG titers increased up to 100 and 1000 fold surpassing 10^5 titers in both species. Thus, the HBsAg-NE vaccine appeared immunogenic in all three animal species tested.

Thermal Stability of HBsAg-NE vaccine

The optimized formulation of HBsAg-NE was evaluated for thermal stability at three test temperatures. The vaccine product was mixed to contain 2.5 mg/ml HBsAg in 20% NE (to obtain a single dose of 20 μg of antigen in a final volume of 8 μl) and aliquoted into capped glass vials for storage at 4±2°C, 25±2°C or 40±2°C. At 6 weeks, 3 months, 6 months and a year after the start of the stability study aliquots of the formulation were evaluated for physical stability in vitro and immunogenicity in vivo.

HBsAg stability in vaccine samples was analyzed by SDS-PAGE with silver staining and antigenicity evaluated with Western blots (Figure 2.7) with the stored samples compared to freshly mixed vaccine at each time point. The protein stains and Western Blots of HBsAg at 6 weeks and 3 months were not different from fresh material and there were no low molecular weight degradation products appreciable at these or any later time points (Figures 2.7A and B). After 6 months of storage (Figure 2.7B), however, the major HBsAg band was not detectable in the 40°C by silver staining or immunoblotting, whereas both 4°C and 25°C stored products were still comparable to freshly mixed vaccine. After 1 year of storage (Figure 2.7C), the 25°C sample was also degraded, while the 4°C stored formulation was intact and comparable to freshly mixed vaccine. The stability of the NE also was evaluated by particle size characterization (Figure

2.7D). The mean diameter (± SD) of freshly mixed HBsAg-NE samples was 0.323±0.016 μm, and there were no significant differences between NE particle sizes of fresh and stored HBsAg-NE samples at any temperature or time point.

Immunogenicity of the vaccine in CD-1 mice was tested at each time point and storage temperature. Mice were immunized then boosted at six weeks post-vaccination, and anti-HBsAg serum IgG responses were determined at 2, 3, 5, 8, 10 and 12 weeks after primary vaccination. There were no significant differences in serum IgG titers elicited by HBsAg-NE vaccine stored at any temperature up to 3 months (Figures 2.8A and B). At 6 months of storage, HBsAg-NE stored at 40°C could elicit and boost HBsAg-specific antibodies, but at a significantly decreased titer when compared to freshly mixed vaccine, while 4°C and 25°C stored vaccines retained complete immunogenicity (Figure 2.8C). After 1 year of storage, 25°C stored HBsAg-NE elicited decreased serum IgG while the 4°C and 25°C stored vaccines again retained complete immunogenicity (Figure 2.8D). This indicated that the vaccine retained immunogenicity for 3 months at 40°C and 6 months at 25°C.

Evaluation of the safety of NE adjuvant and HBsAg-NE Vaccine

Comprehensive evaluation of acute and sub-chronic toxic effect of NE and HBsAg-NE formulations was performed in rodent models and in dogs. Multiple intranasal dose studies (ranging from 2 to 7 total doses as shown in Table 2.2) for NE adjuvant or HBsAg-NE were conducted. No statistically significant changes in subcutaneous temperature or body weight were observed in these species as compared to non-treated control groups (data not shown). Likewise, no observable changes in activity or appetite were noted throughout the study. Hematological and serum biochemical results in rats, guinea pigs, and dogs were within normal physiological range (Table 2.2). No lesions were reported in highly perfused organs including the olfactory bulb and frontal lobe of the brain. Cytotoxicity was not observed in nasal epithelium and other exposed tissues.

The only histological lesion noted was the accumulation of amorphous material that sometimes contained cellular debris from sloughed nasal epithelial cells. None of the lesions were of clinical significance (Table 2.2 and Figure 2.9). For further analysis, serum was collected in mice 24 hours following i.n. vaccination with NEHBsAg and was evaluated for the presence of IL1α IL1β, IL2, IL4, IL5, IL6, IL7, IL9, IL10, IL12, IL13, IL15, IL17, GCSF, GM-CSF, IFN-γ, IP-10, KC, MCP-1, MIP-1α, RANTES, TNF-α using a LINCOplex® Mouse Cytokine/Chemokine kit. Serum concentrations of IL6 significantly exceed those of the non-treated controls (933 pg/ml NE-HBsAg vs. 174 pg/ml for PBS control [*p-value*= 0.053]). The production of IL6, however, occurs in the absence of neutrophilic, macrophagic, or other inflammatory cellular infiltration in directly exposed nasal epithelium (Figure 2.9). Overall, both NE and HBsAg-NE were safe and well tolerated by all animal species tested. Approximately 5% of mice developed nasal obstruction with the emulsion, but this was not observed in larger animals and appeared to be related to the unique nasal anatomy of the mouse.

2.4 DISCUSSION

The commercial hepatitis B vaccines are a remarkable triumph in disease prevention. As one of the first recombinant biological products used as a vaccine, these formulations have a 20 year record of efficacy in preventing hepatitis B and have excellent safety with local reactions from the alum adjuvant being the predominant adverse event [1, 2, 48, 49]. However, hepatitis B remains a significant health issue, especially in the developing world. While efforts of local producers have greatly reduced the cost of the vaccine, the requirement for sterile needles and syringes for administration, and a refrigerated cold chain have conspired to prevent vaccination of many at-risk populations. Because of these issues there is an ongoing interest in producing needle-free and thermally stable hepatitis B vaccines with similar safety and efficacy to the current commercial alum-based vaccines [19, 20, 50].

This study documents the immunogenicity of a novel, mucosal hepatitis B vaccine that is based on a mixture of recombinant HBsAg and nanoemulsion adjuvant. A single nasal immunization of the HBsAg-NE mixture produces a rapid induction of serum anti-HBsAg IgG, which is comparable to that achieved with i.m. vaccination using aluminum salt-based vaccine. Serum IgG responses could be boosted and the titers persisted for the 23 weeks duration of these studies. Normalization carried out by comparison to a standardized human anti-HBsAg serum indicated that anti-HBsAg antibody titers in mice immunized with a nasal HBsAg-NE vaccine corresponded to a greater than 1,000 mIU/ml HBsAg IgG concentration in humans which are considered to be seroprotective against HBV infection [2, 51]. There was also evidence suggesting affinity maturation in the antibody response as serum IgG from animals vaccinated with HBsAg-NE indicated that their avidity matured over time to achieve higher values at 23 weeks than at 5 weeks after vaccination (data not shown). This is important since functional antibody maturation is considered a significant correlate for the protective efficacy of vaccines [52, 53]. The cross-reactive nature of IgG antibodies against the heterologous ayw serotype supports the idea that immunization with one of HBsAg serotypes may produce IgG response broadly reactive with HBsAg epitope variants. This could be of importance for the protective immunity against various serotypes of HBV.

In these studies nasal immunization with HBsAg-NE also induced significant mucosal immunity as documented by IgA and IgG detected in BAL fluids, although the role of mucosal IgA in protecting from a blood-borne pathogen like HBV is not clear. Mucosal immunization with HBsAg-NE also induced antigen-specific T cell responses similar to those reported by our group when using NE as a mucosal adjuvant for gp120, rPA, and vaccinia virus in various mouse strains [40, 41, 54]. In vitro stimulation of splenocytes harvested from vaccinated mice with HBsAg resulted in a cytokine response characterized by significant secretion of hallmark Th1 type cytokines such as IFN-γ and TNF-α, while Th2 type cytokines IL4, IL5 and IL10 showed no antigen-specific response

[55, 56, 57]. In addition to enhancing the magnitude of antibody response, nanoemulsion adjuvant clearly had an effect on the pattern of IgG isotypes, as indicated by prevalence of IgG2 over IgG1 subclass in contrast to vaccination with HBsAg-Alu which produced overwhelming titers of IgG1 antibodies [32, 58]. Prevalence of IgG2b in the overall IgG response provided additional confirmation of a Th1 bias in cellular immunity produced by HBsAg-NE vaccination. However, it is important to note that IgG1 still remained at significant titers, which may suggest co-activation of both Th1 and Th2 immune elements [59]. Although this effect resembles immunostimulation with MPLA, CpG or the other TLR agonists, the lack of any pro-inflammatory compound in the NE and the absence of local nasal inflammation or irritation from the HBsAg-NE argues against activation of these pathways [60, 61]. In general, pro-inflammatory cytokines were not detected systemically in serum with the exception of elevated levels IL6 up to 24 hours following intranasal treatment with NE-HBsAg. Although the role of IL6 in mucosal environment is not fully understood, it has been shown to be play a variety of regulatory functions in development of immune response [62-64].

These studies are significant for a number of reasons. This vaccination produced immunity to HBsAg compatible with aluminum salt-adjuvanted vaccines, but without the need for injection or an inflammatory adjuvant. The ability to produce this level of serum antibodies with nasal immunization is also unique, and shows the potential of this methodology. In addition, the simple approach to formulation of this vaccine makes it suitable to be produced without special equipment. These characteristics should facilitate the use of this vaccine in developing regions of the world. The other advantage of this formulation is its stability. Two mechanisms (electrostatic and hydrophobic interactions) of antigen-lipid association can be documented. The exothermic reaction upon mixing these components also suggests that the mixture is more stable than protein in aqueous solution. The association of the antigen complex with NE through hydrophobic mechanisms seems plausible given the negative change in heat capacity (Cp) and because HBsAg particles contain approximately 20%

host-cell derived lipids [65-67]. Laser diffraction particle sizing and zeta potential measurement indicate that cationic lipid-phase NE droplets associate with HBsAg and remain uniform in size and stable over a broad range of concentrations and temperature conditions. This indicates that the physical association of HBsAg with the lipid phase of NE provides stability to the antigen as well as contributing to the adjuvant capability of NE. Because maintaining cold chain conditions of 4°C to 8°C during inventory, storage and transport contributes significantly to the cost of the currently licensed hepatitis B vaccines, this stability is significant. Since the HBsAg-NE vaccine retained immunogenicity up to 6 months at 25°C and 3 months at 40°C, the vaccine might not require refrigeration for the final stages of distribution. At the least, it indicates that accidental breaks in the cold chain, as often occurs in developing countries, would not necessitate the destruction of the vaccine. Also, the decreases in immunogenicity were readily detected by in vitro analyses (Figures 2.7B and 2.7C), allowing for easy evaluation of vaccine stocks.

Adjuvants have been traditionally developed from pro-inflammatory substances, such as a toxin or microbiological component, found to trigger signaling pathways and cytokine production [68]. Also, enterotoxin-based adjuvants, such as cholera toxin, have been associated with inducing inflammation in the nasal mucosa and with production of the inflammatory cytokines and transport of the vaccine along olfactory neurons into the olfactory bulbs, [69]. Some patients treated with a flu vaccine based on one of these toxins (Nasalflu, Berna Biotech), developed Bell's palsy [70] presumably due to the vaccine in the olfactory bulb. This finding led to Nasalflu being withdrawn, and it is unclear whether other mucosal vaccines using this approach will be acceptable for humans. Our studies indicate no significant inflammation in HBsAg-NE treated animals and there was no evidence of the vaccine in the olfactory bulb. These finds are encouraging and suggest that successfully nasal mucosal adjuvant activity might be achieved without toxicity.

2.5 CONCLUSIONS AND SUMMARY

These studies document that HBsAg-NE is a safe and potent mucosal adjuvant for a novel hepatitis B vaccine. Its unique benefits include needle-free mucosal administration, induction of systemic immunity comparable with conventional vaccines, as well as mucosal and cellular immune responses that are not elicited by injected, aluminum-based hepatitis vaccines. The vaccine has stability that could improve its utility in the developing world. Given the ability to induce potent Th1 cellular immunity, this vaccine also may provide therapeutic benefit to patients with chronic HBV infection who lack cellular immune responses to adequately control the virus.

2.6 TABLES

Particle Size (nm)	Temperature Condition (°C)			
Sample description	**Fresh**	**4**	**25**	**40**
1% W_{80}5EC	355 (±130)	385 (±141)	327 (±168)	353 (±201)
20% W_{80}5EC	368 (±255)	328 (±159)	350 (±166)	337 (±166)
40% W_{80}5EC	331 (±154)	373 (±221)	322 (±178)	340 (±153)
20% W_{80}5EC +0.5 mg/ml HBsAg	373 (±229)	325 (±142)	354 (±193)	347 (±200)
20% W_{80}5EC +2.5 mg/ml HBsAg	341 (±143)	348 (±177)	361 (±227)	347 (±232)

Average particle size 349 (±17); Mean (±SD).

Table 2.1. Consistency of nanoemulsion particle size.

Species/Strain[a]	Treatment		Number of Dose	Dose Volume (ul)	Group Average Histopathological Score[b]				Metabolic Analysis[d]
	NE (%)	HBsAg (ug)			Nasal	Pulmon.	Brain	Other[c]	
Mouse/CD-1	0	20	2[e]	10	0	0	0	0	n/a
	1	20	2[e]	10	0	0	0	0	n/a
	5	20	2[e]	10	1.0±0.9	0	0	0	n/a
	10	20	2[e]	10	0.7±1.1	0	0	0	n/a
	20	20	2[e]	10	1.4±1.3	0	0	0	n/a
	20	0	2[e]	10	1.1±1.7	0	0	0	n/a
Mouse/BALB/c	20	0	4[f]	6	1.2±0.4	0	0	0	n/a
	20	0	7[g]	6	2.0±1.0	0	0	0	n/a
Rat/Wistar	20	32	3[h]	20	0	0	0	0	Normal
Guinea Pig/Hartley	20	32	3[h]	20	0	0	0	0	Normal
Canine/Beagle	20	0	3[e]	200	0	n/a	n/a	n/a	Normal
	20	0	3[e]	400	0	n/a	n/a	n/a	Normal

[a]- The number of animals used for analysis: CD-1 (n = 10), BALB/c, Wistar rats and Hartley guinea pigs (n = 5) and Beagles (n = 1) per group.
[b]- Histological lesions were evaluated on a scale from 0 to 10 with +1 single microscopic focus, +2 at least 2 microscopic foci, +3 more than 3 foci or multiple locally extensive areas of pathology, +4 to +6 were associated increasing severity and more extensive distribution (these lesions could be associated with morbidity), +7 and above had increasing degrees of inflammation (+10 associated with mortality).
[c]- Other tissues evaluated include heart, liver, kidneys, spleen, esophagus, trachea, stomach, intestines, pancreas, and adrenals.
[d]- Metabolic analysis evaluated by standard biochemical serum profile analysis on a IDEXX Vet Test Analyzer™ and performed at the Animal Diagnostic Laboratory through the Unit for Laboratory Animal Medicine at the University of Michigan. Normal indicates all analytes fell within normal expected distributions per species.
[e]- Administered every 2 weeks.
[f]- Administered every 15 minutes.
[g]- Administered every 4 hours.
[h]- Administered every 4 weeks.
doi:10.1371/journal.pone.0002954.t002

Table 2.2. Pre-clinical toxicology evaluation.

2.7 FIGURES

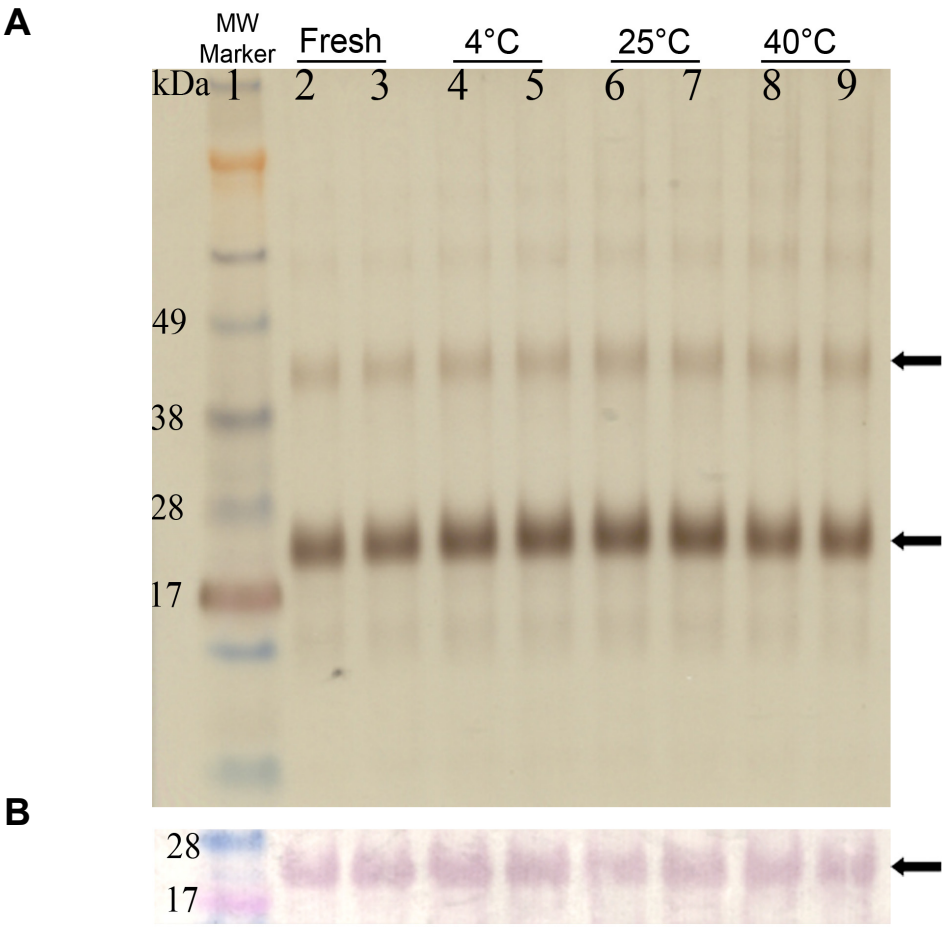

Figure 2.1. Stability of HBsAg. **A)** Silver stained SDS-PAGE: Analysis of freshly prepared vs. 72 hour incubated HBs antigen mixed with 20% NE**.** Conditions of the incubation are specified above the gel. HBsAg monomer and dimer are indicated with arrows at 24 kDa and 48 kDa bands. **B)** Western blot: The protein configuration is identical to as described for SDS-PAGE. HBsAg is detected using a polyclonal anti-HBsAg antibody for all incubation conditions.

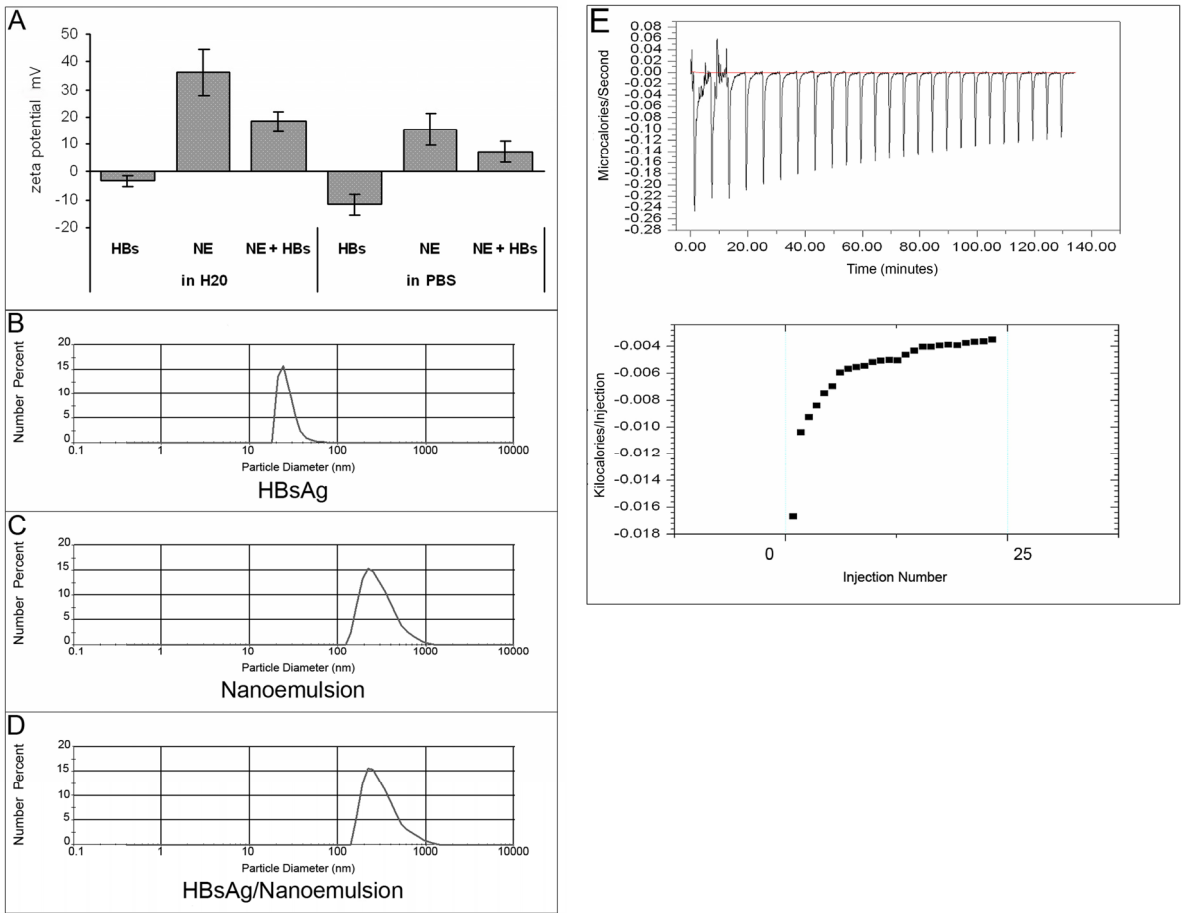

Figure 2.2. HBsAg interaction with NE droplets. Zeta potential: **A)** The zeta potential was measured for HBsAg (2.5 mg/ml), 20% NE and mixture of HBsAg with NE (HBsAg-NE) in water and PBS. Surface charge is reported in mV units. Particle sizing: Size distribution was measured using a laser diffraction particle-sizer. Analysis of HBsAg alone **B)**, NE alone **C)**, and NE with 10 mg/ml of HBsAg **D)**. Data was processed and analyzed using Fraunhofer optical modeling and number weighted averaging (number %). Single population intensity peaks indicate monodisperse populations of HBsAg (28 nm), NE (349 nm), and HBsAg-NE (335 nm). **E)** Calorimetric titration of HBsAg with NE: 25 injections of 1% NE (10 µl/injection) were introduced into a sample cell containing HBsAg (600 µg/ml in PBS) at 30°C. The upper panel shows differences between the sample and reference cell containing PBS. The lower panel shows enthalpy per injection of NE injected versus injection number. An exothermic reaction was measured following the addition of nanoemulsion to an antigen solution. Addition of nanoemulsion to the antigen solution became less energetic as the total concentration of nanoemulsion increased, suggesting that the antigen was being depleted. ΔCp was calculated to be -1.44 [77].

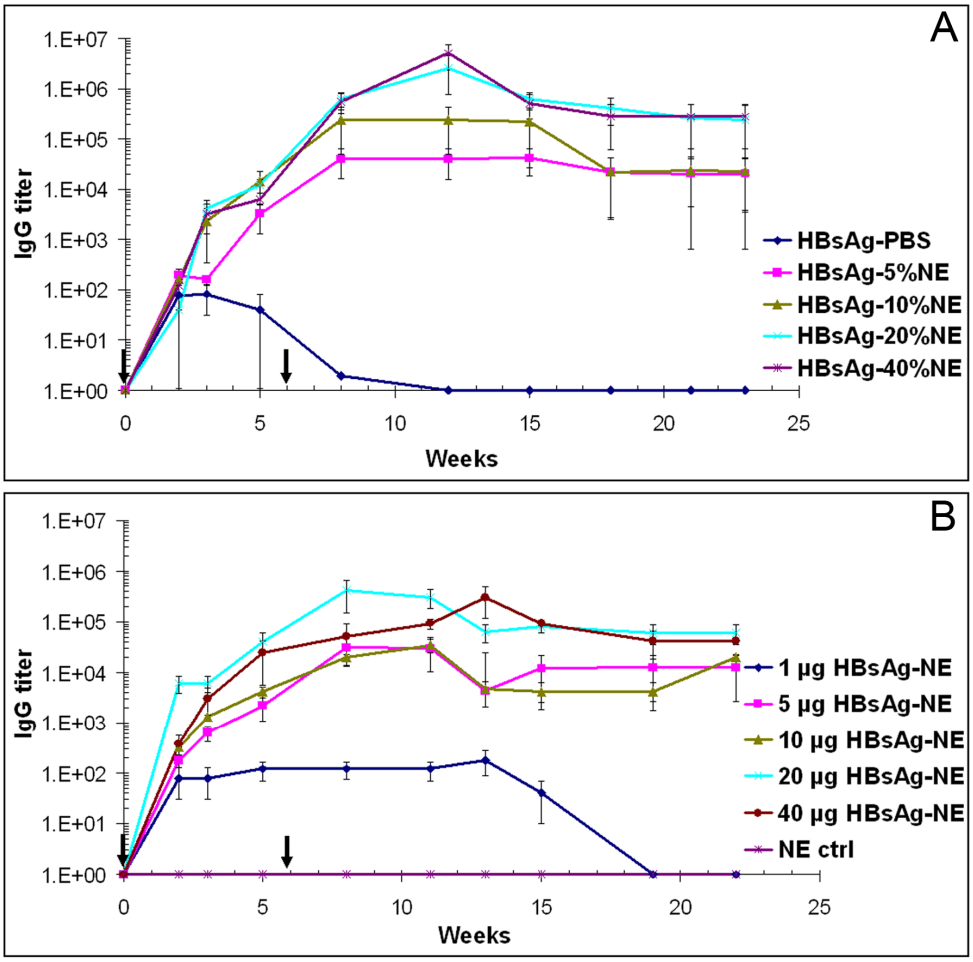

Figure 2.3. Development of IgG response in serum. Effect of NE adjuvant: Mice were immunized intranasally with HBsAg-NE consisting of 20 µg of HBsAg mixed with 0% to 40% concentrations of NE **A)**. Significant statistical difference with *p-value* <0.05 was observed between all HBsAg-NE formulations and HBsAg-PBS vaccine. Antigen dose escalation: Mice were immunized intranasally with 1 µg to 40 µg HBsAg mixed with 20% NE **B)**. A significant statistical difference with *p value* < 0.05 was observed between all 5 µg to 40 µg HBsAg-NE formulations and 1 µg HBsAg-NE vaccine. Serum anti-HBsAg IgG antibody concentrations are presented as mean of endpoint titers in individual sera ±SEM. * indicates a statistical difference (*p-value* <0.05) in the anti-HBsAg IgG titers. Arrows indicate vaccine administration.

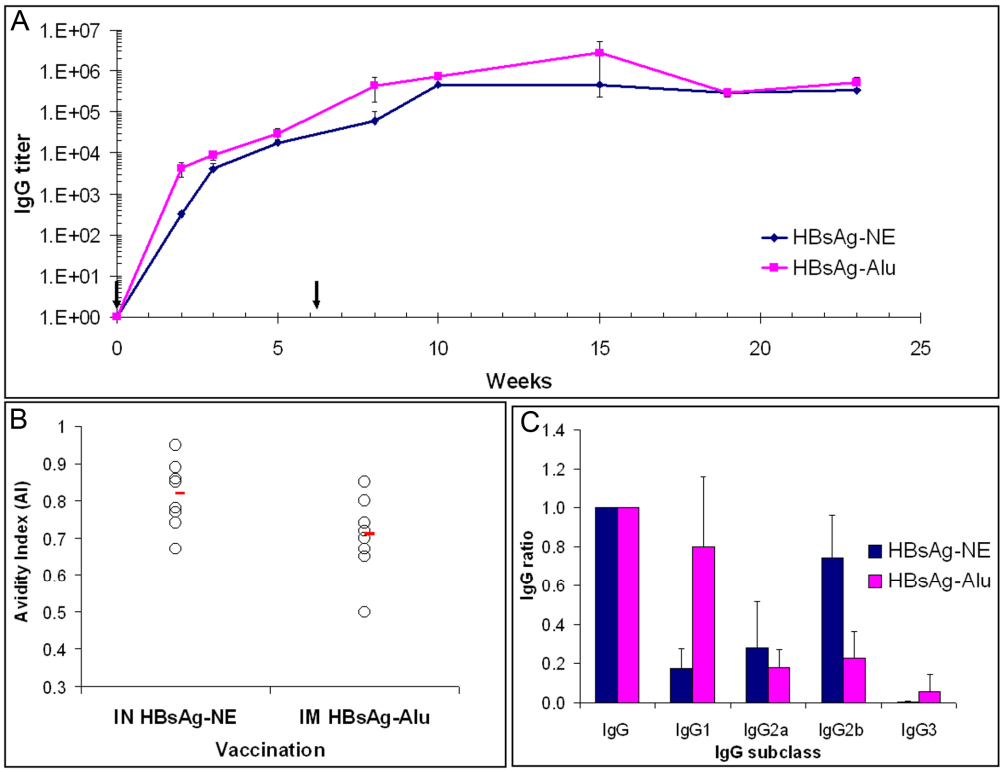

Figure 2.4. Comparison of mucosal NE-based with conventional aluminum-based injectible HBsAg vaccine. Time course of antibody response: Mice were immunized with 20 mg HBsAg. Antigen was mixed with 20% NE for intranasal administration (HBsAg-NE), or adsorbed on aluminum hydroxide (HBsAg-Alu) for intramuscular injections **A)**. Serum anti-HBsAg IgG antibody concentrations are presented as mean of endpoint titers in individual sera ± SEM. * indicates a statistical difference (*p-value* <0.05) in the anti-HBsAg IgG titers. Arrows indicate vaccine administration. Avidity of anti-HBsAg IgG: Analysis of sera from mice immunized i.n. with HBsAg-NE and with i.m. injections of HBsAg-Alu vaccines **B)**. Avidity indexes (AI) were assessed using 1.5 M NaSCN as a discriminating salt concentration. Each circle represents individual AI and lines indicate mean AI value for each group obtained in two independent assays. Serum anti-HBsAg IgG subclass: Anti-HBsAg IgG subclass pattern in mice immunized nasally with HBsAg-NE and injected i.m. with HBsAg-Alu vaccine **C)**. Analysis of sera collected at 22 weeks after initial immunization. The results are presented as ratio of the specific subclass IgG to the overall IgG titer. * indicates statistical difference (*p-value* <0.05) between NE-based and alum-based immunizations.

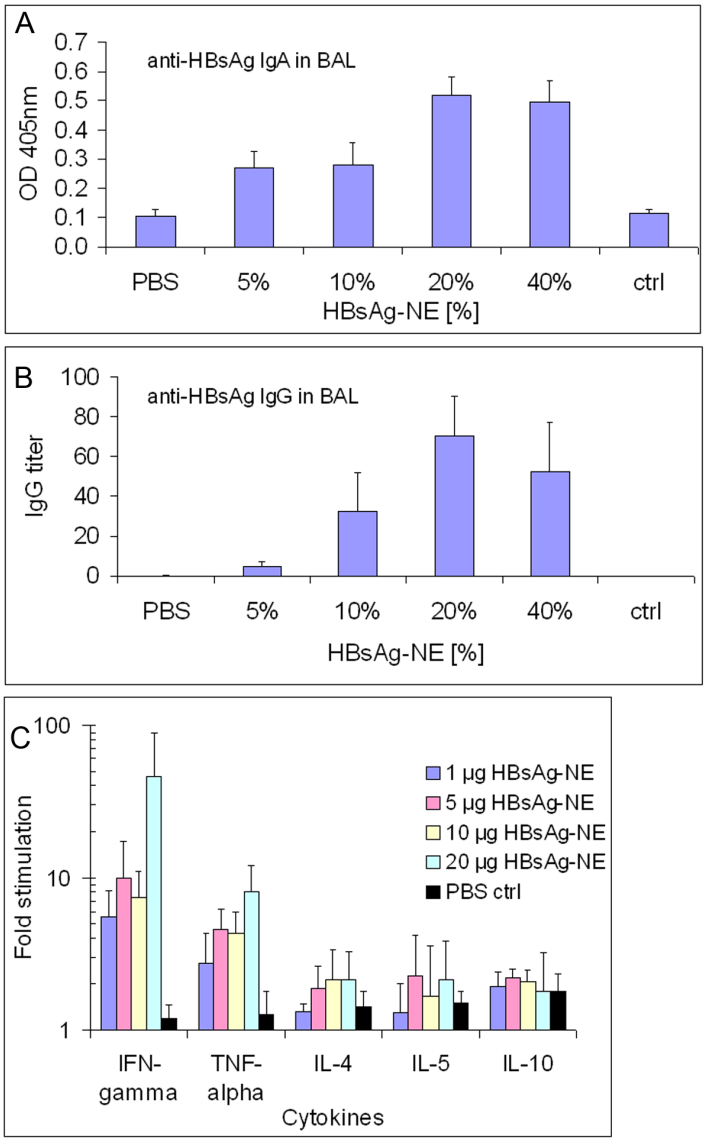

Figure 2.5. Characterization of immune response mucosal and cellular responses to HBsAg-NE. Mucosal antibody measurements were performed in BAL fluids obtained 23 weeks after i.n immunization with HBsAg-NE vaccines. IgA detection: The anti-HBsAg IgA detection was performed with 1:2 dilutions of BAL **A)**. Results are presented as mean values of OD at 405 nm ±SEM. IgG detection: The anti-HBsAg IgG antibody concentrations are presented as end point titers **B)**. Antigen-specific cytokine expression. Pattern of Th1 (IFN-γ and TNF-α) and Th2 (IL4, IL5 and IL10) cytokine expression in vitro in splenocytes from mice intranasally immunized with HBsAg-NE **C)**. Splenocytes were obtained at 23 weeks after initial immunization from mice with HBsAg-20% NE. Results are presented as fold increase of the cytokine production over levels detected in non-stimulated splenocyte cultures.

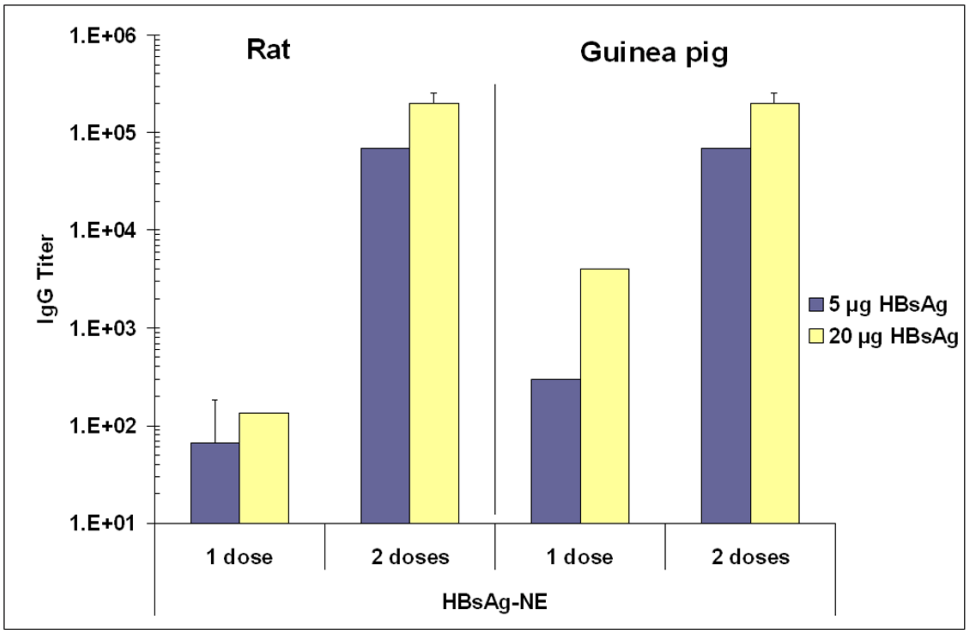

Figure 2.6. Immunogenicity in rats and guinea pigs. Rats and guinea pigs were immunized intranasally with either 5 µg or 20 µg HBsAg mixed with 20% NE. Serum anti-HBsAg IgG antibody concentrations are presented as mean of endpoint titers in individual sera ±SEM. Data represents anti-HBsAg end titers measured 3 weeks after a single dose (1 dose) vaccination and after two vaccinations (2 doses) measured at 7 weeks.

\

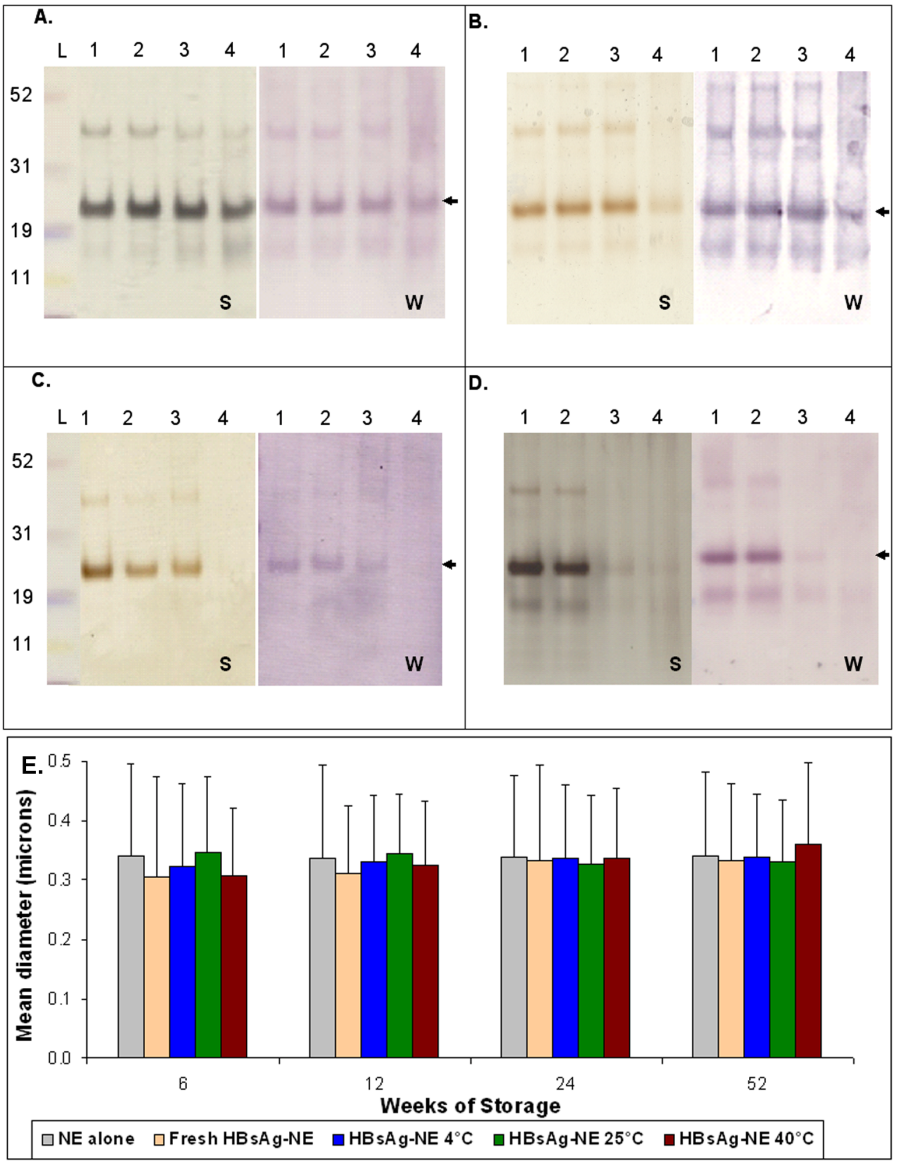

Figure 2.7. In vitro analyses of HBsAg-NE stability. The comparison of HBsAg-NE stored at test temperature conditions to freshly prepared formulation using SDS-PAGE followed by silver staining (S) or Western immunoblotting (W) is shown. Lanes are labeled according to sample storage conditions as follows- 1: fresh, 2: 4°C, 3: 25°C and 4: 40°C. Samples were stored for **A)** 6 weeks, **B)** 3 months, **C)** 6 months or **D)** 1 year (52 weeks) at the three test temperatures. Each lane contains 0.5 µg of antigen. Arrow indicates the HBsAg major band. **E)** Particle size comparison of NE alone to freshly mixed HBsAg-NE and formulation stored up to a year. Mean diameter of particles is shown in microns ± SD.

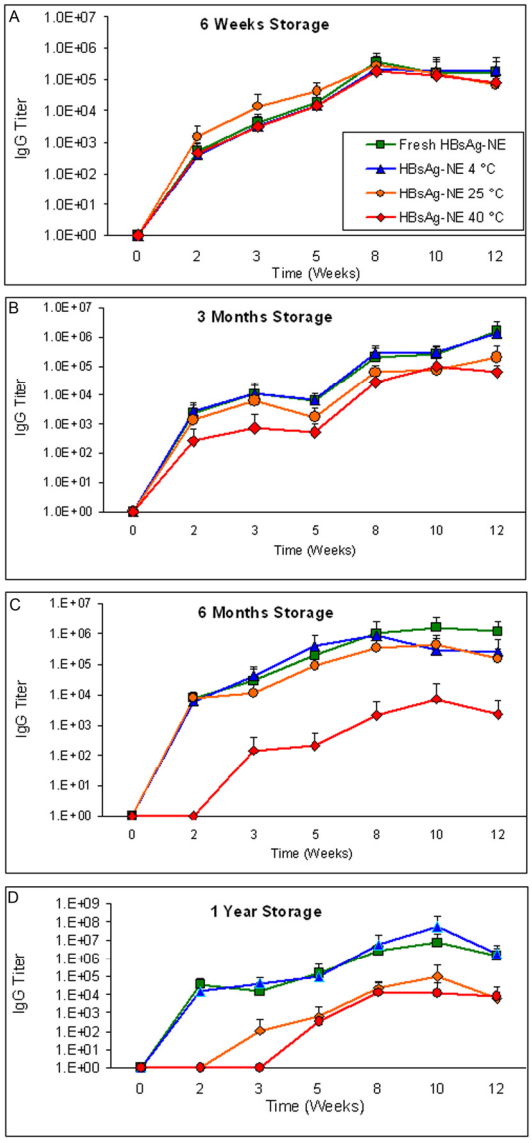

Figure 2.8. In vivo analyses of HBsAg-NE stability. HBsAg specific antibody responses to freshly prepared HBsAg-NE or HBsAg-NE stored under real-time (4°C), accelerated (25°C) and stressed (40°C) temperature conditions are depicted. CD-1 mice were vaccinated with either freshly prepared or stored HBsAg-NE and boosted at 6 weeks. Serum anti-HBsAg IgG antibody concentrations are presented as a mean of endpoint titers in individual sera ± SD. Comparison of serum IgG elicited by freshly prepared HBsAg-NE to formulation stored for **A)** 6 weeks, **B)** 3 months, **C)** 6 months or **D)** 1 year at indicated temperatures. * indicates a statistical difference (*p-value*<0.05) in the anti-HBsAg IgG titers between freshly mixed and stored formulation. Arrows indicate vaccine administration.

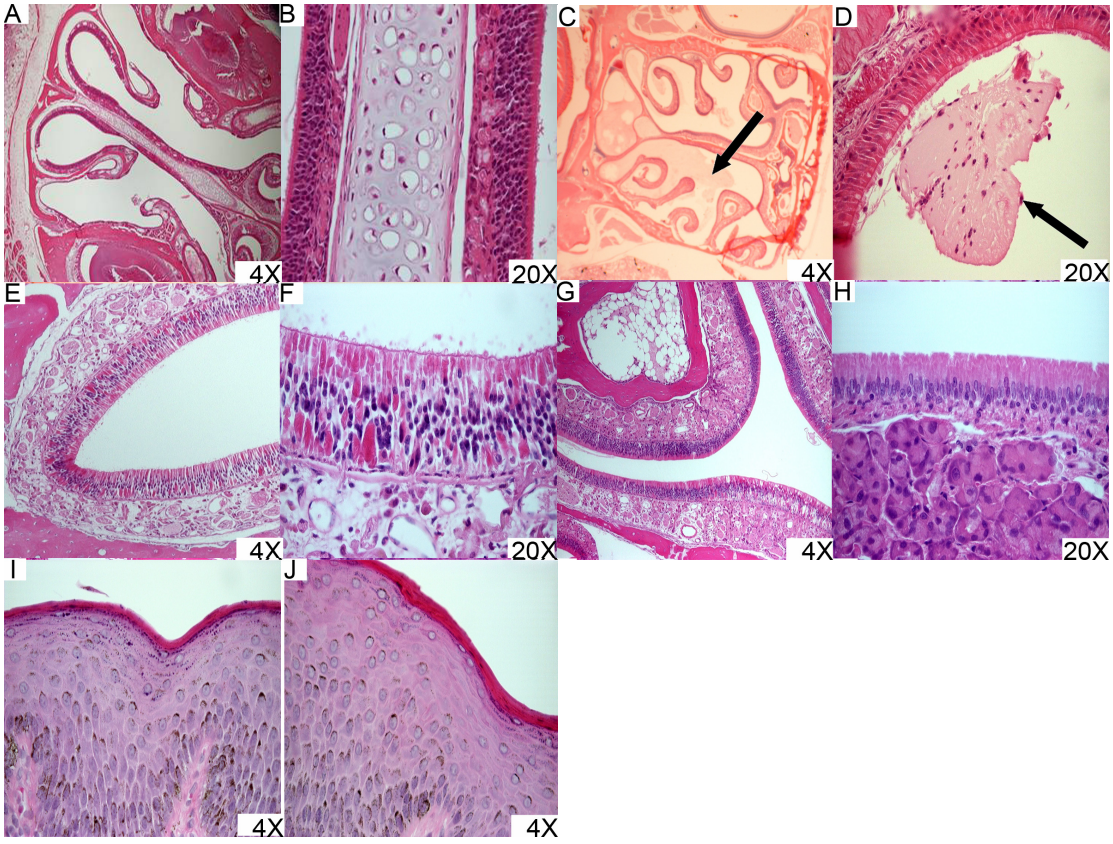

Figure 2.9. Histopathological analysis of nasal tissue exposed to NE adjuvant or HBsAg-NE. Mice: CD-1 mice were vaccinated with HBsAg-NE and primed at 2 weeks. **A–B**) Photomicrographs of H&E stained nasal epithelium collected from mice 14 days following the boost vaccination. Only normal tissue architecture was recorded which indicates a lack of (sub) chronic cytotoxicity or inflammation. **C)** Nasal epithelium collected 24 hours following boost vaccination with HBsAg-NE scored as a +1 grade change according to methodology as described is shown as an example of architectural change. The arrow indicates a single microscopic focus of accumulation of mucoid material and debris in the nasal passages. However, no evidence of epithelial necrosis or inflammatory infiltration of the nasal epithelium is detected. **D)** Nasal epithelium collected 24 hours following boost vaccination with HBsAg-NE scored as a +2 grade. The arrow indicates a single microscopic focus of accumulation of mucoid material and debris in the nasal passages in the absence of inflammatory changes. Architectural change demonstrated in **C** and **D** are considered incidental and can be observed in non-vaccinated mice. Rats and guinea pigs: Nasal epithelium was collected 14 days following final boost vaccination from rats **E–F)** and guinea pigs **G–H)** treated a total of 3 doses of HBsAg-NE administered 14 days apart. Normal tissue architecture is observed suggesting lack of toxicity or inflammation. Dogs: Nasal biopsies were collected 24 hours following the final dose in dogs treated with a total of three doses of NE adjuvant. NE was delivered using a Pfeiffer multidose wide angle sprayer pump in 200 µl/dose **I)** or 400 µl/dose **J)**. No evidence of inflammation or cytotoxicity was detected.

2.8 REFERENCES

1. Assad, S., Francis, A., *Over a decade of experience with a yeast recombinant hepatitis B vaccine.* Vaccine, 1999. 18: p. 57–67.

2. Floreani, A., Baldo, V., Cristofoletti, M., Renzulli, G,, Valeri, A., et al. *Longterm persistence of anti-HBs after vaccination against HBV: an 18 year experience in health care workers.* Vaccine, 2004. 22: p. 608–611.

3. Gesemann, M., Scheiermann, N., *Quantification of hepatitis B vaccine-induced antibodies as a predictor of anti-HBs persistence.* Vaccine, 1995. 13: p. 443–447.

4. CDC, *Global progress toward universal childhood hepatitis B vaccination.* MMWR, 2003. 52: p. 868–870.

5. Giudice, E. L., Campbell, J. D., *Needle-free vaccine delivery.* Advanced Drug Delivery Reviews, 2006. 58: p. 68–89.

6. World Health Organization, Hepatitis B Fact sheet no. 204. 2000.

7. Chisari FV, Ferrari C., *Hepatitis B Virus Immunopathogenesis.* Ann Rev Immunol, 1995. 13: p. 29–60.

8. Peterson, D. L., *The structure of hepatitis B surface antigen and its antigenic sites.* BioEssays, 1987. 6: p. 258–262.

9. Schirmbeck, R., Melber, K., Kuhrober, A., Janowicz, Z. A., Reimann, J., *Immunization with soluble hepatitis B virus surface protein elicits murine H-2 class I-restricted CD8+ cytotoxic T lymphocyte responses in vivo.* J Immunol, 1994. 152: p.110–1119.

10. Seeger, C., Mason, W. S., *Hepatitis B Virus Biology.* Microbiol Mol Biol Rev, 2000. 64: p. 51–68.

11. Gilbert, R. J. C., Beales, L., Blond, D., Simon, M. N., Lin BY, et al., *Hepatitis B small surface antigen particles are octahedral.* PNAS, 2005..14783–14788.

12. Woo, W.-P., Doan, T., Herd, K. A., Netter, H.-J., Tindle, R. W., *Hepatitis B Surface Antigen Vector Delivers Protective Cytotoxic T-Lymphocyte Responses to Disease-Relevant Foreign Epitopes.* J Virol, 2006. 80: p.3975–3984.

13. Lemon, S. M., Thomas, D. L., *Vaccines to Prevent Viral Hepatitis.* N Engl J Med, 1997. 336: p.196–204.

14. Gherardi, R. K., Coquet, M., Cherin, P., Belec, L., Moretto, P., et al., *Macrophagic myofasciitis lesions assess long-term persistence of vaccine-derived aluminium hydroxide in muscle.* Brain, 2001. 124: p.1821–1831.

15. Pittman, P. R., *Aluminum-containing vaccine associated adverse events: role of route of administration and gender.* Vaccine, 2002. 20: S48–S50.

16. Gupta, R. K., *Aluminum compounds as vaccine adjuvants.* Advanced Drug Delivery Reviews, 1998. 32: p. 155–172.

17. Geissler, M., Tokushige, K., Chante, C. C., Zurawski, V. R. Jr., Wands, J. R., *Cellular and humoral immune response to hepatitis B virus structural proteins in mice after DNA-based immunization.* Gastroenterology, 1997. 112: p.1307–1320.

18. Schirmbeck, R., Zheng, X., Roggendorf, M., Geissler, M., Chisari, F. V., et al., T*argeting Murine Immune Responses to Selected T Cell- or Antibody-Defined Determinants of the Hepatitis B Surface Antigen by Plasmid DNA Vaccines Encoding Chimeric Antigen.* J Immunol, 2001. 166: p. 1405–1413.

19. The Bill and Melinda Gates Foundation, *Gates Foundation Grand Challenges in Global Health Initiative*, 2005.

20. Hilleman, M. R., *Overview of the pathogenesis, prophylaxis and therapeusis of viral hepatitis B, with focus on reduction to practical applications* Vaccine, 2001. 19: p. 1837–1848.

21. Davis, S. S., *Nasal vaccines.* Advanced Drug Delivery Reviews, 2001. 51:21–42.

22. Illum, E., Davies, S. S., *Nasal vaccination: a non-invasive vaccine delivery method that holds great promise for the future.* Advanced Drug Delivery Reviews, 2001. 51: p. 1–3.

23. Chen, H., *Recent advances in mucosal vaccine development.* Journal of Controlled Release, 2000. 67: p. 117–128.

24. Neutra, M. R., Kozlowski, P. A., *Mucosal vaccines: the promise and the challenge.* Nat Rev Immunol, 2006. 6: p. 148–158.

25. Isaka, M., Yasuda, Y., Mizokami, M., Kozuka, S., Taniguchi, T., et al. *Mucosal immunization against hepatitis B virus by intranasal co-*

administration of recombinant hepatitis B surface antigen and recombinant cholera toxin B subunit as an adjuvant. Vaccine, 2001. 19: p. 1460–1466.

26. Saraf, S., Mishra, D., Asthana, A., Jain, R., Singh, S., et al., *Lipid microparticles for mucosal immunization against hepatitis B.* Vaccine, 2006. 24: p. 45–56.

27. McCluskie, M. J., Davis, H. L., *Cutting Edge: CpG DNA Is a Potent Enhancer of Systemic and Mucosal Immune Responses Against Hepatitis B Surface Antigen with Intranasal Administration to Mice.* J Immunol, 1998. 161: p. 4463–466.

28. Payette, P., Ma, X., Weertna, R., McCluskie, M., Shapiro, M., et al., Te*sting of CpG-optimized protein and DNA vaccines agains the hepatitis B virus in chimmpanzees for immunogenecity and protection from challenge.* Intervirology, 2006. 49: p. 144–151.

29. Debin, A., Kravtzoff, R., Santiago, J. V., Cazales, L., Sperandio, S., et al., *Intranasal immunization with recombinant antigens associated with new cationic particles induces strong mucosal as well as systemic antibody and CTL responses.* Vaccine, 2002. 20: p. 2752–2763.

30. Jaganathan, K. S., Vyas, S. P., *Strong systemic and mucosal immune responses to surface-modified PLGA microspheres containing recombinant hepatitis B antigen administered intranasally.* Vaccine, 2006. 24: p. 4201–4211.

31. Aguilar, J.C., Acosta-Rivero, N., Duenas-Carrera, S., Morales, Grillo, J., Pichardo, D., et al., *HCV core protein modulates the immune response against the HBV surface antigen in mice.* Biochemical and Biophysical Research Communications, 2003. 310: p. 59–63.

32. Aguilar, J. C., Lobaina, Y., Muzio, V., Garcia, D., Penton, E., et al., *Development of a nasal vaccine for chronic hepatitis B infection that uses the ability of hepatitis B core antigen to stimulate a strong Th1 response against hepatitis B surface antigen.* Immunol Cell Biol, 2004. 82: p. 539–546.

33. Lobaina, Y., Garcia, D., Abreu, N., Muzio, V., Aguilar, J. C., *Mucosal immunogenicity of the hepatitis B core antigen.* Biochemical and Biophysical Research Communications, 2003. 300: p. 745–750.

34. Hepatitis B Foundation, Hepatitis B Clinical Trials. 2007. www.hepb.org.

35. Betancourt, A. A., Delgado, C. A. G., Estevez, Z. C., Martinez, J. C., Rios, G. V., et al., *Phase I clinical trial in healthy adults of a nasal vaccine*

candidate containing recombinant hepatitis B surface and core antigens. International Journal of Infectious Diseases 2007. In Press, Corrected Proof.

36. Zuckerman, J. N., *Protective efficacy, immunotherapeutic potential, and safety of hepatitis B vaccines.* J Med Virol, 2006. 78: p. 169–177.

37. Hamouda, T., Baker, J. R., *Antimicrobial mechanism of action of surfactant lipid preparations in enteric gram-negative bacilli.* Journal of Applied Microbiology, 2000. 89: p. 397–403.

38. Hamouda, T., Hayes, M. M., Cao. Z., Tonda, R., Johnson, K., et al., *A Novel Surfactant Nanoemulsion with Broad-Spectrum Sporicidal Activity against Bacillus Species.* The Journal of Infectious Diseases, 1999. 180: p. 1939–1949.

39. Hamouda, T., Myc, A., Donovan, B., Shih, A. Y., Reuter, J. D., et al., *A novel surfactant nanoemulsion with a unique non-irritant topical antimicrobial activity against bacteria, enveloped viruses and fungi.* Microbiol Res, 2001. 156: p. 1–7.

40. Bielinska, A. U., Chepurnov, A. A., Landers, J. J., Janczak, K. W., Chepurnova, T. S., et al., *A novel killed-virus nasal vaccinia virus vaccine.* Clinical and Vaccine Immunology, 2008. 15: p. 348–358.

41. Bielinska, A. U., Janczak, K. W., Landers, J. J., Makidon, P., Sower, L. E., et al., *Mucosal Immunization with a Novel Nanoemulsion-Based Recombinant Anthrax Protective Antigen Vaccine Protects against Bacillus anthracis Spore Challenge.* Infect Immun, 2007. 75: p. 4020–4029.

42. Bielinska, A. U., Janczak, K. W., Landers, J. J., Markovitz, D. M., Montefiori, D. C., et al., *Nasal immunization with a recombinant HIV gp120 and nanoemulsion adjuvant produces TH1 polarizatied responses and neutralizing antibodies to primary HIV-1 isolates.* AIDS Research and Human Retroviruses, 2007. 24: p. 271–281.

43. Myc, A., Kukowska-Latallo, J. F., Bielinska, A. U., Cao, P., Myc, P. P., et al., *Development of immune response that protects mice from viral pneumonitis after a single intranasal immunization with influenza A virus and nanoemulsion.* Vaccine, 2003. 21: p. 3801–3814.

44. Park, M. H., Song, E. Y., Ahn, C., Oh, K. H., Yang, J., et al., *Two subtypes of hepatitis B virus-associated glomerulonephritis are associated with different HLA-R2 alleles in Koreans.* Tissue Antigens, 2003. 62: p. 505–511.

45. Talaro, K. P., Foundations in Microbiology: Brown, W.C. 1993 pp 806.

46. HogenEsch, H., *Mechanisms of stimulation of the immune response by aluminum adjuvants.* Vaccine, 2002. 20: S34–S39.

47. Katare, Y. K., Panda, A. K., *Immunogenicity and lower dose requirement of polymer entrapped tetanus toxoid co-administered with alum.* Vaccine, 2006. 24: p. 3599–3608.

48. Niu, M. T., Rhodes, P., Salive, M., Lively, T., Davis, D. M., et al., *Comparative Safety of Two Recombinant Hepatitis B Vaccines in Children,: Data from the Vaccine Adverse Event Reporting System (VAERS) and Vaccine Safety Datalink (VSD).* Journal of Clinical Epidemiology, 1998. 51: p. 503–510.

49. Poland, G. A., Jacobson, R. M., *Prevention of Hepatitis B with the Hepatitis B Vaccine.* N Engl J Med, 2004 351: p. 2832–2838.

50. Michel, M. L., Mancini-Bourgine, M., *Therapeutic vaccination against chronic hepatitis B virus infection.* Journal of Clinical Virology, 2005. 34: S108–S114.

51. Van Herck, K., Van Damme, P., Thoelen, S., Meheus, A., *Long-term persistence of anti-HBs after vaccination with a recombinant DNA yeast-derived hepatitis B vaccine: 8-year results.* Vaccine, 1998. 16: p. 1933–1935.

52. Anttila, M. Voutilainen, M. Jantti, V. Eskola, J., Kayhty, H., *Contribution of serotypespecific IgG concentration, IgG subclasses and relative antibody avidity to opsonophagocytic activity against Streptococcus pneumoniae.* Clinical & Experimental Immunology, 1999. 118: p. 402–407.

53. Lambert, P.-H., Liu, M., Siegrist, C.-A., *Can successful vaccines teach us how to induce efficient protective immune responses?* Nat Med, 2005. 11: S54–S62.

54. Bielinska, A. U., Janczak, K. W., Landers, J. J., Markovitz, D. M., Montefiori, D. C., et al., *Nasal immunization with a recombinant HIV gp120 and nanoemulsion adjuvant produces TH1 polarizatied responses and neutralizing antibodies to primary HIV-1 isolates.* AIDS Research and Human Retroviruses, 2008, 24: p. 271–281.

55. Leroux-Roels, G., Van Hecke, E., Michielsen, W., Voet, P., Hauser, P., et al., *Correlation between in vivo humoral and in vitro cellular immune*

responses following immunization with hepatitis B surface antigen (HBsAg) vaccines. Vaccine, 1994. 12: p. 812–818.

56. McClary, H., Koch, R., Chisari, F. V., Guidotti, L. G., *Relative Sensitivity of Hepatitis B Virus and Other Hepatotropic Viruses to the Antiviral Effects of Cytokines.* J Virol, 2000. 74: p. 2255–2264.

57. Wieland, S. F., Guidotti, L. G., Chisari, F. V., *Intrahepatic Induction of Alpha/Beta Interferon Eliminates Viral RNA-Containing Capsids in Hepatitis B Virus Transgenic Mice.* J Virol, 2000. 74: p. 4165–4173.

58. Brewer, J. M., *(How) do aluminium adjuvants work?* Immunology Letters, 2006. 102: p. 10–15.

59. Khajuria, A., Gupta, A., Malik, F., Singh, S., Singh, J., et al., *A new vaccine adjuvant (BOS 2000) a potent enhancer mixed Th1/Th2 immune responses in mice immunized with HBsAg.* Vaccine, 2007. 25: p. 4586–4594.

60. Harandi, A. M., Sanches, J., Eriksson, K., Holmgren, J., *Recent development in mucosal immunomodulatory adjuvants.* Curr Opin Investig Drugs, 2003. 4: p. 156–161.

61. Yoshikazu, Y. Kiyono, H., *New generation of mucosal adjuvants for the induction of protective immunity.* Rev Med Virol, 2003. 13: p. 293–310.

62. Conti, L., Cardone, M., Varano, B., Puddu, P., Belardelli, F., et al., *Role of the cytokine environment and cytokine receptor expression on the generation of functionally distinct dendritic cells from human moncytes.* Eur J Immunol, 2008. 38: p. 750–762.

63. Egan, M. A., Chong, S. Y., Hagen, M., Megati, S., Schadeck, E. B., et al., *A comparative evaluation of nasal and parenteral vaccine adjuvants to elicit systemic and mucosal HIV-1 peptide-specific humoral immune responses in cynomolgus macaques.* Vaccine, 2004. 22: p. 27–28.

64. Sato, A., Hashinguchi, M., Toda, E., Iwasaki, A., Hachimura, S., et al., *CD11b+ Peyer's patch dendritic cells secrete IL-6 and induce IgA secretion from naive B cells.* J Immunol, 2003. 171: p. 3684–3690.

65. Iyer, S. *Mechanism of adsorption of hepatitis B surface antigen by aluminum hydroxide adjuvant.* Vaccine, 2004. 22: p. 1475–1479.

66. Makhatadze, G. I., Privalov, P. L., *Heat capacity of proteins. I. Partial molar heat capacity of individual amino acid residues in aqueous solution: hydration effect.* J Molecular Biology, 1990. 213: p. 375–384.

67. Vanlandschoot, P., Leroux-Roels, G., *Viral apoptotic mimicry: an immune evasion strategy developed by the hepatitis B virus?* Trends in Immunology, 2003. 24: p.144–147.

68. Graham, B. S., *New approaches to vaccine adjuvants:inhibiting the inhibitor.* Plos Medicine, 2006. 3: e57.

69. van Ginkel, F. W., Jackson, R. J., Yoshino, N., Hagiwara, Y., Metzger, D. J., et al., *Enterotoxin-Based Mucosal Adjuvants Alter Antigen Trafficking and Induce Inflammatory Responses in the Nasal Tract.* Infect Immun, 2005. 73: p. 6892–6902.

70. Mutsch, M., Zhou, W., Rhodes, P., Bopp, M., Chen, R. T., et al., *Use of the inactivated intranasal influenza vaccine and the risk of Bell's Palsy in Switzerland.* New Enland Journal of Medicine, 2004. 350: p. 896–903.

71. MicroCal, LLC., VP-ITC MicroCalorimeter User's Manual, 2007. Northhampton, MA:

72. Little, S. F., Webster, W. M., Norris, S. L. W., Andrews, G. P., *Evaluation of an antirPA IgG Elisa for measuring the antibody response in mice.* Biologicals, 2004. 32: p. 62–69.

73. Classen, D. C., Morningstar, J. M., Shanley, J. D., *Detection of antibody to murine cytomegalovirus by enzyme linked immunobasorbent and indirect immunofluorescence assays.* J Clin Microbiol, 1987. 25: p. 600–604.

74. Frey, A., Di Canzio, J., Zurakowski, D., *A statistically defined endpoint titer determination method for immunoassays.* J Immunol Methods, 1998. 221: p. 35–41.

75. Vermont, C. L., van Dijken, H. H., van Limpt, C. J. P., de Groot, R., van Alphen, L., et al., *Antibody Avidity and Immunoglobulin G Isotype Distribution following Immunization with a Monovalent Meningococcal B Outer Membrane Vesicle Vaccine.* Infect Immun, 2002. 70: p. 584–590.

76. Herbert, R. A., Leininger, J. R., Pathology of the Mouse; Maronpot R, ed. 1999. St. Louis: Cache River Press.

77. MicroCal, LLC., VP-ITC MicroCalorimeter User's Manual. MAU130030 Rev. E ed., 2007. Northampton, MA:

CHAPTER 3
NANOEMULSION NASAL MUCOSAL ADJUVANT MECHANISM OF ACTION: INDUCTION OF ANTIGEN SAMPLING AND ROLE OF IL6

3.1 BACKGROUND

There is a critical need for new adjuvants to induce specific immune responses safely in humans, particularly mucosal adjuvants [1]. A major limitation to the development of these adjuvants has been due to the lack of understanding of mucosal adjuvant mechanisms. As described in Chapters 1 and 2, our group has developed a unique soybean oil-based nanoemulsion (NE) with topical bactericidal, fungicidal, and virucidal activity [2-5]. We have shown that mixing antigen or whole organisms with similar formulations to microbiocidal NE formulations results in high titers of serum and mucosal antibodies as well as protective cellular immunity following nasal administration [7-10]. In this chapter, we investigate potential physiological, cellular, and molecular mechanisms by which NE stimulate immunity.

NE adjuvant induces a Th1 biased immune response in mice in the absence of histological inflammation or toxicity [7-12]. As reported in Chapter 2, the simple mixing of antigen with NE cause the antigen to interface with the surface of the emulsion oil droplets at the oil/water interface. This led us to hypothesize that the ability of the NE droplet to penetrate mucosal membranes and facilitate uptake by mucosal antigen presenting cells provided its adjuvant activity, potentially through the recognition of dendritic cell membrane-associated molecules. The latter phenomenon has been shown to be important in the mechanism of action of other mucosal adjuvants such as cholera toxin (CT) and heat labile toxin (LT) [13-15]. In the present work we explore the ability of the NE mucosal adjuvant to induce antigen internalization and sampling by innate

immune cells at early time points *in vitro*, as well as clarifying the trafficking of antigen after nasal application in mice. We also analyze the participation of inflammatory mediators in the adjuvant activity of the NE.

3.2 EXPERIMENTAL METHODS

Animals, cell lines, culture conditions, and reagents

In these studies 8-12 week old female outbred CD-1 mice, inbred BALB/c, IL6 gene deficient mice (IL6(-/-)) [B6.129s2-IL6^{TM1KOPF}/J], and C57BL/6 mice (WT) mice purchased from Jackson Laboratories were used. The mice were housed by the Unit for Laboratory Animal Medicine at the University of Michigan under pathogen-free conditions. These studies were approved by the University Committee on Use and Care of Animals at the University of Michigan. The murine, dendritic cell line Jaws II was obtained from ATCC (CRL-11904) and cultured in RPMI containing 10% bovine fetal serum. E-GFP was acquired from BioVision Research Products. Anti-mouse DEC205-PE conjugated antibody and anti-mouse CD11c-PE conjugated antibody were bought from Miltenyi Biotec. Most of the experiments shown here were accomplished using the nanoemulsion adjuvant formulated in Tween 80 unless specified. The nanoemulsions adjuvants (NE formulated with Tween 80 and NEP407: formulated with P407 detergent) were provided by NanoBio Corporation. The recombinant Hepatitis B surface antigen (HBsAg) was provided by Indian Immunological and the *B. anthracis* rPA was obtained from List Biological Laboratories, Inc. The GM1 was obtained from Matreya LLC. The cholera toxin B subunit (CTB) and rabbit anti-CT antibody were from Sigma Aldrich. Rabbit polyclonal anti E-GFP was acquired from Open Biosystems. Anti-IL6-PE conjugated antibody and anti-CD11c-FITC conjugated antibodies were obtained from BioLegend. Anti-rabbit-rhodamine conjugated, antibody anti-rabbit-alkaline phosphatase conjugated antibody, and anti-mouse-FITC conjugated antibody were procured from KPL. Anti-mouse IgG and IgA-alkaline phosphatase conjugated antibodies were from

Jackson ImmunoResearch Laboratories Inc. Alkaline phosphatase (AP) conjugated rabbit anti-mouse IgG (H&L), IgG1, IgG2a, IgG2b, IgG3, IgA (a chain specific) antibodies were purchased from Rockland Immunochemicals, Inc. Quantum dots (Qtracker 655 non-targeted), ovalbumin Alexa 647 and 488 conjugates, Prolong Gold containing DAPI and DAPI were purchased from Molecular Probes. UE-1 lectin labeled with FITC, and wheat germ agglutinin lectin (WGA) labeled with FITC were purchased from Vector Laboratories.

Antigen and NE internalization into Jaws II and bone marrow-derived, murine dendritic-like cells

To analyze uptake of ovalbumin-Alexa 488 antigen (OVO-Alexa 488) into Jaws II dendritic-like cells, Jaws II cells were incubated for 30 minutes at 37^{o}C with OVO-Alexa 488 10 µg/ml in PBS or with OVO-Alexa 488 10 µg/mL mixed in 0.001% NE. The 0.001% NE concentration was chosen to ensure full viability of cells growing as a monolayer culture. After incubation, cells were washed 3 times with PBS and mounted with the antifade solution ProLong containing DAPI to stain blue the nuclei. The samples were imaged using the Zeiss LSM501 laser confocal microscope using the Argon and Enterprise lasers. The *in vitro* uptake into bone marrow derived dendritic cells was developed using BALB/c mice. Bone marrow derived dendritic cells were generated as described previously [16]. using 100 ng/mL GM-CSF. At 7 to 9 days in culture over 90% of cells expressed CD11c^{+} DC marker as we determined by FACS analyses. For the antigen internalization, 2-3 x 10^{6} cells/well were incubated for 4 hours at 37^{o}C either with 5 µg/mL ovalbumin-Alexa 647 (OVO-Alexa 647) conjugate alone or with OVO-Alexa 647 mixed with nanoemulsion adjuvant. The OVO-Alexa 647-NE mixtures were added the bone marrow derived DC cultures to obtain a 5 µg/mL final concentration of protein and a 0.0001% to 0.01% range of NE concentration. After incubation, cells were washed 3 times with PBS, trypsynized, collected and fixed with 2% paraformaldehyde in PBS. For the FACS analyses cells were resuspended in 0.1% BSA in PBS and fluorescence emission was measured using Becton-Dickinson FACScan. Data were acquired with CellQuest software from Becton Dickinson Immunocytometry Systems and

mean channels fluorescence of acquired samples were analyzed using PC-Lysis software. Jaws II cells were stained with Nile red dye for lipid visualization by incubation for 4 h at 37^{o}C with a range 0.0005% to 0.005% of NE. After incubation, the cells were washed 3 times with cold PBS and fixed with 1.25% formalin in PBS. Lipid staining was performed using Nile red (Sigma) with a slight modification of previously described procedures [17, 18]. A stock solution of Nile red (100 µg/mL) was prepared in DMSO and stored in amber glass vial protected from light. Staining conditions were optimized and carried in situ using freshly prepared 1:100 dilution of Nile red in PBS. The dye solution was incubated with cells for 30 minutes protected from light and followed with two washes with PBS and water. The samples were imaged using the Zeiss LSM501 laser confocal microscope using the HeNe1 laser.

Sampling, staining, and preparation of tissues

To determine the co-localization of the model antigen E-GFP in different DC in mouse tissues 24 hours after nasal vaccination, the mice were nasally immunized (10 µL per nare) using a pipette with a mixture of E-GFP (10 µg/mouse, green fluorescence) with or without the NE adjuvant (20%). The animals were sacrificed 24 hours following immunization, and tissues (nasal epithelium, submandibular lymphoid nodes, thymus, and spleen) were collected in OTC (TissueTek) and frozen by slow immersion in liquid nitrogen. Then 5 µm tissue section slides were prepared in the Center for Organogenesis Morphology Core at the University of Michigan. The tissue sections were blocked for 10 minutes using the Power Block® solution from BioGenex, and stained with the corresponding fluorescent antibodies or control same isotype antibodies overnight at 4^{o}C in a humid chamber in PBS containing 0.1 % BSA. The stained tissue samples were mounted in ProLong containing DAPI (blue nuclear stain), and the imaging was accomplished using a Zeiss LSM501 laser confocal microscopy using HeNe1, Argon, and Enterprise lasers, as described above. The DC markers DEC205 and CD11c were probed with antibody conjugated with PE (red fluorescence). Tissue sections were also were also probed with wheat germ agglutinin (WGA, Vector labs) for the recognition of saccharides on the

surface of epithelial cells [19]. The hematoxylin and eosin staining of paraffin-embedded nasal tissues was accomplished following standard procedures. In order to determine the participation of M cells in the NE-associated antigen sampling, the mice were intranasally immunized with QDOTs plus or minus 20% NE (10 µL per nare containing 6.6 µl of 2 µM solution, Qtracker 655 non-targeted), PBS (10 µL per nare containing 6.6 µL of 2 µM solution, Qtracker 655), or CTB (10 µL per nare containing 6.6 µL of 2 µM solution, Qtracker 655 non-targeted and 10 µg CTB). These mice were sacrificed 30 minutes after inoculation, and the nasal epitheliums were isolated by scraping the tissue from the bone. Just preceding euthanasia, 2 µL per nare of the UE-1-FITC lectin was added to label the luminal surface of M cells. Tissues were mounted with ProLong containing DAPI and analyzed by laser confocal microscopy as described above. The 3D reconstructions of the Z scanning of the nasal epitheliums were accomplished using the Imaris® Suite software from Bitplane AG.

Electron microscopy analysis of nasal tissues

The sinus cavities were excised 24 hours post-vaccination and immersion-fixed in 2.5% glutaraldehyde in 0.05 M cacodylate buffer, pH 7.4, at room temperature for 4 hours. After fixation, the noses were demineralized in 7.5 percent disodium EDTA with 2.5% glutaraldehyde in the same buffer for seven days at room temperature on a rotary shaker, following a protocol adapted from Shapiro et al. [20]. After demineralization, they were rinsed in cacodylate buffer, and then post-fixed for 1.5 hours in one percent osmium tetroxide in buffer. Next, they were dehydrated in an ascending graded series of ethanol and then transferred into three 30 minutes changes of propylene oxide. Then the nasal tissues were infiltrated and embedded in Epon. Ultra-thin sections were viewed without post-staining on a Philips CM100 at 60 kv. The images were recorded digitally using a Hamamatsu ORCA-HR digital camera system, which was operated using AMT software (Advanced Microscopy Techniques Corp.) in the Microscopy and Image Laboratory at the University of Michigan.

In vivo fluorescence in the mice

Groups of 4 mice were inoculated with 10 µL/nare of QDOTs (6.6 µL of 2 µM solution, Qtracker 655 non-targeted, Molecular Probes, OR) plus 20% NE, QDOTs (6.6 µL of 2 µM solution) alone in PBS, QDOTs (6.6 µL of 2 µM solution) plus 20% NE plus GM1 (0.35 mM), or 20% NE alone. In-life fluorescence analysis was accomplished in isofluorane-anesthetized mice using the IVIS Imaging System 200 Spectrum series bioluminometer from Xenogen in the Center for Molecular Imaging at the University of Michigan. The QDOTs were used as a model antigen due to their relatively high level of *in vivo* fluorescence and their ability to interact with the lymphoid tissues in the mice [21].

Nasal immunization with either E-GFP or rPA in NE adjuvant and ELISA of specific serum IgG or secretory IgA and IgG antibodies

The immunizations were performed at day 0 and at week 4. At week 6, the animals were phlebotomized via the lateral saphenous vein. Serum was separated by centrifugation in a microvette CB 300 from Sarstedt, NC. Serum IgG titers were determined by an ELISA method developed in-house (see below). For studies evaluating tolerance development, one group of 5 CD-1 mice were nasally immunized with 10 µL per nare of E-GFP (10 µg) plus 20% NE. As a control, another group of mice were immunized with just the E-GFP protein (10 µg) in PBS with the same volume per nare (10 µL). A group of 5 CD-1 mice were left untreated (naïve control). For studies evaluating the role of IL6 in the signaling pathway for NE adjuvant activity, one group of 5 IL6 (-/-) and one group of WT mice were nasally immunized with 5 µL per nare of rPA (20 µg) plus 20% NE. Controls for this study consisted of one group of IL6 (-/-) mice and one group of WT mice who were immunized with just the rPA protein (20 µg) in PBS with the same volume per nare (5 µL), one group of IL6(-/-) and one group of WT mice who received 20% NE alone, one group of IL6(-/-) and one group of WT mice who were immunized intramuscularly (apaxial administration) of rPA

adsorbed to alum (20 µg rPA + 0.5 mg/mL Alum) in 50 µL total volume, and one group of IL6(-/-) and one group of WT mice who were left untreated (naïve control). Post-mortem bronchioloalveolar lavage were performed as described by Makidon, Bielinska et al. [10]. 18 weeks following prime vaccination for the measurement of secretory IgA and IgG antibodies. Lavagent was stored at -20°C until used. The ELISA assays were developed using immunoabsorbent ELISA plates from Nunclon; the antigen coating was performed with a 0.5 µg/well of either E-GFP or rPA in coating carbonate buffer (Sigma Aldrich) overnight at 4^{o}C. An anti-E-GFP or anti-rPA monoclonal antibody was used as a positive control. The ELISA assays protocol was carried out as we previously described [9,10].

Bronchoalveolar and nasal lavage analysis for cytokines and inflammatory cells

Groups of 5 CD-1 mice were intranasally treated with 20 µL (10 µL/nare) of 20% NE adjuvant in a single dose. Both bronchoalveolar and nasal lavage were performed directly post-mortem either 6 hours or 24 hours following treatment. The pooled nasal and bronchoalveolar lavagent from individual mice was centrifuged at 3500 RPM for 10 minutes (cytospin). Cytospin preparations of samples were fixed (50% methanol-acetone) and stained with Wright-Giemsa stain. Total and differential cell counts were performed on these stained preparations by microscopy. Supernatants from pooled cytospin samples were analyzed for the presence of interleukins IFN-γ, TNF-α, IL6, IL4, and IL17 using a Mouse Cytokine Premixed Lico*plex*® kit (LINCO Research, St. Charles, MO). Briefly, serial dilutions of the lyophilized standard were prepared in deionized water and transferred to appropriate microtiter wells containing diluted antibody-coated bead complexes and incubation buffer. Twenty-five µL of each supernatant sample were transferred to the appropriate wells containing diluted antibody-coated bead complexes and 25 µL incubation buffer. Samples were incubated at room temperature for 2 hours. After washing with assay wash buffer (200 µL/well), a 25 µL detection antibody cocktail was added to the appropriate wells and incubated for 60 minutes. After incubation, 25 µL Streptavidin-

Phycoerythrin was added to each well and incubated for 30 minutes. After a final wash, the plate was analyzed using the Luminex 100 analyzer (Luminex Corp.). A minimum of 50 events per beads complex were collected for each cytokine/sample and median fluorescence intensities were obtained. Cytokine concentrations were calculated based on standard curve data using a MasterPlex™ QT Analysis version 2 (MiraiBio). The results are expressed as mean ± SEM (n = 5). Comparisons between all groups for each respective cytokine were performed by analysis of variances, choosing $p < 0.05$ as significant. Analyses were performed using a Graphpad Prism version 4 (Graphpad Software).

Gene expression assays

Nasal epithelium was harvested 6 hours and 24 hours following nasal immunization (immediately post-mortem) from CD-1 mice. The tissue was collected in OTC and frozen by slow immersion in liquid nitrogen and stored at -80°C until used. Total RNA was extracted per sample using RNeasy (Qiagen) according to the manufacturer's instructions. RNA samples were pooled by groups and then processed by the the UMCCC Affymetrix Core Facility at the University of Michigan using a Ovation Biotin Labeling system from NuGen, Inc and following manufacturer's protocols. Prior to hybridization, the quality of RNA was accessed using an Agilent 2100 Bioanalyzer following protocols established at UMCCC Affymetrix Core. Hybridization, detection and scanning was achieved using a mouse GeneChip® 430 2.0 manufactured by Affymetrix and a Affymetrix Scanner 3000 following manufactures guidelines. Gene expression values were calculated using a robust multi-array average (RMA) [22].

3.3 RESULTS

NE adjuvant induces antigen internalization into dendritic-like cells *in vitro* and enhances lipid internalization of Jaws II cells

We first sought to investigate whether NE could influence the antigen internalization process in DC, which could enhance antigen presentation. As shown in Figure 3.1, we use two different methodologies to document that NE promotes antigen internalization into murine dendritic cells. We observed that NE markedly enhanced internalization of ovoalbumin-Alexa 488 (OVA-Alexa 488) into Jaws II cells (Figures 3.1A through 3.1C). FACS analyses confirmed NE promotes ovoalbumin (conjugated to Alexa 647) internalization into the murine primary bone marrow-derived DC as shown by in Figure 3.1, panels D through F. NE itself was internalized into the DC as documented by the increase in lipid content in Jaws II cells (Figure 3.1 panel G and H). Our results suggest that not only is NE internalized *in vitro* into Jaws II cells, it also promoted antigen internalization into DC antigen-presenting cells.

NE promotes antigen sampling activity in nasal epithelial cells' *in vivo* without disruption of the epithelial barrier

Nasally-applied NE adjuvant was shown not to disrupt the nasal tissues or induce acute inflammation at time points up to 72 hours after application (Figures 3.2A though 3.2C). Incidental lesions that were observed in the nasal epithelium after NE application were also found in control mice (Figure 3.2D through 3.2I), but no inflammation or neutrophilic infiltration is detected. As reported in Chapter 2, occasional lesions did not result in chronic inflammation and were not detected after 24 hours following nasal inoculation [10].

Mucosal antigen presentation often occurs through specialized antigen sampling cells called M cells. Murine M cells uniquely express a surface ligand for the UE-1 lectin [23]. Accordingly, we used FITC-label UE-1 lectin to stain M

cells in nasal epithelium isolated from mice 30 minutes after NE nasal administration. QDOTs were chosen as a surrogate for antigen due to their resistance to fixatives and resistance to degradation by cellular processing and the ability to identifiy their cellular localization. As shown in the laser confocal microscopy galleries and 3-D reconstructions of the Z scanning of immunized nasal epithelium (in Figures 3.3A through 3.3F), the bulk of QDOTs applied to nasal mucosa in PBS appear to internalized through the M cells in the nasal epithelium (Figure 3.3A and 3.3B). However, when NE is added, both QDOTs and UE-1 fluorescence are broadly distributed throughout the nasal epithelium (Figure 3.3C and 3.3D). We used the mucosal adjuvant CTB plus QDOTs as a control. As shown in Figures 3.3E and 3.3F, the fluorescence distribution of QDOTs and UE-1 in the CTB nasally administered mice is similar to that of QDOTs plus the NE adjuvant (Figures 3.3C and 3.3D). This data indicates that both the NE and CTB adjuvants rapidly induce broad nasal cellular internalization of QDOTs and UE-1 lectin not necessarily dependent on the antigen sampling activity of M cells.

TEM was used to examine the ultra-structural cellular effects following NE administration. As shown in Figures 3.4A and 3.4B, the nasal epithelium of a mouse exposed to NE adjuvant contained vesicle-like material homogenously distributed throughout the epithelial cells, with the droplets having an average diameter of 0.479 microns; consistent with the particle size of the NE. Despite the abundant vesicle-like material in the nasal epithelial cells, the morphology of the cells is otherwise normal and tight junctions between adjacent cells are intact (Figure 3.4C). In contrast, nasal epithelium from an untreated mouse was similar in appearance but did not show the cytoplasmic vesicle-like materials (Figure 3.4F). The QDOTs were detected throughout the cytoplasm of cells close to the basal lamina (Figures 3.4D and 3.4E) and in clumps inside the vesicle-like material (Figure 3.4E). The size measurements of this material were consistent with sizes of the QDOTs and NE particles, respectively. This data indicated that

the nasal epithelial cells internalize the both NE and QDOTs, potentially through a macropinocytic-like process that does not disrupt tight junctions between cells.

NE promotes antigen trafficking towards lymphoid tissues *in vivo* after nasal application

To examine the ability at 24 hours post-nasal application of the NE to promote antigen trafficking to lymphoid tissues, we used E-GFP in NE as a model antigen system. As shown in Figures 3.5A through 3.5F, we detected green fluorescence throughout the nasal epithelium, submandibular lymphoid tissue, and thymus (Figures 3.5D through 3.5F). In agreement with previous studies, the E-GFP fluorescence was associated with the majority of the epithelial cells after nasal inoculation with NE adjuvant (Figure 3.5D). The green fluorescence in these tissues was much more intense than for treatment with E-GFP in PBS alone (Figures 3.5A through 3.5C). Brain tissue sections of mice administered NE with E-GFP (particularly of the frontal lobes and olfactory bulbs) were analyzed using anti E-GFP antibody and showed neither E-GFP nor inflammation (Figures 3.5G and 3.5H). This supports the notion that NE does not promote antigen trafficking towards the olfactory bulb through the olfactory nerves.

To identify the cells which internalize the E-GFP, we employed laser confocal microscopy and with dual staining for E-GFP and DC markers (either DEC205 or CD11c red fluorescence) in the nasal epithelium and the thymus. All green fluorescent signals from mice treated with E-GFP-NE co-localized staining with DEC205 and CD11c as shown in the respective profiles (Figures 3.6A, 3.6C and 3.6E). In contrast, no green fluorescence was observed in DCs of mice nasally inoculated with E-GFP in PBS (Figures 3.6B, 3.6D, and 3.6F). Interestingly, 24 hours after nasal inoculation of E-GFP-NE, E-GFP-loaded DCs were not evident in the spleen as shown in Figure 3.6 profiles G and H. This suggests that free E-GFP does not reach the blood circulatory system. These results show that the NE adjuvant promotes E-GFP sampling by DC in the nasal epithelium and traffics the antigen towards the systemic immune system.

To address the possibility that E-GFP trafficking to the thymus may result in induction of antigen-specific tolerance, CD-1 mice were immunized with 10 μg of E-GFP, either with or without NE adjuvant. This resulted in the induction of high levels of E-GFP specific serum IgG antibodies only in animals immunized with E-GFP-NE (titers of 1:362,000 vs 1:18 in animals immunized with E-GFP alone), despite the presence of E-GFP in the thymus and lymphatics (Figures 3.5 and 3.6). The data indicates that nasal application of antigen in NE does not induce tolerance to foreign proteins despite increasing antigen trafficking to the thymus.

NE enhances uptake and dissemination of QDOTs after nasal administration in mice

To confirm that the NE adjuvant promotes antigen sampling and trafficking in mice, we nasally administered QDOTs in NE and followed the bioluminescence in live mice at regular time-points for up to 8 days following inoculation (Figure 3.7). Because the QDOTs have a neutral coating their non-specifically interaction with biological membranes is not expected. We were able to detect dissemination of QDOTs on areas overlying the anatomical location of lymphatic tissues in the animals 24 to 48 hours following nasal application of QDOTs and the NE adjuvant (Figure 3.7, column a). In contrast, in animals treated with QDOTs without NE, fluorescence was not detected in areas consistent with lymphoid tissues, as shown in Figure 3.7, column b. Interestingly, the dissemination of the QDOTs appeared to be inhibited when ganglioside GM1 was present in the mixture containing NE + QDOTs (Figure 3.7, column c). Naïve mice did not show fluorescence (the fifth mouse in each column and column d in Figure 3.7, respectively).

NE induces the production of IL6 in the epithelium

Adjuvants usually induce local inflammation which, in turn, helps to produce immune responses and cause adverse effects. While no local acute inflammatory response was observed histologically with NE nasal application (Figure 3.2), we studied local cytokine production in the nasal mucosa. HBsAg was used as a prototype antigen for these studies. Mice nasally administered NE either alone or with HBsAg were euthanized 6 and 24 hours following application. Nasal and bronchoalveolar lavage was collected to measure the secreted cytokines, and the numbers of neutrophils recruited to the lumen of the nasal epithelium were enumerated. As shown in Figure 3.8, after 24 hours following nasal inoculation with NE, the only cytokine uniquely induced by NE treatment in the lavage was IL6 (Figures 3.8A) but not IFN-γ, TNF-α IL4 or IL17. The production of IL6 was similar regardless of HBsAg presence but higher using the NE formulated with the P407 detergent (NEP407) compared to the Tween 80 containing NE (Figure 3.8A). Despite the increase in IL6, there was only a minimal increase in the neutrophil count in the lavage fluid (Figure 3.8B), and no other inflammatory cells were observed. This data confirms our previous results, as illustrated in Chapter 2, showing IL6 was present in the serum of mice 24 hours following vaccination with HBsAg-NE [10]. In order to determine the origin of IL6 in the bronchoalveolar lavage we prepared frozen sections of nasal tissue 24 hours following nasal treatment with rPA-NE or rPA in PBS. These tissues were stained with fluorescently labeled wheat germ agglutinin lectin and anti-IL6 antibodies. As shown in figure 3.8C and 3.8D, the IL6 is produced mainly by nasal epithelial cells of mice treated with NE but not inmice treated with rPA alone.

Role of IL6 cytokine in the mechanism of action of NE

To study the role of IL6 in the mechanism of action of NE, IL6 gene deficient mice (IL6-/-) and WT mice were nasally vaccinated twice (a prime vaccination and a boost at 4 weeks) with rPA (20 μg) in NE (20%) or with rPA (20 μg) in PBS. Vaccination with NE or NEP407 resulted in equivalent serum and

mucosal IgG and sIgA (Figure 3.9). A statisticaly significant difference in serum anti-rPA IgG and sIgA was observed between IL6-/- and WT mice following the prime and boost with rPA-NE versus rPA-NEP407 plus rPA (Figures 3.9A and 3.9B). The efect of IL6 cytokine on cellular immune responses was evaluated by IgG pattern distribution analysis. As shown in Figure 3.10, immunization with rPA-NE produced over 10 fold prevalence of IgG1 versus IgG2b subclass IgG in IL6-/- mice, and balanced pattern of IgG1 and IgG2b in WT mice. Low titers of IgG2a subclass were detected in both strains of mice. These results suggest that IL6 is involved in NE adjuvant signaling and polarization of the immune response.

Effect of NE on the gene expression of nasal mucosal tissue

To study the effect of NE in the gene expression of nasal tissues, CD-1 mice were nasally immunized with 10 µL per nare of 20% NEP407. These mice were sacrificed 24 hours following treatment and their nasal tissues were isolated to obtain the RNA. As a control, nasal tissue was isolated from mice that were treated with PBS alone. As shown in Figure 3.11A, the expression of 1354 genes was up-regulated and 448 were down-regulated 6 hours following nasal treatment with NEP407. Twenty four hours following treatment, 2496 genes were up-regulated and 3071 were down-regulated. The analysis shows the upregulation of only 1.6% of genes responsible for the production of acute phase inflammatory cytokines including IL6. (Figure 3.11B). No induction of hallmark inflammatory cytokines such as IL4, IL8, and INF-γ was observed. Our results show that chemokines and IL6 are induced in nasal tissue by inoculation with NE adjuvant and the enhanced transcription of these genes probably will impact the development of the overall immune response induced.

3.4 DISCUSSION

Nanoemulsion-based adjuvants are new immunostimulates for induction of vaccine immunity. These formulations efficiently induce mucosal and serum antibodies, as well as produce Th1 cellular immune responses without causing, or requiring, local inflammation [7-10, 12]. However the mechanism of how these compounds induce immunity is not clear. In this chapter, we present several insights into the early events involved in the mechanism of action of NE. We show enhanced antigen sampling in nasal epithelial cells and DC after nasal vaccination in the NE. In addition, the NE adjuvant also promotes rapid antigen trafficking toward lymphoid tissues *in vivo*. These two activities appear to be central to the adjuvant activity of these formulations.

Our work indicates that NE enhances antigen internalization into epithelial and antigen presenting cells. This process however does not seem to be antigen or antigen-presenting cell specific. *In vitro* studies (Figure 3.1) demonstrated that the NE adjuvant enhances antigen sampling by DC while in vivo studies showed that NE adjuvant also induces antigen co-localization with innate DC (Figure 3.4). There are several possible explanations of how NE adjuvant could enhance DC antigen sampling without disruption of the epithelial barrier: First, NE adjuvant may induce DC to directly sample lumenal antigen from the nasal cavity; second, NE could interact with apoptotic epithelial cells that have internalized antigen; and third, NE adjuvant may promote antigen-loaded epithelial cells to pass antigen directly to subepitelial DC. Although these processes have not been extensively studied in the nasal epithelium, they have been reported in intestinal epthelium. In the gut, DCs apparently migrate via chemoreceptor mechanisms towards the lumenal compartment of the epithelium possibly in response to toll-like receptor (TLR) agonists [24-26]. They have been shown to directly sample lumenal microbes through dendrites without disrupting the epithelial barrier [27, 28]. Further, intestinal DCs have been shown to sample apoptotic epithelial cells [29].

Our current investigations are focused in determining which of these mechanisms of DC recruitment and antigen sampling are important in the response to NE adjuvant in the nasal mucosa. Thirty minutes following nasal immunization with NE adjuvant, the nasal epithelium shows a dramatic enhanced staining for the UE-1 ligand –a murine M cell marker (Figure 3.3C and 3.3D). This data suggests that NE non-specifically induces the uptake of the lectin. Differentiation of M cells normally takes at least 24 hours [30, 31] and therefore, the enhanced UE-1 signal is not likely to be specific for differentiation of M cells. We also have shown that NE adjuvant induces broad QDOT internalization and UE-1 staining of epithelial cells in manner similar to CTB. The significance of these findings is currently under investigation.

The finding of antigen within nasal epithelial cells (the presence of vesicle-like material consistent in size to NE particles homogenously distributed in the cytoplasm as shown in Figure 3.4A), is suggestive that as opposed to DC lumenal sampling, antigen-loaded epithelial cells directly interact with resident DC. Some of these epithelial cells demonstrated QDOT loaded vesicles, as shown in Figure 3.4D, residing where the antigen could be delivered to DC (close to the basal lamina). Our data therefore support the hypothesis that the NE promotes antigen sampling by nasal epithelial cells, probably through induction of a pinocytosis of NE with antigen.

Because of the lipid structure of the NE, we hypothesize that NE enhances antigen sampling and trafficking by recognition of membranes and membrane-associated molecules. Thus, NE potentially mimick certain microbial strategies to invade eukaryotic cells. In fact, induction of pinocytosis or phagocytosis in eukaryotic cells by signaling through lipid raft domains is a common theme in microbial pathogenesis. For example, invasion of eukaryotic cells by *Brucella*, Human Immunodeficiency virus type 1, *Afipia felis*, Adenovirus type 2, *Listeria monocytogenes, Leishmania chagasi*, *Legionella pneumophila*, [32-37], and several other microbes [38] is mediated by a lipid raft-activated macropinocytosis or phagocytosis mechanism. A novel finding we are reporting

here is this ability of the NE adjuvant to promote antigen delivery to lymph nodes and the thymus after nasal inoculation (Figures 3.5 and 3.6). In these tissues, E-GFP co-localizes with DEC205 and CD11c DC markers (Figures 3.6C and 3.6E, respectively). The DEC205 cellular marker is expressed by lineages of DC and by thymus cortical epithelial cells which play a central role in antigen internalization and processing [39]. The thymic cortical region has been associated with the T cell positive selection phenomena. Further, DEC205+ epithelial cells are involved in the clearance of apoptotic thymocytes [40]. Despite the E-GFP trafficking to thymus, there is no evidence of tolerance induced. In fact, specific serum IgG antibodies against E-GFP were effectively induced after nasal vaccination with the NE adjuvant. As with intra-thymic vaccines, which have been shown to be safer because they prevent development of autoimmunity [41], antigen trafficking towards the thymus by the NE adjuvant may be important for the safety and efficacy of nasal vaccines requires further experimentation.

A notable finding is that NE enhances whole-body distribution of QDOTs (Figure 3.7). The efficient antigen trafficking may explain why this adjuvant leads to effective immune responses after nasal inoculation with many different antigens. Interestingly, the presence of GM1 in nasal inoculums inhibits systemic dissemination in mice. This suggests that recognition of membrane-associated GM1 may play a role in the early antigen sampling phenomenon occurring at the mucosal tissues and possibly that exogenous GM1 competitively inhibits the interaction of NE/antigen with innate immune cells or that GM1 somehow disrupts the interaction of antigen with NE.

Another unique finding reported in these studies is the lack of inflammation associated with the adjuvant effect of NE. Although there was no evidence of inflammatory associated cytokines, no histological evidence of inflammation, and lack of mucosal gene expression patterns suggestive of inflammation, we detected early production of IL6 in the nasal-bronchoalveolar lavage. The microarray data corroborated the detection of the protein (Figure 3.8

and 3.10B). IL6 production in mucosal tissues has been previously associated with CTB and GM1 interaction *in vivo* and with triggering of mucosal antiviral immune responses [42, 43]. Due to the absence of histolgical inflammation, this acute response probably reflects a specific response to the NE adjuvant by epithelial cells, and it might have a role in mitigating the immune responses. The lack of the induction of other cytokines or inflammatory cell infiltrates suggests a very specific and unique response compared to other adjuvants. Although IL6 appears to be involved in the early signaling pathway, it is apparently not critical for immune response as comparable high titers were achieved in IL6 deficient and WT mice (Figure 3.9).

3.5 CONCLUSSIONS AND SUMMARY

In conclusion, we have shown that NE adjuvant enhances early events in antigen uptake and dissemination in immune cells after nasal vaccination. This leads to efficient antigen trafficking towards lymphoid tissues and the thymus, and results in the induction of immunity. Based on these findings we propose that NE functions, in part, as a delivery vehicle to mediate initial contact with the cell surface and then to facilitate subsequent active antigen uptake by resident DCs.

3.6 FIGURES

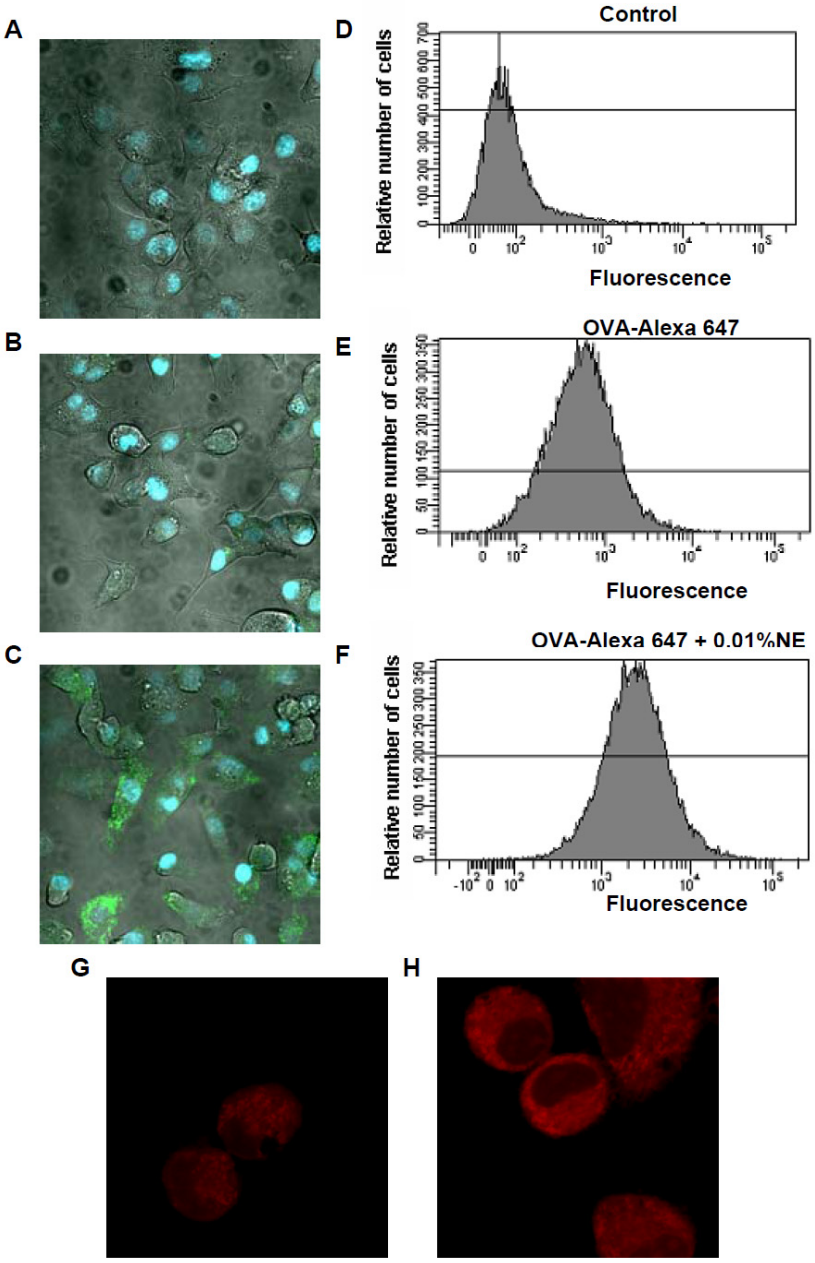

Figure 3.1. ***In vitro*** **NE adjuvant induces antigen internalization into murine dendritic-like cells and enhances lipid staining of Jaws II dendritic-like cells.** By fluorescent microscopy, internalization of OVA-Alexa 488 (green fluorescence) into Jaws II dendritic-like cells was demonstrated in **A** through **C**, the nuclei is stained blue with DAPI. The A image shows the cells treated with the cell culture media; B shows cells treated with just fluorescent OVA-Alexa 488 10ug/ml; and C shows the cells after 2 h exposed to fluorescent OVA-Alexa 488 10 ug/ml plus 0.001% NE. Using FACs internalization of OVA-Alexa 647 into bone marrow dendritic-like cells was measured in **D** through **F**. Bone-marrow derived DC treated with cells culture media in **D**, just OVA-Alexa 647 in **E** and OVA-Alexa 647 plus NE 0.01% in **F**. In **G** and **H** are shown images of Nile red staining of Jaws II dendritic-like cells pretreated with NE in **G** or pretreated with just PBS in **H**.

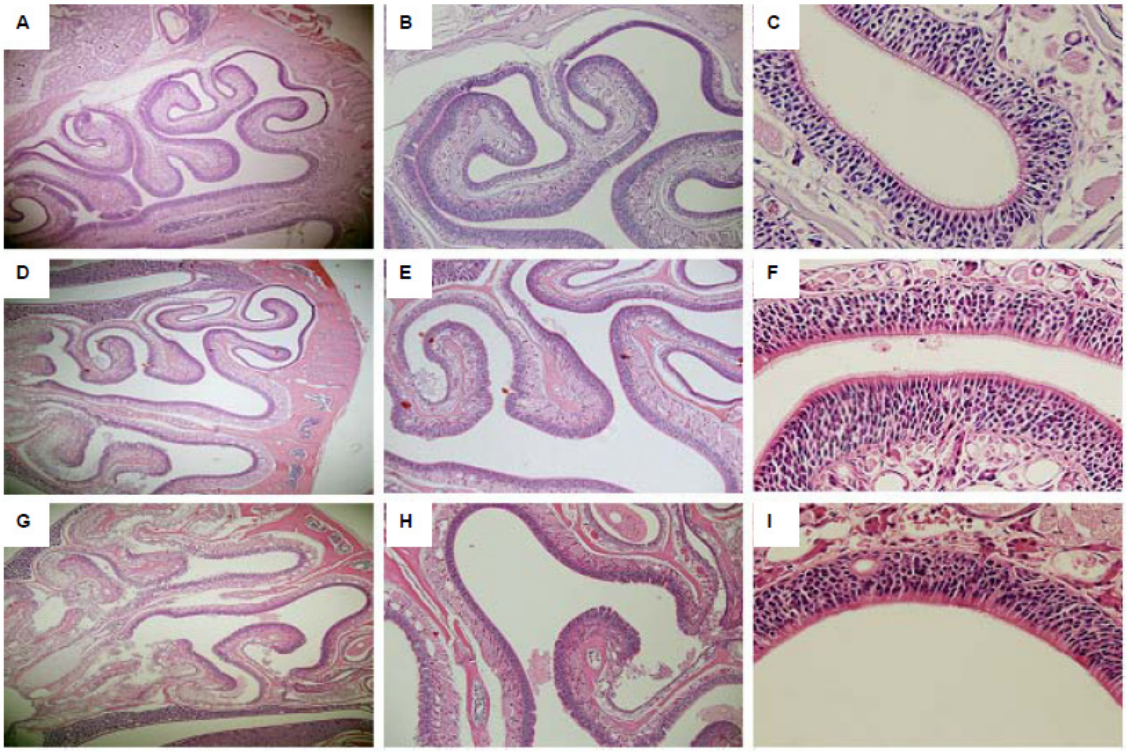

Figure 3.2. Histopathological analysis of nasal tissue sections. Shown are photomicrographs of hematoxylin-eosin staining of coronal tissue sections of paraffin embedded heads using an Olympus BX 51 microscope. First row **A** to **C** shows control mouse nasally inoculated with PBS alone (**A** using 4x objective; **B** using 20x objective; and **C** using a 40x objective). The second row **D** to **F** are pictures from a mouse treated with 20% NE alone (**D** using 4x objective; **E** using 20x objective; and **F** using a 40x objective). And in the last row **G** to **I** a set of potomicrographs of the mouse nasally vaccinated with 20% NE plus 10 µg of HBsAg (**G** using 4x objective; **H** using 20x objective; and **I** using a 40x objective).

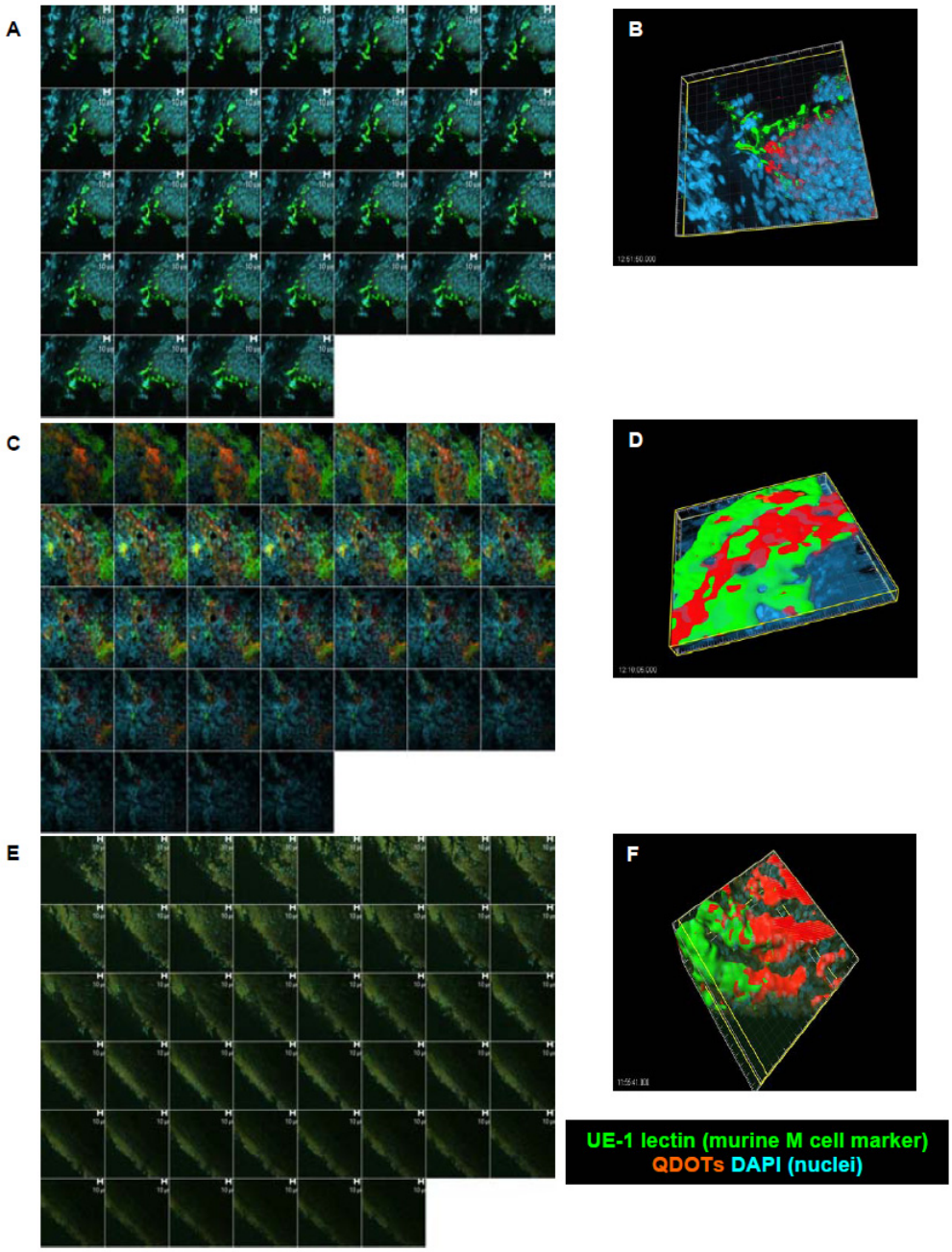

Figure 3.3: ***In vivo*** **NE promotes broad sampling activity by nasal epithelial cells.** Shown here are the analyses of Z scanning of murine nasal epithelium after 30 m nasal vaccination with QDOTs (red) using laser confocal microscopy: galleries in **A, C**, and **E** and the respective 3D reconstruction views in **B**, **D**, and **F** (see supplemental material with the respective 3D animations) using the Imaris software. Figures **A** and **B** show the nasal epithelium of a mouse immunized with QDOTs plus PBS; **C** and **D** show the nasal epithelium of a mouse vaccinated with QDOTs plus 20% NE; **E** and **F** show the nasal epithelium from a mouse immunized with QDOTs and CTB. Just before euthanasia 2 µl of the UE-1-FITC (green) lectin were added to the nares to label the surface of the M cells, and the samples of nasal tissues were mounted with ProLong containing DAPI (blue nuclei).

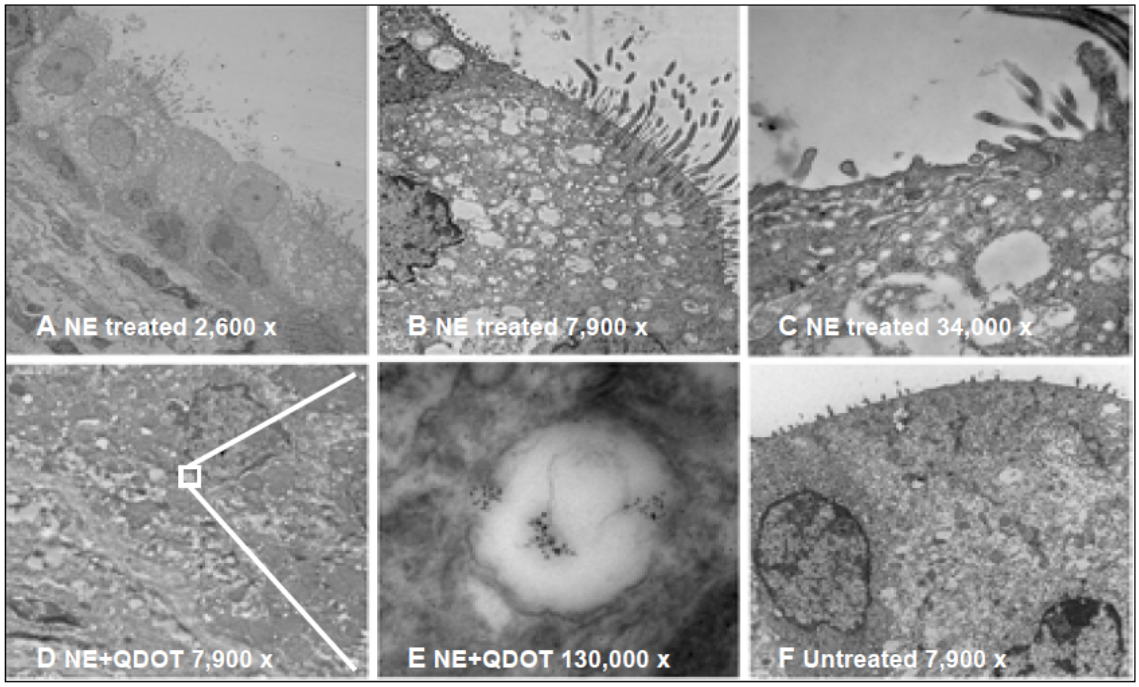

Figure 3.4. ***In vivo*** **NE promotes nasal epithelial cells' sampling activity without disruption of the epithelial barrier.** Images of the TEM analysis of murine nasal epithelium 24 h after nasal inoculation are shown from **A** through **F**. Shown in **A** through **E** is the nasal epithelium of a mouse treated with 20% NE adjuvant; the vesicle-like material was measured (average diameter is 0.479 microns). **D** and **E** show the nasal epithelium of a mouse nasally inoculated with QDOTs plus NE adjuvant; in the **D** overview (magnification 7,900 x) the white square shows the area amplified in the **E** view at up to 130,000 x magnification. In **E** the vesicle-like structure containing clumps of QDOTs, the diameter measured 0.455 microns on average and the QDOT-like material spread in the cytoplasm measured on average 0.005 microns. In Figure **F** shows a picture of the nasal epithelium of a control animal without treatment.

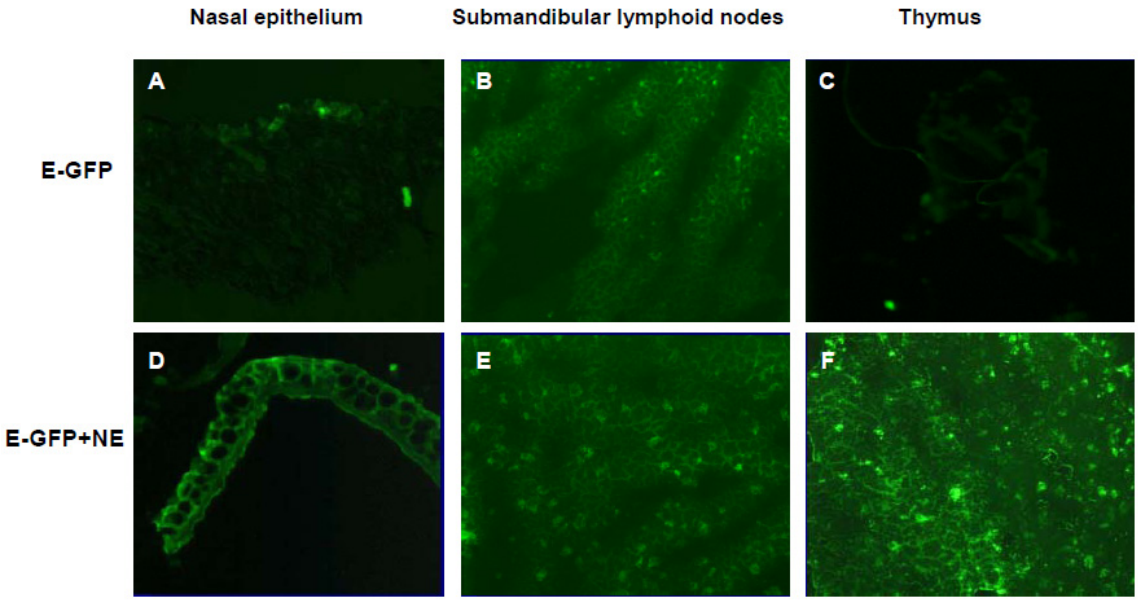

Figure 3.5. ***In vivo*** **effect of NE adjuvant in E-GFP trafficking towards lymphoid tissues.** Mice were nasally inoculated either with E-GFP in PBS (**A**, **B**, and **C**) or with E-GFP with 20% NE (**D**, **E** and **F**). After 24 h, cryo-sections of tissues were prepared and analyzed using an inverted fluorescent microscope (magnification 40 x). Showing in **A** and **D**: the nasal epithelium; in **B** and **E**: the submandibular lymphoid nodules; and in **C** and **F**: the thymus. **G** and **F** show the profile of fluorescence through the red line is shown for tissue sections of olfactory bulb obtained after 24 h of nasal vaccination. The tissue sections were stained with anti E-GFP antibody in **G** or without the primary antibody in **H** from a mouse nasally vaccinated with 20% NE plus E-GFP.

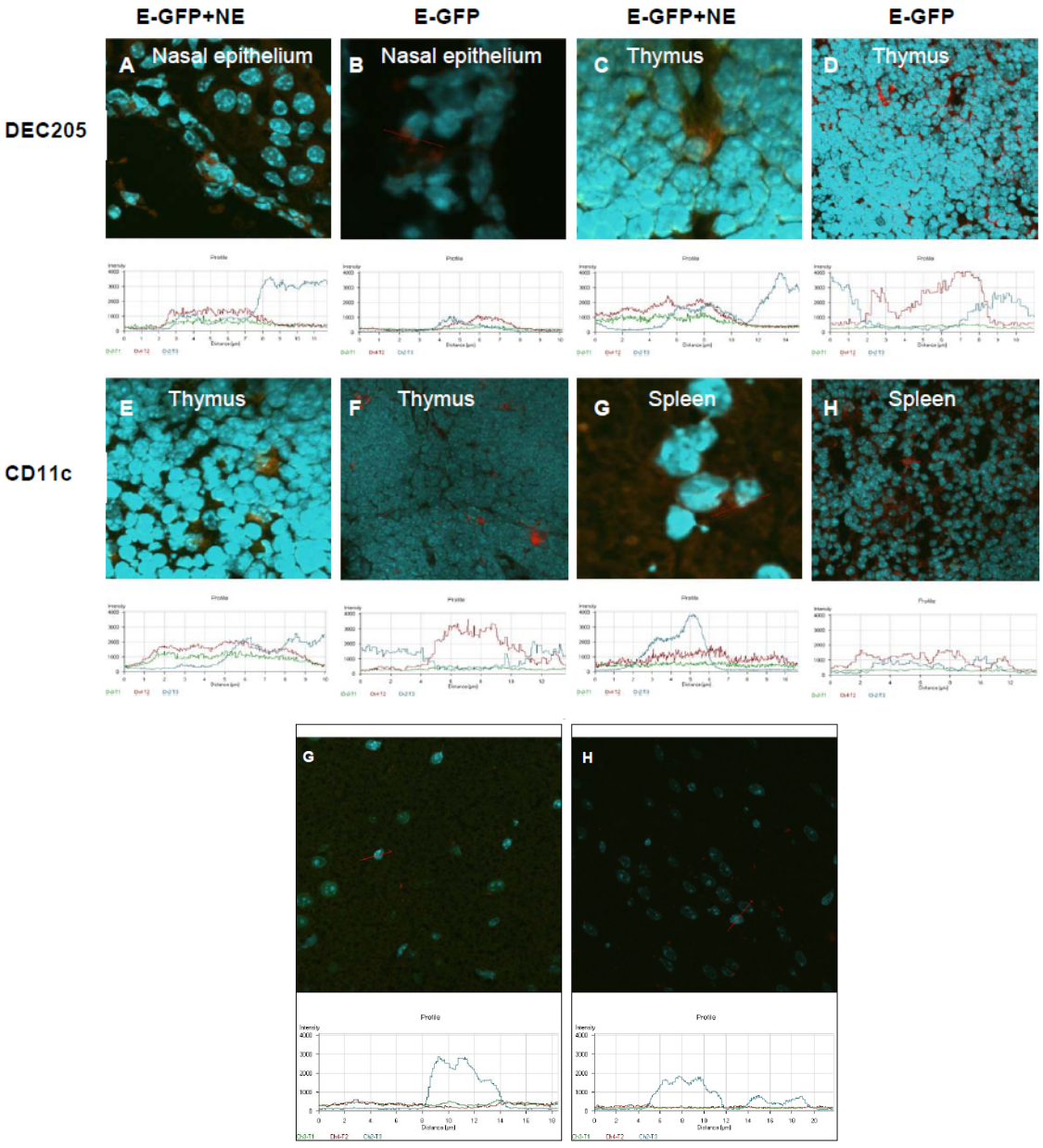

Figure 3.6. ***In vivo*** **NE adjuvant promotes co-localization of E-GFP with DC.** After 24 h of nasal inoculation, frozen sections of the tissues were prepared. In **A** through **D**, frozen tissue sections were stained with anti-DEC205 antibody (red: PE conjugated) and, in **E** through **H**, with anti-CD11c (red: PE conjugated) and were analyzed by laser confocal microscopy profiles. Profiles measure the fluorescence intensity through a red line in each image. ProLong (molecular Probes) containing DAPI was used to prepare the samples for microscopy analysis and to stain the nuclei blue. Profiles **A**, **E**, **C**, and **G** were obtained from mice immunized with NE plus E-GFP and profiles **B**, **F**, **D**, and **H** are from mice immunized with just E-GFP. Profiles A and B show the nasal epithelium; **C**, **D**, **E** and **F** are profiles from the thymus; and **G** and **H** profiles show spleen sections.

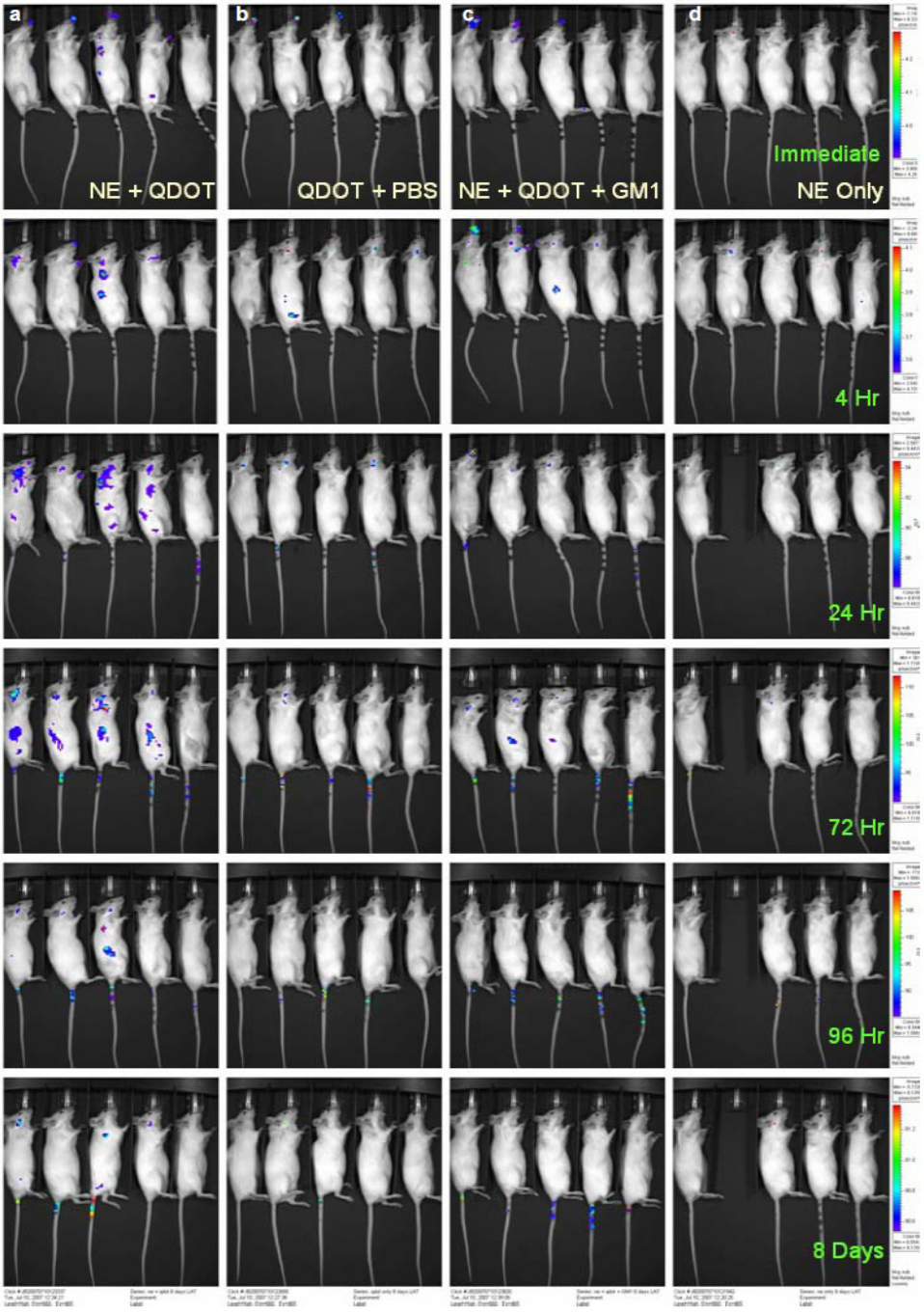

Figure 3.7. ***In vivo*** **effect of the NE adjuvant in the dissemination of quantum dots after nasal vaccination of mice.** Groups of 4 mice were nasally inoculated with QDOTs plus 20% NE, column a; QDOTs in PBS, column b; QDOTs plus 20% NE plus GM1 (0.35 mM), column c; and 20% NE only, column d. Then through time and up to 8 days the whole mouse fluorescence was measured in the IVIS Imaging System 200 Spectrum series bioluminometer from Xenogen at the Center for Molecular Imaging, University of Michigan. The fifth mouse in each group to the right is a naïve mouse. One mouse died in the group treated with the NE from a nasopharyngeal obstruction.

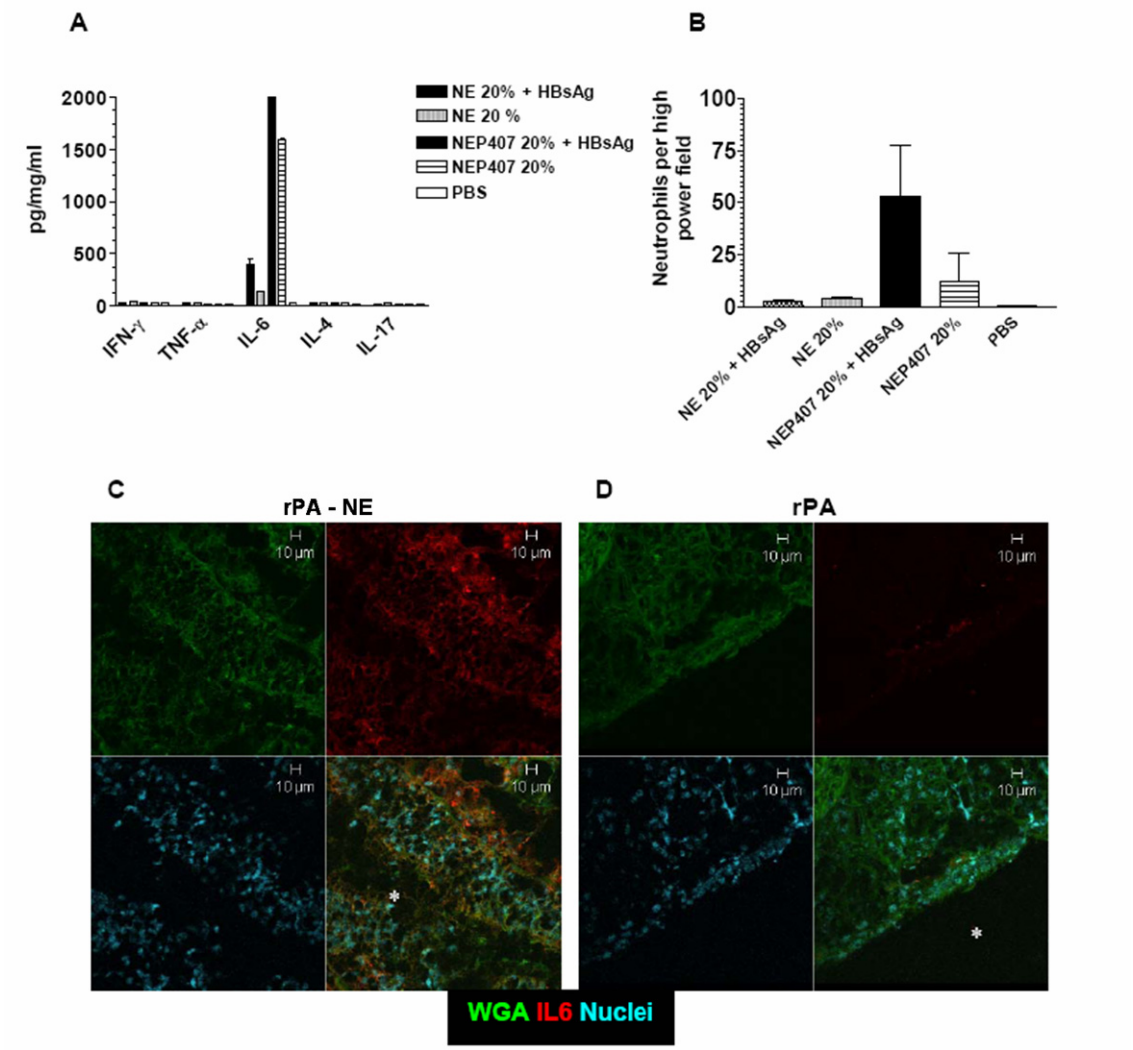

Figure 3.8. Effect of NE adjuvant in cytokines and neutrophils infiltration into the nasal lumenal cavity and identification of IL6 producing cells. After nasal inoculation, the cytokine profile was determined in nasal-bronchoalveolar lavage after 24 hours **A)** by Luminex assay. After 24 h the cellular content of the lavage were pelleted (cytospin) and microscopically analyzed for the presence and number of neutrophils after Giemsa staining **B)**. Shown are the averages ± SEM of 5 different focal views for each group, *: *p-value* <0.01 by student's t-test analyses. Nasal epithelium was harvested from mice 24 hours after treatment with rPA-NE **C)** or rPA alone **D).** The tissues were probed with wheat germ agglutinin (WGA) lectin [green] and anti-Il6 antibodies [red].

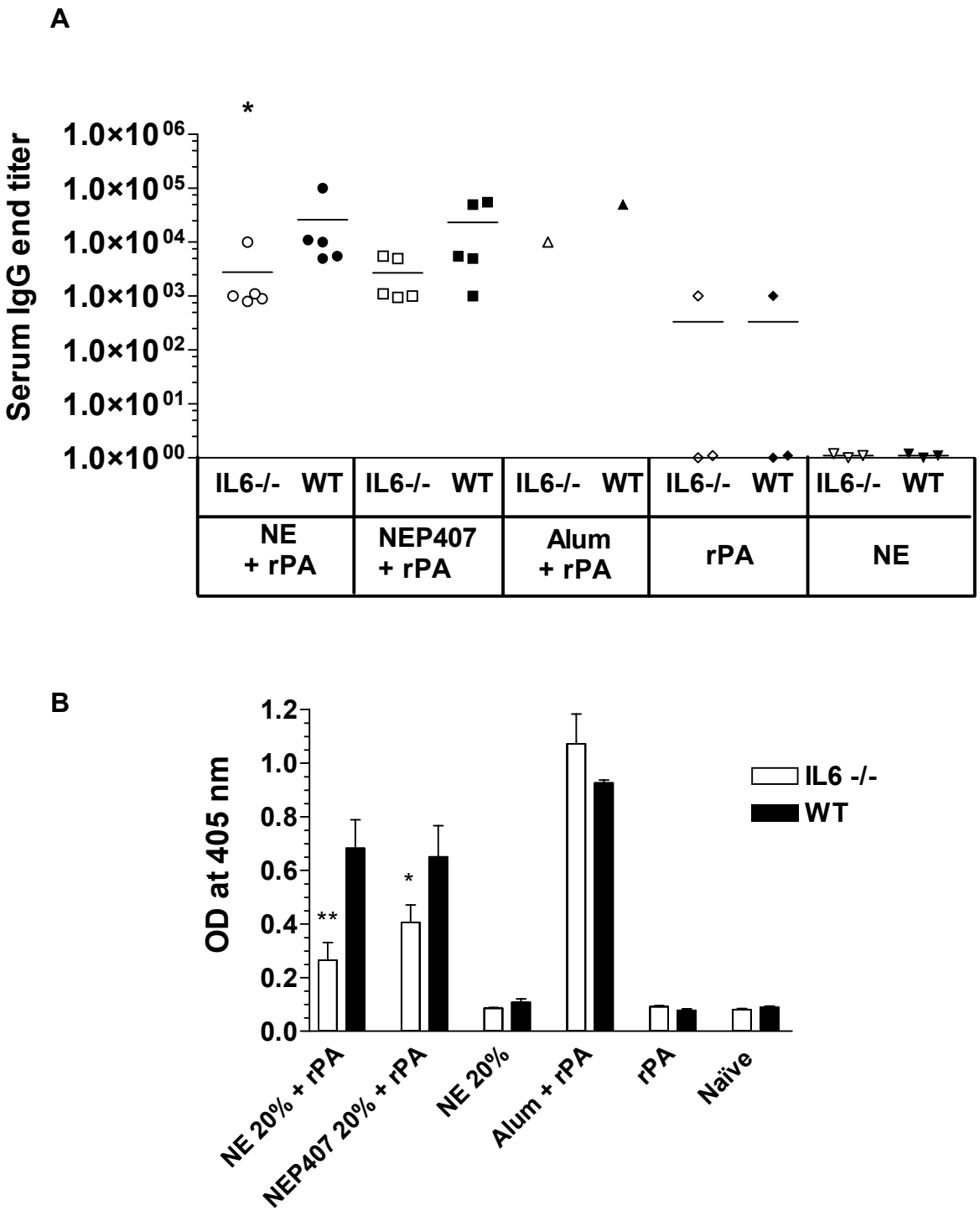

Figure 3.9. Antigen specific antibodies produced in the IL6 deficient mice. Shown are the rPA specific antibodies induced after 14 weeks of vaccine (prime at 0 week and boost at 4 weeks) in the IL6 deficient (IL6 -/-) and the wild type C57BL/6 (WT) mice. It is shown in A the serum end titers reach for IgG and in B the sIgA from bronchoalveolar lavage, respectively. All the animals were immunized by the nasal route except those vaccinated with Alum plus rPA (intramuscular injection). *p<0.05 and **p<0.01 as determined by Mann Whitney analysis in A, and student's t-test in B, respectively.

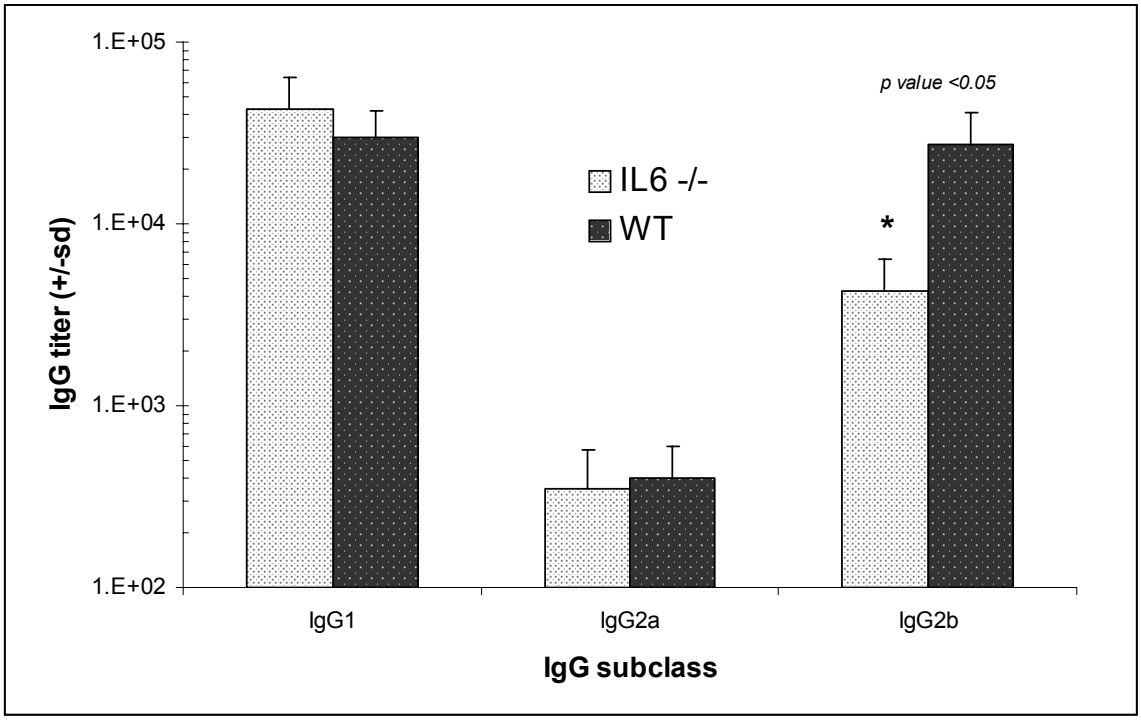

Figure 3.10. Anti-PA IgG subclass analysis in IL6-/- mutant and WT mice. Immunization with rPA-NE produced over 10 fold prevalence of IgG1 over IgG2b subclass IgG in IL6-/- mice, and balanced pattern of IgG1 and IgG2b in WT mice. Low titers of IgG2a subclass were detected in both strains of mice. * indicate significant IgG2b titer difference between IL6-/- and WT mice (*p-value* <0.05).

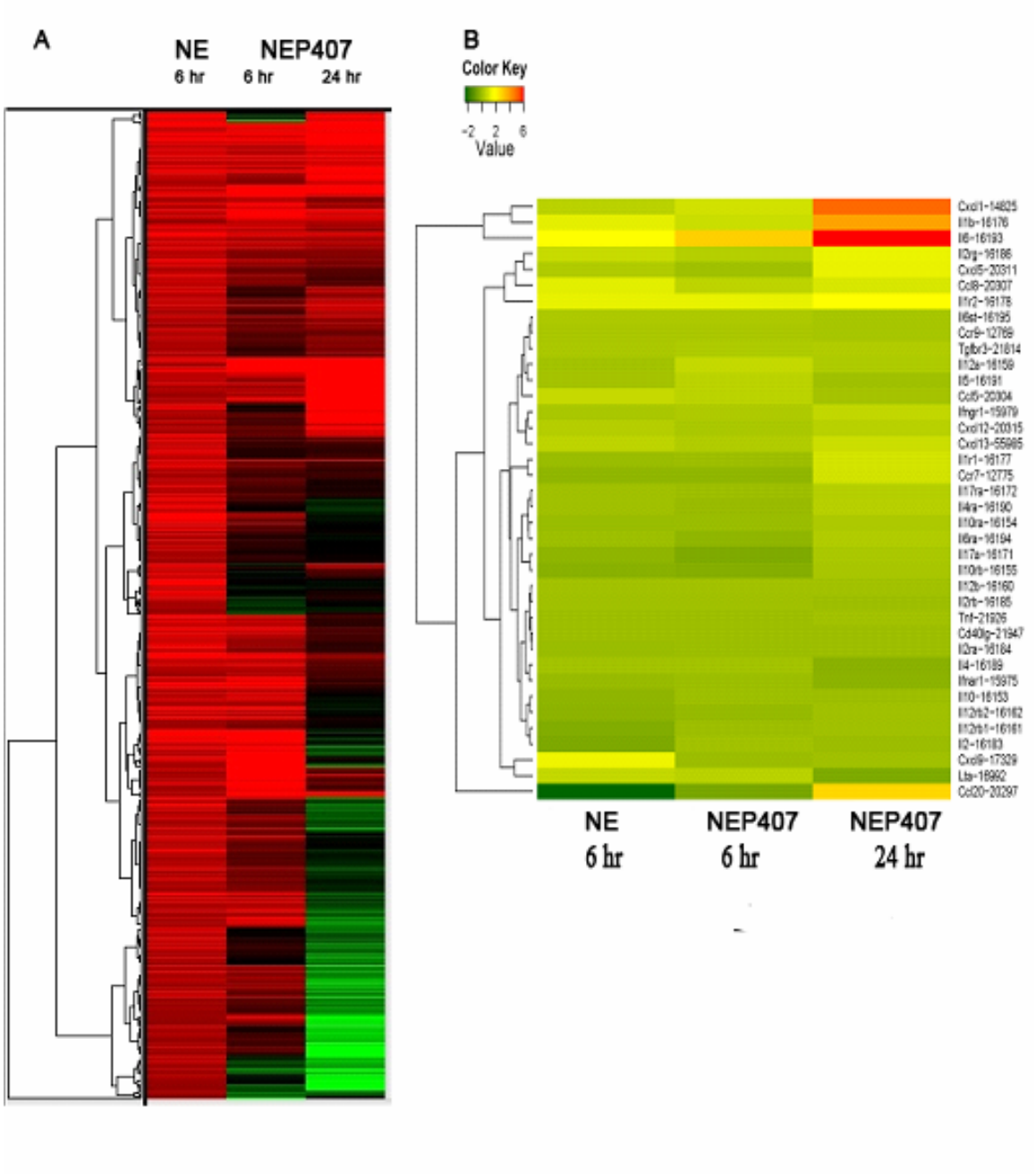

Figure 3.11. Gene expression patterns changes following i.n. treatment with either NE or NEP407 A) Hierarchal clustering of over 1400 gene transcripts up-regulating with NE or NEP407 treatment for 6 or 24 hours and **B)** Clustering of a group of 38 genes regulating inflammatory expression patterns. Statistical analysis of gene expression was performed using Bioconductor analysis and the DAVID acquisition program. Gene transcription was considered changed when detected as ≥ 2 fold difference as compared to non-treated controls. Red = up-regulation and green = down regulation, yellow = not changed.

3.7 REFERENCES

1. Neutra, M.R. and P.A. Kozlowski, *Mucosal vaccines: the promise and the challenge.* Nat Rev Immunol, 2006. 6(2): p. 148-158.

2. Chepurnov, A.A., et al., *Inactivation of Ebola virus with a surfactant nanoemulsion.* Acta Tropica, 2003. 87(3): p. 315-320.

3. Hamouda, T., et al., *A novel surfactant nanoemulsion with a unique non-irritant topical antimicrobial activity against bacteria, enveloped viruses and fungi.* Microbiological Research, 2001. 156(1): p. 1-7.

4. Hamouda, T., et al., *A novel surfactant nanoemulsion with broad-spectrum sporicidal activity against Bacillus species.* The Journal of Infectious Diseases, 1999. 180(6): p. 1939-49.

5. Myc, A., et al., *The fungicidal activity of novel nanoemulsion (X8W60PC) against clinically important yeast and filamentous fungi.* Mycopathologia, 2003. 155(4): p. 195-201.

6. Hamouda, T. and J.R. Baker, *Antimicrobial mechanism of action of surfactant lipid preparations in enteric Gram-negative bacilli.* Journal of Applied Microbiology, 2000. 89(3): p. 397-403.

7. Bielinska, A.U., et al., *A Novel, Killed-virus Nasal Vaccinia Vaccine.* Clinical and Vaccine Immunology, 2007: p. CVI.00440-07.

8. Bielinska, A.U., et al., *Mucosal Immunization with a Novel Nanoemulsion-Based Recombinant Anthrax Protective Antigen Vaccine Protects against Bacillus anthracis Spore Challenge.* Infection and Immunity, 2007. 75(8): p. 4020-4029.

9. Myc, A., et al., *Development of immune response that protects mice from viral pneumonitis after a single intranasal immunization with influenza A virus and nanoemulsion.* Vaccine, 2003. 21(25-26): p. 3801-3814.

10. Makidon, P.E., et al., *Pre-Clinical Evaluation of a Novel Nanoemulsion-Based Hepatitis B Mucosal Vaccine.* PLoS ONE, 2008. 3(8): p. e2954.

11. Donovan, B.W., et al., *Prevention of murine influenza A virus pneumonitis by surfactant nano-emulsions.* Antiviral Chemistry & Chemotherapy, 2000. 11(1): p. 41-9.

12. Bielinska, A.U., et al., *Nasal Immunization with a Recombinant HIV gp120 and Nanoemulsion Adjuvant Produces Th1 Polarized Responses and Neutralizing Antibodies to Primary HIV Type 1 Isolates.* AIDS Res. Hum. Retroviruses, 2008. 24(2): p. 271-281.

13. Nawar, H.F., et al., *Mutants of Type II Heat-Labile Enterotoxin LT-IIa with Altered Ganglioside-Binding Activities and Diminished Toxicity Are Potent Mucosal Adjuvants.* Infection and Immunity, 2007. 75(2): p. 621-633.

14. De Haan, L., et al., *Role of GM1 binding in the mucosal immunogenicity and adjuvant activity of the Escherichia coli heat-labile enterotoxin and its B subunit.* Immunology, 1998. 94(3): p. 424-430.

15. Grdic, D., et al., *Splenic Marginal Zone Dendritic Cells Mediate the Cholera Toxin Adjuvant Effect: Dependence on the ADP-Ribosyltransferase Activity of the Holotoxin.* Journal of Immunology, 2005. 175(8): p. 5192-5202.

16. Lardon, F., et al., *Generation of dendritic cells from bone marrow progenitors using GM-CSF, TNF-alpha, and additional cytokines: antagonistic effects of IL-4 and IFN-gamma and selective involvement of TNF-alpha receptor-1.* Immunology, 1997. 91(4): p. 553-9.

17. Greenspan, P., E.P. Mayer, and S.D. Fowler, *Nile red: a selective fluorescent stain for intracellular lipid droplets.* J. Cell Biol., 1985. 100(3): p. 965-973.

18. Genicot, G., et al., *The use of a fluorescent dye, Nile red, to evaluate the lipid content of single mammalian oocytes.* Theriogenology, 2005. 63(4): p. 1181-1194.

19. Jang, M.H., et al., *Intestinal villous M cells: An antigen entry site in the mucosal epithelium.* PNAS, 2004. 104(16): p. 6110-6115.

20. Shapiro, F., et al., *Transmission electron microscopic demonstration of vimentin in rat osteoblast and osteocyte cell bodies and processes using the immunogold technique.* The Anatomical Record, 1995. 241(1): p. 39-48.

21. Ballou, B., et al., *Sentinel Lymph Node Imaging Using Quantum Dots in Mouse Tumor Models.* Bioconjugate Chem, 2007. 18(2): p. 389-396.

22. Irizarry, R.A., et al., *Use of Mixture Models in a Microarray-Based Screening Procedure for Detecting Differentially Represented Yeast Mutants* Stat Appl Genet Mol Biol, 2003. 2(1): p. article 1.

23. Gebert, A., et al., *The Development of M Cells in Peyer's Patches Is Restricted to Specialized Dome-Associated Crypts.* Am. J. Pathol., 1999. 154(5): p. 1573-1582.

24. Niedergang, F. and M.-N. Kweon, *New trends in antigen uptake in the gut mucosa.* Trends in Microbiology, 2005. 13(10): p. 485-490.

25. Niess, J.H. and H.-C. Reinecker, *Dendritic cells in the recognition of intestinal microbiota.* Cellular Microbiology, 2006. 8(4): p. 558-564.

26. Novak, N. and T. Bieber, *2. Dendritic cells as regulators of immunity and tolerance.* Journal of Allergy and Clinical Immunology, 2008. 121(2, Supplement 2): p. S370-S374.

27. Rescigno, M.M., et al., *Dendritic cells shuttle microbes across gut epithelial monolayers.* Immunobiology, 2001. 204(5): p. 572-81.

28. Rescigno, M., et al., *Dendritic cells express tight junction proteins and penetrate gut epithelial monolayers to sample bacteria.* Nature Immunology, 2001. 2(4): p. 361-7.

29. Huang, F.-P., et al., *A Discrete Subpopulation of Dendritic Cells Transports Apoptotic Intestinal Epithelial Cells to T Cell Areas of Mesenteric Lymph Nodes.* J. Exp. Med., 2000. 191(3): p. 435-444.

30. Takeuchi, T., et al., *Proliferation and cellular kinetics of villous epithelial cells and M cells in the chicken caecum.* Journal of Anatomy, 1998. 193(2): p. 233-239.

31. Takeuchi, T. and T. Gonda, *Cellular kinetics of villous epithelial cells and m cells in rabbit small intestine.* The Journal of Veterinary Medical Science, 2004. 66(6): p. 689-93.

32. Schneider, B., et al., *Lipid Microdomain-Dependent Macropinocytosis Determines Compartmentation of Afipia felis.* Traffic, 2007. 8(3): p. 226-240.

33. Watarai, M., et al., *Legionella pneumophila Is Internalized by a Macropinocytotic Uptake Pathway Controlled by the Dot/Icm System and the Mouse Lgn1 Locus.* J. Experimental Medicine, 2001. 194(8): p. 1081-1096.

34. Watarai, M., et al., *Modulation of Brucella-induced macropinocytosis by lipid rafts mediates intracellular replication.* Cellular Microbiology, 2002. 4(6): p. 341-355.

35. Liu, N.Q., et al., *Human Immunodeficiency Virus Type 1 Enters Brain Microvascular Endothelia by Macropinocytosis Dependent on Lipid Rafts and the Mitogen-Activated Protein Kinase Signaling Pathway.* Journal of Virology, 2002. 76(13): p. 6689-6700.

36. Imelli, N., et al., *Cholesterol Is Required for Endocytosis and Endosomal Escape of Adenovirus Type 2.* Journal of Virology, 2004. 78(6): p. 3089-3098.

37. Seveau, S., et al., *Role of lipid rafts in E-cadherin- and HGF-R/Met-mediated entry of Listeria monocytogenes into host cells.* J. Cell Biol., 2004. 166(5): p. 743-753.

38. Blanco, L.P., *Gangliosides' role in cellular interactions witht microbes and immune cell activation*, *Glycolipids: New Research*, D. Sasaki, Editor. 2008, Novapublishers: New York.

39. Jiang, W., et al., *The receptor DEC-205 expressed by dendritic cells and thymic epithelial cells is involved in antigen processing.* Nature, 1995. 375(6527): p. 151-155.

40. Small, M. and G. Kraal, *In vitro evidence for participation of DEC-205 expressed by thymic cortical epithelial cells in clearance of apoptotic thymocytes.* International Immunology, 2003. 15(2): p. 197-203.

41. Fridkis-Hareli, M. and E. Reinherz, *New approaches to eliciting protective immunity through T cell repertoire manipulation: the concept of thymic vaccination.* Med Immunol, 2004. 3(1): p. 2.

42. van Ginkel, F.W., et al., *Enterotoxin-Based Mucosal Adjuvants Alter Antigen Trafficking and Induce Inflammatory Responses in the Nasal Tract.* Infection and Immunity, 2005. 73(10): p. 6892-6902.

43. Xing, Z., et al., *Adenoviral-Mediated Gene Transfer of Interleukin-6 in Rat Lung Enhances Antiviral Immunoglobulin A and G Responses in Distinct Tissue Compartments.* Biochemical and Biophysical Research Communications, 1999. 258(2): p. 332-335.

CHAPTER 4
FORMULATION AND DEVELOPMENT OF NANOEMULSION-BASED VACCINES AND DELIVERY THROUGH NASAL SPRAYER DELIVERY SYSTEMS

4.1 BACKGROUND

The development of heat-stable and needle-free vaccines is considered critical to some populations [1]. On a global scale, traditional vaccines have successfully reduced the burden of infectious diseases, including tetanus, diphtheria, pertussis, poliomyelitis, rubella embryopathy, and measles [2]. Despite these remarkable accomplishments, vaccine preventable diseases continue to cause significant morbidity and mortality, especially in developing populations. Recently, immunization frequency in many undeveloped countries has actually declined for adults and children [3]. The disparity of vaccine coverage in these areas results from a number of compounding problems, including the requirement for sterile needles, the cost and burden associated with non-interrupted cold chain handling, political strife and civil unrest, weak health service delivery systems, underfunding, and poor management . Adding to the problem, the unsafe use of needle injections have been linked to the transmission of life-threatening infections such as hepatitis B and C, HIV, Ebola, Lassa virus infections, and malaria [4]. However, until recently, there have been relatively low levels of interest in developing new vaccines designed to safely prevent the predominant diseases in the developing world [1, 3].

In light of these limitations, the development of successful thermally-stable and needle-free mucosal vaccines is undoubtedly becoming a pressing consideration for the scientific community. Fortunately, a number of non-invasive delivery routes, including nasal, ophthalmic, pulmonary, transdermal,

buccal, rectal, and vaginal, are available for which vaccine technologies are under development [5, 6]. Among these routes, nasal vaccine delivery seems most promising, given the accessibility of the mucosal tissue, the interface of a range of systems, the relative lack of barriers such as the stratum corneum, the proven track record of therapeutic nasal drug delivery technologies, and improvement patient compliance [6]. Despite the many attractive features of nasal vaccination [7-12], only one intranasal vaccine has been approved for human use [12]. Experimental vaccines which consist of live attenuated virus re-assortment strains have the potential to provide long-lasting humoral and cell-mediated immunity, but they bear the potential risk of reversion to virulence and carry considerable logistical and bio-safety problems associated with storage, particularly in the developing world [7]. Many experimental vaccines consisting of killed or purified antigens are typically poorly immunogenic and require inflammatory adjuvants [7, 13].

Thermally-stable nanoemulsion (NE), as described in Chapters 1-3, is a promising non-inflammatory mucosal adjuvant for needle-free nasal immunization. We have previously demonstrated protective immunity in a variety of antigen systems (including recombinant protein) and animal models, suggesting a possible utility of NE-based vaccines for use in developing populations [14-18]. The successful use of NE-based vaccines, however, poses serious challenges. One such challenge is optimization of the platform for thermal stability and potency. In Chapter 2, we reported that the potency of a prototype mucosal nanoemulsion-based hepatitis B vaccine (HBsAg-NE) remains unaffected for at least 6 weeks when stored at 40°C [18]. Assessment of the effect of the diluent for NE-based vaccines may be important because, considerable differences in potencies related to the diluent have been documented at least for alum-based vaccines [19]. Another challenge for successful mucosal vaccines is the ability to accurately and repeatedly dispense very small quantities of the NE-based preparations to relevant areas of the nasal mucosa (potentially targeting lymphoid tissues). The delivery performance of any aerosol introduced via the nasal cavity depends on many factors, such as

the design of the pump, the physical properties of the formulation, and the position of administration [20-24]. In this present chapter, we have examined the effects of phosphate buffered saline (PBS) versus sodium chloride (NaCl) diluents on the thermal stability profile and potency of NE-based vaccines and the potential to efficiently deliver them using commercially available nasal sprayer devices.

4.2 EXPERIMENTAL METHODS

Nanoemulsion, proteins, and general reagents

Nanoemulsion (NE), provided by the NanoBio® Corporation, was supplied as a Tween 80-based (W_{80}5EC) mixture manufactured as previously described [18]. For these studies, three proteins (Ovalbumin, Alkaline Phosphatase, and Hepatitis B surface antigen) were used to evaluate thermal stability, immunogenicity, and sprayer function. Ovalbumin–Grade V (OVA), porcine intestinal alkaline phosphatase (AlkP), and bovine serum albumin (BSA) were purchased from Sigma and dissolved in either sterile-filtered, phosphate-buffered saline (Mediatech) or sterile-filtered saline (Hospira). Recombinant adw serotype hepatitis B surface antigen (HBsAg) was supplied by Human Biologicals Institute (Indian Immunologics, Ltd.). HBsAg was made using GMP procedures and was purified from *Pichia pastoris* transfected with plasmid pPIC3K. Alkaline phosphatase (AP) conjugated rabbit anti-mouse IgG (H&L) antibody was purchased from Rockland Immunochemicals, Inc.

Preparation of OVA-NE and HBsAg-NE mixtures

Ovalbumin-nanoemulsion (OVA-NE), alkaline phosphatase-nanoemulsion (AlkP-NE), and hepatitis B surface antigen-nanoemulsion (HBsAg-NE) formulations were prepared by vigorously mixing the protein solution with the concentrated NE. Final salt concentrations were adjusted to either 150 mM PBS

or 0.9% saline (pH 7.03). For the physico-chemical analysis and sprayer studies, the OVA-NE was formulated at 3.125 mg/mL OVA in a range of 0.28% to 40% NE (v/v). The AlkP-NE was prepared with 16.7 mg/mL AlkP in 20% NE. For intranasal immunizations, the OVA-NE dose was 3.125 µg/mL OVA in 20% NE, and the HBsAg-NE doses ranged from 0.625 or 2.5 mg/ml HBsAg in 20% NE. For the rheological and sprayer characteristic studies, the HBsAg-NE was prepared with 0.04 mg/ml HBsAg in 20% NE.

Determination of the effects of formulation on thermal stability and potency

OVA was chosen as a surrogate antigen since it is a well-defined and frequently utilized antigen for immunological and vaccine studies [25]. To determine the effects of the diluent on thermal stability, two formulations were characterized; each consisting of an either OVA-NE diluted with 0.9% NaCl or 150 mMol PBS. Each preparation was evaluated for long-term (8-10 months) thermal stability and immunogenicity. The OVA-NE mixtures were stored in 2 mL glass vials with phenolic rubber-lined caps (Wheaton Science Products) at room temperature (~ 25°C) and in standard lighting conditions. The vials were filled with minimal air contained above the OVA-NE mixture. The thermal stability of the NE adjuvant was evaluated visually and by particle size characterization. Protein stability was determined by SDS-PAGE immunoblotting and *in vivo* potency. The NE mixture was considered stable if there was no visual evidence of creaming, settling, or phase separation. The NE itself was deemed stable if the lipid droplet size remained consistent with freshly mixed product (~339 +/-161 nm for OVA-NE with 150 mMol PBS and 318 +/-143 nm for OVA-NE with 0.9% NaCl). The stored samples were maintained until either NE instability was evident or degradation of the protein was detected. For visual analysis of thermal stability, the closed vials were inspected against an incandescent backlight at regular intervals for evidence of creaming, settling, or phase separation. The visual appearance of the mixture was scored on a scale ranging from 0 to 6 according to the following criteria: 6 = normal (homogenous) visual appearance, 5 =

flocculant gradient without distinct boundaries, 4 = clear distinct boundary re-dispersible with minimal mechanical disturbance (clear portion < 25% total volume), 3 = same as 4 with the clear portion representing 25 to 50% of the total volume, 2 = same as 4 with the clear portion representing 51 to 75% of the total volume, 1 = clear distinct boundary re-dispersible with the clear portion > 75% total volume, and 0 = irreversible phase separation. Care was taken not to disturb or shake the mixture during the visual inspection.

Mice, Immunization Procedures, Sample Collection, and Antibody Measurement

Pathogen-free, outbred CD-1 mice (females 6-8 weeks old) were purchased from Charles River Laboratories and housed in SPF conditions with food and water available ad libitum in accordance with the standards of the American Association for Accreditation of Laboratory Animal Care (AAALAC). All mouse procedures performed for this study were conducted with the approval of the University of Michigan University Committee on Use and Care of Animals (UCUCA).

The mice were immunized with either OVA-NE or HBsAg-NE (*n = 5* per group) administered nasally, six weeks apart. All intranasal immunizations were conducted in mice anesthetized with isoflurane, using the IMPAC 6® anesthesia delivery system. The anesthetized mice were held in a supine position and 8 µl (4 µl/nare) of NE/HBsAg solution was administered slowly to the nares using a micropipette tip.

Whole blood samples were obtained from the lateral saphenous vein every 14 days following prime immunization. The serum was separated by centrifugation at 3500 RPM for 15 minutes after allowing coagulation for 30 to 60 minutes at room temperature. The serum samples were stored at -20° C until analyzed.

Anti-OVA- or HBsAg-specific IgG levels were determined by ELISA. Nunc Microtiter Maxisorb™ plates (Roskilde, Denmark) were coated with 5 µg/mL (100 µl) of HBsAg in a coating buffer (50 mM sodium carbonate, 50 mM sodium bicarbonate, pH 9.6) and incubated overnight at 4^{o}C. The protein solution was removed and the plates were incubated with blocking buffer (PBS with 1% dry milk) for 30 minutes at 37^{o}C. For antibody detection, the serum samples were serially diluted in 0.1% BSA in PBS. Aliquots of 100 µL/well were added to the plates and incubated for 1 hour at 37^{o} C. The plates were washed three times with R&D Systems 1X washing buffer followed by 1 hour incubation at 37°C with anti-mouse IgG alkaline phosphatase (AP)-conjugated antibody, then washed three times and incubated with AP substrate Sigma Fast^{TM} (Sigma). The optical density (OD) was measured using a Spectra Max 340 ELISA reader (Molecular Devices) at 405 nm with the reference wavelength of 690 nm after a 45-minute incubation step. Serum antibody concentrations were defined as endpoint titers (the reciprocal of the highest serum dilution producing an OD above cutoff value). The cutoff value will be determined as the OD of the corresponding dilution of control sera+2 (standard deviations) and plate background [26, 27].

Nasal spray pumps and preparation

The Pfeiffer SAP-62602 Dispenser (130 µL/actuation) and BD Hypak SCF 0.5 mL Accuspray^{TM} sprayer systems were kindly provided by Pfeiffer of America and the Becton, Dickinson, and Company. These systems were evaluated for the suitability of dispensing intranasal NE-based vaccines. The Pfeiffer 62602 is a metered multi-dose mechanical pump designed for nasal pharmaceutical delivery applications and was developed as a modular system and manufactured with CFR-compliant materials to include an 18/415 screw enclosure and gasket system. To contain the samples with the Pfeiffer pump, we used 5-mL U Save™ VB1 3F glass vials manufactured by Saint-Gobain Desjonqures (SGD). The BD Accuspray device, manufactured with CFR-compliant materials, is constructed in a pre-metered glass syringe configuration

and dispenses up to 500 µl, depending on the initial loading methodology. For these studies, the BD syringes were preloaded with 130 µl of samples in order to retain dispensing volume consistent with the Pfeiffer system. Prior to analysis, both devices were briefly soaked in 1% liquinox solution in order to remove any residue from manufacturing and thoroughly rinsed with sterile distilled H_20, then dried at 37°C for 30 minutes. For sample dispensing, the Pfeiffer pump was secured tightly to the SDG vials containing NE mixtures 24 hours prior to testing. Prior to testing, the pump was primed by manual actuation at least five times in agreement with manufacturer's directions. For the BD sprayer, a plunger rod and stopper were then placed into the syringe barrel and the chamber was then pressurized according to manufacturer recommendations using a BD Hypak NSCF hand stoppering tool 24 hours preceding testing.

Determination of the effects of pump actuation on protein-NE stability

The consistency of the emulsion oil-phase particle size was used to assess nanoemulsion stability. Dispensed NE (+/- OVA) was collected from either the Pfeiffer or BD systems using a sterile Fisher Scientific 15 mL polypropylene tube. An aliquot of the collected sample was used in an LS230 particle sizing instrument (Beckmann-Coulter) fitted with a small-volume module. The procedure was conducted in accordance to manufacturer's directions. Particle size distributions were calculated using a Fraunhofer optical model and number weighted averaging over an average of three 60-second measurement cycles. The data was analyzed using SOFTmax Pro© ver. 2.2.1 software.

The protein stability in the protein-NE mixtures was analyzed using PAGE and Western techniques. Samples were reduced using DTT and electrophoresed by SDS-PAGE. Protein electrophoresis was conducted using 4-12% Bis-Tris gels and MES running buffer (Invitrogen). Gels were either stained using an Invitogen SilverQuest™ silver staining kit or transferred to 0.45 micron-sized PVDF Immobilon-P membranes (Millipore). Established immunoblotting

procedures were followed [18]. Ovalbumin-specific bands were detected using rabbit anti-ovalbumin polyclonal antibody (RDI) and mouse anti-rabbit IgG-alkaline phosphatase conjugated antibody with the chromogenic substrate NBT/BCIP (Roche Diagnostic Corp.).

Measurement of Alkaline phosphatase enzymatic activity was used as a more sensitive method to assess the effects of pump actuation on protein stability. AlkP-NE samples were prepared and stored for 24 hours as detailed above. Pre-dispensed samples were collected and compared to mixtures dispensed through either the Pfeiffer or BD sprayers. The samples were diluted 1:1000 in distilled H_20 in order to avoid NE turbidity effect on the optical density measurements. Diluted samples were then aliquotted into individual wells on a 96-well flat-bottom non-treated assay plate to provide a final concentration of 334 ng of AlkP/100 µL. SIGMA FAST™ p-Nitrophenol Phosphate (pNPP) was used as a chromogenic substrate for an AlkP. Optical density measurements of the solutions were collected 15 minutes, 30 minutes, and 1 hour after the introduction of the pNPP substrate solution using a SpectraMax 340 spectrophotometer at 405 nm, 450 nm, 490 nm, and 650 nm. The data was analyzed using SOFTmax Pro© ver. 2.2.1 software.

Determination of the effects of sprayer actuation on the potency of NE-based vaccines

In order to evaluate the effects of dispensing NE-based vaccines through the nasal sprayer systems, *in vivo* immunogenicity studies were conducted in mice. HBsAg-NE was dispensed through either the BD or Pfeiffer system, and the dispensed mixture was collected in 15-mL polystyrene vials. Either pre-actuated or post-actuated HBsAg-NE samples were used to nasally vaccinate the mice, as described above. Serum anti-HBsAg IgG titers were measured using ELISA.

Determination of the consistency of dispensing NE using nasal sprayers

The consistency of the NE spray volume was evaluated by two methods. First, the intrinsic turbidity of the NE was measured to quantify the sprayer output. In order to determine a NE dilution concentration that falls within a measurable linear range, a standard NE turbidity curve was generated by 1:10 to 1:1000 dilutions of NE stock. The optical density was measured using a Milton Roy 1001 spectrophotometer at 405 nm. Based on the standard curves, the optimal dilutions for measurement were identified to be > 1:100 of the 100% NE stock. For volume comparison studies, both the Pfeiffer and BD (n=3 devices/manufacturer and 6 sprays/device) sprayers were manually actuated (~130 µL each actuation) such that the entirety of the emitted NE was dispersed into a 15 mL polypropylene vial. Thirteen mL of distilled H_20 was then added to the vial, and the vial was centrifuged at 1000 RPM for 60 seconds to assure that all of the dispensed NE was combined in the solution. The optical density was then measured.

Spray weights were also used to confirm dose consistency. For these studies, the nasal spray pumps were weighed before and after actuation, using a calibrated AB204 Mettler Toledo enclosed gram scale. These studies were also conducted with 3 Pfeiffer and 3 BD sprayers. Spray weights were averaged based on 6 actuations per pump.

Determination of Physical Properties of NE Potentially Influencing Nasal

Viscosity

The rheology of the NE or the HBsAg-NE was measured using a AR-G2 (TA Instruments) control stress rheometer. The measurements were performed at room temperature (25°C) with a 2° 6-cm steel cone and plate geometry to mimic the conditions during the sprayer characterization studies. Using a pipette, samples of 5%, 10%, 20 % and 40% NE or 0.04 mg/mL HBsAg – 20% NE were carefully loaded into the rheometer, and the mixture was allowed to equilibrate

for at least 5 minutes prior to analysis. A solvent trap was used to avoid evaporation. The rheology flow curves were produced using the steady state flow test, whereby the shear rate ($\dot{\gamma}$), was increased gradually from 10^{-1} (s^{-1}) up to 10^{3} (s^{-1}). Hysteresis curves were generated by gradually increasing the shear rate from 10^{-1} (s^{-1}) to 10^{2} (s^{-1}) where shear rate remained constant at 10^{2} (s^{-1}) for 30 minutes. The shear rate was then gradually returned to the starting point under the same conditions.

Surface tension

NE-air surface tension was calculated using the surface capillary rise tensiometer method [28]. Microcaps® precision 20-µl capillary tubes (Drummond Scientific Company) were carefully inserted into 5%, 10%, 20% or 40% NE, 0.04 mg/mL HBsAg – 20% mixtures just to the point of contact. The mixture was allowed to equilibrate in the capillary tube. Using a precision caliper Model 14-468-17 (Fisher Scientific), the height of the column in the capillary tube was measured. The contact angle θ (the angle the tangent to the surface of the NE makes with the side of the capillary tube) was measured after scanning the tube with a Hewlett Packard 5300c scanner. In all solutions containing NE, θ =90°. The condition of the equilibrium of a column of height *h* is approximated by:

$$h = (2\gamma_{1a}\cos\theta)/\rho g r$$

where γ_{1a} is the liquid-air surface tension, ρ is the density of the liquid, r is the radius of the capillary tube (0.0223 inches), and g is the gravity acceleration constant [29]. The validity of the experimental design was confirmed by comparing it to the established values for water, glycerol, and ethanol.

Determination of Nasal Spray Characteristics

Droplet size distribution (DSD)

Droplet-size analysis of the 0.04 mg/mL HBsAg- 20% NE aerosols was conducted by laser diffraction using a Malvern Spraytec with RT Sizer software. A Proveris Scientific NSx-MS Actuation Station and Image Therm NSx Actuation Station were used to actuate the BD and Pfeiffer pumps, respectively. DSD measurements were performed at room temperature (~25°C) with a 300-ms test duration, and the data acquisition rate was set at 1000 Hz by the Malvern Spraytec Software. The selection of the actuation-force settings represented the forces typically applied by a majority of individuals. The following actuation parameters for BD sprayers were set using SprayVIEW NSx Automated Actuation Station software: 14-mm stroke length, 60-mm/sec velocity, 3000-mm/sec² acceleration, 30-ms initial delay, 150-ms hold time, and the position of the nasal spray tip relative to the edge of the Malvern Spraytec detector lens cover was 7.25 cm. The actuation parameters for Pfeiffer pumps were as follows: symmetric profile, 4.69-mm stroke length, 33-mm/sec velocity, 1526-mm/sec^2 acceleration, 30-msec initial delay, and 252-ms hold time. The droplet size distribution was characterized by the following metrics: volume distribution (Dv10, Dv50, Dv90) and Span and percentage (%) less than 9 µm per the FDA CMC guidance on *Nasal Spray and Inhalation Solution, Suspension, and Spray Drug Products—Chemistry, Manufacturing and Controls Documentation, July 2002*. Dv50 is defined as when the volume median diameter or 50% of the distribution is contained in droplets that are smaller than this value while the other half is contained in droplets that are larger than this value. Similarly, the Dv10 and Dv90 values indicate that 10% and 90%, respectively, of the distribution is contained in droplets that are between these values. Span quantifies the spread of the droplet size distribution and is calculated by the following equation:

$$\text{Span} = (Dv90-Dv10)/Dv50$$

The stable phase from the acquired histogram for each actuation was manually

selected to analyze the droplet size distribution (DSD). Neither the BD nor Pfeiffer systems required shaking. The Pfeiffer pump was manually actuated 5 times just prior to sample analysis for priming, whereas the BD sprayer did not require priming. Five units each of BD and Pfeiffer pumps were tested.

Spray Pattern

Spray pattern tests were performed from the analysis of a two-dimensional image of the emitted plume. Spray-pattern studies of 0.04 mg/mL HBsAg- 20% NE aerosols were conducted using SprayVIEW NSP, which is a non-impaction laser sheet-based instrument. As in DSD studies, a Proveris Scientific NSx-MS Actuation Station and an Image Therm NSx Actuation Station were used to actuate the BD and Pfeiffer pumps with the same actuation parameters described above. The spray pattern was measured with the SprayVIEW NSP using the following parameters: a 3-cm distance to the laser beam (orifice to tip distance), a 500-Hz frame rate, 500 images were acquired per device, a 2.0 lens aperture, a 9-mm Fujinon lens, 22-cm and 25-cm camera position vertical (from the top) for the BD and Pfeiffer sprayers respectively, 5-cm and 15-cm camera position horizontal (from the right) for BD and Pfeiffer sprayers respectively, an 8.6-cm laser position horizontal (from the left), and a gradient pallet. The spray pattern is characterized by the following metrics: Dmax, Dmin, ovality ratio, and % area per the FDA CMC guidance for *Nasal Spray and Inhalation Solution, Suspension, and Spray Drug Products* (2002) and the FDA draft guidance for industry: *Bioavailability and Bioequivalence Studies for Nasal Aerosols and Nasal Sprays for Local Action,* April 2003. Dmax is defined as the longest diameter measured on the resulting spray pattern image. Dmin is the shortest diameter measured on the resulting spray pattern image. Dmax and Dmin must pass through the center (weighted for image intensity) of the spray pattern image. The ovality ratio is the ratio of Dmax to Dmin. This ratio provides a quantitative value for the overall shape of the spray. Percent area indicates the percent of the area

that the emitted plume filled the established screening area. Five units each of BD and Pfeiffer pumps were tested.

Plume Geometry

The SprayVIEW NSP with the Proveris Scientific NSx-MS Actuation Station (for the BD sprayers) and the Image Therm NSx Actuation Station (for the Pfeiffer pumps) were used to mechanically actuate the sprayer units for plume geometry studies on the 0.04 mg/mL HBsAg- 20% NE aerosols. The actuation parameters did not deviate from those used for DSD and spray pattern analysis. Sprayview NSP parameters established for spray pattern determination remained consistent, with the following exceptions: 250 images were acquired, the camera position vertical (from the top) was set to 12.8 cm (BD) and 10.8 cm (Pfeiffer), the camera position horizontal (from the right) was set to 24.0 cm, the laser position horizontal (from the left) was set to 10.1 cm, and the laser position height (from the top) was set to 16.8 cm (BD) and 14.3 cm (Pfeiffer). The plume geometry was characterized by the following metrics: spray angle (the angle of the emitted plume measured from the vertex of the spray cone and spray nozzle) and plume width (the width of the plume at a given distance from the spray nozzle) per *FDA Guidance for Industry: Nasal Spray and Inhalation Solution, Suspension, and Spray Drug Products—Chemistry, Manufacturing and Controls Documentation, July 2002* and FDA draft guidance for industry: *Bioavailability and Bioequivalence Studies for Nasal Aerosols and Nasal Sprays for Local Action,* April 2003 . Five units each of the BD and Pfeiffer pumps were tested.

Statistics

Data were expressed as mean ± standard deviation (SD) and were subjected to statistical analyses of variance (ANOVA) using the Student *t* and Fisher exact tests. The analyses were done with 95% confidence limits and two-tailed tests. Probability values of <0.05 were considered statistically significant.

4.3 RESULTS

Formulation and effects of diluent on thermal stability of NE-based vaccines

Regardless of the diluent, mixtures of OVA-NE remained visually homogenous (score 6) at all time points in this study up to 10 months. Lipid particle size did not significantly change in all cases throughout the 10-month duration of the study, confirming the visual inspection results (Figure 4.1).

SDS-PAGE and immunoblotting studies demonstrated absence of OVA degradation. The antigenic epitopes remain intact in the presence of NE for up to 8 months in PBS-diluted samples and 6 months for NaCl-diluted samples (Figures 4.2A and 4.2B). OVA-specific, higher-molecular-weight bands were detected by immunoblotting at all time points. However, the absence of lower-molecular-weight bands and the retained intensity of the major OVA band indicate a lack of protein degradation. Significant decreases in the intact OVA protein was observed by 10 months for the PBS-diluted samples and at 8 months for the NaCl-diluted samples (Figure 4.2C). However, no lower-molecular-weight OVA-specific products were detected in any of the tested samples.

In light of these findings *in vivo* potency was tested in CD-1 mice using OVA-NE stored for 6-8 months duration of time respectively. Immunogenicity, measured as serum anti-OVA IgG titers, was compared to mice vaccinated with freshly prepared OVA-NE mixtures. Anti-OVA serum IgG responses were determined at 12 weeks after primary vaccination. No significant differences in potency between the freshly prepared versus the stored samples were observed. However, stored OVA-NE with 0.9% NaCl trended toward reduced potency at 6 months (Figure 4.3).

Effects of nasal spray pumps on physico-chemical stability of NE-based vaccines

Sprayer Effects on NE and Protein

To ascertain the effects of dispensing NE-based vaccines through nasal spray pumps, the physico-chemical stability characteristics of the inoclum. Dispensing with either the Pfeiffer of the BD Accuspray did not change the particle size of NE alone or the OVA-NE (Figures 4.4A and 4.4B). The integrity of the OVA was not affected by actuation through either system. Silver-stained electrophoresed gels containing samples collected from the pre-spray and post-spray samples (Figure 4.5A) showed no evidence of protein degradation. We compared the activity of an enzyme (AlkP) in pre- and post-spray samples as a slightly more sensitive way of determining the possibility of epitope changes associated with sprayer actuation. The AlkP-NE was collected and enzyme activity was measured prior and post-dispensing through either the Pfeiffer or the BD sprayer systems. AlkPhos activity was not affected after dispensing AlkP-NE through either sprayer (Figure 4.5B).

Sprayer effects on Immunogenicity

Immunogenicity studies were performed using HBsAg as a representative antigen. For these studies, mice were vaccinated with either 20 µg HBsAg + 20% NE or 5 µg HBsAg + 20% NE to accentuate potential differences at lower concentrations. Intranasal vaccination with either pre- or post-sprayed samples resulted in comparable high levels of anti-HBsAg serum IgG antibodies. Titers reached 10^3 to 10^4 titers prior to the boost and 10^4 to 10^5 following the boost, respectively (Figures 4.6A and 4.6B). No significant differences in antibody response at any time point in the study between the pre- and post-sprayed samples were observed for either sprayer system ($p < .05$).

In vitro nasal spray characterization using NE-based vaccines

Volume Consistency

Spectrophotometric and spray weight studies were used to quantitatively evaluate the consistency of delivery using both the Pfeiffer and BD systems. Using the inherent turbidity of NE, pre- and post-dispensed samples (consisting of a broad range of NE concentrations) were measured for optical density. As shown in Figure 4.7A, a broad concentration range is emitted consistently (minimal standard deviation error bars) with either the BD or Pfeiffer systems. Also, spray weight measurements demonstrated volume consistency with either sprayer system (Figure 4.7B).

Viscosity

To gain an understanding and to explore the relationship between the rheological properties of NEs and their spray characteristics, viscosity studies were conducted using a range of NE concentrations and protein-NE formulations. The shear-rate dependent viscosity is reported in Figure 4.8A; a NE concentration-dependent increase in viscosity was observed (η = 0.0011 Pa-s [10% NE], =0.0015 Pa-s [20% NE and 0.04 mg/mL HBsAg + 20% NE], =0.0037 Pa-s [40% NE]). There was no change in the viscosity with the addition of protein. In order to assess shear-induced degradation, a hysteresis of the rheology curve was investigated wherein the shear rate was slowly ramped up and maintained at a relatively high rate for 30 minutes prior to ramp-down. The process appeared to be reversible with no prominent hysteresis in the viscosity profile, and there was therefore no evidence of shear-induced degradation (Figure 4.8B).

Surface Tension

The surface tension of the NE-air interface was experimentally determined using the capillary rise tensiometer method. As expected, a surfactant concentration-

dependent decrease in surface tension was observed for NE concentrations ranging from 2.5% to 20% (Figure 4.8C). Surface tension significantly increased between 20% NE and 40% NE by 1.7 dynes (*p val* = 6.0 x 10^{-3}). There was not a significantly different surface tension between 2.5% NE and 40% NE groups, however. The addition of HBsAg increased the surface tension significantly by 1.3 dynes (*p val* = 1.3 x 10^{-3}).

DSD Measurement

Differences in 0.04 mg/mL HBsAg-20% NE DSD profiles were observed between the BD and Pfeiffer units (Table 4.1). For example, 80 % of the BD emitted spray contained droplets ranging in size from 128 µm and 406.66 µm (Dv10 - Dv90) with a Dv50 Value of 251.50 µm. The Dv10 - Dv90 for the Pfeiffer emission ranged from 14.44 µm to 59.33 µm, with a Dv50 value of 29.43 µm. In addition, 3.11% of the BD emission measured less than 9 µm in size, whereas there were no detectable droplets smaller than 9 µm for Pfeiffer units.

Spray Pattern and Plume Geometry

Considerable differences in the spray pattern and plume geometry were also observed between the BD and Pfeiffer units (Tables 4.1 and 4.2 and Figure 4.9). The NE dispensed in a narrow oval shape (ovality = 3.636 spray diameters ranging from 1.8 mm to 4.6 mm, spray angle of 9.8°, and plume width of 5.1 mm) in the BD sprayers as compared to the Pfeiffer units (ovality = 1.152, spray diameters ranging from 39.5 mm to 45.4 mm, spray angle of 74.8°, and plume width of 46.2 mm).

4.4 DISCUSSION

NE-based vaccines offer a significant advantage over traditional vaccines, because of their potent adjuvant ability, long shelf life at non-refrigerated temperatures, and needle-free delivery [18]. Inherent safety profiles associated

with recombinant proteins which are often manufactured and diluted in either PBS buffer or non buffered NaCl solutions lend attractiveness to their use in NE-based mucosal vaccines [15, 16, 18]. Practical use of NE-based vaccines, however, requires formulation optimization of antigen and NE mixtures. One of the aims of this study was to characterize the effects of PBS versus non-buffered saline diluents on the thermal stability and immunogenicity of NE-based vaccines. Our results indicate that antigen integrity was unaltered in the nanoemulsion solution and that its *in vivo* potency remained intact for at least 8 months when stored at room temperature and diluted in PBS and at least 6 months (at room temperature) when diluted in NaCl. The nanoemulsion remained physically stable regardless of the antigen or dilution during all time points during the study. These studies are consistent with previous studies showing HBsAg-NE retained full potency for at least 12 months at 4°C, 6 months at 25°C and 6 weeks at 40°C. The major factors influencing the thermal stability of HBsAg-NE were entropically driven thermodynamic association and electrostatic interactions of the HBsAg and the NE [18]. Based on the present results, we propose that the effects of the buffered versus the non-buffered sodium diluents influence the electrostatic relationship between protein and the NE. The change in protein-NE interaction may result in the difference in thermal stability profiles. Studies designed to further evaluate the thermodynamic and electrostatic relationships of the antigen and the NE are currently underway in our laboratory.

For use in developing populations, NE-based vaccines should be manufactured at low cost and formulated for easy administration, perhaps by non-highly trained medical personnel using commercially available nasal sprayer delivery devices. In these studies, we investigated the potential to accurately, efficiently, and reproducibly deliver NE-based vaccines using standard nasal sprayer devices which have been approved for human use. The physico-chemical stability and immunogenicity of NE-based vaccines were found to be unaffected by actuation through the nasal sprayer devices tested. Either sprayer

produced consistency dose volume of the NE with a variance of less than 1%. This consistency is well within the U. S. Food and Drug Administration Center for Drug Evaluation and Research (FDA CDER) guidelines governing the use of nasal and inhalation spray drug products. Recommendations in this report suggest that the pump spray weight delivery acceptance criteria should control the weight of the individual sprays to be within 15 % of the target weight and that their mean weight be within 10% of the target [30].

The characteristics of nasal aerosol generation are shown to be dependent on a combination of actuation force, viscosity, rheological properties, surface tension, and pump design [22, 23]. A concentration-dependent decrease in surface tension and a respective increase in DSD are expected to increase with a higher total surfactant [23]. In these studies our data verify this relationship in part in that dilute NEs (with lower concentrations of surfactants) exhibit a higher surface tension compared to less dilute concentrations of NEs (with higher surfactant concentrations). Nasal deposition patterns of aerosolized substances, however, are more difficult to predict with *in vitro* modeling and are influenced by a number of pump-related factors, including DSD, viscosity, spray pattern, plume angle and administration angle, impaction, and sedimentation characteristics [21, 31, 32]. The most significant anatomical influence is the airway constriction and turbulence that occur at the nasal valve. This area, which is the primary focus of impaction, has been suggested as the limiting barrier preventing anti-rostral distribution . While most spray pumps that produce DSD exceeding 10 μm in size deposit substances in the anterior region of an MRI-reconstructed sinus replica, pumps producing sprays with small plume angles have been shown to be capable of reaching the turbinate region with deposition efficiencies approaching 90% . Minimal dependence on droplet size, viscosity, or device was observed in those studies [31].

The nasal distribution patterns of other experimental muco-adhesive substances have significant alterations in nasal deposition patterns resulting from

changes in DSD profiles primarily impacted by the viscosity [23]. In this study, we have reported that a NE behaves as a Newtonian fluid, as evidenced by the constant viscosity at a given temperature regardless of the rate of shear. Further, as the shear rate was increased, there was no evidence of shear thinning or physical changes in the material over forces well exceeding those encountered during actuation. Based on the predicted inertial impaction of the large droplet size of NE-based vaccine produced by (128.47 μm – 404.66 μm for BD and 14.44 μm to 59.33 μm for Pfeiffer), the spray angle, and plume geometry reported in these studies, the NE-based vaccines are expected to be efficiently deposited mainly in the anterior region of the human sinus with both sprayer units [21, 31]. Because of the larger spray angle (74.8° ± 1.86), the Pfeiffer pumps potentially may distribute over a broader surface in this area. However, deposition with the BD pump, which produces a relatively small spray angle (9.8° ± 3.61) and a spray pattern exhibiting a relatively small diameter (ranging from 1.8 mm ± 1.4 to 4.6 mm ±0.57), is expected mainly in the anterior region, but some deposition in the turbinate regions may occur [21, 31]. The expanded theoretical NE deposition pattern of the BD units may be limited by DSD characteristics and would be highly dependent on an administration angle [31]. Further studies are warranted to determine the actual deposition patterns in the human sinus. Although numerous investigators have suggested that targeting to nasal-associated lymphoid tissue (NALT) may be a superior method of inducting nasal immunization [33-35], we have shown that a NE adjuvant promotes efficient trans-mucosal antigen delivery to innate immune cells in non-NALT regions. In those studies, we demonstrate broad nasal epithelium uptake in the anterior and turbinate sinus regions and then subsequent trafficking of the fluorescent protein to the sub-mandibular lymphoid nodes and thymus within 24 hours after application without appreciable involvement of the NALT [36-37]. In this respect, both sprayers would likely produce NE deposition patterns appropriate for immune induction.

4.5 CONCLUSIONS AND SUMMARY

In summary, the results of this study support the use of NE for use as a nasopharyngeal vaccine adjuvant in either industrialized or in un-developed populations. Our study furthers this goal by demonstrating improved thermal stability and potency by using PBS as a diluent for NE-based vaccine formulations. This may be an antigen-dependent phenomenon and further detailed investigations on candidate NE-based vaccines are needed. We have also demonstrated that NE-based vaccines do not require specially engineered delivery devices, a characteristic which may promote cost-efficient delivery to developing populations. Future studies will assess the actual distribution of NE-based vaccines within the nasal cavity, following intranasal dispensing with sprayers. Such studies will further characterize the potential utility of a NE as a nasopharyngeal adjuvant.

4.6 FIGURES

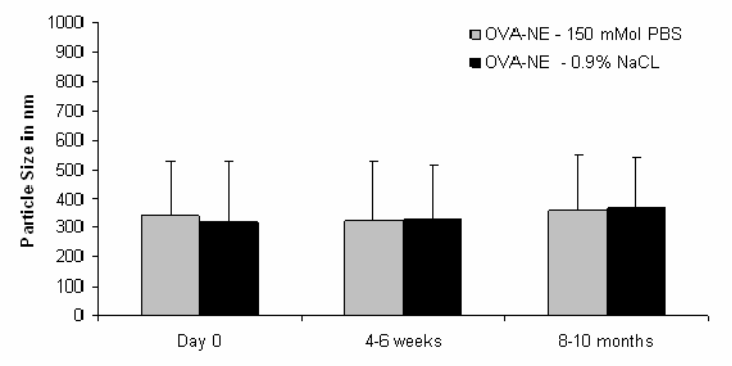

Figure 4.1. Evaluation of the effects of diluent on OVA-NE thermostability-Particle size characterization of NE OVA-NE. Particle size was not significantly different (*p-value* < 0.05) for either OVA-NE with 150 mMol PBS or 0.9% NaCl at any time during the study.

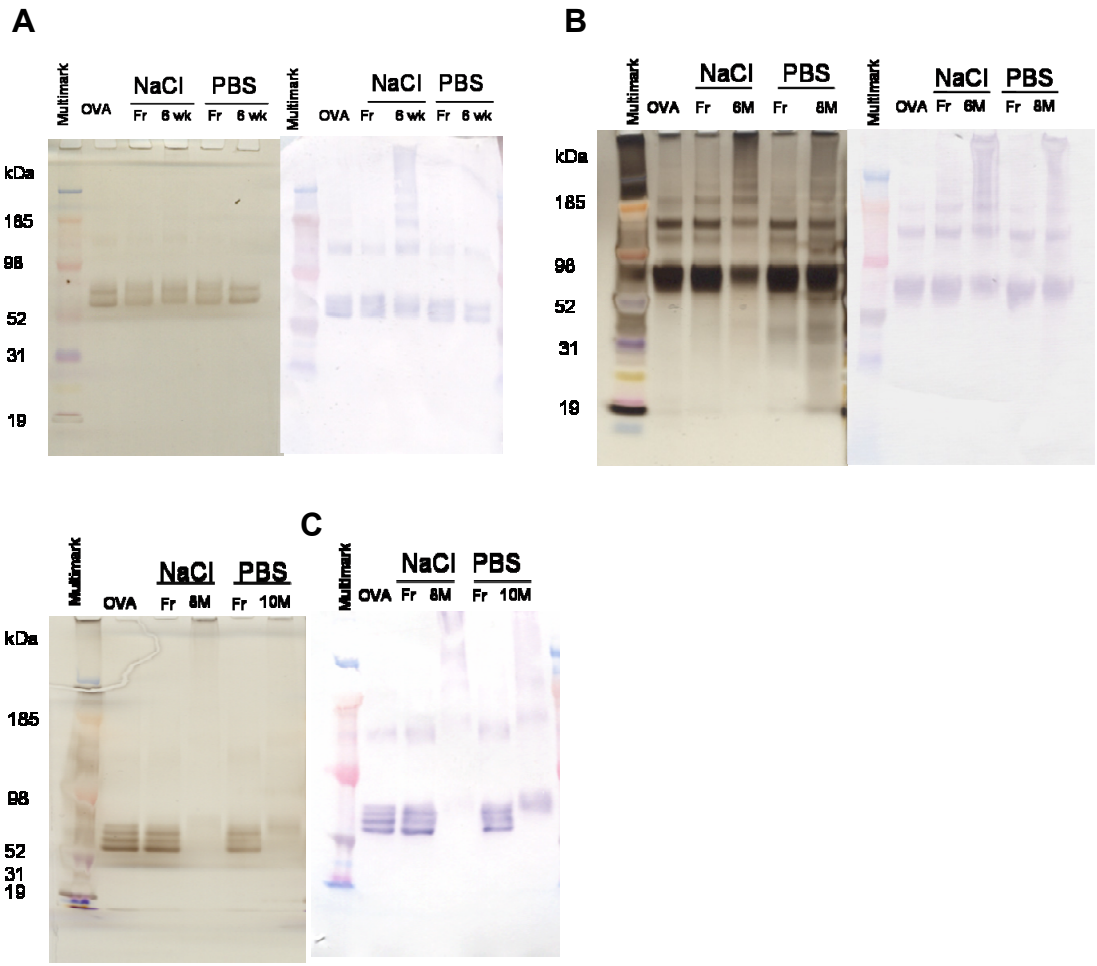

Figure 4.2. Physico-chemical Evaluation of the effects of diluent on OVA-NE The comparison of OVA-NE stored at room temperature conditions to freshly prepared formulation using SDS-PAGE followed by silver staining or Western immunoblotting is shown. Lanes are labeled according to sample storage conditions as follows- Lane 1: MW standard, lane 2: OVA (non-incubated), lanes 3-4: fresh prepared versus stored OVA-NE with 0.9% NaCl, lanes 5-6: fresh prepared versus stored OVA-NE with 150 mMol PBS. Samples were stored for **A)** 6 weeks, **B)** 6 months (0.9% NaCl mixtures) and 8 months (PBS mixtures), or **C)** 8 months (0.9% NaCl mixtures) and 10 months (PBS mixtures). Each lane contains 0.5 µg of antigen.

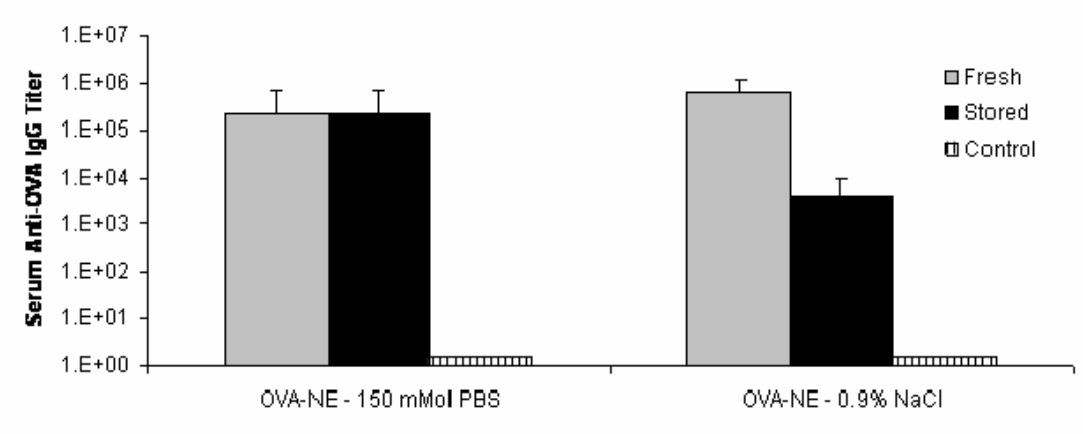

Figure 4.3. ***In vivo*** **potency evaluation of the effects of diluent on OVA-NE.** OVA specific antibody responses to freshly prepared OVA-NE or OVA-NE stored at room temperature (25°C) conditions are depicted. CD-1 mice were vaccinated with either freshly prepared or stored OVA-NE and boosted at 6 weeks. Control mice were not vaccinated. Serum anti-OVA IgG antibody concentrations measured at 6 weeks following boost vaccination are presented as a mean of endpoint titers in individual sera ± SD. Comparison of serum IgG elicited by freshly prepared OVA-NE to formulation stored for 8 months (OVA-NE with 150 mMol PBS) or 10 months (OVA-NE with 0.9% NaCl). No statistical differences (*p-value* <0.05) between freshly mixed and stored formulation IgG titers were observed.

A

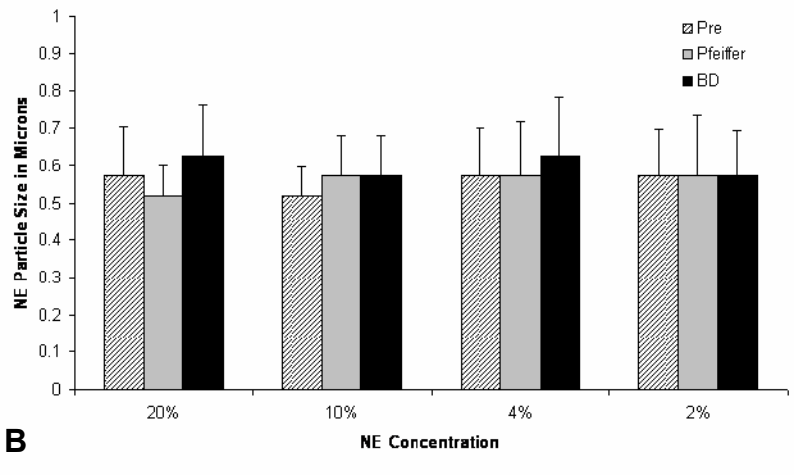

B

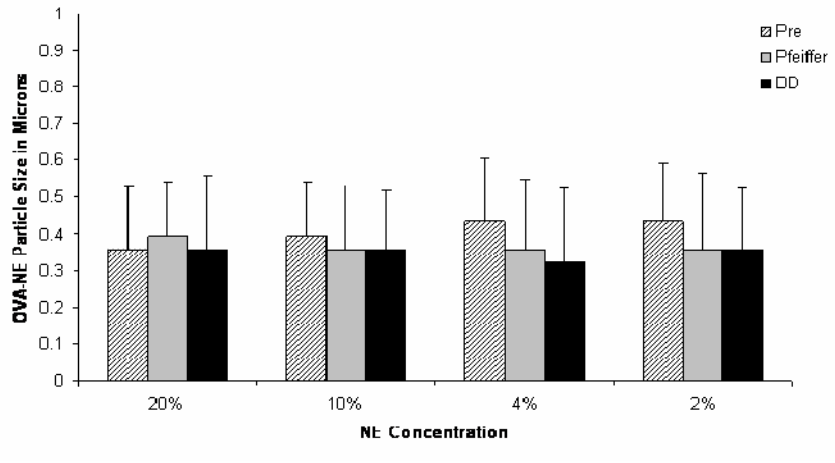

Figure 4.4. Effects of dispensing OVA-NE through commercially available nasal sprayers on NE stability. A) Particle size characterization of NE and **B)** OVA-NE. Note that particle size did not change after dispensing NE or OVA-NE through either the BD Accuspray or Pfeiffer sprayer systems.

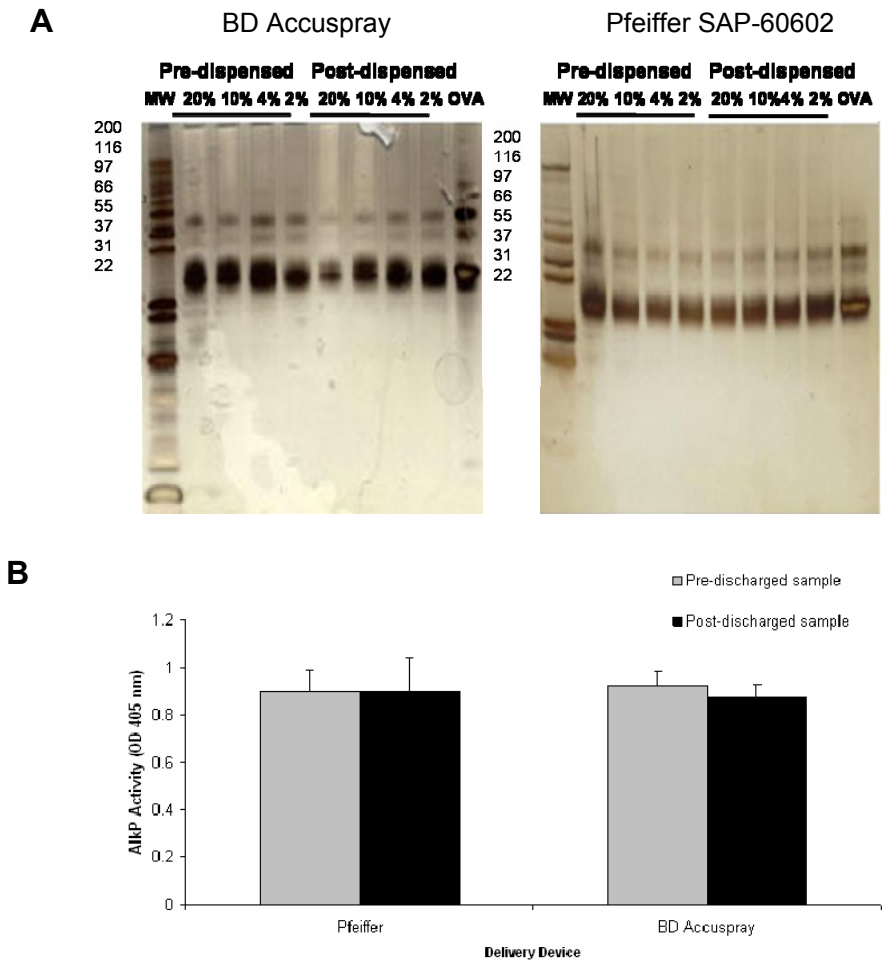

Figure 4.5. Physico-chemical evaluation of the effects of spraying OVA-NE through the Pfeiffer SAP-62602 or the BD Accuspray. A) The comparison of OVA-NE mixtures dispensed through either the BD Accuspray (left panel) or Pfeiffer sprayers (right panel) to freshly prepared (non-dispensed) formulations using SDS-PAGE followed by silver staining is shown. Lanes are labeled according to sample storage conditions as follows—Lane 1: MW standard, lanes 2-5: pre-dispensed OVA-NE (NE concentrations are listed above the respective lanes), lanes 6-9: post-dispensed OVA-NE, lane 10: OVA (non-dispensed). Each lane contains 0.5 mg of antigen. **B)** Comparison of AlkP enzymatic activity AlkP-OVA in pre-dispensed mixtures versus samples dispensed through the BD Accuspray and Pfeiffer sprayers. Activity in post-dispensed samples was not significantly different (*p-value* < 0.05) in comparison to pre-dispensed mixtures for either sprayer system.

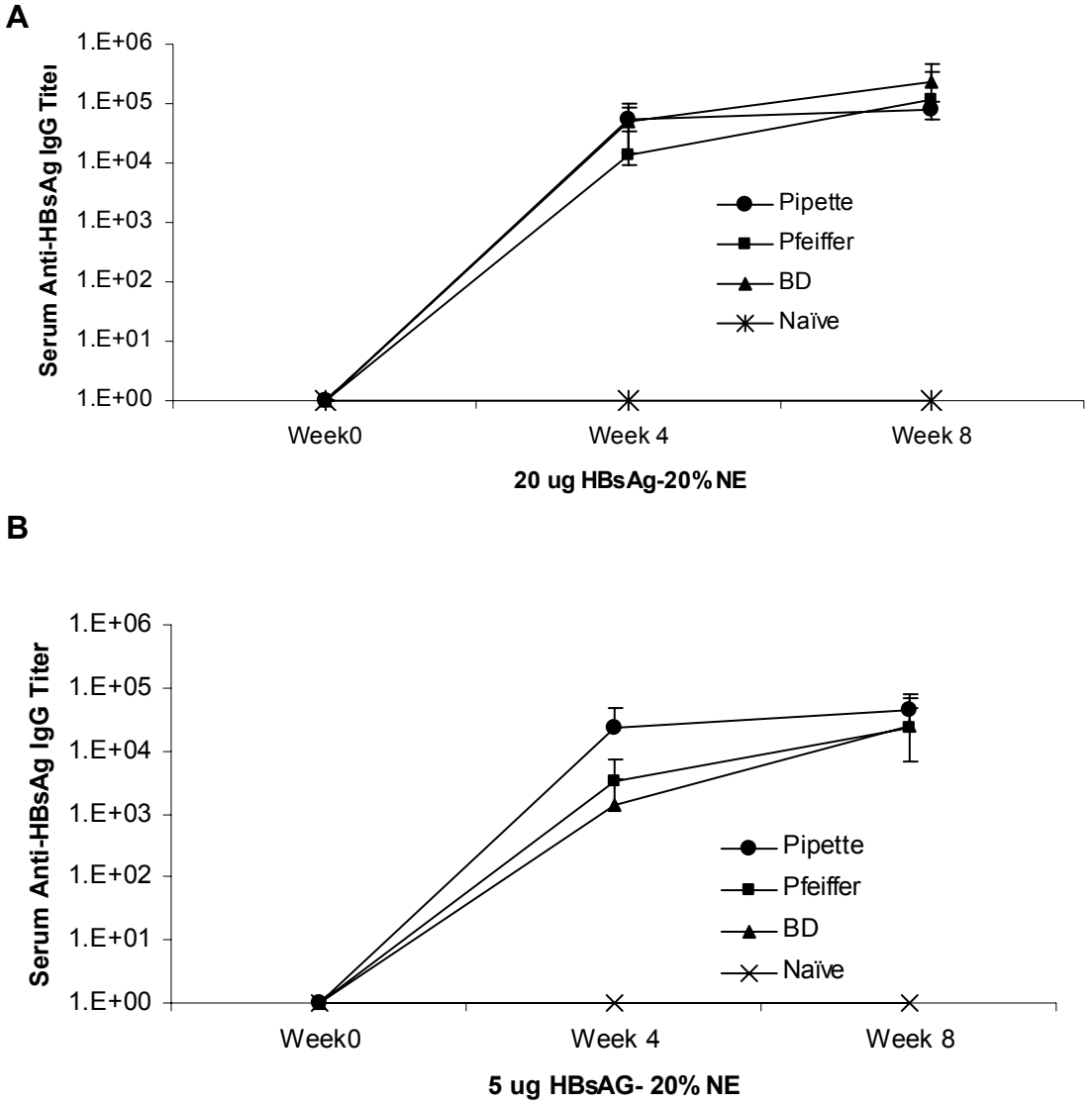

Figure 4.6. Evaluation of the effects of spraying OVA-NE through the Pfeiffer SAP-62602 or the BD Accuspray on *in vivo potency.* Antibody responses to OVA-NE actuated through either the BD Accuspray or Pfeiffer sprayer systems compared to non-sprayed mixtures are depicted. Mice were vaccinated with 20% NE + 20 µg OVA **A)** or 20% NE + 5 µg OVA **B)** and boosted at 6 weeks. Serum anti-OVA IgG antibody concentrations measured at 0, 4 and 8 weeks following prime vaccination are presented as a mean of endpoint titers in individual sera ± SD. No statistical difference (*p-value* <0.05) between sprayed and non-sprayed IgG titers was observed for either sprayer system.

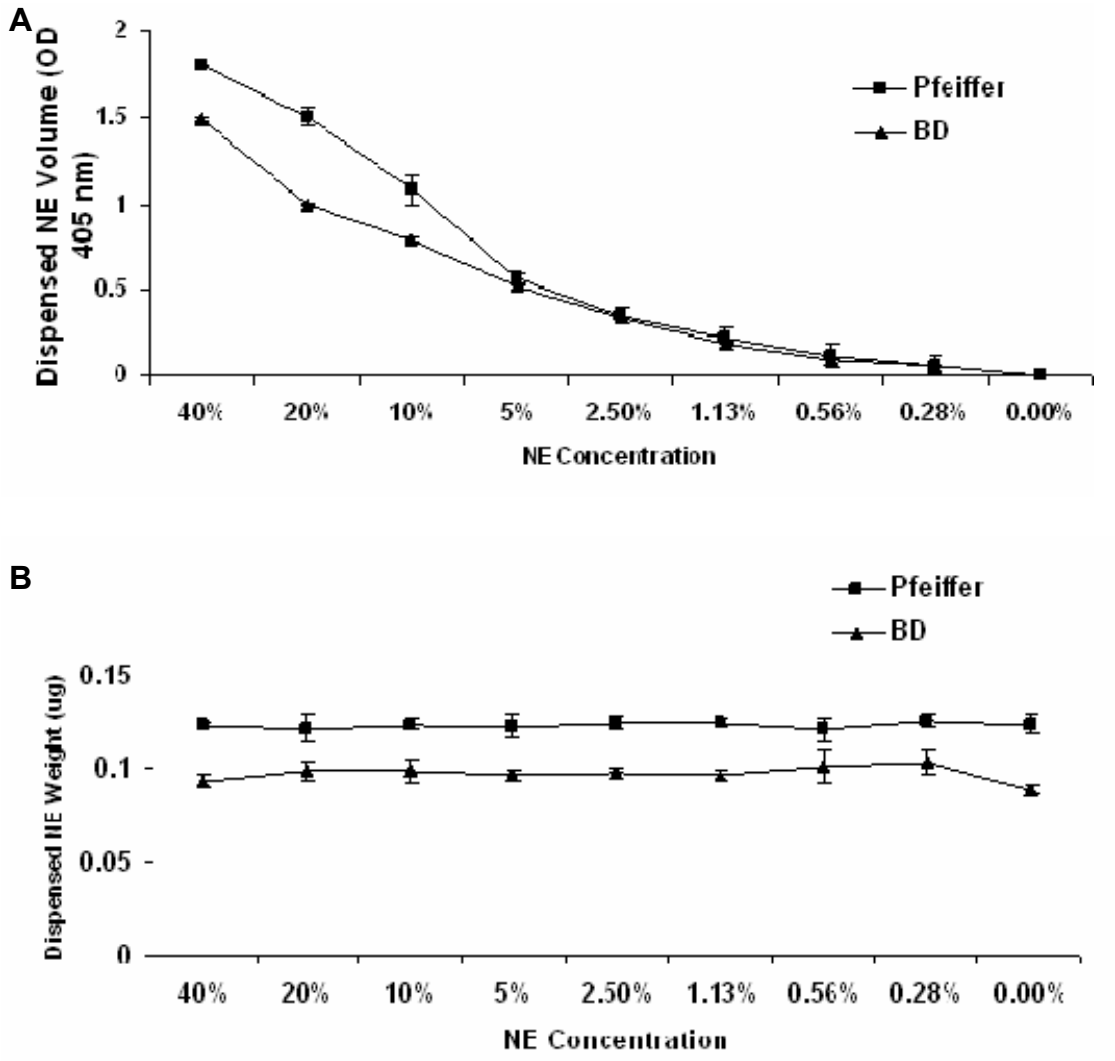

Figure 4.7. Evaluation of consistency in dispensed NE volume using commercially available nasal sprayer systems. A) Spectrophotometric analysis and **B)** spray weight characterization of the volume of NE dispensed in a single spray using either the BD Accuspray or Pfeiffer sprayer systems. Variation in spray volume is presented as a mean of optical density or spray weight ± SD. The difference in measured optical density and spray weight between the Pfeiffer and BD sprayers is explained by the inherent dead space within the BD sprayer nozzle and does not reflect a difference in the ability to deliver NE.

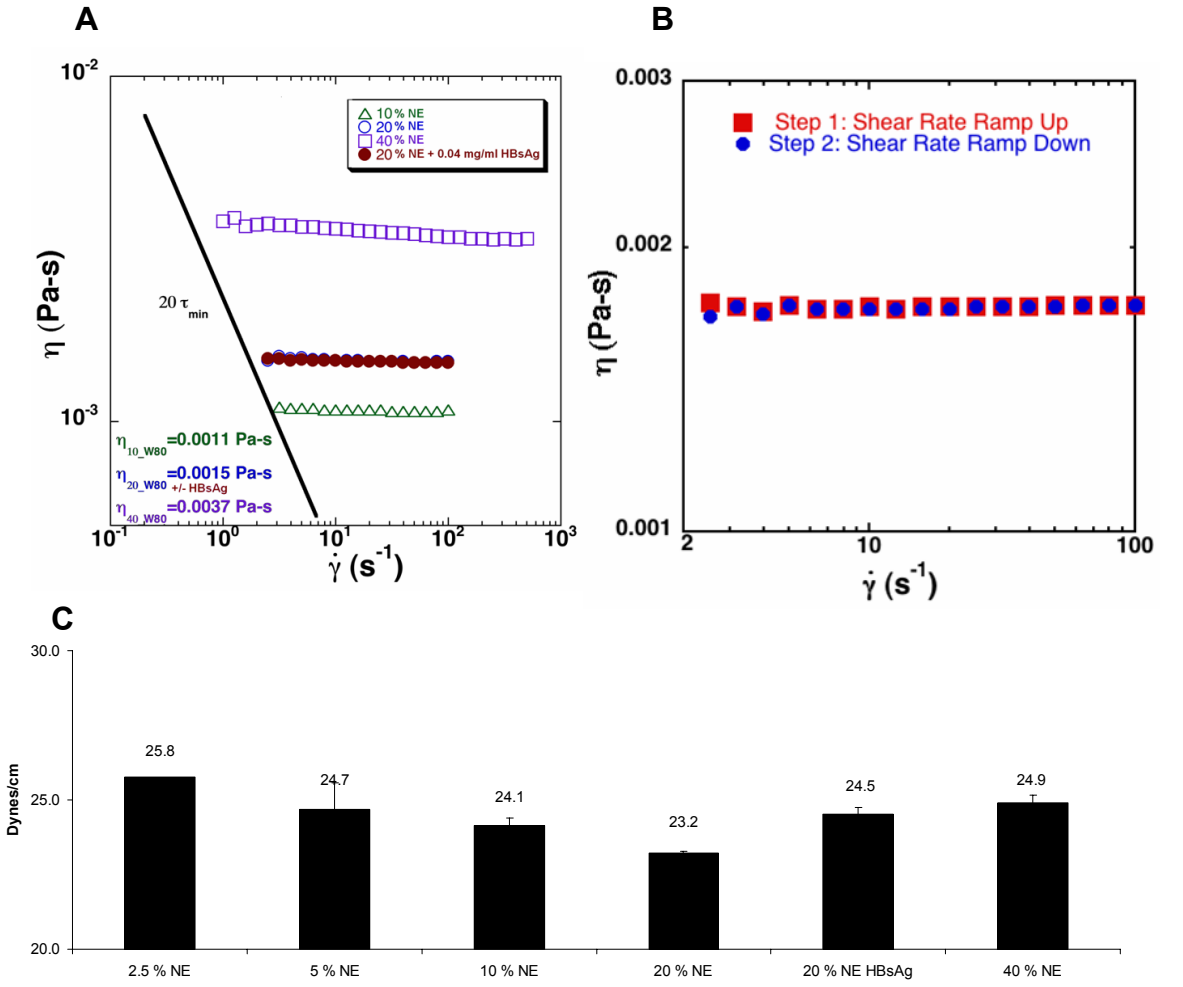

Figure 4.8. Rheological evaluation and surface tension characterization of NE and HbsAg-NE. A) Shear viscosity of solutions of NE at various concentrations and HBsAg-NE are depicted. Rheological measurements were performed using an AR-G2 (TA Instruments, Newcastle, DE) control stress rheometer by linearly increasing the shear stress from 10^{-1} (s^{-1}) to 10^{3} (s^{-1}). **B)** A hysteresis curve was generated by gradually increasing the shear rate from 10^{-1} (s^{-1}) to 10^{2} (s^{-1}) where shear rate remained constant at 10^{2} (s^{-1}) for 30 minutes. The shear rate was then gradually returned to the starting point under the same conditions. Viscosity (η) is reported in Pa-s units. **C)** Changes in surface tension at varying NE concentrations calculated using capillary rise tensiometry. Note that as the concentration of NE from 2.5 to 20% (and therefore surfactant concentration) increases, a statistically significant (*p*-value < 0.5) decrease in surface tension was observed. However, no significant change in surface tension was observed in the HBsAg-NE and 40% NE mixtures as compared to the 2.5% NE.

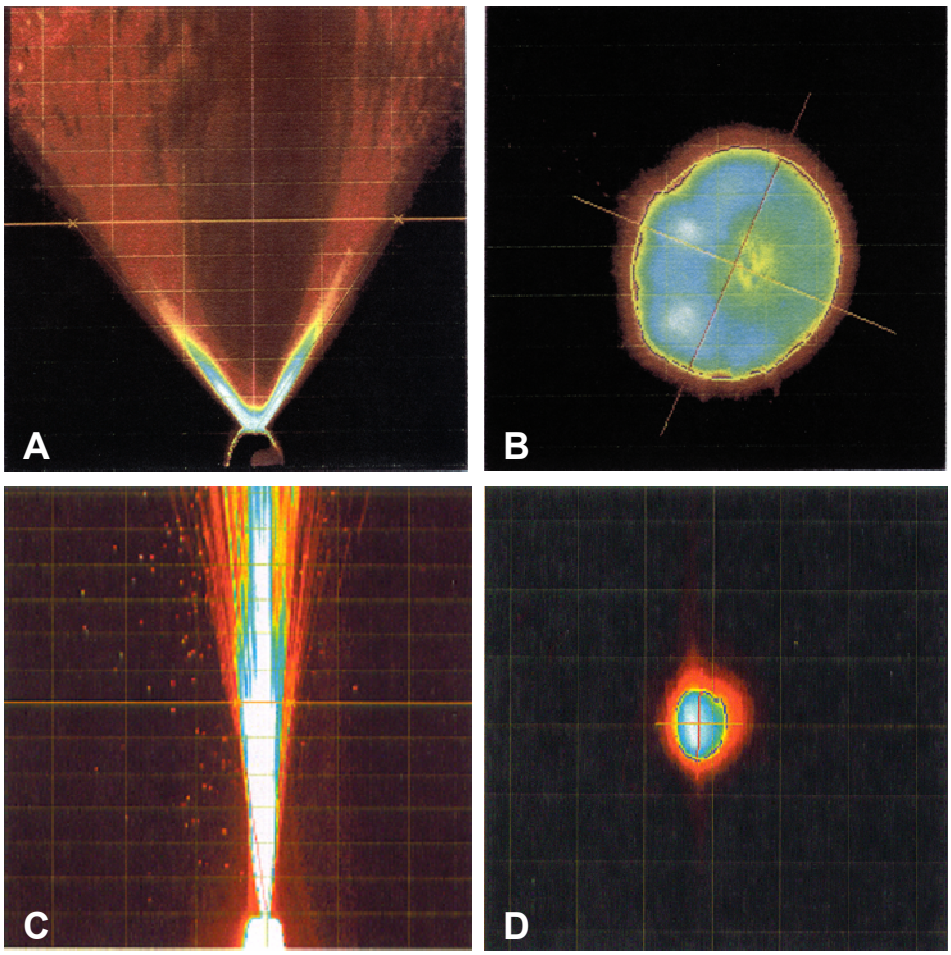

Figure 4.9. Plume Geometry and Spray-pattern characteristics for nasal sprayer systems. Influence in pump design on the emission of HBsAg-NE. Plume geometry is represented for **A)** Pfeiffer and **C)** BD Accuspray devices. Spray pattern is visualized at a distance of 3-cm from the pump orifice for **B)** Pfeiffer and **D)** BD Accuspray units.

4.7 TABLES

BD Accuspray					
	Dv10	Dv50	Dv90	Span	< 9 µm
	Size (µm)				
Mean	128.00	251.50	404.66	1.11	0.00
STD	21.79	31.90	21.00	0.15	0.00
%CV	16.96	12.68	5.19	13.27	0.00
Pfeiffer					
	Dv10	Dv50	Dv90	Span	< 9 µm
	Size (µm)				
Mean	14.44	29.43	59.43	1.53	3.11
STD	0.21	1.23	3.91	0.06	0.39
%CV	1.48	4.19	6.58	4.20	12.49

Table 4.1. Droplet size analysis of dispensing HBsAg-NE through commercial BD Accuspray or Pfeiffer sprayer systems. Each data column represents the average ± SD of six actuations. %CV is the coefficient of variance.

BD Accuspray				
Spray Pattern	Dmin	Dmax	Ovality Ratio	% Area
	Size (mm)			
Mean	1.8	4.6	3.636	0.6
STD	1.40	0.57	1.89	0.52
%CV	76.77	12.46	52.04	89.92
Plume Geometry	Spray Angle (degrees)		Plume Width (mm)	
Mean	9.8		5.1	
STD	3.61		1.88	
%CV	36.80		36.57	
Pfeiffer				
Spray Pattern	Dmin	Dmax	Ovality Ratio	% Area
	Size (mm)			
Mean	39.5	45.4	1.152	16.2
STD	0.87	2.35	0.05	1.02
%CV	2.21	5.18	3.99	6.28
Plume Geometry	Spray Angle (degrees)		Plume Width (mm)	
Mean	74.8		46.2	
STD	1.86		1.40	
%CV	2.49		3.02	

Table 4.2. Spray pattern and plume geometry characterization of dispensing HBsAG-NE through commercial BD Accuspray or Pfeiffer sprayer systems. Each data column represents the average ±SD of six actuations. %CV is the coefficient of variance.

4.8 REFERENCES

1. Miller, M.A. and A.R. Hinman, *Economic analyses of vaccine policies [Chapter 57]*, in *Vaccines*, S.A. Plotkin and W.A. Orenstein, Editors. 2004, Elsevier Inc.: Philadelphia, PA.

2. Heininger, U., *The success of immunization—shovelling its own grave? .* Vaccine, 2004. 22(15-16): p. 2071-2072.

3. Miller, M.A. and J.T. Sentz, *Disease and Mortality in Sub-Saharan Africa*, in *Disease and Mortality in Sub-Saharan Africa*, D.T. Jamison , et al., Editors. 2006, The Internation Bank for Reconstruction and Development/The World Bank: Washington, D. C.

4. Simonsen, L., et al., *Unsafe injections in the developing world and transmission of bloodborne pathogens: a review.* Bull World Health Organ., 1999. 77(10): p. 789-800.

5. Almeidaa, A.J. and E. Soutob, *Solid lipid nanoparticles as a drug delivery system for peptides and proteins.* Advanced Drug Delivery Reviews, 2007. 59(6): p. 478-490.

6. Keldmann, T. (2006) *Nasal drug delivery: Rapid onset via a conveient route*. OnDrugDelivery, 4-7.

7. Sharma, S., et al., *Pharmaceutical Aspects of Intranasal Delivery of Vaccines Using Particulate Systems.* Journal of pharmaceutical sciences, 2008. E PUB ahead of print.

8. Onorato, I.M., et al., *Mucosal immunity induced by enhance-potency inactivated and oral polio vaccines.* J Infect Dis, 1991. 163: p. 1-6.

9. McGhee, J.R. and J. Mestecky, *In defense of mucosal surfaces.Development of novel vaccines for IgA responses protective at the portals of entry of microbial pathogens.* Infect Dis Clin North Am, 1990. 4: p. 315–341.

10. Mestecky, J. and J.R. McGhee, *Prospects for human mucosal vaccines.* Adv Exp Med Biol 1992. 327: p. 13–23.

11. Brandtzaeg, P., *Overview of the mucosal immune system.* Curr Top Microbiol Immunol, 1989. 146: p. 13-25.

12. Slutter, B., N. Hagenaars, and W. Jiskoot, *Rational design of nasal vaccines.* Journal of Drug Targeting, 2008. 16(1): p. 1-17.

13. Moingeon, P., J. Haensler, and A. Lindberg, *Towards the rational design of Th1 adjuvants.* Vaccine 2001. 19: p. 4363–4372.

14. Myc, A., et al., *Development of immune response that protects mice from viral pneumonitis after a single intranasal immunization with influenza A virus and nanoemulsion.* Vaccine, 2003. 21: p. 3801–3814.

15. Bielinska, A.U., et al., *Mucosal Immunization with a Novel Nanoemulsion-Based Recombinant Anthrax Protective Antigen Vaccine Protects against Bacillus anthracis Spore Challenge.* Infect Immun, 2007. 75: p. 4020-4029.

16. Bielinska, A.U., et al., *Nasal immunization with a recombinant HIV gp120 and nanoemulsion adjuvant produces TH1 polarizatied responses and neutralizing antibodies to primary HIV-1 isolates.* AIDS Research and Human Retroviruses 2007. 24: p. 271-281.

17. Bielinska, A.U., et al., *A novel killed-virus nasal vaccinia virus vaccine.* Clinical and Vaccine Immunology 2008. 15: p. 348–358.

18. Makidon, P.E., et al., *Pre-Clinical Evaluation of a Novel Nanoemulsion-Based Hepatitis B Mucosal Vaccine.* PLoS ONE, 2008. 3(8): p. e2954.

19. Sawtell, J. A., Ream, A. J., *Observations on the Effect of the Diluent Used for Diluting Challenge Toxin in theClostridium botulinum Potency Test*. Biologicals, 1995. 23(3): p. 249-251.

20. Harris, A.S., et al., *Effect of viscosity on particle size, deposition, and clearance of nasal delivery systems containing desmopressin.* Journal of Pharmaceutical Sciences, 1988. 77: p. 405-408.

21. Cheng, Y.S., et al., *Characterization of nasal spray pumps and deposition pattern in a replica of the human nasal airway. J. Aerosol. Med*., 2001. 14: p. 267-280.

22. Suman, J.D., et al., *Validity of in vitro tests on aqueous spray pumps as surrogates for nasal deposition.* Pharm Res., 2002. 19(1): p. 1-6.

23. Dayal, P., M.S. Shaik, and M. Singh, *Evaluation of different parameters that effect droplet-size distribution from nasal sprays using the Malvern Spraytec.* Journal of pharmaceutical sciences, 2004. 93(7): p. 1725-1742.

24. Guo, C., et al., *Assessment of the influence factors on in vitro testing of nasal sprays using Box-Behnken experimental design.* European Journal of Pharmaceutical Sciences, 2008. In Press.

25. Lillard, J.W.J., et al., *Lymphotactin Acts as an Innate Mucosal Adjuvant.* The Journal of Immunology, 1999. 162: p. 1959-1965.

26. Classen, D.C., J.M. Morningstar, and J.D. Shanley, *Detection of antibody to murine cytomegalovirus by enzyme linked immunobasorbent and indirect immunofluorescence assays.* J Clin Microbiol, 1987. 25: p. 600-604.

27. Frey, A., J. Di Canzio, and D. Zurakowski, *A statistically defined endpoint titer determination method for immunoassays.* J Immunol Methods, 1998. 221: p. 35-41.

28. Batchelor, G.K., *An Introduction to Fluid Dynamics*, ed. G.K. Batchelor. 2000, Cambridge, UK: The Press Syndicate of the University of Cambridge.

29. Sears, F.W. and M.W. Zemanski, *University Physics*. 2nd ed. 1955, London, UK: Addison Wesley.

30. (CDER), *Guidance for Industry Nasal Spray and Inhalation Solution, Suspension, and Spray Drug Products - Chemistry, Manufacturing, and Controls Documentation*, US Food and Drug Administration, Editor. 2002, U.S. Department of Health and Human Services Rockville, MD.

31. Foo, M.Y., et al., *The influence of spray properties on intranasal deposition.* Journal of Aerosol Medicine, 2007. 20(4).

32. Vidgren, M.T. and H. Kublik, *Nasal delivery systems and their effect on deposition and absorption. Adv. Drug Deliv. Rev.*, 1998. 29: p. 157-177.

33. Reddy, S.T., et al., *In vivo targeting of dendritic cells in lymph nodes with poly(propylene sulfide) nanoparticles* J Control Release. , 2006. 112(1): p. 26-34.

34. Kiyono, H. and S. Fukuyama, *NALT- versus Peyer's-patch-mediated mucosal immunity.* Nat Rev Immunol. , 2004. 4(9): p. 699-710.

35. Goetsch, L., et al., *Targeting of Nasal Mucosa-Associated Antigen-Presenting Cells In Vivo with an Outer Membrane Protein A Derived from Klebsiella pneumoniae.* Infect Immun. , 2001. 69(10): p. 6434–6444.

36. Blanco, L.P., et al. *Insights into the Mucosal Adjuvant Mechanism of a Soybean Oil Nanoemulsion (SO-NE): Participation of GM1 Ganglioside.* in *Eleventh Annual Conference on Vaccine Research*. 2008. Baltimore, MD.

37. Makidon, P.E., et al. *Nanoemulsion Enhances Intracellular Uptake and Localization of Antigen to Regional Lymphoidal Tissue.* in *15th Annual Department of Internal Medicine Research Symposium*. 2007. University of Michigan, Ann Arbor, MI.

CHAPTER 5
NASAL IMMUNIZATION WITH A NANOEMULSION-BASED *BURKHOLDERIA CENOCEPACIA* OUTER MEMBRANE PROTEIN VACCINE PROTECTS AGAINST EXPERIMENTAL LUNG INFECTIONS IN MICE

5.1 BACKGROUND

In Chapter 5, I discuss the development of a NE-based mucosal vaccine designed for prohylaxis against cystic fibrosis (CF)-associated pathogens. CF results in the functional impairment of innate respiratory defense mechanisms, providing an appropriate environment for colonization of pathogenic bacterial species such *Staphylococcus aureus* and *Haemophilus influenzae* and a number of opportunistic species such as *Pseudomonas aeruginosa, Achromobacter xylosoxidans, Stenotrophomonas maltophilia, Ralstonia spp.*, *Pandoraea spp.,* and the *Burkholderia* cepacia complex (Bcc) species [1]. Bcc belongs to a group of up to 17 closely and phylogenetically related saprophytic gram-negative bacilli, most of which are capable of forming biofilm [1-4]. They are particularly difficult pathogens to treat and are associated with increased rates of morbidity and mortality in CF patients, and they are among the most antimicrobial-resistant bacterial species encountered in human infection [1, 5]. Once colonies are established, the unremitting infection and the associated inflammation is rarely eliminated, resulting in progressive lung disease ending in pulmonary failure and death [1, 6]. While therapeutic progress has been made in preserving functional pulmonary physiology by managing nutrition and mucoidal secretions, little progress has been made in therapeutic interventions for the prevention and management of Bcc infections [1, 5]. At present, no vaccines effective against Bcc are available.

Because Bcc colonization occurs on the respiratory mucosa, the development of a mucosal vaccine may be of value, as this route of vaccination has been associated with both mucosal and systemic immunity [7-11]. Mucosal vaccine development, though, has been limited largely because of the lack of effective mucosal adjuvants [7]. Outer membrane proteins (OMPs), the major surface antigens of Bcc, are considered potential protective epitopes for vaccine development. Bertot et al. have previously described robust immunity and protection in an experimental infection model after nasal vaccination with OMPs from *B. multivorans* adjuvanted by adamantylamide dipeptide (AdDP) and have demonstrated the potential protective value of anti-Bcc immune responses [12].

This study examines the use of a novel oil-and-water nanoemulsion (NE) as a mucosal adjuvant for a *B. cenocepacia* OMP vaccine. We have previously demonstrated that these NEs have broad antimicrobial activity [1, 13-16] and are safe and effective non-inflammatory mucosal adjuvants for killed virus-based and recombinant protein-based vaccines [9-11, 17, 18]. In this chapter, I characterized *B. cenocepacia* OMPs, assessed the induction of both mucosal and systemic anti-OMP antibodies, evaluated the ability of sera from mice vaccinated with *B. cenocepacia* to neutralize *B. cenocepacia* and *B. multivorans,* and tested for protective immunity after *B. cenocepacia* pulmonary infection was experimentally induced.

5.2 EXPERIMENTAL METHODS

B. cenocepacia Strain K56-2 Stock Maintenance and Culture

Burkholderia cenocepacia strain K56-2 was provided by the *Burkholderia cepacia* Research Laboratory and Repository (BcRLR), University of Michigan, Ann Arbor, MI. This isolate has been identified to the species level by polyphasic analyses using phenotypic and genotypic assays at the BcRLR (48). K56-2 is a clinical isolate and has been commonly used for *Burkholderia* molecular

microbiology and genomic studies [19]. It is a representative of the transmissible and virulent ET12 lineage. This makes it a logical choice for vaccine studies and it was selected because of the transmissible and virulent phenotype associated with this strain [20, 21]. *Burkholderia multivorans* ATCC 17616 was used for cross-strain neutralization assays. Both K56-2 and ATCC 17616 strains were stored at -80^{o}C in Lauria-Bertani broth with 15% glycerol and recovered from frozen stock on Mueller-Hinton (MH) agar overnight at 37^{o}C.

B. cenocepacia Outer Membrane Protein (OMP) Preparation

A 250-mL overnight culture of K56-2 in brain-heart infusion media was centrifuged at 3500 rpm for 20 minutes. The cell pellet was washed several times with phosphate-buffered saline (PBS), re-suspended in 75 mL of 1mM EDTA in PBS (pH 8.0), and then incubated for 30 minutes at room temperature. Post-incubation, the bacteria were passed several times through a 26-gauge needle (BD) using high pressure. Cell lysis was achieved with Triton X-100 (Sigma) added to a final concentration of 2% and incubated for 10 minutes at room temperature. Mechanical separation was performed on the preparation with multiple rounds of sonication (1 minute each). The sonicated lysates were then centrifuged for 10 minutes at 6000g twice with the supernatant retained after each spin. Following the second centrifugation, the supernatant was centrifuged at 100,000g for 1 hour at 4°C. The resulting pellet was then resuspended in endotoxin-free PBS. The rough OMP preparation was then purified (endotoxin-depleted OMP) with an endotoxin-removal column (Pierce) according to manufacturer's instructions. The flow-through fractions were stored at −80 °C until required.

OMP Analysis

The protein contained within the OMP preparation was quantified using BCA Assay (Pierce). Western blots and silver stain were performed using 4-12%

Bis-Tris Gels (Invitrogen) and the NuPAGE electrophoresis and transfer buffers (MES, Invitrogen). Western blot and silver staining was performed according to established protocol as described by Makidon, Bielinska et al. [8]. To quantify endotoxin contaminate, OMP was diluted 1:100 in endotoxin-free PBS and was analyzed using the Limulus Amebocyte Lysate (LAL) Kinetic-QCL (Lonza). Endotoxin was detected at 1.93 endotoxin units/mg in the endotxin-depleted OMP preparation. The DNA contaminant removal was verified by agarose-EtBr gel electrophoresis. Equal concentrations of OMP fractions before and after processing were run on a 1% agarose gel (Gibco) with ethidium bromide added. A ddH2O and 6X loading dye was added to each of the samples and then loaded onto the gel. Gels were run at 80V and imaged on a UV table (Figure 5.1C).

OMP Sequencing and Verification

Sample Preparation

The protein sample was separated by SDS-PAGE. The protein band immunostained with the highest intensity (~17 KDa) on Western blot (See Figure 5.1B was excised and subjected to in-gel digestion. In-gel digestion was performed at the Protein Structure Facility at the University of Michigan according to procedures by Rosenfeld et al. and Hellman et al. [22, 23]. A gel slice containing 5-pmol bovine serum albumin (BSA) was analyzed in parallel as a positive control.

Mass Spectrometry

HPLC-Electrospray Ionization (ESI) Tandem Mass Spectrometry (MS/MS) was performed on a Q-tof premier mass spectrometer (Waters Inc) fitted with a nanospray source (Waters Inc.). The mass spectrometer was calibrated with a mass accuracy within 3 ppm. On-line capillary HPLC was performed using a Waters UPLC system with an Atlantis C18 column (Waters, 100-mm inner

diameter, 100-mm length, 3-mm particle size). Digests were desalted using an online trapping column (Waters, Symmetry C18, 180-mm inner diameter, 20-mm length, 5-mm particle size) before being loaded onto the Atlantis column. HPLC separations were accomplished with a linear gradient of 3 to 75% acetonitrile in 0.1% formic acid in 75 minutes, flow rate 500 nl/min. A data-dependent tandem mass spectrometry approach was utilized to identify peptides in which a full scan spectrum (survey scan) was used, followed by collision-induced dissociation (CID) mass spectra of all ions in the survey scan with a peak intensity rising above 20 counts per second. The survey scan was acquired in V+ mode over a mass range of 50-2000 Da with lockmass correction (Gu-Fibrinopeptide B, $[M+H]^{2+}$: 785.8426) and charge state peak selection (2+, 3+ and 4+). The MS/MS scans were acquired for 5 seconds with collision energy control by charge state recognition.

Data Analysis and Bioinformatics

Tandem mass spectra were acquired using Mass Lynx software (Version 4.1). Raw data files were first processed for lockmass correction, noise reduction, centering, and deisotoping using the Protein Lynx Global Server software Ver. 4.25 (Waters Inc.). The generated peaklist files containing the fragment mass spectra were subjected to database searches using the ProteinLynxGlobal Server and Mascot (Matrix Science Inc., Boston, MA) search engines and Swiss Prot and NCBI databases, as well as the *Burkholderia cenocepacia* database downloaded from the Sanger Institute web site (http://www.sanger.ac.uk).

Preparation of Nanoemulsion-based OMP (OMP-NE) vaccine

NE was provided by NanoBio Corporation. OMP-NE formulations were prepared by vigorously mixing the endotxin-depleted OMP preparation (Figure 5.1.A Lane F) with concentrated NE, using PBS as the diluent. For the intranasal

immunizations OMP-NEs were formulated to contain either 0.25 μg/μL or 0.75 μg/μL OMPs mixed in 20% (v/v) NE.

Animals and immunization procedures

Pathogen-free, outbred CD-1 mice (females 6–8 weeks old) were purchased from Charles River Laboratories. The mice were housed in groups of five in standard pathogen-free (SPF) conditions with food and water available ad libitum in accordance to the standards of the American Association for Accreditation of Laboratory Animal Care. The use of these mice was approved by the University of Michigan University Committee on Use and Care of Animals (UCUCA). The mice (n=10 per group) were vaccinated with two administrations of either OMP-NE vaccines four weeks apart. Intranasal (i.n.) immunizations were performed in mice anaesthetized with isoflurane using the IMPAC$^{6®}$ anesthesia delivery system. The anesthetized animals were held in a supine position and 20 μL (10 μL/nare) of OMP-NE vaccine was administered slowly to the nares using a micropipette tip. Mice were immunized with either 15 μg OMP + 20% NE, 15 μg OMP in PBS, 5 μg OMP + 20% NE, or 5 μg OMP in PBS.

Phlebotomy, bronchioalveolar lavage, and splenocyte collection

Blood was collected from the saphenous vein every 21 days throughout the duration of the study. The terminal sample was obtained by cardiac puncture immediately following euthanasia. Whole blood samples were separated by centrifugation at 3500 rpm (15 minutes) following coagulation. The serum samples were stored at -20°C until analyzed.

Bronchioalveolar lavage (BAL) fluid was obtained from the mice immediately following euthanasia as described by Makidon et al. [8]. Briefly, a 22-gauge catheter (Angiocath, B-D) attached to a syringe was inserted into the distal trachea and 1.4 mL of PBS with protease inhibitors (Complete Mini-tabs,

Roche) was introduced into the bronchi and lungs and then subsequently removed.

In vitro measurement of the cytokine response was determined using the spleens of the vaccinated mice. Spleens were mechanically disrupted to obtain single-cell splenocyte suspension in PBS. Red blood cells were lysed with ACK buffer (150 mM NH4Cl, 10 mM KHCO3, 0.1 mM Na2EDTA) and removed by washing the cell suspension twice in PBS. The splenocytes were then resuspended in RPMI 1640 medium supplemented with 2% FBS, 200 nM L-glutamine, and penicillin/streptomycin (100 U/mL and 100 mg/mL).

Enzyme-linked immunosorbent assay (ELISA)

Serum IgG and secretory IgA and IgG were determined by ELISA against OMP. OMP was prepared at 15 µg/mL in coating buffer (Sigma) and 100 µL was applied per well to Polysorb plates (Nunc) for a 4°C overnight incubation. Serum from the mice was diluted in 0.1% BSA/PBS. Either diluted serum or undiluted BAL was then added to the plates for an overnight incubation at 4°C. Following a 16 hour incubation, the plates were washed 4X with wash buffer (R & D systems) and an alkaline phosphatase conjugated anti-mouse IgG (H&L), IgG1, IgG2a, IgG2b, IgA (a chain-specific) (Rockland Immunochemicals, Inc) antibody was added at 1:2000 or 1:1000 respectively in 0.1% BSA/PBS. After 1-hour incubation at 37°C, the plates were washed again (4X) and PNPP substrate (Sigma) was added. The plates were read at 405-nm and end titers based on naïve animal levels. Levels of IgA normalized to total protein content.

Evaluation of the immunogenic effects of LPS and of the 17 KDa OmpA

In addition to western blot analysis as shown in Figure 5.1B, serum lipoprotein-specific and lipopolysaccharide-specific IgG antibodies were measured using ELISA. Briefly, 96-well Polysorb assay plates (Nunc) were coated with 0.05 µg/well of either crude OMP, endotoxin-depleted OMP (Lane F

figure 5.1A), or LPS (List Biological Laboratories). Murine serum collected 8 weeks following prime and 4 weeks following boost immunization with 15 µg OMP + 20% NE was serially diluted in 0.1% BSA/PBS and then added to the coated wells. The ELISA procedure was performed as described.

To evaluate the immunogenic contribution of LPS contained within the OMP-based vaccinne, an enzymatic protein digest was performed using 250 µg of PCR grade recombinant proteinase K (Roche) in 100 µl of either the crude OMP preparation or the endotoxin-depleted OMP preparation. Proteinase k was incubated with the OMP preparations for 16 hours at room temperature. The protein digestion was verified using a silver-stained SDS-PAGE run as previously described. LPS and OMP-protein specific epitopes were evaluated using western blot analysis probing with serum from mice vaccinated with either OMP-NE or OMP in PBS as previously described.

In order to evaluate the immunoreactivity of the 17 KDa lipoprotein, (OmpA), 1 µg/lane of the endotoxin-depleted OMP preparation was run using 4-12% Bis-Tris gels and transferred onto a PVDF membrane as described [8]. The membrane was stained with Ponceau-s stain for band localization. The 17 KDa band was cut from the membrane and placed in 1 mL of dilute serum (1:2500, 1:5000 or 1:10000) for at least 1 hour. The adsorbed serum was then used for standard ELISA IgG measurement as previously described.

Luminex analysis of cytokine expression

Freshly isolated mouse murine splenocytes were seeded at $4x10^6$ cells/mL (RPMI 1640, 2% FBS) and incubated for 72 hours with OMPs (15 µg/mL) or PHA-P mitogen (2 µg/mL) as a control. Cell culture supernatants were collected and analyzed for the presence of cytokines using Luminex™ multi-analyte profiling beads (Luminex Corporation, Austin, TX), according to the manufacturer's instructions.

Measurement of serum antibody neutralization

B. cenocepacia strain K56-2 and *B. multivorans* strain ATCC 17616 antibody-compliment neutralization activity was assayed using serum harvested from mice 6 weeks following primary i.n. vaccination. Twenty-five µL of serum (serial diluted 1x, 2x, 3x, 4x, or 5x) was added to 25 µl of a solution containing 1 $x10^3$ K56-2 or *B. multivorans* supplementing MH medium in microculture plates (Nunc). The plates were incubated at 37°C for 48 hours. Controls included 25 µL serum with 25 µL of sterile 1x PBS and 50 µL of MH medium containing $1x10^3$ bacteria. Following incubation, the wells were mixed using a sterile pipette tip. Ten µL of solution was plated on *Burkholderia* selective agar (BCSA) media (Fisherbrand) [24] on polystyrene culture plates and incubated for 72 hours at 37°C prior to manual CFU enumeration.

Pulmonary bacterial challenge

The bacterial challenge studies were performed in immunized mice 10 weeks following primary vaccination (n = 5/group) or non-vaccinated control mice (n = 10) using a modified version of the chronic pulmonary model of *B. cepacia* infection described previously [12, 25, 26]. Briefly, 5 $x10^7$ of K56-2 suspended in 85 µL of PBS was instilled through a trans-tracheal catheter extending to the bifurcation of the main-stem bronchi in anesthetized mice. The mice were maintained for a period of 6 days. Prior to the challenge study, the mice were non-surgically implanted with programmable temperature transponders (IPTT-3000, Bio Medic Data Systems, Inc.) for non-invasive subcutaneous temperature measurement with a handheld portable scanner (DAS-6002, Bio Medic Data Systems, Inc.). In-life analysis included monitoring the clinical status of each animal by evaluating the following metrics: body weight, body temperature, food consumption, and activity.

Immediately following euthanasia, pulmonary tissues and the spleen were collected in sterile conditions and each organ was placed into individual containers containing 1 mL of 1x PBS (Mediatec Inc). The tissue was then homogenized using a Tissue Tearor™ (Biospec Products Inc.) for 50 seconds on

ice. Serial dilutions (:10^2 to 1:10^8) of the homogenate were plated onto separated BCSA plates. All plates were then incubated for 72 hours at 37°C prior to manual CFU enumeration.

Whole blood was collected in tubes containing EDTA (BD) immediately following euthanasia. Anti-coagulated blood was processed to determine total peripheral lymphocytes and mononuclear lymphocytes by the Animal Diagnostic Laboratory at the University of Michigan, using a HEMAVETH 950 hematology analyzer (Drew Scientific, Inc.) in accordance to manufacturer's recommendation.

Statistics

Antibody end-titer results are expressed as mean ± standard error of the mean (SEM) or ± standard deviation (SD). The statistical significance for these studies was determined by ANOVA (analysis of variance) using the Student t and Fisher exact tests and two-tailed tests. For the bacterial challenge studies, the distribution of the colonization response was highly skewed, and therefore the data was transformed (natural log transformation) for data normalization. The normalized mean bacterial response in the lung and spleen were compared using an independent samples test with a two sided *p-value*. *P values* <0.05 were considered to be statistically significant. All analyses were done with 95% confidence limits.

5.3 RESULTS

Identification of immunoreactive proteins

Immunoreactive proteins were identified using western blots analyzing endotoxin-extracted OMP preparations probed with sera from mice immunized with either OMP-NE (Figure 5.1B) or OMP in PBS. Major reactive bands were

documented at 62 KDa, 45 KDa, 17 KDa, and 10 KDa molecular weights in both cases. However, while using the same serum diltuon for probing, the intensity of the bands were much higher when using serum from mice immunized with the NE-based vaccine as compared to the blot probed with serum from mice immunized with the OMP in PBS prepation.

The protein band staining with the highest intensity was associated with the 17 KDa proteins. For the purpose of protein identification, the 17 KDa band was isolated from the gel and identified by MALDI-TOF analysis. The protein was identified as *Burkholderia cepacia* outer membrane lipoprotein (OmpA) with a MW of 16.396 KDa [27, 28]. Sequence analysis using BLAST confirmed that these proteins are present in other closely related *Burkholderia* species (Table 5.1). A high degree of protein homology (87.9% sequence homology) was identified in numerous strains of *Burkholderia* and *Ralstonia* (Table 1). The 62 KDa, 45 KDa, 17 KDa, and 10 KDa bands correlated to the silver-stained patterns by overlay analysis (Figure 5.1A). Oligonuleotides were not evident in the either the crude OMP or the endotoxin-depleted OMP preparations (Figure 5.1C).

Intranasal immunization with OMP-NE induces serum anti-OMP antibodies

The humoral and cell-mediated immune responses to the OMP-NE vaccine were characterized *in vivo* in the mice. Intranasal vaccination with either 5 µg or 15 µg OMP preparations mixed in 20% NE (OMP-NE) resulted in high serum titers of OMP-specific IgG antibodies of 2.8×10^5 and 5.1×10^5 within 6 weeks, respectively, following primary vaccination (Figure 5.2). Non-adjuvanted OMPs were immunogenic and resulted in serum anti-OMP IgG titers of 1.9×10^4 and 3.8×10^4 six weeks following primary i.n. immunization. However, NE-adjuvanted treatment groups responded significantly higher (13 to 30 fold) than non-adjuvanted groups at all time points following the boost ($p < 0.05$). Further, mice vaccinated with OMP in PBS did not demonstrate a significant boost effect following the second vaccination.

Intranasal OMP-NE and OMP in PBS vaccination produce mucosal immunity

In order to further characterize the OMP-NE vaccine, we evaluated its ability to elicit specific antibody production in bronchiolar secretions. Mucosal antibody production is an important characteristic for protection against *Burkholderia* colonization since secretory antibodies are thought to be critical effectors in protection against mucosal respiratory pathogens. Mucosal immune responses were measured in bronchioalveolar lavage (BAL) fluid of animals immunized with 5 μg OMP 20% NE and 5 μg OMP in PBS. OMP-specific IgA and IgG antibodies were detected in samples obtained 6 weeks after initial immunization (Figure 5.3A). Comparable levels of anti-OMP antibodies were detected in BALs in mice immunized either with OMP-NE or OMP without NE adjuvant.

OMP-NE immunization yields a balanced Th1/Th2 cellular response

OMP-specific cellular responses were characterized in splenocytes obtained 6 weeks following primary vaccination with 5 μg OMP + 20% NE. The cells were stimulated with OMP and then evaluated for specific cytokine production. Although the acute-phase Th1 cytokines INF-γ and TNF-α were either not induced or minimally increased (TNF-α =1.94-fold increase, *p-value* = 0.04), the IL2 (a TH1 cytokine) production increased 16.96-fold (*p-value* = 0.0001) in splenocytes harvested from vaccinated as compared to non-vaccinated mice (Figure 5.3B). The IL2 response suggests prior T-cell stimulation by OMPs and is indicative of an antigen-specific response. The Th2 cytokines IL4 and IL10 were also measured. IL4 was minimally induced (2.23-fold increase, *p-value* = 0.01), whereas IL10 did not increase in splenocytes from vaccinated vs. non-vaccinated mice.

The analysis of the serum IgG subclass was also used to assess the Th-type bias of the cellular response. The pattern of IgG subclass distribution shows that i.n. immunization with OMP-NE produced increased levels of Th1-type

IgG2b versus Th2-type IgG1 subclass antibodies (*p-value* =0.00046) (Figure 5.4). In comparison, immunization with OMP in PBS produced similar levels of IgG1 and IgG2b antibodies (Figure 5.4). The pattern of splenic cytokine expression and the IgG subclass results suggested a balanced Th1/Th2 response to OMP-NE vaccination.

Antibody response is directed toward OMP lipoprotein and LPS

It has been previously documented that LPS is intrinsically associated with *Burkholderia* spp. OMP preparations [12].To further investigate the specificity of immune response and to evaluate the possible role of endotoxin in *B. cencocepacia* OMP preparations, serum from mice immunized with OMP-NE was analyzed using ELISA with either crude OMP, endotoxin-depleted OMP, or LPS. The highest IgG levels were detected in the endotoxin-depleted and crude OMP preparations. However, the serum also contained significant levels of anti-LPS antibodies (Figure 5.5A). The statistical analysis indicated a *p-value* of 0.001 and 0.01 for the endotoxin depleted OMP and the crude OMP preparations as compared to the LPS respectively.

For clarification of the role of endotoxin in the OMP preparation, a proteolytic digest of the crude OMP and endotoxin-depleted OMP preparations were performed. The immunogenic epitopes were evaluated by western blot analysis comparing serum antibodies generated in mice vaccinated with OMP in PBS versus from mice vaccinated with OMP-NE (Figure 5.5B). The results clearly indicated that antibody specificity in the non-digested OMP preparations was directed toward specicic proteins contained within the OMP preparation (62 KDa and 17 KDa). This was confirmed by the disappearance of the protein bands in the proteolyticaly digested preparations. Further, using the same serum dilutions, the intensity of the staining was consistently higher in the blots probed with serum from mice immunized with NE-based vaccines as compared to mice immunized with OMP in PBS preparations. These results confirm the

measurement of at least a 13-fold decrease in antibody concentration in mice vaccinated with OMP in PBS preparations as compared to mice vaccinated with OMP-NE (Figure 5.2).

The immunodominant response, as determined by Western blot analysis, appeared to be the 17 KDa lipoprotein (Figure 5.1C). In order to verify this finding and to further explore the immunogenic contribution of the 17 KDa lipoprotein, an ELISA was performed comparing serum from vaccinated mice to the same serum absorbed to the lipoprotein. The anti-OMP IgG measured significantly higher (*p-value = 0.05*) in the non-absorbed serum, as compared to the absorbed serum (OD=3.153 vs. 2.937), suggesting that the 17 KDa band is a contributor to immunogenicity with this OMP.

Intranasal vaccination with OMP-NE results in cross-protective neutralizing serum antibody

B. cenocepacia neutralizing antibodies were determined using a colony reduction assay. The mice intranasally vaccinated with 15 µg OMP + 20% NE or 5 µg OMP 20% NE produced serum-neutralizing antibodies that inhibited 98.3% or 92.5% of *B. cenocepacia* colonies, respectively, as compared to serum from non-vaccinated mice (Figure 5.6A). The mice vaccinated with non-adjuvanted OMP also demonstrated a relatively high level of inhibition, resulting in 46.7% (15 µg OMP in PBS) and 33.3% (5 µg OMP in PBS) CFU reduction. The statistical analysis showed that B. cenocepacia was significantly inhibited in NE-vaccinated mice as compared those who were immunized with the OMP preparation alone (*p-value* = 0.03 for 15 µg OMP + 20% NE and 09,9x10-5 for 5 µg OMP + 20% NE).

To evaluate if the OMP-NE can produce cross-reactive protection, serum from mice vaccinated with 15 µg OMP 20% NE was also incubated with an equal volume of *B. multivorans*. *B. multivorans* was selected because it is the most common isolate cultured from CF patients infected with Bcc organisms [29].

In this study, the serum inhibited *B. multivorans* by 80.1% and 49.8% in mice vaccinated with OMP-NE and OMP without adjuvant, respectively, suggesting the generation of cross-protective antibodies following immunization with either OMP-NE or OMP in PBS (Figure 5.6B).

Immunization with OMP-NE protects against pulmonary *B. cenocepacia* challenge and reduces incidence of sepsis

The protective effect of intranasal immunization was also tested in a mouse model of lung infection. *B. cenocepacia* pulmonary clearance was evaluated 6 days following intratracheal inoculation in mice that were intranasally immunized with the OMP-NE or the OMP without an adjuvant. Vaccination with 15 µg OMP + 20%NE resulted in significantly higher rates of pulmonary clearance (*p-value* =0.0092) as compared to the non-vaccinated mice (Figure 5.7A). At day 6, the average pulmonary bacterial load was 22.5 ± 26.2 CFU in mice vaccinated with 15 µg OMP + 20% NE, compared to 1.28 $x10^6$ ± 3.36 x 10^6 CFU/lung in non-vaccinated mice, representing a greater than 5-log reduction in the bacterial load.

Splenic colonization following pulmonary inoculation with *B. cenocepacia* was evaluated as a means of assessing sepsis (Figure 5.7B). Vaccination with 15 µg OMP + 20% NE significantly reduced the incidence of bacteria in the spleens 6 days following the pulmonary challenge of individual mice from an average of 1.12 x 10^3 ± x 10^3 CFU/spleen in non-vaccinated mice to 2.5 ± 5 CFU/spleen in vaccinates (*p-value* = 0.0307). Although no colonies were recovered from the spleens of mice vaccinated with 15 µg OMP in PBS, a statistical significance was not achieved that was attributed to the loss of 2 out of the 5 mice during the challenge.

Intranasal immunization with OMP-NE attenuates systemic illness after *B. cenocepacia* infection

B. cenocepacia infection resulted in greater loss of thermoregulation in the non-vaccinated mice than in the mice immunized with OMP-NE or OMP without the adjuvant (Figures 5.8A and 5.8B). The mean body temperature 6 days following infection with *B. cenocepacia* was significantly lower for the non-vaccinated mice than for the mice vaccinated with 15 µg OMP + 20% NE (*p val* = 0.008), 5 µg OMP + 20% NE (*p val* = 0.008), or 5 µg OMP without the adjuvant (*p-value* = 0.01). Although there was a trend in the mean body weight of vaccinated versus non-vaccinated mice infected with *B. cenocepacia,* this difference was not statistically significant (Figure 5.7B).

The total peripheral leukocyte counts determined at the time of sacrifice in the non-vaccinated mice were significantly higher from the values observed for the mice vaccinated with 15 µg OMP + 20% NE (*p-value* = 0.047), 5 µg OMP + 20% NE (*p-value* = 0.026), or 5 µg OMP in PBS (*p-value* = 0.032) (Table 5.2). The polymorphonuclear leukocyte counts for the non-vaccinated mice were also significantly higher than those for the mice vaccinated with 15 µg OMP + 20% NE (*p-value* = 0.02), 5 µg OMP + 20% NE (*p-value* = 0.024), or 15 µg OMP in PBS (*p-value* = 0.04), suggesting that immunization with OMP ± NE resulted in decreased systemic disease following infection with *B. cenocepacia* (Table 5.2).

5.4 DISCUSSION

Given the morbidity, co-morbidities, and sensitivity to inflammation associated with CF [1, 6], the development of safe and efficacious adjuvants is crucial to producing vaccines to protect against Bcc in people with CF. We demonstrate that mucosal immunization with formulations containing OMPs from *B. cenocepacia* mixed with the NE, an experimental non-inflammatory and safe mucosal adjuvant [8], elicited robust Bcc-specific serum and mucosal immune responses and a balanced Th1/Th2-type bias. The OMP-NE produced antibodies capable of neutralizing *B. cenocepacia* and cross-neutralizing *B.*

multivorans. We have also documented the decrease in time of *B. cenocepacia* clearance after experimental infection.

In these studies a single nasal immunization with OMP-NE produced a rapid induction of serum anti-OMP IgG, which was subsequently boosted. Immunization wither either OMP-NE or OMP alone was capable of inducing antigen-specific T cell responses and secretory antibody responses, as documented by induction of IL2 and secretory IgA and IgG. Mucosal and cell-mediated immunity are thought to be critically important to preventing Bcc colonization because infecting bacteria primarily reside within the airway lumen in the sputum, the airway epithelial surface fluid, and the bronchial mucosa [1].

A novel finding that we report in this manuscript is the immune response associated with a 17 KDa OmpA protein. Here, we have shown that the 17 KDa lipoprotein fractions stained with the highest intensity on western blot (Figure 5.1B). Although it was clear that at least 4 antigenic protein bands were identified on the western blot analysis including the 17 KDa band, it is possible that numerous different proteins of the same size could contained within the endotoxin-depleted OMP preparation could confound the specificity. Further *in vivo* studies using size or charge seperated proteins are necessary for clarification. This discovery of immunogenicity of the 17 KDa OmpA proteins adds to the scarce data existing for Bcc vaccine development and suggests a rationale for the use of epitopes contained within the 17KDa OmpA for generation of antibodies not previously described in patients infected with Bcc. The development of anti-OmpA proteins may be important because this protein has been shown to be critical for host-cell adherence [30]. Further, OmpA has been used to target nasal mucosa-associated dendritic cells [31]. Up to this point, very little has been known about the humoral immune response to *B. cepacia* infection in CF [32]. Investigators have previously reported that anti-*B. cepacia* OMP IgG antibodies were developed in CF patients co-infected with *B. cepacia* and *P. aeruginosa*, causing speculation of antigenic crossreactivity [33,

34]. Others have reported serum IgG and sputum IgA antibodies to *B. cepacia* lipopolysaccharide (LPS) core antigen, flagella antigens, exopolysaccharides, and elastase, among others, in infected patients [35-38]. However, none of these antibodies are thought to be protective. Bertot et al. suggested that the protective IgG and IgA response in the mice was independent of LPS contamination in their preparation. The specificity of response was against 90 KDa, 72 KDa, 66 KDa, and 60 KDa lipoproteins in that study.

Adding to the potential utilitity of the OMP-NE vaccne, cross neutralization of *B. cenocepacia* and of the *B. multivorans* with serum from mice vaccinated with OMP-NE vaccination was demonstrated in these studies. The cross-reactivity of OMP-specific antibodies suggests that vaccination with OMP-NE may prevent chronic colonization with Bcc. Cross-reactivity is associated at least in part with the 17 KDa lipoprotein, as suggested by the BLAST findings reporting antigenically conserved epitopes on numerous Bcc and non-Bcc strains. Future vaccine studies using recombinant-derived 17 KDa lipoprotein and the NE adjuvant would be helpful in assessing the immunogenicity of this protein.

A second novel finding that we are reporting here involves the use of the chronic lung infection model. It is understood that animal models of *B. cenocepacia* infection are limited due to the obscure virulence and lack of lethality associated with pulmonary colonization [32]. Bertot et al. and others suggest that establishment of a chronic *B. cenocepacia* infection cannot be achieved, even with a neutropenic model [12, 25, 26]. In these studies, the establishment of a chronic *B. cenocepacia* infection was achieved using a solution containing 5 x 10^7 K56-2 organisms intranasally. Although *B. multivorans* is isolated from the lungs of CF patients with more frequency, K56-2 was chosen for our experimental vaccine studies because of the transmissible and virulent phenotype of this strain [21]. Immunization with K56-2 OMPs-NE resulted in a dramatic decrease of CFU in the lungs of mice, compared to the lungs of non-immunized mice (Figure 5.6A). Although there was no clear

reduction in the severity of systemic disease, pulmonary bacterial clearance a was significantly enhanced in OMP-NE mice. Likewise, Fewer CFU were identified in the spleens of OMP-NE-or OMP in PBS vaccinated mice, compared to non-vaccinated groups (Figure 5.6B). These results suggest that the mucosal OMP-NE vaccine produced protective immunity and reduced the likelihood of sepsis, adding support to the claim that increased mucosal immunity in the airways as a result of mucosal vaccination may help prevent chronic colonization with Bcc in patients with CF [12].

It is important to note that although immunization with OMP in PBS resulted in comparable immunity to OMP-NE in numerous instances, important differences were observed. For example, we have shown that immunization with OMP without adjuvant results in relatively high titers of IgG but is 13 to 30 times less immunogenic and did not boost in mice as compared to OMP mixed with NE adjuvant (Figure 5.2). Although the reponse with OMP-NE is primarily directed toward specific protein contained within the preparation (Figure 5.5B), OMP is undoubtably antigenic also due to the endotoxin content inseparable from the OMP. Additionally, the OMP preparation may contain antigenic cytoplasmic or wall-associated proteins not eliminated in the generation of the OMP solution. There were also important differences in the functionality of the immune response elicited between OMP-NE and OMP without adjuvant. Mice immunized with OMP-NE neutralized higher levels of *B. cenocepacia* than those vaccinated with OMP alone (Figure 5.6). Although the pulmonary challenge showed a clear difference in protection in immunized versus non-immunized mice, the differences in response between OMP-NE and OMP without adjuvant were less clear (Figures 5.7, 5.8, and table 5.2). The similarities in the response profile between the OMP-NE and the OMP in PBS preparations may be due to the technical limitations and the variability of the challenge model [32]. Further, it is possible that the nanoemulsion adjuvant may promote the activation and binding of T-cell epitopes. The induction of epitope specific T-cell responses

theroretically may enhance the clearance of the *B. cepacia* organism, but studies analyzing this claim will be necessary.

5.5 CONCLUSIONS AND SUMMARY

In summary, our study indicates that NEs appear to be effective mucosal adjuvants for a *B. cenocepacia* OMP vaccine. These formulations induce robust, and specific humoral and cellular responses, resulting in protective immunity. The 17 KDa OmpA shows potential for future vaccine development. This study provides a rational basis for vaccine design using NE-adjuvanted vaccines in combination with recombinant OMP protein.

5.6 FIGURES

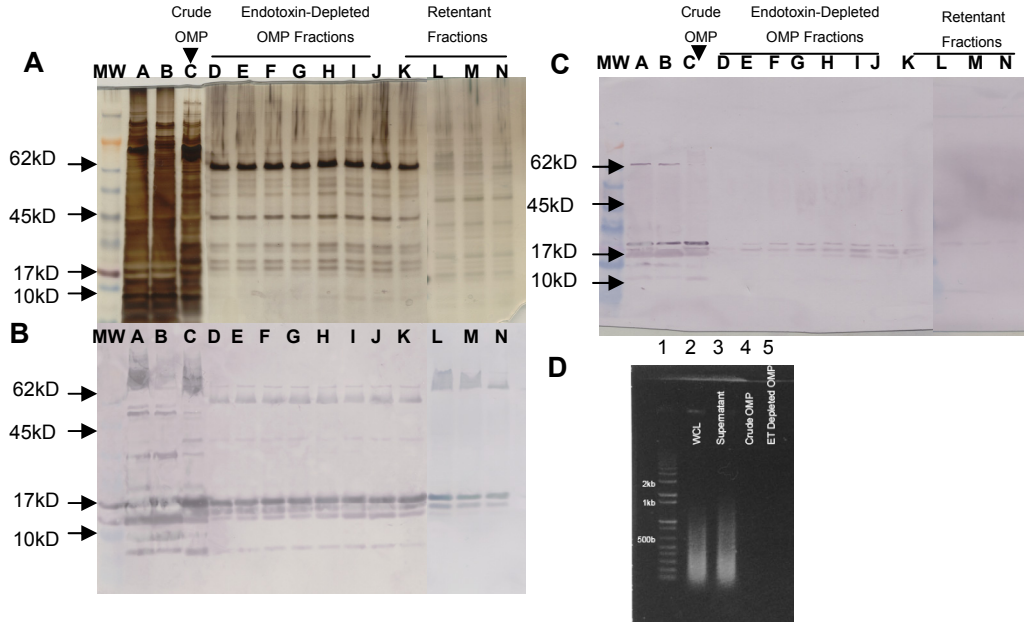

Figure 5.1. OMP Analysis **A)** The 4-12% SDS-PAGE was loaded on a volumetrically normalized basis to track the progression of the protein from its most crude form to its cleanest form. In lane A, protein from the supernatant produced after the 6000xG centrifugation was loaded. An equal volume of the supernatant from the 100,000xG centrifugation was loaded into lane B. Lane C was loaded with the Crude OMP (the re-suspended pellet fraction of the 100,000xG spin). Lanes D-J were loaded with the endotoxin-depleted OMP fractions (the successive flow-through portions of the endotoxin column). Lanes K-N were loaded with the endotoxin column retentant fractions (the successive fluid regenerated from the column after the addition of sodium deoxycholate). **B)** Western blot probed with serum from mice immunized with the endotoxin-depleted OMP prep at 1:1000 in 5% Milk/PBST and secondarily probed with an AP-conjugated anti-mouse antibody. **C)** Western blot probed with serum from mice immunized with the OMP in PBS prep at 1:1000 in 5% Milk/PBST and secondarily probed with an AP-conjugated anti-mouse antibody. **D)** Agarose gel electrophoresis of the OMP preparation. Lane 1 is loaded with a DNA ladder. Lane 2 is loaded with the cell lysate (WCL) before separation by high speed centrifugation, Lane 3 is loaded with the resulting supernatant following the 100,000xG spin (lane B in the Silver and western blot above), Lane 4 is loaded with the crude OMP preparation (lane C in the Silver and western blot above), and lane 5 is loaded with the endotoxin (ET) depleted OMP fraction (lane E in the Silver and western blot above).

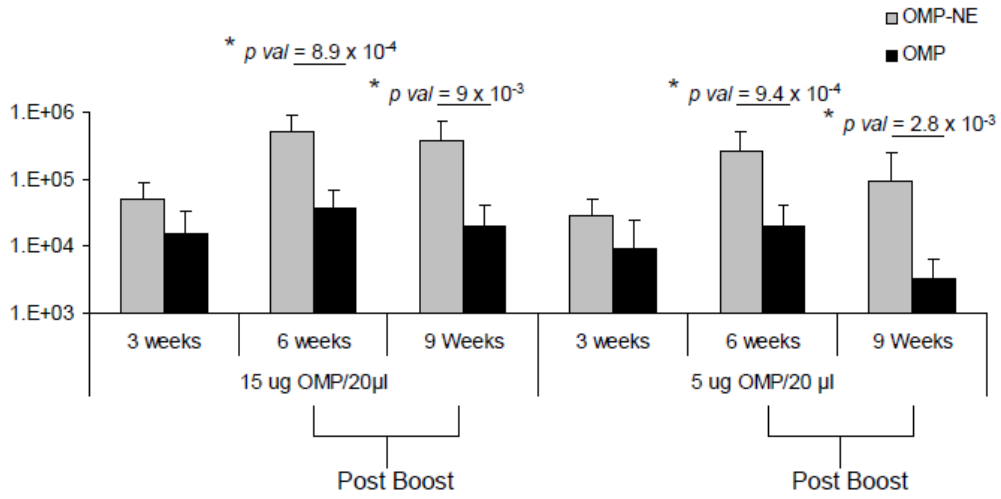

Figure 5.2 Humoral immune response to *B. cenocepacia* OMP-NE. IgG response in serum post-immunization with the OMP preparation with or without nanoemulsion. Response was measured via ELISA using plates coated with the OMP preparation. Significant statistical difference with *p value* <0.05 were observed for the 6 and 9 week (2 and 5 weeks following boost) samples between nanoemulsion-adjuvanted OMP formulations and OMP-PBS formulations for either concentration. Serum anti-OMP IgG antibody concentrations are presented as mean of endpoint titers in individual sera ±SEM. * indicates a statistical difference (*p- value* <0.05) in the anti-OMP IgG titers.

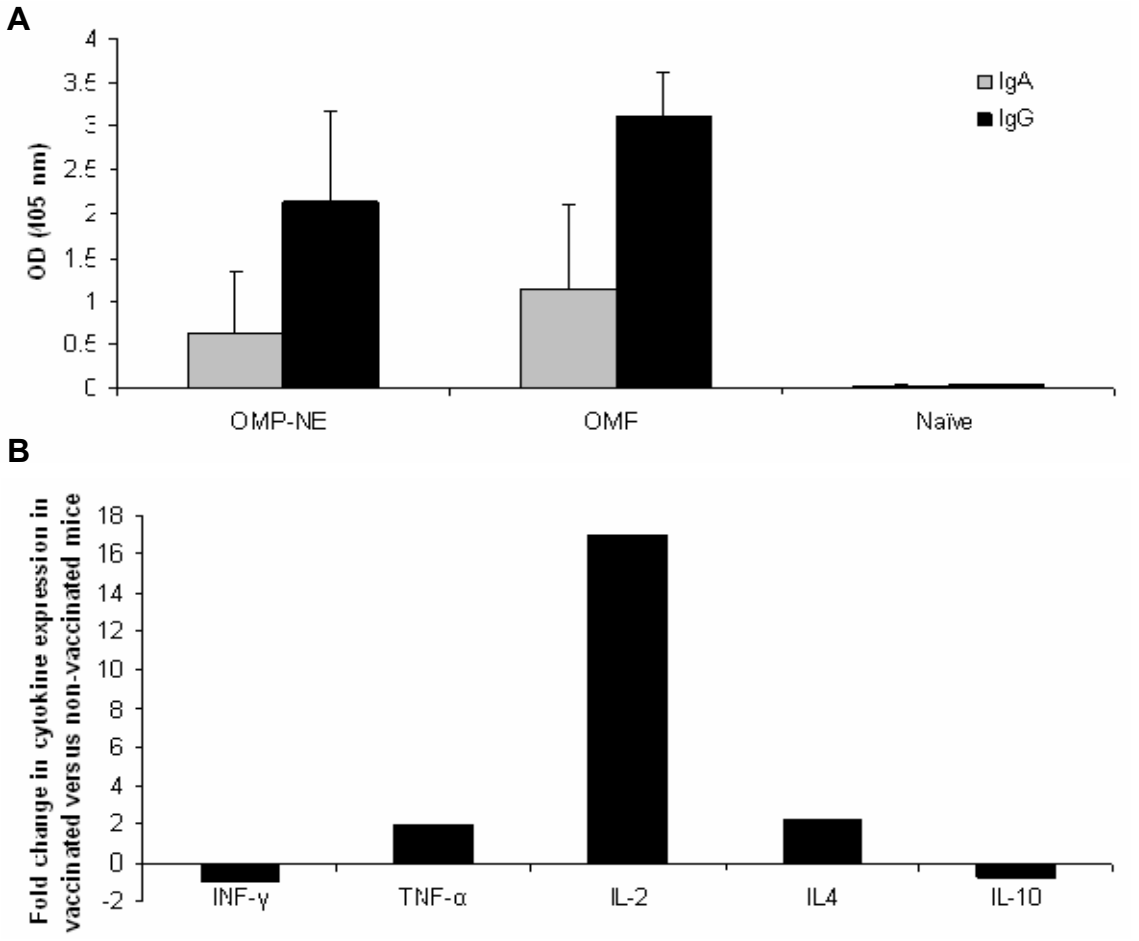

Figure 5.3. Mucosal and splenic cytokine response analysis of *B. cenocepacia* OMP-NE. A) Mucosal response to the OMP vaccination with or without nanoemulsion. IgA and IgG measured in BAL solution via ELISA using plates coated with the OMP preparation. The OD levels were normalized to total protein content within the samples. **B)** Cytokine profiling of splenocytes of mice immunized with 5 µg OMP + 20% NE. Cytokines were measured in media taken from splenocytes activated with endotoxin-depleted OMP preparation. 1.5ug OMP prep was used to activate $4x10^4$ splenocytes in RPMI medium. Media was removed from the splenocytes on day 3 post-activation and analyzed using the Mouse Cytokine/Chemokine Kit from Linco. Data is represented as fold change in vaccinated mice vs. naïve mice.

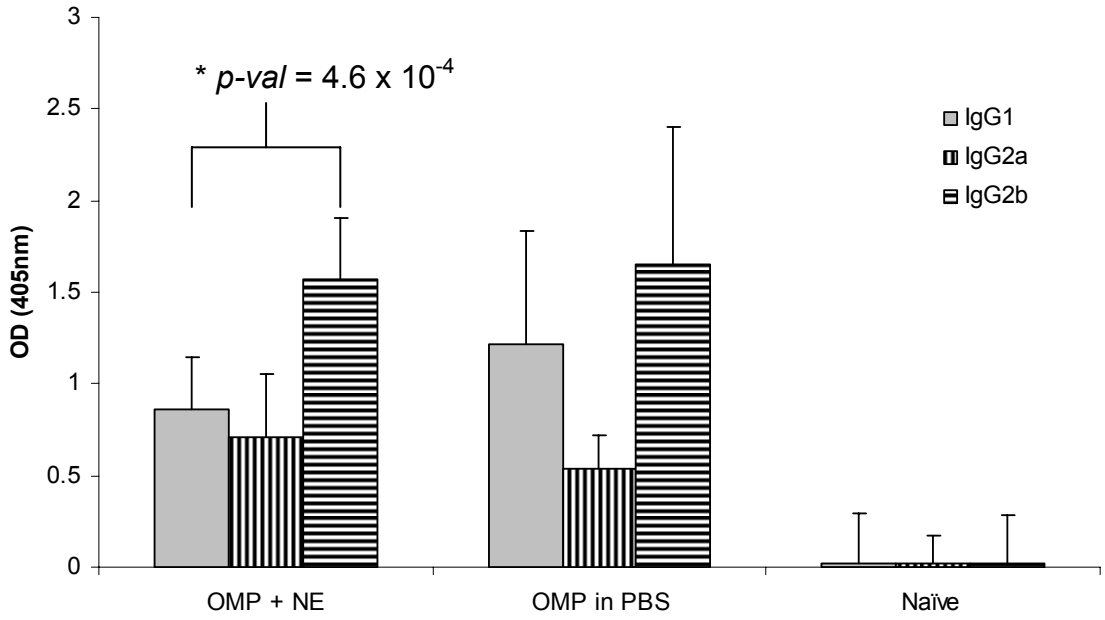

Figure 5.4. IgG Subtype Analysis. Serum from naïve mice and mice immunized with 5 µg OMP +/- 20% NE was analyzed for antibody subtype distribution. The results are presented as ratio of the specific subclass IgG to the overall IgG titer. * indicates statistical difference (*p-value* <0.05) between IgG2b and IgG1 subtypes.

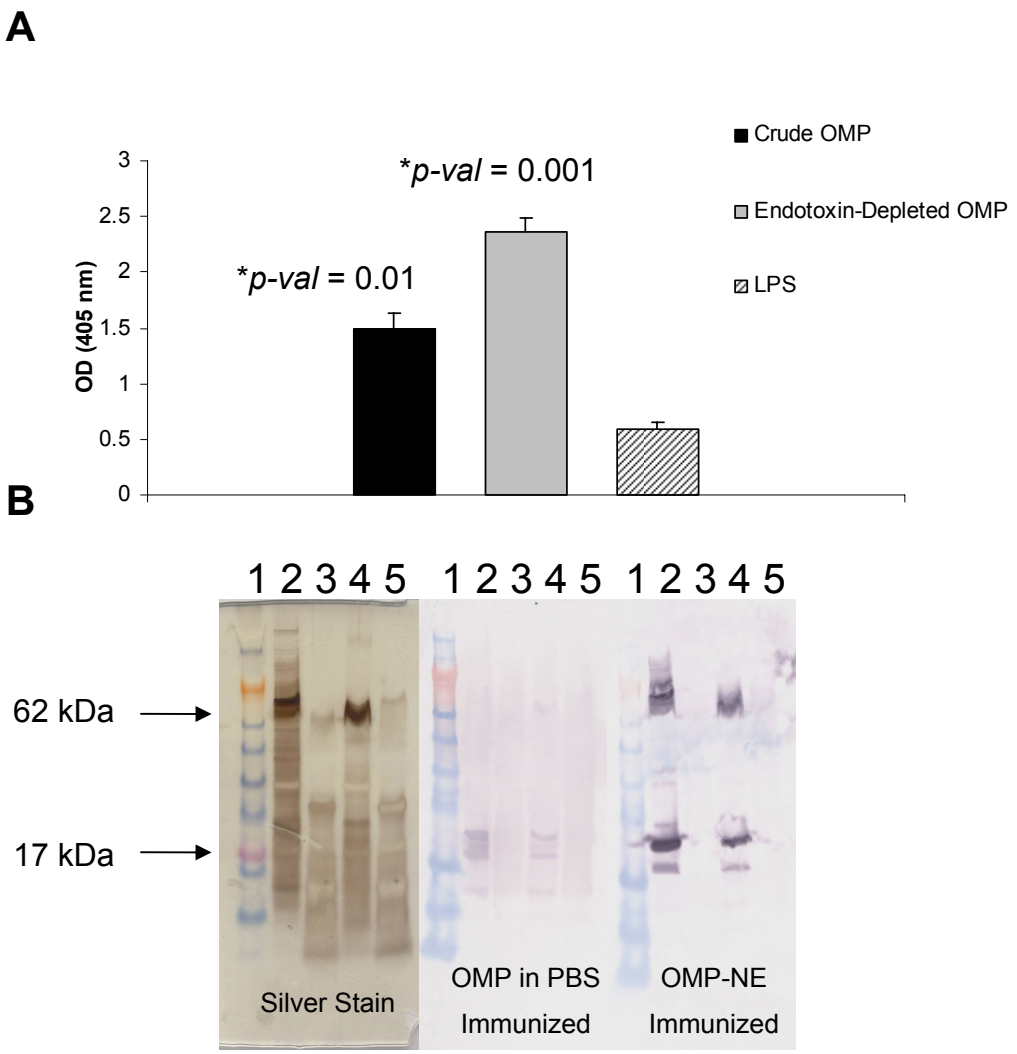

Figure 5.5. Evaluation of the immunogenic effects of LPS and of the 17 KDa OmpA. A) In order to determine the antigen specificity of the response to the OMP preparation-based vaccine**,** 96 well plates were coated with either crude OMP preparation, endotoxin-depleted OMP preparation, or LPS for standard ELISA serum IgG analysis using serum from mice vaccinated with 15 µg OMP-20% NE. Results are presented as mean values of OD at 405 nm ±SEM. The levels of responses were compared to LPS only. **B)** Silver-stained SDS gel and western blots of the crude OMP preparation (lane 2), the enzymatically digested crude OMP preparation (lane 3), the endotoxin-depleted OMP preparation (lane 4), and the enzymatically digested endotoxin-depleted OMP preparation (lane 5). A protein ladder was loaded into lane 1. Western blots were probed with serum from either OMP in PBS or OMP-NE immunized mice as indicated.

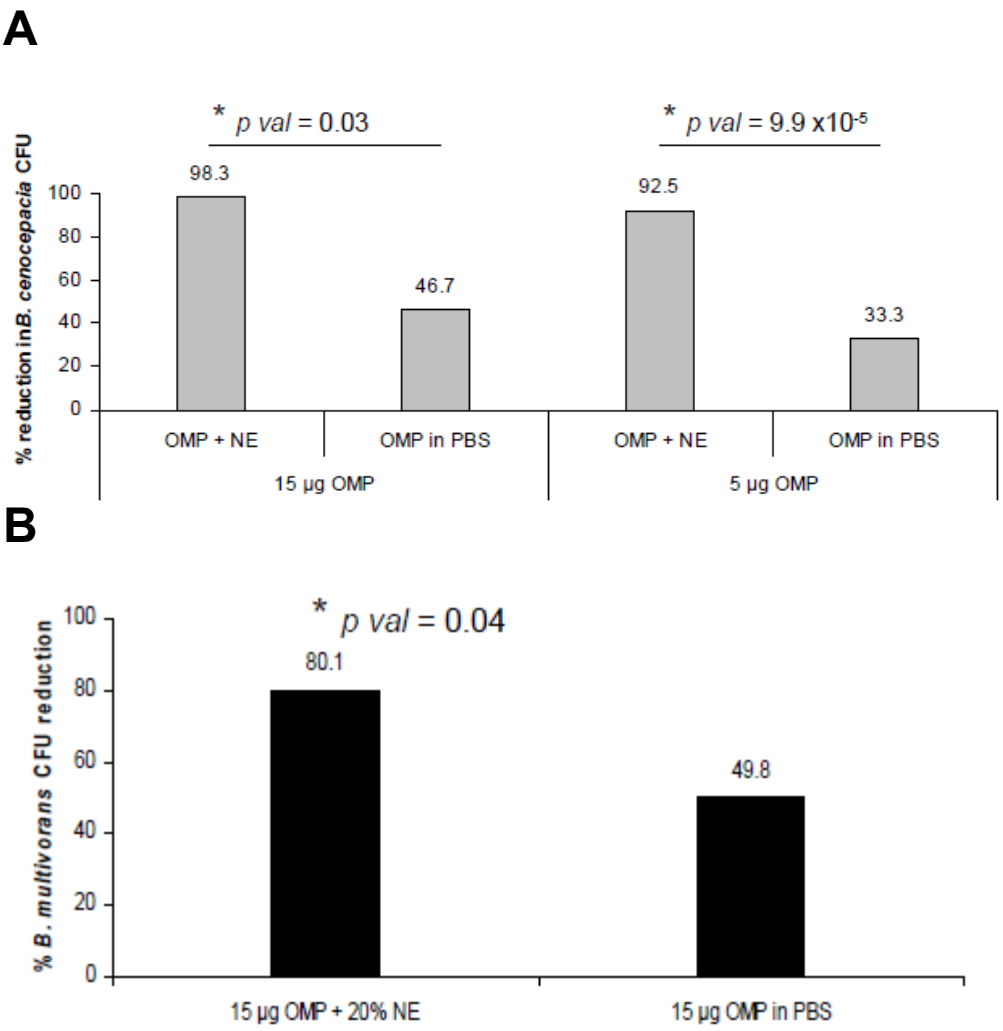

Figure 5.6. Serum Neutralization Assay. A) Serum diluted 1:5 from immunized or naïve mice was mixed in equal volumes with *B. cenocepacia* (10^7 CFU) and broth and incubated 48 hours at 37°C. Following incubation, the solution was plated out on BCSA plates and incubated for 72 hours at 37°C for colony enumeration. The percent reduction in CFU was plotted against samples with naïve serum. A statistical difference (*p-value* <0.05) in neutralizing activity was observed between serum from mice immunized with OMP-NE and serum from mice immunized with OMP in PBS formulations. **B)** Cross neutralizing activity of the antibodies produced from mice vaccinated mice, serum from mice immunized with 15 µg OMP + 20% NE was diluted 1:3 and mixed with equal volumes of *B. multivorans* (10^7 CFU) and broth and incubated 48 hours at 37°C. As above, the solution was plated out on BCSA plates and incubated for 72 hours at 37°C for colony enumeration following incubation. The percent reduction in CFU was plotted against samples with naïve serum. A statistical difference (*p-value* <0.05) in neutralizing activity was observed between serum from mice immunized with OMP-NE and serum from naïve mice.

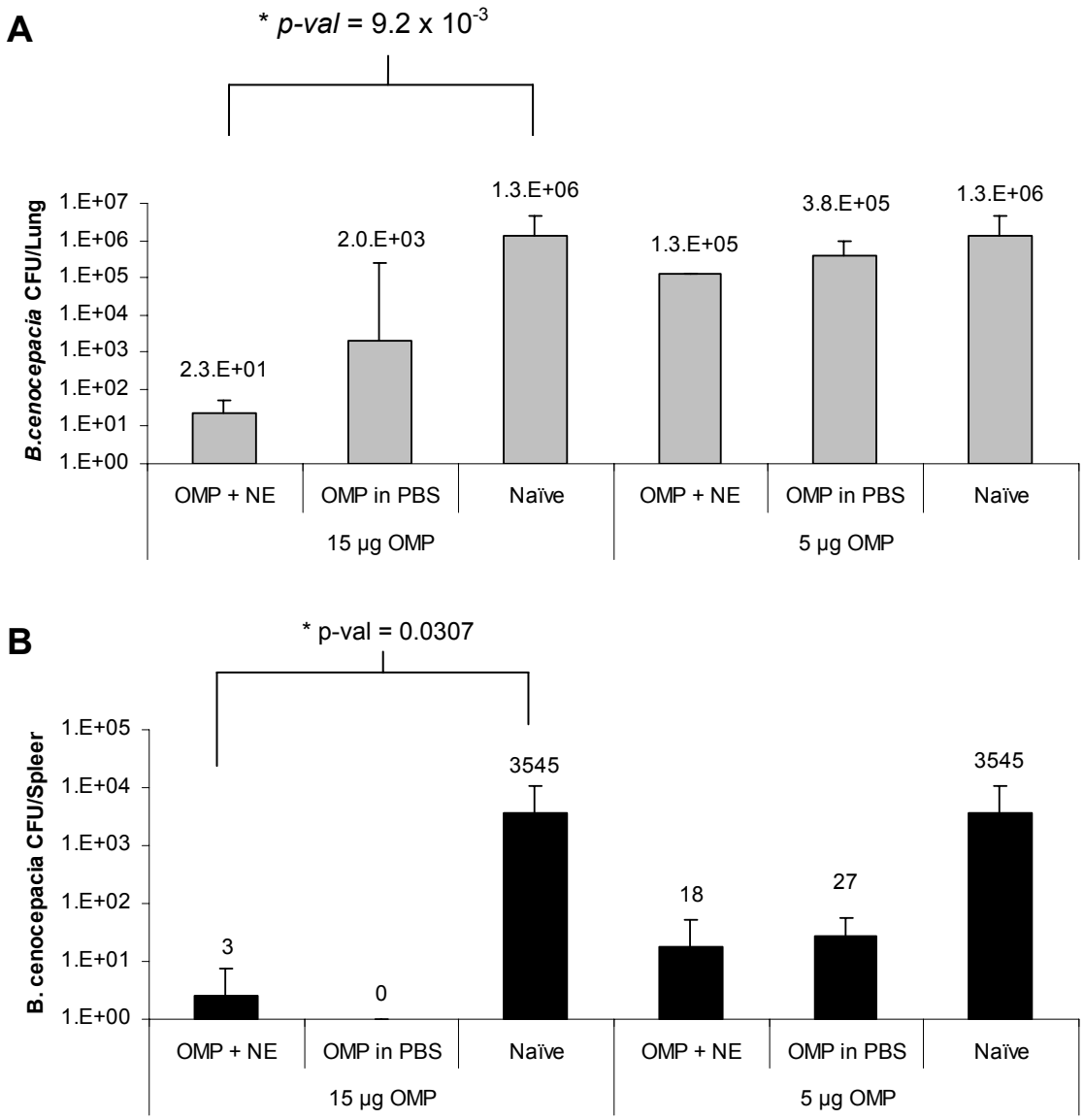

Figure 5.7. Pulmonary and splenic colonization assay. A) Pulmonary tissue CFU and **B)** Splenic tissue CFU. Vaccinated or naïve mice (n=5/group) were placed under general anesthesia and were challenged with $5X10^7$ *B. cenocepacia* in PBS. The mice were euthanized at 6 days post-challenge. Lungs and spleens were homogenized under sterile conditions in PBS and the homogenate was diluted. The dilution samples were plated to BCSA plates and incubated 72 hours at 37°C prior to CFU enumeration.

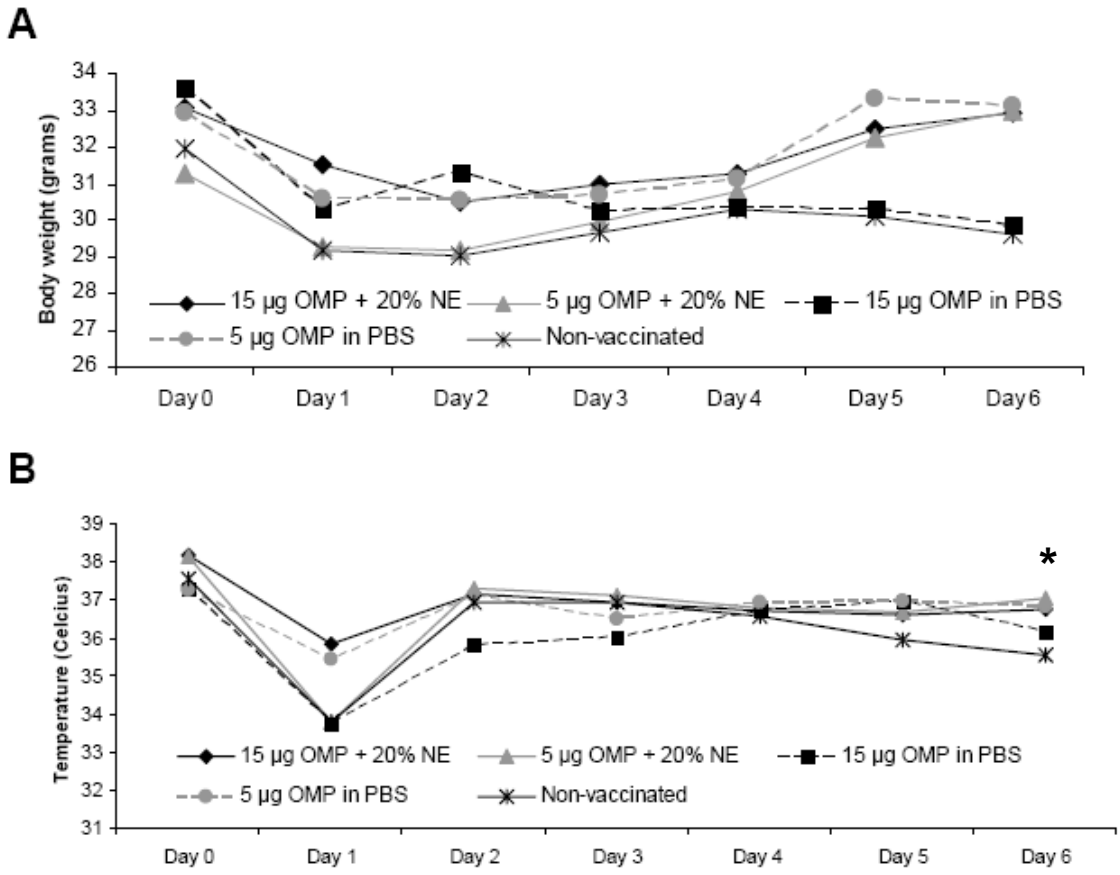

Figure 5.8. Morbidity monitoring. A) Change in body weight and **B)** change in subcutaneous temperature in CD-1 mice following pulmonary challenge with $5x10^7$ *B. cenocepacia* organisms. * indicates a statistic difference in subcutaneous temperature of vaccinated versus non-vaccinated mice (*p-value* < 0.05).

5.7 TABLES

Omp-A like sequences alignment	Organisms	Identity (%)
LDDKANAGAVSTQPSADNVAQVNVDPLNDPNSPLAKRSIYFDFDSYSVKDEYQPLLQQHAQYLKSHPQRHVLIQGNTDERGTSEYNLALGQKRAEAVRRALALLGVADSQMEAVSLGKEKPLATGHDEASWAQNRRADLVYQQ	*B. cenocepacia*	100
LDDKANAGAVSTQPSADNVAQVNVDPLNDPNSPLAKRSIYFDFDSYSVKDEYQPLLQQHAQYLKSHPQRHVLIQGNTDERGTSEYNLALGQKRAEAVRRALALLGVADSQMEAVSLGKEKPLATGHDEASWAQNRRADLVYQQ	*B. dolosa*	100
LDDKANAGA+STQPSADNVAQVNVDPLNDPNSPLAKRSIYFDFDSYSVKDEYQPLLQQHAQYLKSHPQRHVLIQGNTDERGTSEYNLALGQKRAEAVRRALALLGVADSQMEAVSLGKEKP ATGHDEASWAQNRRADLVYQQ	*B. multivorans*	98
LDDKANAGAVSTQPSADNVAQVNVDPLNDPNSPLAKRSIYFDFDSYSVKDEYQPL+QQHAQYLKSHPQRHVLIQGNTDERGTSEYNLALGQKRAEAVRRA+ALLGV DSQMEAVSLGKEKP A+GHDEASWAQNRRADLVYQQ	*B. ambifaria*	96
LDDKAN-AGAVSTQPSADNVAQVNVDPLNDPNSPLAKRSIYFDFDSYSVKDEYQPLLQQHAQYLKSHPQRHVLIQGNTDERGTSEYNLALGQKRAEAVRRA+ALLGV DSQMEAVSLGKEKP ATGHDEASWAQNRRADLVYQQ	*B. vietnamiensis*	97
LD+KANAGA+STQP+ +NVAQV VDPLNDPNSPLAKRSIYFDFDSYSVKDEYQPL+QQHAQYLKSHPQRHVLIQGNTDERGTSEYNLALGQKRAEAVRRA+ALLGVADSQMEAVSLGKEKP A GHDEASWAQNRR+DLVYQQ	*B. ubonensis*	92
LD+ AN- GAVSTQP+ +NAQV VDPLNDPNSPLAKRS+YFDFDSYSV+D+YQPLLQQHAQYLKSHPQRH+LIQGNTDERGTSEYNLALGQKRAEAVRRAL+LLGV DSQMEAVSLGKEKP+A GHDEASWAQNRRADLVYQQ	*B. thailandensis*	88
LD+ AN- GAVSTQP+ ++VAQVNVDPLNDPNSPLAKRSIYFDFDSYSVKD+YQ LLQQH+QYLKSHPQRHVLIQGNTDERGTSEYNLALGQKRAEAVRR+L+L+GV DSQMEAVSLGKEKP ATGHDE+SWAQNRRADLVYQQ	*B. graminis*	88
LD+ AN- GAVSTQP+ +NVAQV VDPLNDPNSPLAKRS+YFDFDSYSV+D+YQ LLQQHAQYLK HPQRH+LIQGNTDERGTSEYNLALGQKRAEAVRRAL+LLGV DSQMEAVSLGKEKP+A GHDEASWAQNRRADLVYQQ	*B. oklahomensis*	87
LD+ AN G-AVSTQP+ +NVAQV VDPLNDPNSPLAKRS+YFDFDSYSV+D+YQ LLQQHAQYLKSHPQRH+LIQGNTDERGTSEYNLALGQKRAEAVRRAL+LLGV D+QMEAVSLGKEKP+A GHDEASWAQNRRADLVYQQ	*B. pseudomallei*	87
LD+ AN G-+VS QP+ ++VA V VDPLNDPNSPLAKRSIYFDFDSYSVKD+YQ LLQQHAQYLKSHPQRH+LIQGNTDERGTSEYNLALGQKRAEAVRR+L+L+GV DSQMEAVSLGKEKP ATGHDE+SWAQNRRADLVYQQ	*B. xenovorans*	86
LD+ AN- G VS QP+ ++VA VNVDPLNDPNSPLAKRSIYFDFDSYSVKD+YQ LLQQHAQYLKSHPQRHVLIQGNTDERGTSEYNLALGQKRAEAVRR+L+L+GV DSQMEAVSLGKEKP ATGHDE+SWAQNRRADLVYQQ	*B. phytofirmans*	86
LD+ A – GA QP+ ++VA VNVDPLNDPNSPLAKRSIYFDFDSYSVKD+YQPLLQQHAQYLKSHPQRHVLIQGNTDERGTSEYNLALGQKRAEAVRR+L+LLGV DS+MEAVSLGKEKP ATGHDEASWAQNRRADLVYQQ	*B. phymatum*	86
LDD + +GA- A NVA V+V--DPLNDPN PLAKRS+YFDFDSYSVK +YQ +LQ H+QYL S+ R +LIQGNTDERGTSEYNLALGQKRAEAVRR+LA +GV DSQMEAVSLGKEKP ATGHD+ASWA+NRRAD+VY	*R. metallidurans*	73
LDD ANAGA AD-- V V+V--DPLNDPNSPLAKRS+YFDFDSYSVK EYQ +L +HA+YL S+ R +LIQGNTDERGTSEYNLALGQKRAEAVRR+LA +GV+DSQMEAVSLGKEKP +TGHDEA+WA+NRRAD+ Y	*R. eutropha*	73
LDD--K G +T NV V+V--D L DPNSPLAKRS+YFDFDSY+VK EYQ LL QHA+YL+SH QR VLIQGNTDERGTSEYNLALGQKRAEAVRRAL+ GV DSQMEAVSLGKEKP ATGHDE SWAQNRR+D+VY	*R. solanacearum*	74

Table 5.1. Sequence alignment of OmpA-like domains. The sequence underlined was obtained from the analysis of the high immune reactive protein in the outer membrane preparation of *B. cenocepacia*. Shown are the sequence alignments resulting from the BLAST analysis. The eleven residues in red are strictly conserved among all the Omp-A family members characterized as described by Grisot and Buchanan (2004).

Immunization Group	Mean total Peripheral Leukocyte Concentration (10^9/L)	Mean Polymorphonuclear Leukocyte Concentration (10^9/L)
15 µg OMP + 20% NE	5.41 ± 2.28 *	2.58 ± 0.48 *
15 µg OMP in PBS	5.26 ± 2.13	2.56 ± 0.55 *
5 µg OMP + 20% NE	4.36 ± 0.85 *	1.99 ± 0.20 *
5 µg OMP in PBS	5.41 ± 1.48 *	3.23 ± 0.29
Non-Vaccinated	9.59 ± 5.31	7.29 ± 1.35

Table 5.2. Total leukocyte and polymorphonuclear leukocyte serum enumeration following challenge. Vaccinated or naïve mice (n=5/group) were placed under general anesthesia and were trans-tracheally challenged with $5X10^7$ *B. cenocepacia* in PBS. The mice were euthanized at 4 or 6 days post-challenge and blood from a cardiac puncture was collected in tubes with EDTA. The blood was analyzed for total and mononuclear lymphocytes using the HEMAVETH 950 analyzer. * indicates statistical difference (*p value* <0.05) between immunized and non-immunized animals.

5.8 REFERENCES

1. LiPuma, J.J., et al., *In vitro activity of a novel nanoemulsion against Burkholderia and other multi-drug resistant cystic fibrosis-associated bacterial species.* Antimicrob Agents Chemother. , 2008. Epub ahead of print.

2. Eberl, L. and B. Tummler, *Pseudomonas aeruginosa and Burkholderia cepacia in cystic fibrosis: genome evolution, interactions and adaptation. .* Int J Med Microbiol 2004. 294: p. 123-131.

3. Al-Bakri, A.G., P. Gilbert, and D.G. Allison, *Immigration and emigration of Burkholderia cepacia and Pseudomonas aeruginosa between and within mixed biofilm communities. .* J Appl Microbiol, 2004. 96: p. 455-463.

4. Tomlin, K.L., S.R.D. Clark, and C. Howard, *Green and red fluorescent protein vectors for use in biofilm studies of the intrinsically resistant Burkholderia cepacia complex.* J Microbiol Methods, 2004. 57: p. 95-106.

5. LiPuma, J.J., *Update on Burkholderia cepacia complex.* Current Opinion in Pulmonary Medicine, 2005. 11: p. 528-533.

6. Boucher, R., M.R. Knowles, and J. Yankaskas, *Mason: Murry & Nadel's Textbook of Respiratory Medicine*. 4th ed, ed. R.J. Mason. 2005, Philadelphia, PA:: Elsevier Inc.

7. Davis, S.S., *Nasal vaccines. .* Adv. Drug Deliv. Rev., 2001. 51: p. 21-42.

8. Makidon, P.E., et al., *Pre-Clinical Evaluation of a Novel Nanoemulsion-Based Hepatitis B Mucosal Vaccine.* PLoS One, 2008. 3(8): p. e2954.

9. Bielinska, A.U., et al., *A novel killed-virus nasal vaccinia virus vaccine.* Clinical and Vaccine Immunology, 2008. 15: p. 348-358.

10. Bielinska, A.U., et al., *Nasal immunization with a recombinant HIV gp120 and nanoemulsion adjuvant produces TH1 polarizatied responses and neutralizing antibodies to primary HIV-1 isolates.* AIDS Research and Human Retroviruses, 2007. 24: p. 271-281.

11. Bielinska, A.U., et al., *Mucosal Immunization with a Novel Nanoemulsion-Based Recombinant Anthrax Protective Antigen Vaccine Protects against Bacillus anthracis Spore Challenge.* Infect Immun, 2007. 75: p. 4020-4029.

12. Bertot, G.M., et al., *Nasal Immunization with Burkholderia multivorans Outer Membrane Proteins and the Mucosal Adjuvant Adamantylamide Dipeptide Confers Efficient Protection against Experimental Lung Infections with B. multivorans and B. cenocepacia.* Infect. Immun., 2007. 75(6): p. 2740–2752.

13. Hamouda, T., et al., *A novel surfactant nanoemulsion with a unique non-irritant topical antimicrobial activity against bacteria, enveloped viruses and fungi.* Microbiological Research, 2000. 156(1): p. 1-7.

14. Hamouda, T., et al., *A novel surfactant nanoemulsion with a unique non-irritant topical antimicrobial activity against bacteria, enveloped viruses and fungi.* Microbiol Res, 2001. 156(1): p. 1-7.

15. Hamouda, T. and J.R. Baker, *Antimicrobial mechanism of action of surfactant lipid preparations in enteric Gram-negative bacilli.* Journal of Applied Microbiology, 2000. 89(3): p. 397-403.

16. Myc, A., et al., *The fungicidal activity of novel nanoemulsion (X8W60PC) against clinically important yeast and filamentous fungi.* Mycopathologia, 2002. 155(4): p. 195-201.

17. Makidon, P.E., et al., *Pre-Clinical Evaluation of a Novel Nanoemulsion-Based Hepatitis B Mucosal Vaccine.* PLoS ONE, 2008. 3(8): p. e2954.

18. Myc, A., et al., *Development of immune response that protects mice from viral pneumonitis after a single intranasal immunization with influenza A virus and nanoemulsion.* Vaccine, 2003. 21: p. 3801-3814.

19. Coenye, T. and P. Vandamme, *Burkholderia Molecular Microbiology and Genomics* 1ed. Horizon Scientific Press. 2007, Oxford, UK: Taylor & Francis.

20. Johnson, W.M., S.D. Tyler, and K. Rozee, *Linkage analysis of geographic and clinical clusters in Pseudomonas cepacia infections by multilocus enzyme electrophoresis and ribotyping.* J. Clin. Microbiol., 1994. 32(4): p. 924-930.

21. Sajjan, U.S., et al., *A type IV secretion system contributes to intracellular survival and replication of Burkholderia cenocepacia.* Infect Immun, 2008. Epub ahead of print.

22. Rosenfeld, J., et al., *In-gel digestion of proteins for internal sequence analysis after one- or two-dimensional gel electrophoresis.* Analytical Biochemistry, 1992. 203(1): p. 173-179.

23. Hellman, U., et al., *Improvement of an "In-Gel" digestion procedure for the micropreparation of internal protein fragments for amino acid sequencing.* Analytical Biochemistry, 1995. 224(1): p. 451-455.

24. Henry, D.A., et al., *Identification of Burkholderia cepacia isolates from patients with cystic fibrosis and use of a simple new selective medium.* J Clin Microbiol 1997. 35: p. 614-619.

25. Chu, K.K., et al., *Differential persistence among genomovars of the Burkholderia cepacia complex in a murine model of pulmonary infection.* Infect. Immun. , 2002. 70: p. 2715-2720.

26. Chu, K.K., et al., *Persistence of Burkholderia multivorans within the pulmonary macrophage in the murine lung.* Infect. Immun. , 2004. 72: p. 6142–6147.

27. Ortega, X., et al., *Reconstitution of O-specific lipopolysaccharide expression in Burkholderia cenocepacia strain J2315, which is associated with transmissible infections in patients with cystic fibrosis.* Journal of Bacteriology, 2005. 187(4): p. 1324-1333.

28. Plesa, M., et al., *Conservation of the opcL gene encoding the peptidoglycan-associated outer-membrane lipoprotein among representatives of the Burkholderia cepacia complex.* Journal of Medical Microbiology, 2004. 53: p. 389-398.

29. Baldwin, A., et al., *Elucidating Global Epidemiology of Burkholderia multivorans in Cases of Cystic Fibrosis by Multilocus Sequence Typing.* J Clin Microbiol., 2008. 46(1): p. 290-295.

30. Dabo, S.M., A.W. Confer, and R.A. Quijano-Blas, *Molecular and immunological characterization of Pasteurella multocida serotype A:3 OmpA: evidence of its role in P. multocida interaction with extracelluar matrix molecules.* Microb Pathog, 2003. 35(4): p. 147-157.

31. Goetsch, L., et al., *Targeting of nasal mucosa-associated antigen-presenting cells in vivo with an outer membrane protein A derived Klebsiella pneumoniae.* Infect Immun, 2001. 69(10): p. 6434-6444.

32. Hendry, J., et al., *Antibody Response to Burkholderia cepacia in Patients with Cystic Fibrosis Colonized with Burkholderia cepacia and Pseudomonas aeruginosa.* Journal of Infection, 2000. 40: p. 164-170.

33. Aronoff, S.C. and R.C. Stern, *Serum IgG antibody to the outer membrane antigens of Pseudomonas cepacia and Pseudomonas aeruginosa in cystic fibrosis. .* J Infect Dis 1988. 157: p. 934-940.

34. Lacy, D., et al., *Serum IgG response to B. cepacia outer membrane antigens in cystic fibrosis:assessment of cross-reactivity with P. aeruginosa.* FEMS Immunology and Medical Microbiology 1995. 10: p. 253-262.

35. Nelson, J.W., J.R.W. Govan, and G.R. Barclay, *Pseudomonas aeruginosa flagellar antibodies in serum, saliva and sputum from patients with cystic fibrosis. Serodiag Immunother Inf Dis* 1990. 4: p. 351-361.

36. Brett, M.M., A.T.M. Ghonheim, and J.M. Littlewood, *Serum IgG antibodies in patients with cystic fibrosis with early P. aeruginosa infection.* Arch Dis Child 1987. 62: p. 357-361.

37. Doring, G. and N. Hoiby, *Longitudinal study of immune response to Pseudomonas aeruginosa antigens in cystic fibrosis. . Infect Immun*, 1983. 42: p. 197-201.

38. Nelson, J.W., et al., *Serum IgG and sputum IgA antibody to core lipopolysaccharide antigen from Pseudomonas cepacia in patients with cystic fibrosis. .* J Med Microbiol 1993. 39: p. 39-47.

CHAPTER 6
CONCLUSIONS AND OUTLOOK

The search for new-generation mucosal vaccines is an area of intense investigation. Novel mucosal vaccines hold great promise for the prevention of existing and emerging infectious disease, but none have been approved for human use. It is clear that the development of safe and effective mucosal adjuvants capable of stimulating humoral and cell-mediated immunity is critical to the advancement of mucosal vaccinology. This dissertation has examined the potential utility of a novel nanoemulsion as a new-generation nasopharyngeal adjuvant for humans.

In Chapter 2, I explored several aims. First, we characterize the profile of immunity stimulated by NE. This profile is useful for the understanding of the adjuvant mechanism and as a basis for the development of future NE-based vaccines. The immunological profile we assert is summarized as follows:

- A robust and sustained systemic IgG, mucosal IgA, and strong antigen-specific cellular immune responses were observed.
- Intranasal vaccination with HBsAg-NE stimulates a robust protective immunity in rodents.
- HBsAg-NE immunization resulted in significantly higher serum IgG anti-HBsAg avidity, compared to the IgG from HBsAg-Alu vaccinated mice.
- A Th1 polarized immune response was indicated by IFN-γ and TNF-α cytokine production and elevated levels of the IgG2 subclass of HBsAg-specific antibodies.

I have demonstrated that NE is an effective and strong mucosal adjuvant for a recombinant protein. The utility of the material is based on the ability of the NE to stabilize antigen in non-refrigerated conditions for prolonged periods of time. In order to develop a clear understanding of the factors that contributes to thermal-stability and immunogenicity, Chapters 2 and 4 examined the physical relationship between antigen and NE and evaluated the effects of buffered and non-buffered salt diluents. These findings can be summarized as follows:

- HBsAg-NE retains full immunogenicity for a year at 4°C, 6 months at 25°C and 6 weeks at 40°C.
- OVA-NE retains full immunogenicity for 8 months at 25°C when formulated with PBS and for 6 months when formulated with NaCl.
- The mechanism of thermal stability relates to a thermodynamically favorable and electrostatic association of NE and antigen.
- Thermal stability is enhanced by formulating NE-based vaccines with buffered salt when compared to non-buffered diluents.

The physico-chemical characterization of HBsAg-NE and OVA-NE presented in Chapters 2 and 4 suggest that NE is thermal stable. Therefore circumvention of strict cold-chain storage conditions for NE is possible under certain circumstances. Studies in Chapter 2 had determined that the simple mixing of antigen with NE causes the antigen to interface with the the emulsion oil droplets at the oil/water interface. This led us to hypothesize that the ability of the NE droplet to penetrate mucosal membranes and facilitate uptake by mucosal antigen-presenting cells provided its adjuvant activity, potentially through the recognition of dendritic cell membrane-associated molecules. This may be partially explained in Chapter 3 by the enhanced DC internalization and enhanced physiologic trafficking of antigen-NE, compared to antigen alone. Antigens that have a thermodynamically unfavorable interaction or that display electrostatic repulsion to the oil-phase of the NE and therefore reside primarily in the aqueous phase may act similarly to antigen without NE adjuvant. We hypothesize that decreased cellular internalization and physiological trafficking

would result for antigens that do not favorably associate with the oil phase of the emulsion, compared to those that exhibit favorable relationships. Ongoing studies designed to evaluate this relationship after mixing antigen with cationic, neutral and anionic NE are underway. If our hypothesis is correct, these types of physico-chemical analysis could serve as an important screening method for predicting immunogenicity for new-generation NE-based vaccines.

As stated previously, the development of effective mucosal vaccines depends on the discovery of safe adjuvants and the ability to successfully deliver them to the appropriate tissues of the human sinus. The final aim of Chapter 2 was to assess the safety of applying NE to the nasal mucosa. This was accomplished using a variety of animal models. The suitability of dispensing NE-based vaccines through commercially available sprayer pumps was examined in Chapter 4. The findings of these studies can be summarized as follows:

- Comprehensive pre-clinical toxicology evaluation demonstrated that NE is safe and well tolerated in multiple animal models.
- NE-based vaccines are not physically or chemically altered and retain their potency following actuation through two commercially available nasal sprayer devices.
- NE-based vaccines are expected to be efficiently deposited in inductive tissues mainly in the anterior region of the human sinus and therefore do not require specially engineered delivery devices.

In Chapter 3, we examine the apparently unique adjuvant activity associated with NE. Understanding the mechanism of adjuvant activity associated with NE is important from the standpoint of future development of the platform and formulation optimization. Perhaps as important, these studies may illuminate previously undescribed innate immune pathways. The mechanism of NE adjuvant action findings are summarized below:

- NE promotes antigen and NE lipid internalization in the Jaws II dendritic cell line and bone marrow-derived murine dendritic-like cells *in vitro*.

- NE promotes broad nasal epithelial uptake and subsequent trafficking of antigenic protein to the submandibular lymph nodes and thymus within 24 hours of intranasal vaccination *in vivo*.
- NE promotes trans-epithelial antigen loading of mucosal DC and trafficking towards lymphoid tissues without inducing inflammation or massive cellular infiltration.
- IL6 is induced in the bronchoalveolar secretions by nasal epithelial cells, following intranasal vaccination with NE-based vaccines.
- IL6 appears to be important in the adjuvant signaling pathway and for T-helper cell polarity but is not critical for IgG immune response.
- A unique set of immunomodulatory cytokine/chemokine-associated genes chemotactic for innate lymphocytes and dendritic cells are induced following intranasal vaccination with NE-based vaccines, compared to Alum, MF59, and CpG. These genes are associated with the induction of IL6, Cxcl1, Ccl20, IL1β and are important chemoattractants for mucosal DC.
- Hallmark inflammation is not evident after NE-based vaccination

Although this thesis makes some important contributions to the understanding of the NE adjuvant mechanism, the complexity and multi-factorial nature of the exact mechanism has, suffice to say, left many outstanding questions. There are several ways in which to improve our understanding of the adjuvant mechanism. There are, for example, a number of key innate factors such as TLR receptors, NLR, inflamasomes, and NF-κB proteins that may interact with NE. Studying the interaction of these proteins in *in vitro* and *in vivo* studies should further clarify the mechanistic pathway of the NE adjuvant. The information may provide critical insight into formulation optimization for different antigen systems or approaches.

Chapter 5 serves as the capstone section for this thesis. The intent of this chapter was to utilize the knowledge gained from studies reported in Chapters 2-

4 for the development of a NE-based mucosal vaccine using a pathogen-derived antigen. To this end, *B. cenocepacia* OMP was chosen not only because of the critical importance of advancing the understanding of Bcc prophylaxis but also because it represents a type of protein not yet evaluated with NE adjuvant. The important findings regarding the development of an experimental *B. cenocepacia* OMP-NE are summarized as follows:

- Intranasal vaccination with *B. cenocepacia* OMP-NE stimulates a robust systemic IgG, mucosal IgA and IgG, and antigen-specific cellular immune responses.
- A novel finding is that an immune response is associated with a 17 KDa OmpA.
- A balanced Th1/Th2 polarized immune response was indicated by IFN-γ, IL2, and IL4 cytokine production and elevated levels of the IgG2b subclass of OMP-specific antibodies.
- Vaccination resulted in the production of *B. cenocepacia*-neutralizing antibodies and cross-neutralizing antibodies for *B. multivorans*.
- Using a mouse model of chronic pulmonary infection, we demonstrated enhanced clearance of *B. cenocepacia* from the lungs of vaccinated animals which correlated with neutralizing antibodies for *B. cenocepacia*.

My results indicate that NE is an efficient adjuvant for *B. cenocepacia* OMP intranasal immunization. Mucosal immunity to *B. cenocepacia* elicited by intranasal vaccination with OMPs and NE could prevent the early steps of colonization and infection with *Bcc* organisms. The 17 KDa OMP shows potential for future vaccine development. This study provides a rational basis for vaccine design using NE-adjuvanted vaccines in combination with recombinant OMP protein.

In summary, the findings reported in this dissertation support the continued development of nanoemulsion adjuvant as a new-generation mucosal vaccine adjuvant. Understanding the mechanisms of adjuvation, the safety profiles, and

formulation optimization is critical as NE-based vaccines approach human clinical trials. As such, there remains a great deal of work to be accomplished, not only on NE formulations already utilized, but also on those currently being developed and for those yet to be developed to combat emerging diseases. These future efforts combined with work presented in this dissertation will play a critical role in advancing the science of new-generation mucosal vaccine adjuvants.